Room temperature methods of direct arylation for conjugated polymer and small molecule synthesis

Amy L. Mayhugh

A dissertation

submitted in partial fulfillment of the

requirements for the degree of

Doctor of Philosophy

University of Washington

2022

Reading Committee:

Christine K. Luscombe, Chair

Gojko Lalic

Alshakim Nelson

Program Authorized to Offer Degree:

Chemistry

University of Washington

Abstract

Room temperature methods of direct arylation for conjugated polymer and small molecule synthesis

Amy L. Mayhugh

Chair of the Supervisory Committee:
Professor Christine K. Luscombe
Materials Science & Engineering

Direct arylation polymerization (DArP) offers numerous benefits over classical methods of cross-coupling polymerization, although improvements are still warranted to increase simplicity and reduce cost. Room temperature transformations are an attractive approach, requiring an efficient C-H arylation process while providing insights into mechanistic features allowing for good reactivity with reduced thermal energy availability. This work investigates room temperature direct arylation, emphasizing the underlying mechanisms that differ between room temperature conditions and the more common elevated temperatures. Two different transformations are investigated as room temperature direct arylation methods for heterobiaryls: DArP-prepared polyindole and benzofuran direct arylation. Both conditions are shown to proceed through non-traditional mechanisms, facilitating room temperature reactivity. Despite good small molecule regioselectivity, regiodefects are high in polyindole and regioselectivity is a concern should the benzofuran method be used for DArP. These results demand greater study into approaches for improving selectivity. The unpredicted regiodefects in these polymerizations provide a strategy for understanding selectivity and reactivity trends not readily observable in the corresponding small molecule reaction due to the exceptional monomer conversion required for polymerization.

ACKNOWLEDGMENTS

This work would not have been possible without the support of my advisor Christine Luscombe. Her sharp technical expertise, patient temperament, and willingness to provide time, space, and support for me to sort through research questions has been immensely valuable to my development as an independent scientist.

The Luscombe group's support has added to my scientific training. The entire group has made an impact on me and my work by sharing their expertise, editing manuscripts, and building comradery in our graduate school experiences. My broader organic division cohort has also been a source of shared resources, brainstorming, and encouragement.

The Clean Energy Institute and the NSF Center for Selective C-H Functionalization have been critical to broadening my scientific perspective and developing a holistic skillset.

Thank you to my undergraduate advisor Dave Cordes. My experience at Pacific University could not have been a more positive, collaborative, engaging, and supportive introduction to the chemical sciences.

I am so grateful for the endless support, patience, and encouragement showed to me by my community. Thank you for reminding me the value of this degree is in gaining wisdom much more than knowledge. Wendy and Svea: thank you for always answering the phone and making me feel like we are in this together. Chris: thank you for being a good listener, believing in me and reminding me to do the same. Erin and Kat: thank you for your friendship and celebrations since Day 1. You each get a slice of this degree.

There are so many people to thank who have contributed to the completion of this work, for all of whom I am so thankful.

TABLE OF CONTENTS

LIST OF ABBREVIATIONS

Ac	Acetyl
BHT	2,6-Di-tert-butyl-4-methylphenol
Bpy	2,2-Bipyridine
CDC	Cross dehydrogenative coupling
CMD	Concerted-metalation deprotonation
CPME	Cyclopentyl methyl ether
CTP	Catalyst transfer polymerization
Cy	Cyclohexyl
CyJohnPhos	(2-Biphenyl)dicyclohexylphosphine
D-A	Donor-Acceptor
DArP	Direct arylation polymerization
dba	Dibenzylideneacetone
DCAP	Direct C-H Amidation Polymerization
DCE	1,2-Dichloroethane
DCM	Dichloromethane
DG	Directing group
DMAc	N,N-Dimethylacetamide
DMF	N,N-Dimethylformamide
DMSO	Dimethyl sulfoxide
DP	Degree of polymerization
dppe	1,2-Bis(diphenylphosphino)ethane

*e*CMD	Electrophilic concerted-metalation deprotonation
E_{dist}	Distortion energy
EDTA	Ethylenediaminetetraacetic acid
EI	Electron ionization
E_{int}	Interaction energy
Equiv	equivalence
Et	Ethyl
EtOH	Ethanol
GC-MS	Gas chromatography-mass spectrometry
H	Hour
Hex	Hexyl
3-HET	3-hexylesterthiophene
3-HT	3-hexylthiophene
HFIP	1,1,1,3,3,3-Hexafluoropropan-2-ol
HOMO	Highest occupied molecular orbital
HRMS	High resolution mass spectrometry
i-Pr	isopropyl
JohnPhos	(2-Biphenylyl)di-tert-butylphosphine
KIE	Kinetic isotope effect
LUMO	Lowest occupied molecular orbital
MALDI-TOF MS	Matrix-assisted laser desorption/ionization-time of flight mass spectrometry

Me	Methyl
MeOH	Methanol
MHz	Megahertz
M_n	Number average molecular weights
Mol	Mole
N	Number of π electrons
n	Number of repeat units in a polymer
ND	Not determined
NDA	Neodecanoic acid
NMR	Nuclear magnetic resonance

Abbreviations for NMR splitting patterns:

- s: singlet
- d: doublet
- t: triplet
- q: quartet
- p: pentet
- m: multiplet
- br: broad
- dd: doublet of doublets
- dt: doublet of triplets
- ddt: doublet of doublet of triplets

Oxi-DArP	Oxidative direct arylation polymerization

p	Conversion to polymer
P3HT	Poly(3-hexylthiophene)
PBX	1-Pivaloyloxy-1,2-benziodoxol-3(1*H*)-one
Ph	Phenyl
PhMe	Toluene
PIn	Poly(indole)
PivOH	Pivalic acid
ppm	Parts per million
ProDOT	3,4-Propylenedioxythiophene
R	Stoichiometric ration of reactants
R_f	Retention factor
RR	Regioregularity
rt	Room temperature
S_EAr	Electrophilic aromatic substitution
SET	Single electron transfer
S_NAr	Nucleophilic aromatic substitution
$S_{RN}1$	Radical-nucleophilic aromatic substitution
t-Bu	Tert-butyl
t-BuBrettPhos	2-(Di-tert-butylphosphino)-2′,4′,6′-triisopropyl-3,6-dimethoxy-1,1′-biphenyl
t-BuXPhos	2-Di-tert-butylphosphino-2′,4′,6′-triisopropylbiphenyl
TEMPO	(2,2,6,6-Tetramethylpiperidin-1-yl)oxyl

THF	Tetrahydrofuran
TMEDA	Tetramethylethylenediamine
TM	Transition Metal
TS	Transition State
XPhos	2-Dicyclohexylphosphino-2′,4′,6′-triisopropylbiphenyl

LIST OF FIGURES

LIST OF SCHEMES

Chapter 1. Introduction

*Sections within Chapter 1 have been adapted from a previously submitted article: Reprinted with permission from *J. Am. Chem. Soc.* **2022**. Copyright 2022 American Chemical Society.

1.1 Conjugated Polymers

Conjugated polymers, marked by their alternating double and single bonds, are a class of materials having received significant study since the discovery of their semiconducting properties in the 1970s by Shirakawa, Heeger, and MacDiarmid.[1,2] The most basic of these materials, polyacetylene, exemplifies the extended π-conjugation that provides conjugated polymers with semiconducting properties. As the conjugation length increases, greater electron delocalization occurs through overlapping p orbitals, and the energy distance between the HOMO and LUMO decreases to form a narrow band gap (**Figure 1.1**).[3] For inorganic materials, decreasing the band gap present in between the valence and conduction band edges changes a material from an insulator, to a semiconductor, and eventually when the band edges overlap, to a conductor. Analogously, sufficiently narrowing the distance between a polymer's HOMO and LUMO levels gives conjugated polymers semiconducting properties. Thus, structural features impacting the polymer's band gap, such as molecular weight, directly impact the electronic properties of the material.

Rationally designed polymers can maximize electronic and mechanical properties of a conjugated polymer for a particular application, based on the relationship between molecular structure and observed properties. Since polyacetylene was first studied, complex molecular structures have been designed that leverage the structure/property relationship between a given

material and its electronic performance to achieve high performance polymers. Common design strategies exist for achieving these materials,[3–5] and some of these are listed as follows. Commonly, donor-acceptor (D-A) copolymers are used to narrow the band gap through a push-pull electronic effect.[6,7] The band gap can be further tuned by modification of the polymer side chain with either electron-rich or electron-deficient groups.[8,9] An additional strategy uses repeat units containing fused heterocycles to improve π-electron flow on the polymer chain by favoring quinoid structures along the backbone.[10,11] While there are many considerations when designing conjugated polymers, these examples demonstrate the chemical structures' influence on electronic properties.

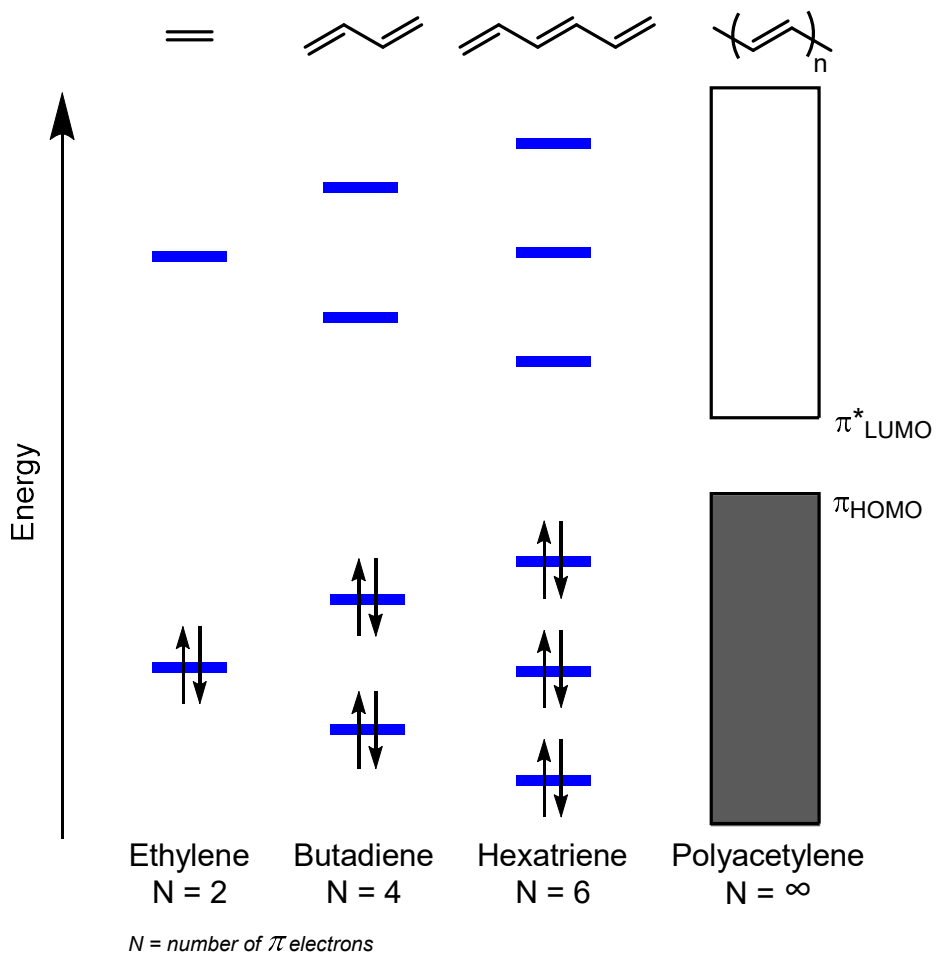

Figure 1.1 Effect of increasing conjugation length on HOMO-LUMO levels in polyacetylene

The precise structural control at an atomic level make conjugated polymers a broad and dynamic class of materials, with different structures meeting the needs of a diverse range of applications.[12–15] These applications take advantage of polymers' potential for large-scale, solution-based processing. Moreover, conjugated polymers are lightweight, can be flexible and deformable, demonstrate good biocompatibility, and demonstrate mixed conductivity. These properties allow for applications including thin displays with increased flexibility,[13] large-scale fabrication of laminate solar cells,[16] bio-based sensors,[17] and stretchable electronics[14] among others. In order to achieve these applications commercially, materials must achieve suitable

electronic performance, while maintain good stability and desired mechanical properties. In addition, their preparation must be cost-efficient, sustainable, and reliable in order to be a viable product.[18] Lastly, serious consideration is needed to their long-term environmental life cycle if these materials are to be produced at a commercial scale.[19,20]

1.2 Polycondensation Reactions

Currently, conjugated polymers are produced using conventional methods of cross-coupling; typically the Stille or Suzuki polymerization is used. While catalyst transfer polymerizations (CTP) have been investigated to prepare poly(3-hexylthiophene) (P3HT) and analogs in a controlled chain polymerization,[21,22] the vast majority of conjugated polymers are prepared with cross-coupling polymerizations which are polycondensation reactions (**Scheme 1.1**). These methods are favored as they offer high enough reactivity to yield high molecular weight materials, a challenging requirement for polycondensation reactions which require extremely high conversion to achieve high molecular weights.[23] Additionally, these methods feature monomer prefunctionalization with reactive species, typically an organometallic group. By installing reactive functional groups, excellent regioselectivity can be achieved at the desired cross-coupling sites. While these methods are valuable for their reactivity, reliability, and site-selectivity, they also have limitations. As polycondensation reactions require equimolar monomer loading, monomer purity is essential to achieve the highest molecular weights. In the case of organostannane monomers, for example, purification can be tricky and impurities are a problem. These monomers are also highly toxic, and produce stoichiometric amounts of organostannane waste which must be sequestered and quenched. Additionally, the reaction steps required to

install the intermediate reactive functional groups add work, increase waste and increase cost of the transformation.

Scheme 1.1 Conventional methods of cross-coupling polymerization

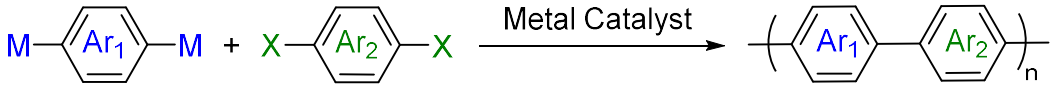

M =	SnR_3	Stille Coupling	X = I, Br, Cl, OTf, etc.
	$B(OR)_2$	Suzuki Coupling	
	ZnR	Negishi Coupling	
	MgX	Kumada Coupling	
	Li	Murahashi Coupling	

Cross-coupling polymerizations are an example of a polycondensation reaction, where difunctionalized molecules undergo repeated substitution while extruding small molecule byproducts. Here, polymer chains grow slowly by reacting throughout the reaction medium, such that every monomer is used to from short chain oligomers on the way to long polymers (**Figure 1.2A**). These reactions are in contrast to chain polymerizations, where an initiator forms an active chain end, selectively adding monomers one-by-one such that a long polymer can exist in the same solution as monomer units. As such, initiators are required for chain polymerization but not for polycondensation reactions. Similarly, polycondensation reactions do not undergo termination and can continue to react presuming no side reactions have caused decomposition of the necessary reactive functional groups. On the other hand, chain polymerizations involve termination after which the polymer chains end are not active for continued growth.

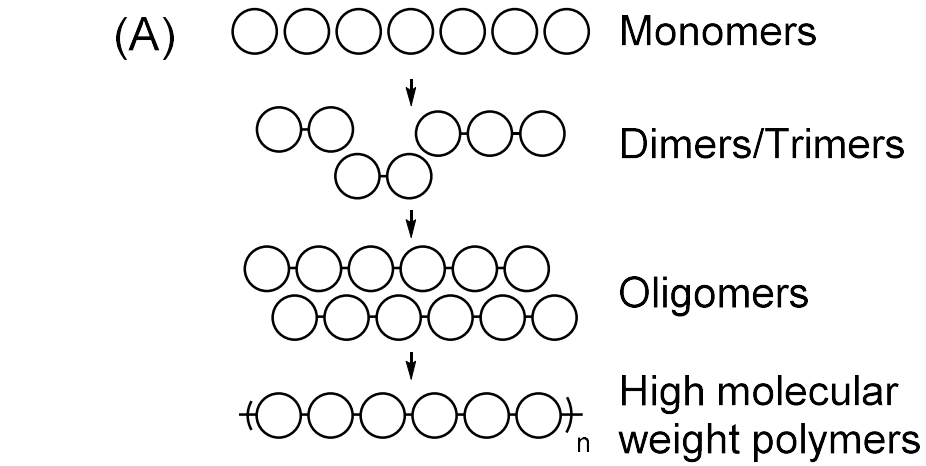

(B)

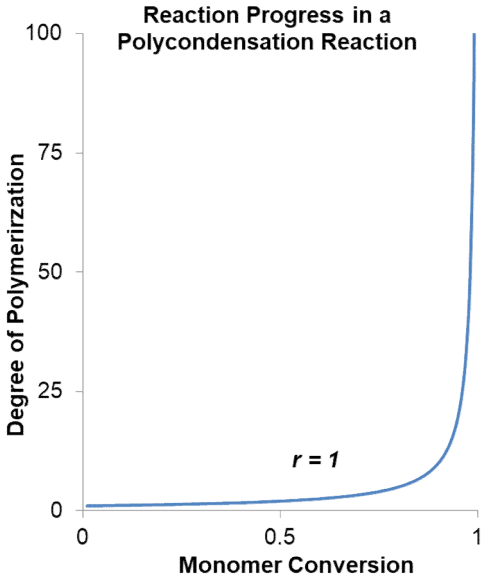

Monomer Molar Ratio	DP at 99% Conversion	DP at 95% Conversion
1	100	20
0.99	67	18
0.98	50	17
0.95	28	13
0.90	16	10

Figure 1.2 Qualitative and quantitative representation of polycondensation reactions

Polycondensation reactions have been modeled extensively, providing valuable insight into how to understand the behavior of these reactions, and how to optimize for high molecular weights. One way to think about polycondensation reactions is that every n-mer displays the same effective reactivity as the monomer, in contrast to chain polymerization where the growing polymer chain reacts preferentially to monomers (**Figure 1.2A**).[24] In polycondensation reactions, the same coupling is repeated extensively until long chains are produced. This has been described

mathematically by the Carothers equation, indicating that exceptionally high conversion is needed for achieving high molecular weights (**Equation 1**, **Figure 1.2B**).[23]

$$DP = \frac{1 + r}{1 + r - 2rp} \quad \textbf{(1)}$$

Here, the degree of polymerization (DP) is related to the stoichiometric ratio of monomer coupling partners (r), and the fraction of reacted monomer functional groups (p). The Carothers equation is a simple relationship governed by a few assumptions which are not always realized in polycondensation reactions.[25] Firstly, all reactive groups are assumed to be equally reactive, meaning that a monomer will react with either a monomer or growing polymer chain without preference. Additionally, this model assumes an equilibrium polymerization with complete solubility of monomers and polymers.[23]

In addition to very high conversion, equimolar monomer loading is required to achieve high molecular weight polymers. This can be shown mathematically, where in **Equation 1**, when r is one, the Carothers equation simplifies to:

$$DP = \frac{1}{1 - p} \quad \textbf{(2)}$$

Equation 2 demonstrates how when perfect stoichiometry is achieved, the degree of polymerization is only related to p. More frequently, perfect stoichiometry is not achieved. Even in a seemingly excellent scenario where r = 0.99 and p = 0.99, the maximum DP is only 67, and DP declines readily as r and p further deviate from one. This is demonstrated in the table in **Figure 1.2B**: as the monomer molar ratio deviates from one, the maximum accessible DP decreases. Practically, the Carothers model of polycondensation reactions makes monomer purity essential for achieving perfect stoichiometry, which can be challenging with the reactive

organometallic monomers often used in cross-coupling polymerizations. It also demands transformations with exceptionally high conversions.

1.3 C-H Bond Functionalization

The direct functionalization of C-H bonds has revolutionized synthetic chemistry, presenting an efficient and atom economic pathway to prepare molecules through novel disconnections. Within conjugated polymer synthesis, C-H arylation has seen broad study for improving conventional methods of cross-coupling polymerization. Rather than monomer prefunctionalization inherent to conventional cross-coupling methods, C-H arylation allows C-C bond formation between an aryl halide and an unfunctionalized coupling partner (**Scheme 1.2**). As an alternative to traditional cross-coupling polymerizations, using C-H functionalization reduces the number of synthetic steps required, reducing both labor and waste produced while simultaneously making highly pure monomers easier to access. Additionally, particularly in the case of the Stille coupling, stoichiometric amounts of toxic intermediates are not required.

Scheme 1.2 C-H functionalization compared with traditional methods

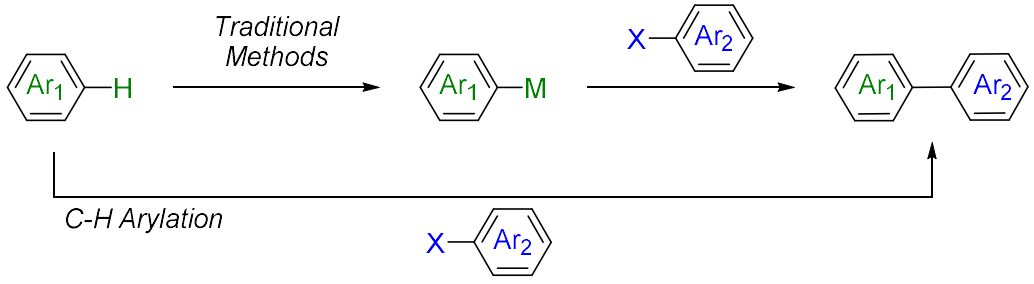

While C-H arylation has a number of attractive features over conventional cross-coupling methods, there are still challenges. Regioselective transformations are an important albeit challenging goal in this area of work, as most organic molecules have multiple, similar C-H bonds present. Creating systems that sufficiently activate only the desired C-H bond to achieve

high yielding and selective transformations can be a challenge. As C-H bonds in other contexts can be considered inert, elegant systems are often required to achieve high yielding regioselective reactions. Within the C-H functionalization methodology, there are several commonly used perspectives adopted to address these problems. Although examples may not fit clearly into a single perspective, it is a helpful way to structure the thought process of addressing selectivity problems within C-H functionalization. Two of these approaches will be discussed, one focuses on precise catalyst design to influence selectivity and reactivity while the other uses substrates' structure to control the reaction's outcome.

Catalyst-controlled selectivity seeks to tune the electronic and steric properties of a transition metal catalyst in order to optimize the reactivity, chemoselectivity, and site-selectivity for the desired transformation (**Scheme 1.3**).[26] C-H bonds within a given molecule show differing rates of C-H functionalization in all cases, although these differences are often too small to achieve a single product. By focusing on catalyst design and conditions optimization, it is possible to bias the formation of a single product without needing to make changes to the substrate through protecting groups, directing groups, or other fundamental changes. There are a number of examples in the literature for this approach, including reactions featuring sp^2-sp^2 C-C bond forming events.[26–30] This approach is attractive as without having to modify a substrate, reagents and catalysts can be varied to achieve the desired product. For circumstances where a particular structure is needed, including in drug development and complex monomer synthesis, catalyst-controlled selectivity allows more flexibility in synthetic design.[31,32]

Scheme 1.3 Regiodivergent C-H functionalization achieved via catalyst-control

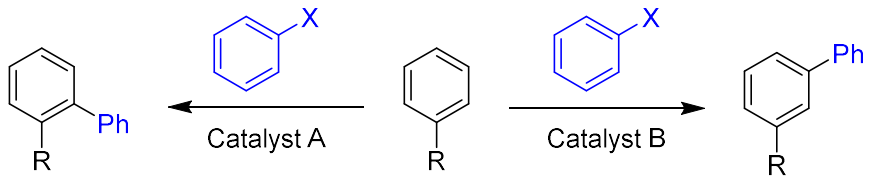

Substrate-controlled selectivity leverages meaningful reactivity differences between C-H bonds on a molecule to control product selectivity. These reactivity differences can be influenced by choosing electronically activated substrates, directing groups attached to the molecule, or by transient directing groups.[33] The situation is straightforward when the innate electronic bias of the desired substrate provides sufficient selectivity (**Scheme 1.4A**) or it is possible without compromising on molecular design to have blocking groups at competing C-H sites. Often times, selectivity is insufficient when relying on just the substrates' properties. Directing groups are a particularly common and effective strategy to increase innate substrate selectivity; these groups chelate to the catalyst, guiding it to a specific reaction site. Directing groups can be preinstalled stoichiometrically to the molecule, which then requires subsequent removal analogous to a protecting group (**Scheme 1.4B**).[34] Alternatively, transient directing groups allow for installation and removal in situ; transient directing groups can be used catalytically or stoichiometrically and can be covalently attached or use weak interactions (**Scheme 1.4C**).[35] While the catalyst and ligand selection influence the outcomes, this research perspective focuses primarily on modifying the substrate to achieve control while catalyst-controlled primarily focuses on using different catalysts to achieve different selectivity.

Scheme 1.4 Strategies for substrate-controlled site-selectivity

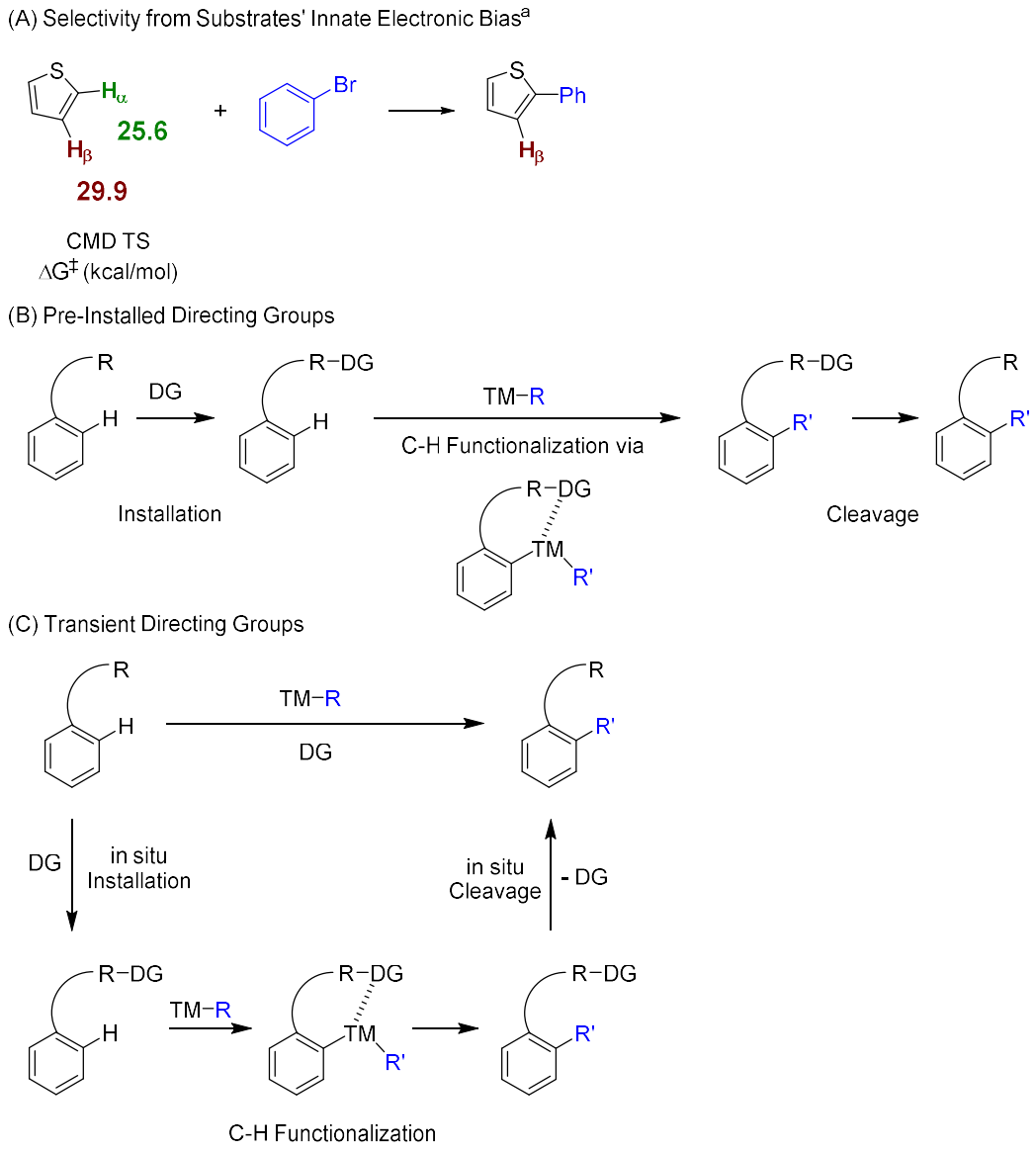

[a] Free energy values from ref. 36. DG = directing group

1.4 C-H Arylation in Conjugated Polymer Synthesis

C-H arylation can be achieved through direct arylation, where cross-coupling occurs between an aryl halide and an aromatic C-H bond. Oxidative direct arylation is another, similar approach to achieve C-H arylation, where homocoupling or cross-coupling occurs between two

aromatic C-H bonds. In these cases, selectivity is primarily controlled by the innate reactivity of the substrate for heteroarenes.[37] Both of these methods have been investigated extensively as polymerizations. Direct arylation polymerization (DArP) offers facile cross-coupling selectivity compared to oxidative direct arylation polymerization (Oxi-DArP), while Oxi-DArP presents the most efficient cross-coupling pathway to prepare polymers (**Scheme 1.5**).[38–40] Compared to conventional methods of cross-coupling polymerizations (e.g. Stille and Suzuki), DArP and Oxi-DArP present an elegant alternative, improving atom and step economy, cost, and monomer toxicity. As conjugated polymers have a wide range of potential commercial applications, finding synthetic methods that are both economically and ecologically viable at a commercial scale is an important research goal that C-H arylation polymerizations seek to address.

Scheme 1.5 C-H arylation polymerizations

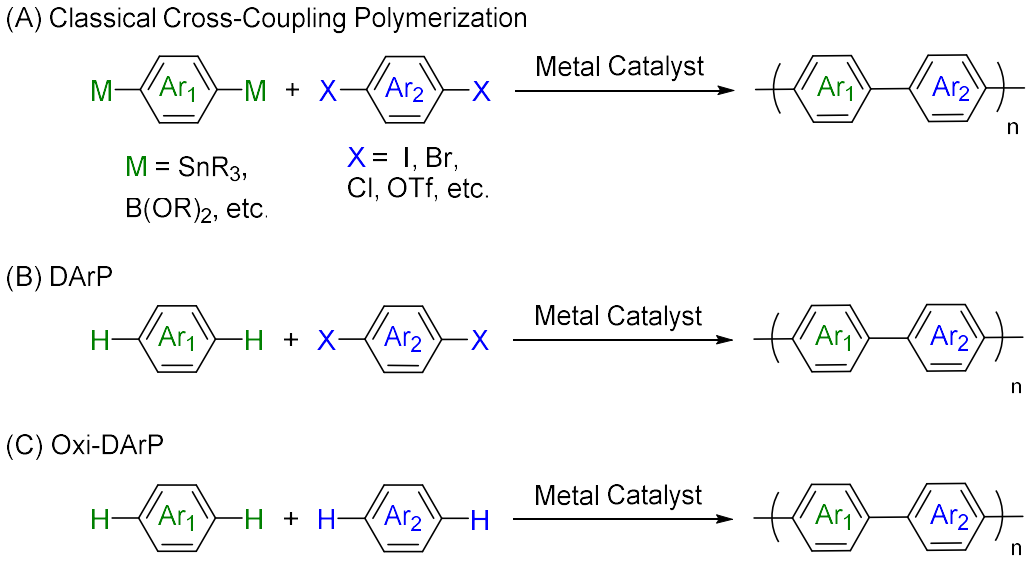

When considering regioselectivity for heteroarenes, oftentimes there is sufficient electronic activation by the heteroatom for good site-selectivity.[36] In small molecule reactions the small amounts of a regioisomers produced allows for the product to be isolated via purification

techniques. In other cases, regioisomers formation can be mitigated by shorter reaction times with slightly lower starting material conversion, thus avoiding tricky purifications. However, in polymerizations, producing even small amounts of an undesired regioisomer is detrimental as they are permanently incorporated into the polymer chain. This makes very high regioselectivity essential for polymerization success. In small molecule arylations of simple arenes and sometimes heteroarenes, directing groups are often utilized to achieve desired selectivity.[41] Despite their potential to alleviate difficulties achieving regioregular polymers via DArP, directing groups are uncommon in polymerizations due to their impact on the molecular design, and potential to facilitate cross-linking.

1.5 Mechanisms in Direct Arylation

Understanding the mechanism governing DArP can aid in improving selectivity outcomes. Substantial work has been completed investigating potential mechanism for direct arylation. Most commonly, direct arylation occurs through a concerted-metalation deprotonation (CMD) pathway.[36,37,42] That being said, under particular conditions, activation barriers can be lowered for other mechanisms and/or increased for the CMD pathway allowing for mechanisms such as Heck-type arylation to occur.[43–45] Electrophilic aromatic substitution (S_EAr) is another commonly considered mechanism. As these different mechanisms can lead to different reactivity trends and selectivity, understanding the operating mechanism can be important for optimization. In CMD, a ligated carboxylate assists in deprotonation at the same time as a C-Pd bond is being formed (i.e. concertedly, **Scheme 1.6B**), rather than in a stepwise fashion producing a σ-complex intermediate one would expect in an S_EAr mechanism.[36] CMD catalysts feature electron rich, organometallic transition metal species with aryl ligands from the oxidative addition product. In

terms of regioselectivity, CMD typically favors low pK_a C-H bonds and sterically accessible sites – a trend that has been broadly demonstrated to usefully describe the reactivity and selectivity patterns in currently known DArP methods.[46]

Scheme 1.6 CMD mechanism and distortion-interaction analysis[a]

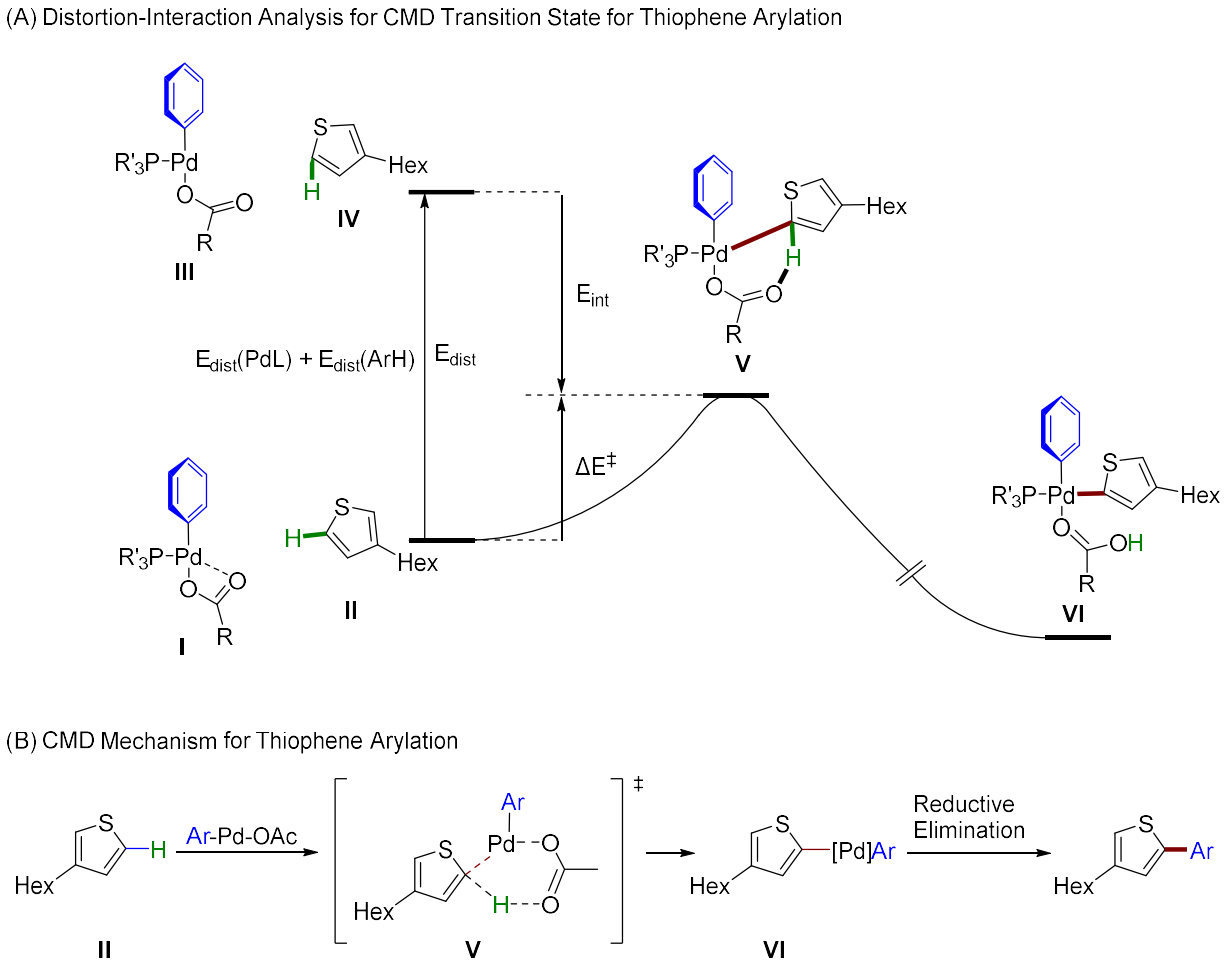

[a]Adapted from ref. 37,46.

CMD transition states can be understood using the distortion-interaction analysis, which considers both geometric and electronic factors influence reactivity and regioselectivity (**Scheme 1.6A**).[37,46] The geometric distortion that occurs when the catalyst and arene assume their transition state (TS) geometries (**III** and **IV**) presents an energetic cost (E_{dist}, distortion energy).

After this, the electronic interaction of the TS geometries of the catalyst and arene provide an energy gain (E_{int}, interaction energy) through forming **V** from **III** and **IV**. This interaction forms the TS structure. Depending on the balance of E_{dist} and E_{int}, the C-H arylation regioselectivity is governed by either the cost of E_{dist}, the gain of E_{int}, or a mixture of the two. Previous computational work has grouped a number of heteroarenes into three classes based on these three groupings.[36] Thiophene, a notable structural group in conjugated polymers, is part of a class of heteroarenes where for different C-H bonds the difference between both the energy cost of E_{dist} and the energy gain of E_{int} determine the regioisomers produced.

Beyond standard CMD, other mechanisms have also been discussed for direct arylation and need to be considered when considering reactivity outcomes in direct arylation systems. CMD can be thought of as part of a continuum, with proton abstraction on one end, a stepwise S_EAr mechanism with a σ-complex intermediate on the other, and a fully concerted transition state in the middle. Here, it has been suggested that CMD and electrophilic CMD (*e*CMD) mechanisms exist with asynchronous, concerted transition states. This means that for standard CMD the C-H bond cleavage is more advanced in the transition state than C-Pd bond forming, and for *e*CMD C-Pd bond forming is more advanced than C-H bond breaking (**Scheme 1.7**)[47,48] While classical CMD often favors more acidic sites that are more sterically accessible,[46] *e*CMD catalysts preferentially activate a substrate's π-basic sites, and can enable functionalization at more sterically hindered C-H bonds.[49] The location of a CMD process on this continuum is characteristic of the transition metal complex itself, and it is not reflective of the substrate's identity, allowing for catalyst-controlled regioselectivity.[47] Thus, by changing the catalyst from an electron-rich organometallic species to a more electron-poor inorganic metal complex, an *e*CMD mechanism is favored over standard CMD and regioselectivity can be switched from the

more acidic to the more basic C-H bond. *e*CMD can be a useful concept to describe unexpected regioselectivity outcomes in direct arylation reactions that otherwise indicate a CMD mechanism over S_EAr.

Scheme 1.7 Stepwise-concerted continuum for C-H arylation

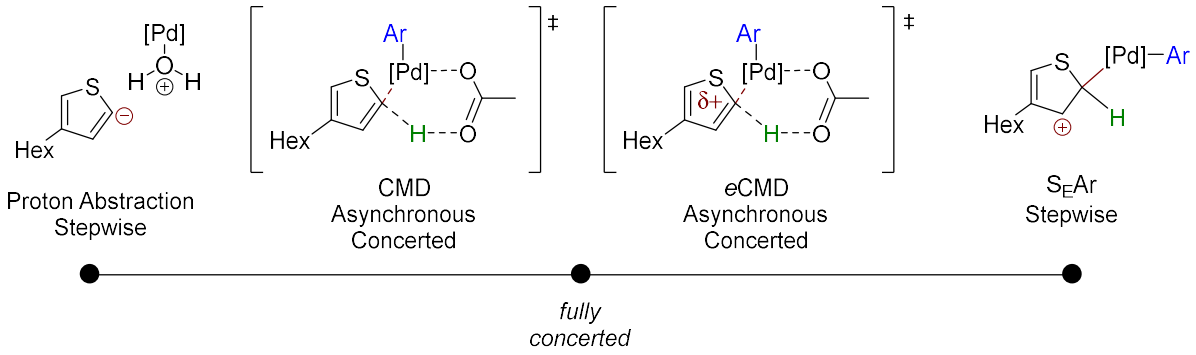

A growing number of reports evidencing Heck-type arylation are present in the literature.[43–45,50] Heck-type direct arylation is similar to the common Heck olefination reaction which features oxidative addition, alkene insertion, *syn*-β-hydride elimination, and catalyst regeneration.[51] In the classical Heck olefination reaction, bond rotation is a key step to afford the proper geometry for *syn*-β-hydride elimination, which is required for the reaction to proceed. Unlike in alkene cross-coupling, the arene substrates in direct arylation are cyclic making bond rotation impossible. Thus, there is no *syn*-hydride for elimination. This has been investigated computationally, and *anti*-β-hydride elimination or a base-assisted E2 elimination could occur to allow a Heck-type carbopalladation mechanism.[45] Thus, Heck-type direct arylation may occur via oxidative addition, carbopalladation, β-hydride elimination, and catalyst regeneration (**Scheme 1.8**). Heck-type arylation has been shown to be in competition with a CMD process, which can be tuned by catalyst design.[45] Since Heck-type arylation can demonstrate different

regioselectivity outcomes than a CMD process,[30,45] understanding the mechanism governing desired reactivity is important for optimizing catalyst selection.

Scheme 1.8 Heck-type direct arylation

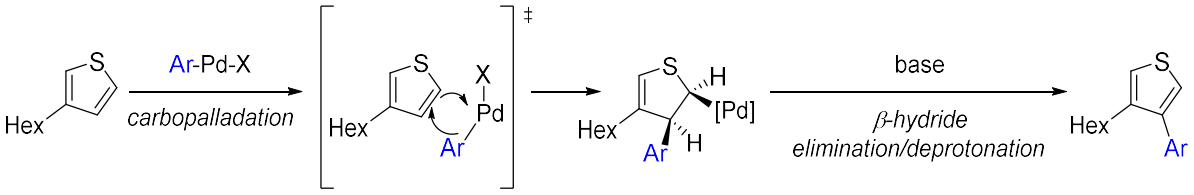

1.6 DArP Conditions and Regioselectivity Outcomes

Many different conditions have been successfully investigated for DArP; they can be organized into two main classes of conditions.[39] The first breakthrough in utilizing C-H activation for polymer synthesis came from Lemaire and co-workers, synthesizing poly(3-alkylthiophene)s from 2-iodo-3-alkylthiophenes.[52] However, the oligomers produced had low molecular weights of ~3 kg/mol, limiting broader interest in this strategy in the following years.[53,54] Small molecule methodology from Fagnou et al. introduced adding a carboxylate,[55] leading to the advent of currently utilized DArP conditions. These Fagnou-derived conditions feature $Pd(OAc)_2$, polar coordinating solvents (e.g. DMAc, DMF), a base (e.g. K_2CO_3, KOPiv, NaOAc), and a carboxylic acid.[55] A phosphine ligand may or may not be present under Fagnou-derived conditions. Secondly, Ozawa-derived conditions feature a palladium catalyst (e.g. Herrmann-Beller, Pd_2dba_3), a nonpolar solvent (e.g. THF, PhMe), a base (Cs_2CO_3), and a phosphine ligand.[56] A carboxylic acid may or may not be added to the reaction. The discovery of these conditions has been essential for accessing regioregular, high molecular weight polymers.

Achieving regioregular materials via DArP has been an active area of research, leading to improved fundamental understanding of the principles guiding regioselectivity and conditions

that reliably produce regioregular polymers.[57–59] One such area of focus has been on the carboxylic acid's identity. As a ligand and proton shuttle, the carboxylic acid lowers the CMD TS's energy requirements. By choosing judiciously, the identity of the carboxylic acid can have a significant influence on molecular weight and polymer yield. While it would seem reasonable for the carboxylic acid's pK_a to influence the rate of the CMD deprotonation, pK_a is not a useful guide. Rather, the size of the acid is the most important variable to consider when screening acids.[60] For example, larger groups including neodecanoic acid (NDA) are often found to be superior to smaller acids like pivalic acid (PivOH) and acetic acid.[61] A separate area of focus has been on understanding the regioselectivity outcomes based on a given monomers' substituents, especially which monomer is halogenated.[58] Here, halogenation is known to have a significant activating effect leading to loss of regioselectivity. Thus, the halogenated coupling partner should be chosen carefully.

While significant progress has been made in using conditions to improve the breadth and quality of DArP-prepared polymers, there are still challenges the method faces. As the field grows, new monomers are desired that offer improved performance for varied applications, are more affordable, and/or are more sustainable. At the same time, improved conditions are needed that use earth-abundant metals, reduce catalyst loading, use green solvents, and feature both mild reagents and low reaction temperatures. Generally speaking, the incorporation of new monomers and conditions will continue to present similar challenges to all DArP conditions: good regio- and chemoselectivity, yield, and molecular weight. These challenges present opposing needs often encountered in DArP syntheses: the need for a fast enough reaction to access high molecular weights on a reasonable timespan and the need for high selectivity. Oftentimes, by increasing the speed of the reaction, selectivity is compromised. Thus, new DArP conditions

developed must be able to increase reactivity at the desired C-H arylation site while simultaneously minimizing reactivity at undesired sites. In the current literature, the primary conditions-based variables used to address these challenges are the catalyst (loading, ligands), the bulkiness of an additive, which coupling partner is halogenated, reaction time, and reaction temperature.[59] Finding conditions that encourage or suppress different mechanisms for direct arylation is another strategy that may improve reaction outcomes.

1.7 Room Temperature Methods

Reaction temperature has a significant impact on a polymerizations' yield and molecular weight. Oftentimes, due to the very high reactivity needed for high molecular weight materials prepared using polycondensation techniques, DArP reactions are run at reflux. For Ozawa-derived conditions, superheated THF is a common feature.[56] These high temperatures help achieve materials with suitably high molecular weights and yields by increasing the rate of the reaction. Increasing the reaction temperature can have a deleterious effect on regioregularity, providing enough thermal energy to make the undesired reaction sites more accessible to CMD-mediated arylation. This creates a scenario where high reactivity (observed through molecular weight and yield) has to be balanced with suitably high selectivity.

Many DArP conditions optimization screenings investigate some temperature variations, although typically near the boiling point of the solvent. For solvents frequently utilized, this means temperatures in excess of 100 °C (e.g., DMF at 153 °C, DMAc at 165 °C, PhMe at 110 °C, 1,4-dioxane at 101 °C). Limited low temperature studies have been performed on DArP systems. One such report systematically investigated the effect of temperature between 120 °C and room temperature on DArP-prepared P3HT, reporting on M_n, yield, and regioregularity.[62]

The report shows a clear improvement to regioregularity with decreasing temperature (rr = 89% at 20 °C vs. 82% at 120 °C), albeit a concurrent loss in yield and molecular weight is also observed (**Scheme 1.9**).

Scheme 1.9 Temperature's effects on DArP-prepared P3HT[a]

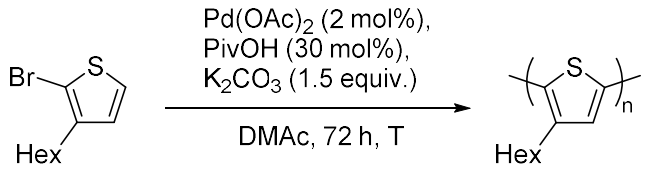

Entry	Temperature (°C)	M_n (kg/mol)	RR (%)	Yield (%)
1	120	39	82.6	13
2	95	22	87.3	39
3	70	21	87.7	44
4	45	24	88.9	39
5	20	14	89.3	9

[a]Adapted from ref. 62.

Room temperature reactions present an interesting approach for improving regioregularity outcomes in polymerizations. In addition to the potential improvement to selectivity, performing reactions at room temperature decreases the cost and energy required to produce a material, particularly at large scales. Notably, room temperature methods can increase functional group tolerance for heat-labile functionalities present on a molecule. In the polymerization literature, other than the P3HT system found in **Scheme 1.9** no other examples of room temperature DArP are known at the time of writing this dissertation. In general, limited room temperature polymerizations are known for conjugated polymers. A room temperature method of Stille polymerization has been reported, where a thioether coupling partner is activated in the place of haloarenes.[63] There have been several early reports of photomediated, room temperature polymerizations of conjugated polymers. These systems are able to achieve oligo- and polymeric

materials at room temperature, using light as an energy source in place of heat. Some of these photomediated systems use Grignards,[64] while others occur without prefunctionalization.[65] That being said, mechanistically, these systems are very different than C-H arylation via catalytic transition metal activation.

Despite the limited studies presented in the polymerization literature, the small molecule direct arylation literature has several high yielding, highly selective examples of direct arylation that occur readily at room temperature.[43,66–69] The small molecule systems present an intriguing collection highly reactive conditions that are able to proceed at room temperature. These room temperature conditions provide a good starting point for developing methods of room temperature DArP, which could improve regioregularity with a lower cost and more facile method. In addition, studying room temperature methods presents an opportunity to foster greater understanding of direct arylation reactivity. As most direct arylation transformations require elevated temperature to proceed within a practical timespan, the mechanistic features enabling specific transformations to proceed at ambient temperature can inform greater fundamental insight into direct arylation systems. Understanding reactivity trends can allow for developing the next generation of DArP conditions that proceed readily under facile conditions.

Chapter 2. Room temperature Pd/Ag direct arylation enabled by a radical pathway

*The work in Chapter 2 is adapted from a previously published article: *Beilstein J. Org. Chem.* **2020,** *16,* 384–390; DOI: 10.3762/bjoc.16.36

2.1 Introduction

While significant progress has been made in DArP, C-H bonds are more challenging to functionalize than their C-M counterparts used in conventional cross-coupling polymerizations. Known DArP conditions have limited monomers that can produce polymers with both high molecular weight and regioregularity, and elevated reaction temperatures are typically required.[70] Mild conditions for C-H functionalization is of growing interest within the broader synthetic community as an opportunity to improve functional group tolerance, and environmental impact.[71,72] While many direct arylation systems occur under neutral conditions and without the need for strong oxidants or reductants, few proceed at ambient temperatures.[39,70] To our knowledge, only one example of room temperature DArP exists, polymerizing P3HT to an acceptably high number average molecular weight of 14 kg/mol, although in 9% yield.[59] Room temperature DArP would improve the simplicity of conjugated polymer synthesis, and reduce the energy requirements.

Small molecule reactions can help predict a method's utility in polymerizations, as DArP proceeds through a polycondensation process. Generically, a small molecule reaction is a candidate for adaptation to a polymerization when it is highly regioselective, and high yielding. Under polycondensation conditions a high yielding reaction is essential for producing a high

molecular weight material,[23] which directly influences the quality and electronic performance of the material.[59,73] More specific to this work, the direct arylation method should be catalytic, directing-group free and at room temperature; a handful of such methods have been reported.[43,66–69] One such method, an indole/iodoarene direct arylation method reported by Larrosa is notable: proceeding in high yields, at room temperature, and with no reported regioselectivity issues (**Scheme 2.1**).[66] This system is hypothesized to proceed under mild conditions due to a highly electrophilic Pd catalyst generated in situ by dissociation of the carboxylate ligand. In this chapter, the mechanism of room temperature direct arylation and DArP is investigated by using the method reported by Larrosa to synthesize a conjugated polymer, polyindole (PIn). Small molecule mechanistic studies were undertaken that will help future development of mild, efficient DArP conditions.

Scheme 2.1 Indole and iodobenzene direct arylation[a]

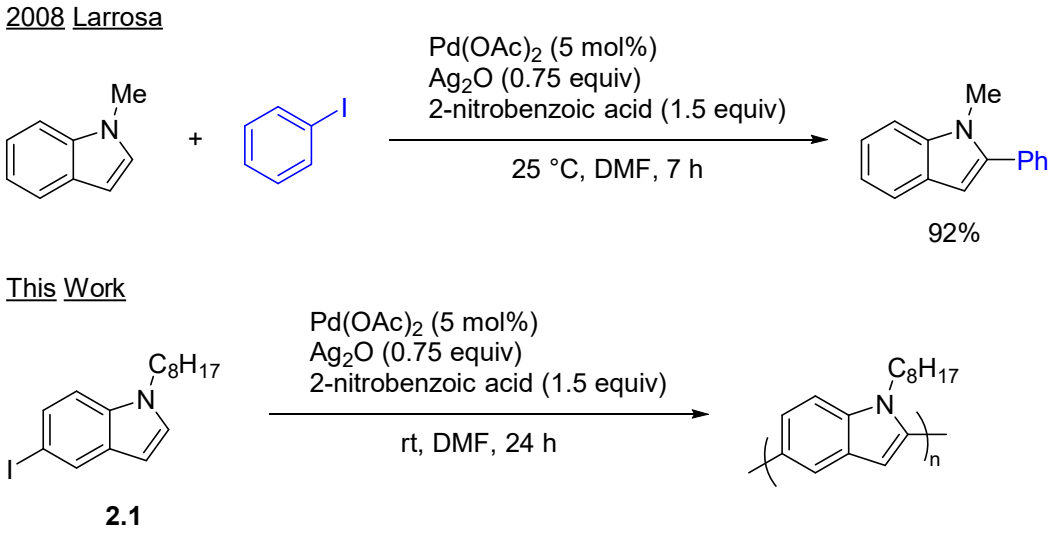

[a]top: adapted from ref. 66.

2.2 Results and Discussion

Initial attempts to polymerize iodoindole monomer **2.1** using the reported conditions (**Scheme 2.1**) produced oligomers with an unanticipated coupling pattern in good yield (87%) (**Figure 2.1**, **Figure 2.5**). The ^{1}H NMR signals from the C2-*H*, C3-*H* on the pyrrole ring and the N-C*H*$_2$-R on the alkyl chain indicate the product is highly branched.[74] Comparing the monomer's spectrum to the polymer's shows large peaks from unfunctionalized pyrrole rings at the chain ends with a ratio of interior to end groups of 1:0.57. While low molecular weight also contributes to the large signals from the chain ends, there are a few factors that indicate branching is occurring: firstly, the large variety in C3-H signals; secondly, the relative integration of the C2-H/C3-H signals to the N-CH$_2$-R signals show that for every indole unit, there is less than one H on the pyrrole ring (**Scheme 2.9**). Finally, branching is evidenced by the discrepancy in molecular weight as calculated for a linear polymer by ^{1}H NMR compared with that indicated by MALDI-TOF MS (**Figure 2.2**). Due to the high regioselectivity in small molecule couplings, defects to this extent were unexpected.

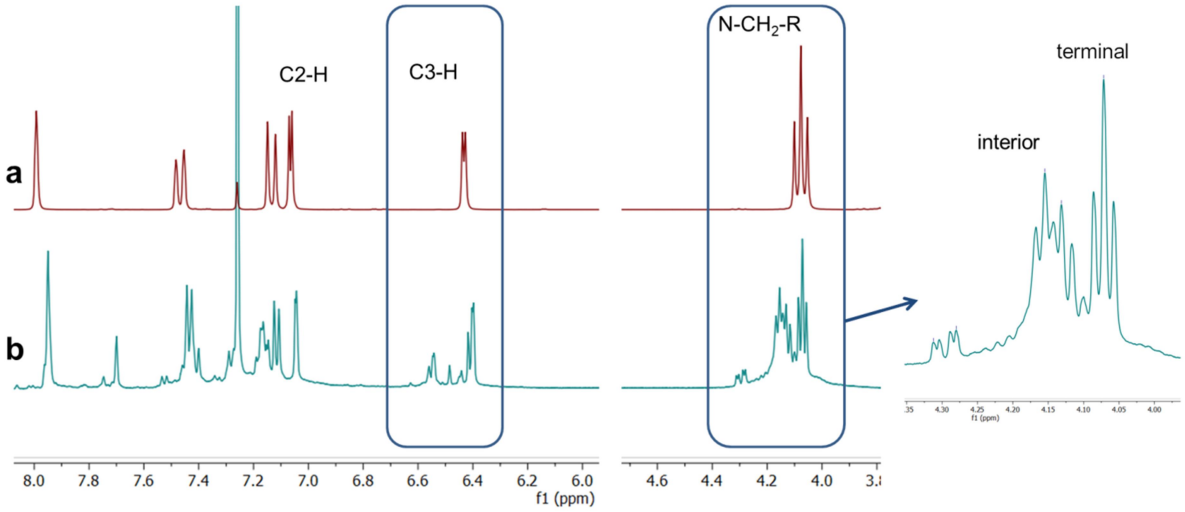

Figure 2.1. ^{1}H NMR (500 MHz, $CDCl_3$) of (a) monomer **2.1** (b) PIn.

MALDI-TOF MS was collected for PIn to further clarify the nature of the coupling pattern (**Figure 2.2**, **Figure 2.4**). The repeat unit corresponds to C/H-C/I coupling (m/z = 227) as expected for direct arylation. In contrast to the expected I/H end groups, the mass spectrum indicates various incorporations of nitrobenzene into the polymer chains. The 2-nitrobenzoic acid used to form a silver carboxylate in the reaction system is the origin of the nitrophenyl group. Three different types of chains are represented, corresponding to incorporation of I/nitrophenyl, H/nitrophenyl, and two nitrophenyl end groups.

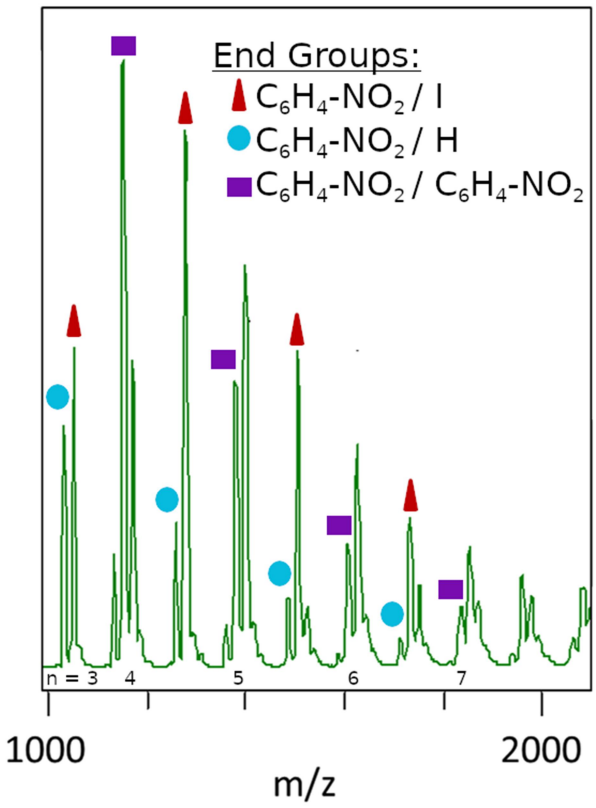

Figure 2.2. MALDI-TOF MS of PIn, indicating octylindole repeat units with three different types of end groups. These include 2-nitrophenyl, iodine, and hydrogen.

2-Substituted benzoic acids in general, and 2-nitrobenzoic acid in particular, are reactive substrates in decarboxylative couplings reactions.[75,76] However, more forceful conditions are typically required than used in the room temperature system. Indeed, a very similar Pd/Ag system has been reported for decarboxylative coupling between indole and 2-nitrobenzoic acids at 110 °C.[77] Under such conditions, silver carboxylates decompose to produce carbonyl and phenyl radicals, which could explain the origin of nitrobenzene incorporation.[78,79] When radical trapping agent (2,6-di-tert-butyl-4-methylphenol) (BHT) was added to the polymerization conditions, no polymerization occurred (**Scheme 2.2**). Additionally, the reaction was completely inhibited when

run in the dark. These results indicate that visible light may be responsible for radical generation in the polymerization.

Scheme 2.2. Polymerization control experiments[a]

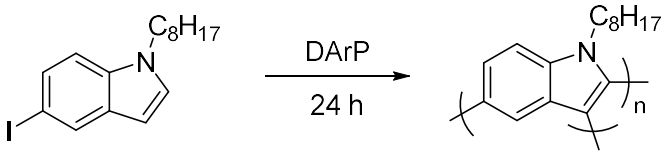

2.1

Entry	Variation	Yield (%)
(1)	BHT (1 equiv.)	0
(2)	Dark	0
(3)	No $Pd(OAc)_2$	0

[a]Conditions: $Pd(OAc)_2$ (5 mol%), Ag_2O (0.75 equiv.), 2-nitrobenzoic acid (1.5 equiv.), DMF, rt.

To further investigate the possibility of a radical-mediated reaction, additional radical capture experiments were performed for the small molecule reaction using 1-methylindole and iodobenzene (**Scheme 2.3**). Similar results were observed for 1-octylindole and iodobenzene (**Scheme 2.8**). In all cases, coupling was completely suppressed by the addition of ((2,2,6,6-tetramethylpiperidin-1-yl)oxyl) (TEMPO) and BHT. Moreover, Ph-BHT was observed by GC-MS when BHT was added. Similar to the polymerization trials, coupling was inhibited when the standard conditions were run in the dark. Both the Ph-BHT adduct and continued poor reactivity in the dark provides growing evidence for a radical mechanism. Moreover, the observed behavior appears to be common between the iodoindole monomer and iodobenzene/indole system, rather than a phenomenon unique to an electron-rich iodoindole.

Scheme 2.3. Small molecule control experiments[a]

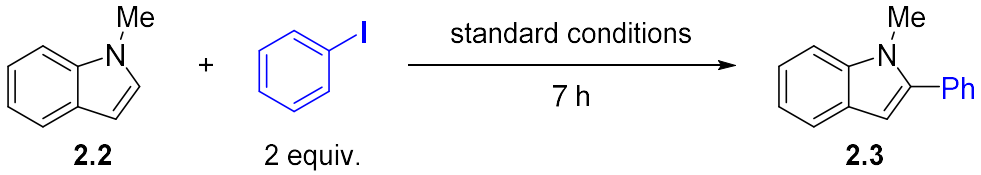

2.2 2 equiv. **2.3**

Entry	Variation	Yield (%)[b]
(1)	None	85[c]
(2)	BHT (2 equiv.)[d]	0
(3)	TEMPO (2 equiv.)	0
(4)	Dark	20

[a]Conditions: $Pd(OAc)_2$ (5 mol%), Ag_2O (0.75 equiv), 2-nitrobenzoic acid (1.5 equiv), DMF, rt. [b]Determined by ^1H NMR using ethylene carbonate as an internal standard. [c]Isolated yield. [d]Ph-BHT adduct observed by GC-MS.

The growing evidence for a phenyl radical in the catalytic cycle is in contrast to the typically proposed mechanisms for direct arylation (**Scheme 2.4**). Amongst these mechanisms, the most widely accepted is the concerted metalation-deprotonation (CMD) pathway.[80] Within the indole direct-arylation literature, however, there remains much discussion of an electrophilic metalation mechanism, with the majority of experimental evidence supporting this pathway.[81–85] In this case, when C2 selectivity is observed it is theoretically from a C3/C2 Pd migration, as S_EAr selectivity favors C3 for indole. A third possible mechanism is a Heck-type carbopalladation. This mechanism has been recently supported by ^{13}C and ^2H KIE experiments for the arylation of benzo[b]thiophene, although with C3 selectivity.[43] In contrast to these pathways, the radical trap and dark experiments reported above indicate a hybrid Pd(I) radical species induced by visible light is involved in the catalytic cycle. This type of mechanism has been previously proposed for aryl and alkene alkylations,[86,87] but not for direct arylation systems.

Scheme 2.4. Commonly proposed direct arylation mechanisms

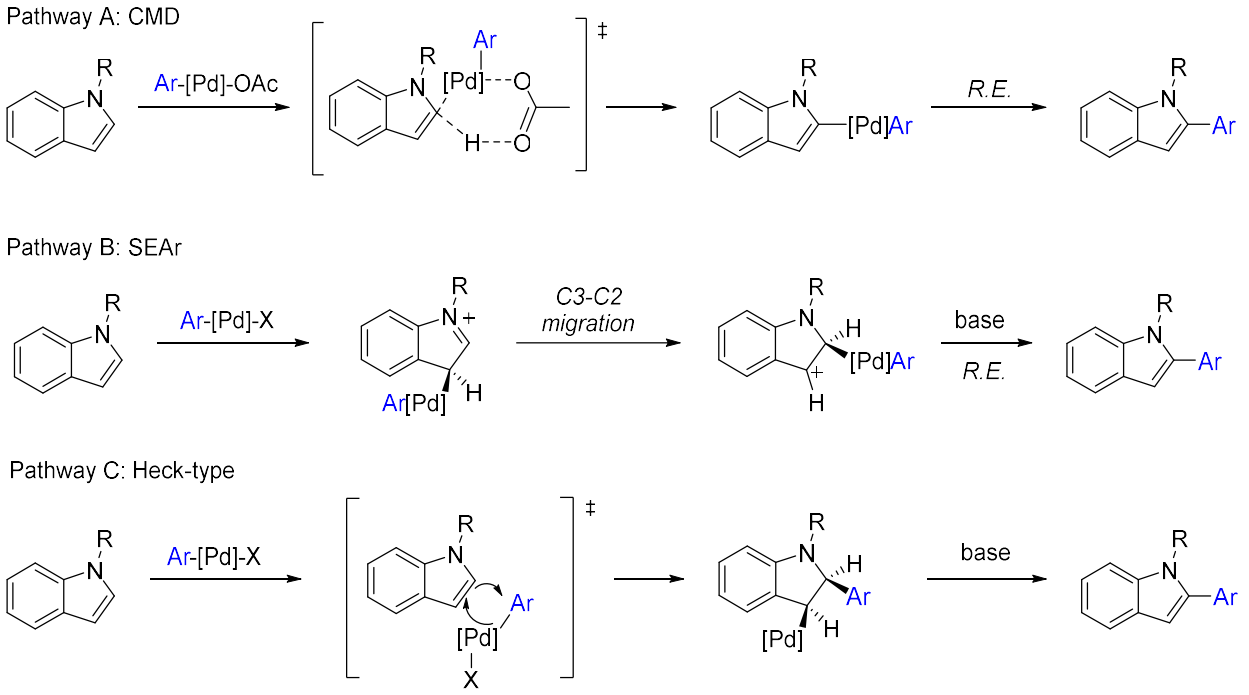

A possible mechanism is outlined in **Scheme 2.5**, informed by the previous reports.[86–89] The aryl iodide **2.4** undergoes SET with an excited palladium(0) species to form hybrid palladium-radical intermediate **2.5**. This carbon-centered radical can then add to the indole. From here, three different pathways to rearomatize **2.7** are possible, eventually affording the arylated product **2.10**. Pd(0) can be regenerated by a base; in this case, the silver carboxylate. This accounts for the formation of a carboxylate radical **2.11**, explaining the presence of 2-nitrophenyl incorporation into the polymer chain. Additionally, this explains the formation of a phenyl radical at room temperature, and the poor control in which the nitrophenyl groups are incorporated into the chain.

There are limited examples across the aryl C-H functionalization literature indicating a transition-metal catalyzed radical process, limited largely to cobalt catalysis.[90,91] While there are several reports of palladium-catalyzed systems for room temperature direct arylation (i.e. no

directing group, transition-metal catalyzed), a radical mechanism has not been previously discussed. Some of these reports indicate a marked difference in selectivity between elevated and ambient temperatures, which we found may be due to a change in mechanism (**Scheme 2.7, Figure 2.3**).[68]

Scheme 2.5. Proposed mechanism for palladium radical involved reaction.

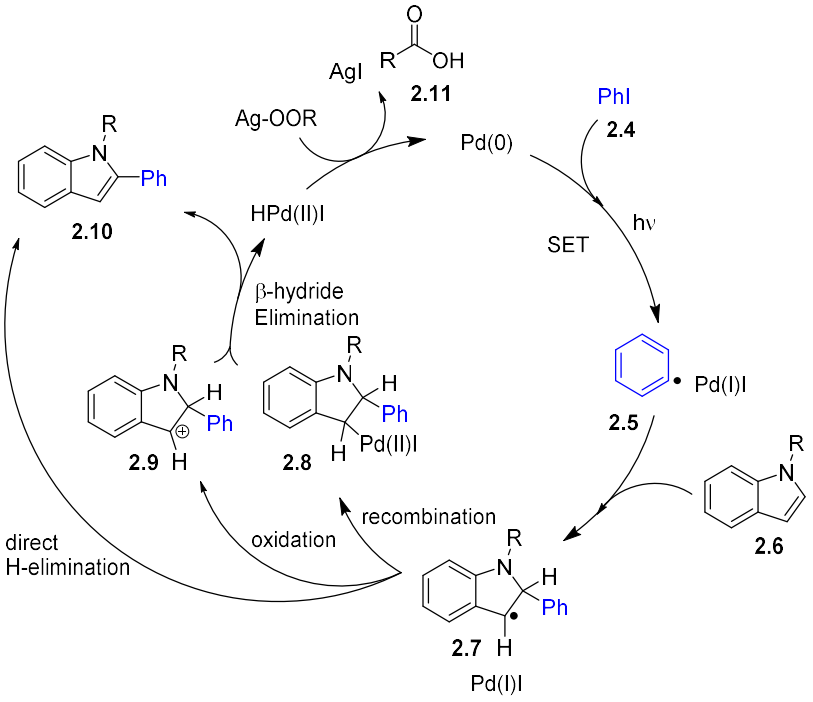

We hypothesized that other known palladium-catalyzed room temperature direct arylation methods could also proceed by a single electron process. Two such Pd/Ag methods were investigated: a method for benzothiophene arylation,[68] and a method for fluoroarene coupling (**Scheme 2.6**).[69] First the published results were replicated, then radical traps were introduced. In these cases, BHT completely eliminated the formation of product **2.12** and partially inhibited the conversion to product **2.13**. In both cases the arene-BHT adduct was observed by GC-MS as shown in the inset of **Scheme 2.6**. Due to the increased inhibition found in **Scheme 2.6A**, light

sensitivity was also probed, where the reaction's yield declined to 16% when run in the dark. While more extensive studies are needed to conclusively indicate a radical mechanism, the trap experiments and room temperature reactivity indicate that a radical-mediated mechanism similar to the indole direct arylation may be governing the observed reactivity. Particularly for the benzothiophene conditions, a similar photosensitivity is observed that indicates an atypical and interesting process may be proceeding.

Scheme 2.6. Radical trap effects on room temperature direct arylation literature methods[a]

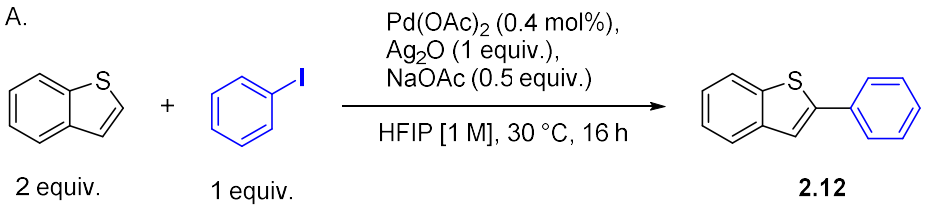

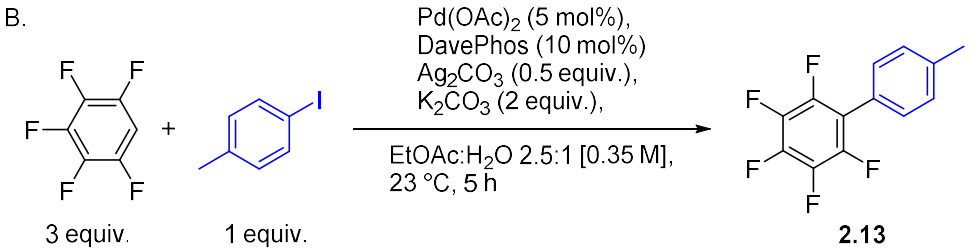

Observed by GC-MS

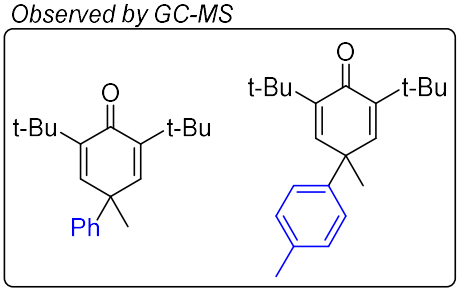

Variation	2.12 Yield (%)[b]	2.13 Yield (%)[b]
None	79[c]	52
BHT (1.1 equiv.)	0	30
Dark	16	ND

[a]Scheme A: adapted from ref. 68; Scheme B: adapted from ref. 69. [b]Determined by ^{1}H NMR against an internal standard. [c]Isolated yield

2.3 Conclusion

In conclusion, in the midst of investigating room temperature DArP, we have discovered room temperature palladium-catalyzed direct arylation may often be governed by radical processes. Based on the use of radical scavengers and experiments in the dark, it has become evident that a light-mediated SET is likely involved in the reported coupling of indole with iodobenzene. Moreover, other substrates such as benzo[b]thiophene and pentafluorobenzene appear to undergo a radical-mediated Pd/Ag room temperature direct arylation. This is a useful insight for advancing the direct arylation knowledge base, and serves as inspiration for designing new polymerization systems that proceed under mild conditions, improving energy requirements and scalability. Work is ongoing to leverage this insight into new direct arylation methods utilizing palladium involved radicals.

2.4 Supplementary Information

2.4.1 *High Temperature Conditions*

Scheme 2.7. High temperature trials[a]

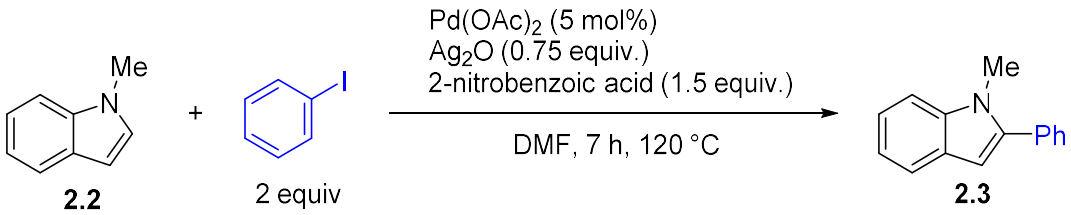

Entry	Variation	Conversion (%)[a]	Yield (%)[a]
(1)	None	99	63
(2)	Dark	99	70
(3)	BHT (1.1 equiv.)	45	25

[a]Determined by [1]H NMR using ethylene carbonate as an internal standard. Other products include 2,3-dipheny-1-methylindole.

Figure 2.3. Silver mirroring is not observed at high temperature.

2.4.2 *Additional Radical Trap Experiments*

Scheme 2.8. 1-octylindole and iodobenzene radical trap experiments

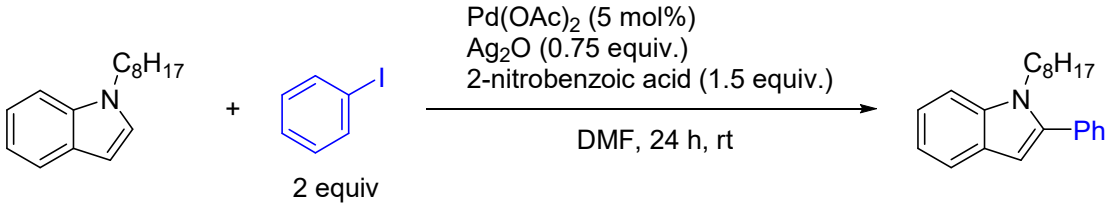

Entry	Variation	Yield (%)[a]
(1)	TEMPO (1.1 equiv)	Trace
(2)	Dark	Trace
(3)	No $Pd(OAc)_2$	0

[a]Determined by GC-MS.

2.4.3 *Branching Models*

In an ideal case, there are only small peaks from the terminal pyrrole ring's contribution. In this work, the ^{1}H NMR for PIn showed integration values for the chain ends and the midchain groups were relatively similar, indicating a similar number of terminal repeat units to interior repeat units.

Scheme 2.9 Models demonstrating branching in PIn

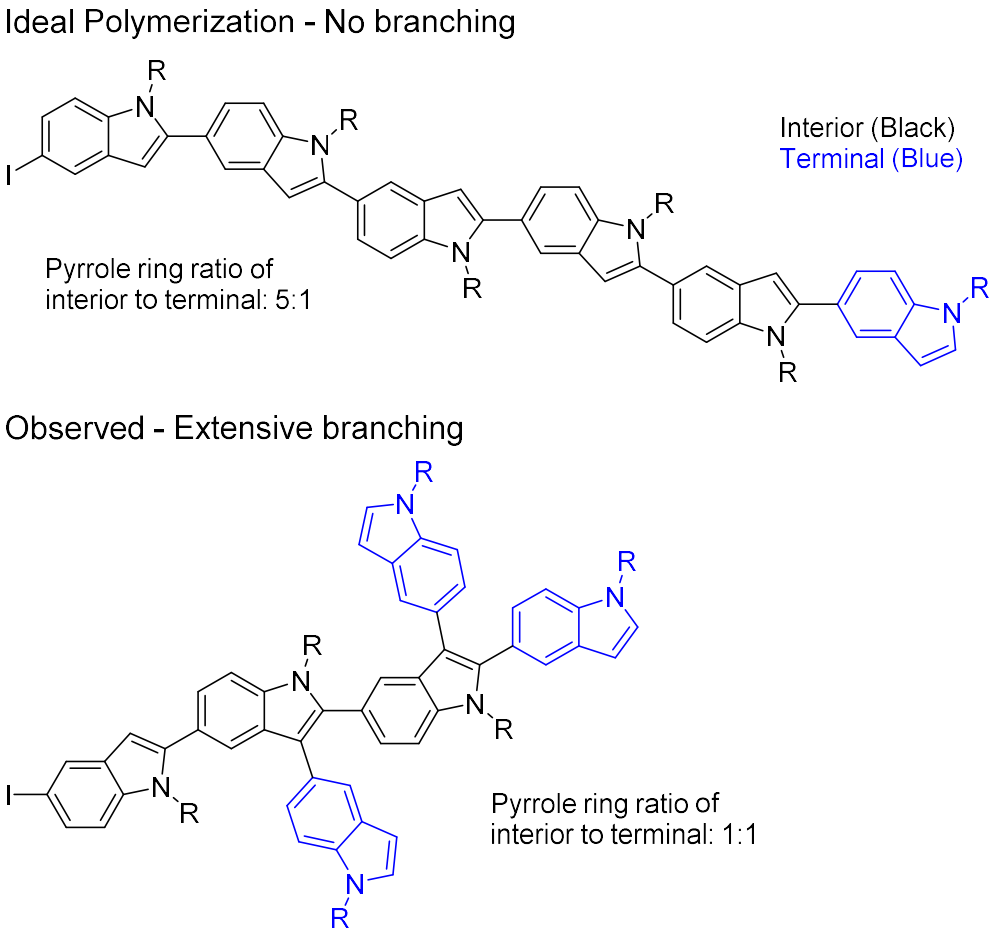

2.4.4 *General Information*

All reactions were carried out under nitrogen atmosphere using standard Schlenk techniques unless otherwise noted. NMR spectra were recorded on Bruker AV-300 and AV-500

spectrometers operating at 300 and 500 MHz, respectively. NMR chemical shifts (δ) are reported in parts per million (ppm) downfield of tetramethylsilane and are referenced relative to the residual solvent signal for ^{1}H NMR ($CDCl_3$ (7.26 ppm)) and ^{13}C NMR ($CDCl_3$ (77.16 ppm). ^{19} F NMR was referenced against hexafluoroisopropanol (-76.4 ppm). When indicated, ethylene carbonate was used as an internal standard for quantitative NMR and stored under nitrogen between uses. An Agilent 5973 Gas Chromatograph - Mass Spectrometer (EI) was used to perform GC-MS analysis. MALDI-TOF MS was collected using a Bruker AutoFlex II instrument with a terthiophene matrix. DMF and THF were dried and degassed on an Inert PureSolv solvent purification system. Deuterated solvents were stored over 4 Å molecular sieves. All other reagents and chemicals were purchased from Sigma-Aldrich or Tokyo Chemical International and used without purification. Column chromatography was performed using VWR Common Silica Gel 60 Ǻ.

2.4.5 *Direct Arylation Procedures*

Polymerizations: To a flame-dried Schlenk tube was added $Pd(OAc)_2$ (5 mol%, 0.025 mmol), Ag_2O (0.75 equiv., 0.15 mmol), and 2-nitrobenzoic acid (1.5 equiv., 0.3 mmol). Radical trapping agents were added at this time (1.1 equiv., 0.22 mmol). The flask was evacuated and backfilled with N_2 three times. DMF was added (0.5 M), followed by iodoindole (1 equiv., 0.2 mmol). The reaction was allowed to stir at room temperature (22 °C). After the required time, the reaction mixture was filtered through silica using CH_2Cl_3 to transfer and concentrated to dryness. The product was purified using Soxhlet extraction under N_2 with MeOH and collected with $CHCl_3$.

General Procedure – Small Molecule: Based on the literature method [66]. To an oven-dried vial was added $Pd(OAc)_2$ (5 mol%, 0.025 mmol), Ag_2O (0.75 equiv., 0.15 mmol), 2-nitrobenzoic acid

(1.5 equiv., 0.3 mmol), and BHT if used (1.1 equiv., 0.22 mmol). The flask was evacuated and backfilled with N_2 three times. DMF was added (0.5 M), followed by indole (1 equiv., 0.2 mmol) and the iodoarene (2 equiv., 0.4 mmol). The reaction was allowed to stir at room temperature (22 °C). After the required time, the reaction mixture was filtered through silica using CH_2Cl_2 to transfer and concentrated. Purification was performed using column chromatography (hexanes/EtOAc).

Dark Trials: The general procedures are followed with the following changes: before adding reagents, the flask is wrapped in aluminum foil. After the allotted time, while still wrapped in foil the reaction mixture is quenched with 2 mL saturated EDTA solution, extracted with 5 mL CH_2Cl_2 three times, dried over $MgSO_4$, filtered, and concentrated.

2.4.6 *Starting Materials Characterization*

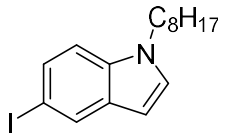

5-iodo-1-octylindole (2.1): To a flame-dried 3-neck round bottom flask was charged 5-iodoindole (1 equiv., 4.1 mmol). THF was added (10 mL). The flask was cooled to -78°C and sodium hydride (60% dispersion in mineral oil, 1.2 equiv., 4.9 mmol) was added against N_2.After stirring for one hour, iodooctane (1.5 equiv., 6.2 mmol) was added and the reaction was allowed to stir overnight at room temperature. The mixture was diluted with H_2O, and extracted 3 times with Et_2O. The combined organic layers were washed with brine, dried over $MgSO_4$, filtered, concentrated, and purified by column chromatography (hexanes with EtOAc gradient) to obtain a yellow oil (58%). R_f = 0.3 (hexanes) **^{1}H NMR** (300 MHz, $CDCl_3$) δ 7.99 (t, *J* = 1.6 Hz, 1H), 7.47 (dd, *J* = 8.7, 1.6 Hz, 1H), 7.13 (d, *J* = 8.6 Hz, 1H), 7.07 (d, *J* = 3.1 Hz, 1H), 6.43 (d, *J* = 3.1

Hz, 1H), 4.08 (t, *J* = 7.1 Hz, 2H), 1.82 (p, *J* = 7.1 Hz, 2H), 1.31 (q, *J* = 4.5, 3.8 Hz, 10H), 0.92 (td, *J* = 6.8, 1.7 Hz, 3H). **^{13}C NMR** (126 MHz, $CDCl_3$) δ 135.13, 131.21, 129.89, 129.69, 129.61, 129.52, 128.64, 111.46, 100.34, 82.74, 46.58, 31.85, 30.26, 29.24, 27.02, 22.71. **GC-MS** (EI) calculated for [M]+ 355.1, found 355.1

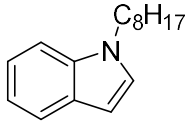

1-octylindole: Prepared according to the literature procedure, and exhibited matching spectral data.[92] A clear oil was obtained in 65% yield. R_f = 0.25 (hexanes) **^{1}H NMR** (500 MHz, $CDCl_3$) δ 7.78 (d, *J* = 7.9 Hz, 1H), 7.46 (d, *J* = 8.2 Hz, 1H), 7.34 (t, *J* = 7.6 Hz, 1H), 7.28 – 7.21 (m, 1H), 7.21 – 7.17 (m, 1H), 6.62 (t, 1H), 4.19 (t, *J* = 7.2 Hz, 1H), 1.97 – 1.91 (m, 2H), 1.45 – 1.38 (m, 11H), 1.03 (t, *J* = 7.0 Hz, 2H). **^{13}C NMR** (126 MHz, $CDCl_3$) δ 135.92, 128.56, 127.67, 121.21, 120.86, 109.31, 100.77, 46.30, 31.75, 30.19, 29.13, 26.96, 22.58, 14.04. **GC-MS** (EI) calculated for [M]+ 229.2, found 229.3

2.4.7 *Products Characterization*

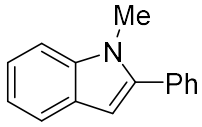

2-phenyl-1-methylindole (2.3): prepared according to the literature procedure and exhibited matching spectral data.[66] White crystals were obtained in 85% yield. R_f = 0.2 (98:2 hexanes:EtOAc) **^{1}H NMR** (300 MHz, $CDCl_3$) δ 7.64 (d, *J* = 7.7 Hz, 1H), 7.58 – 7.32 (m, 6H), 7.15 (t, *J* = 7.4 Hz, 1H), 6.57 (s, 1H), 3.76 (s, 3H). **^{13}C NMR** (126 MHz, $CDCl_3$) δ 141.57, 138.36, 132.87, 129.38, 128.48, 127.97, 127.85, 121.66, 120.47, 119.85, 109.59, 101.66, 31.15. **GC-MS** (EI) calculated for [M]+ 207.1, found 207.1

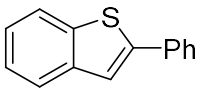

2-phenylbenzothiophene (2.12): Prepared according to the literature procedure and exhibited matching spectral data.[68] The title compound was obtained as a white solid in 79% yield. R_f = 0.4 (hexanes) **^{1}H NMR** (300 MHz, $CDCl_3$) δ 7.84 (d, J = 7.4 Hz, 1H), 7.78 (d, J = 7.0 Hz, 1H), 7.73 (d, J = 7.2 Hz, 2H), 7.55 (s, 1H), 7.44 (t, J = 7.4 Hz, 2H), 7.34 (ddd, J = 8.6, 5.3, 1.7 Hz, 3H). **^{13}C NMR** (126 MHz, $CDCl_3$) δ 140.70, 139.52, 134.31, 128.95, 128.27, 126.51, 124.51, 124.31, 123.56, 122.27, 119.45. **GC-MS** (EI) calculated for [M]+ 210.1, found 210.2

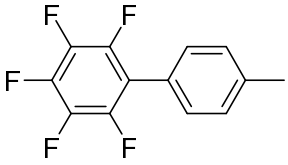

4-Methyl-2,3,4,5,6-pentafluoro-1,1-biphenyl (2.13): Prepared according to the literature procedure, and exhibited matching spectral data.[69,93] The title compound was obtained as a white solid in 52% yield. R_f = 0.45 (hexanes) **^{1}H NMR** (300 MHz, $CDCl_3$) δ 7.31 (s, 4H), 2.43 (s, 3H). **^{13}C NMR** (excluding C_6F_5, 75 MHz, $CDCl_3$) δ 139.58, 130.15, 129.61, 123.57, 21.45. **^{19}F NMR** (470 MHz, $CDCl_3$) δ -144.50 (dd, J = 26.3, 9.4 Hz), -157.25 (t, J = 22.4 Hz), -162.45 -164.41 (m). **GC-MS** (EI) calculated for [M]+ 258.2, found 258.1

Radical Trap Adducts:

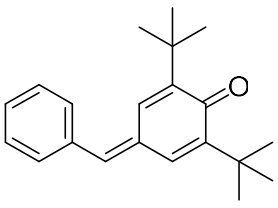

GC-MS (EI) calculated for [M]+ 294.2, found 294.3

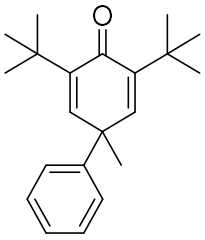

GC-MS (EI) calculated for [M]+ 296.2, found 296.3

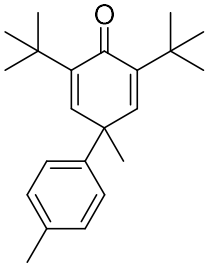

GC-MS (EI) calculated for [M+] 310.2, found 310.2

2.4.8 *Polyindole Characterization*

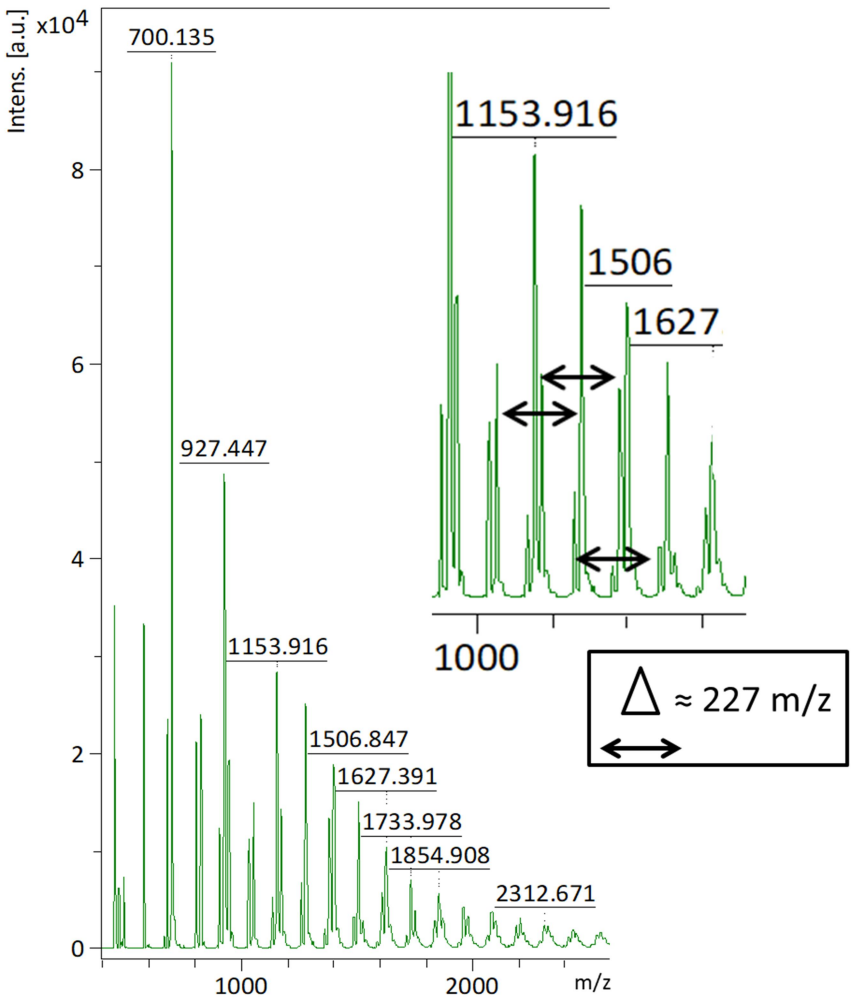

n	2 C_6H_4-NO_2 / I	C_6H_4-NO_2 / H	2 C_6H_4-NO_2
1	-	-	472
2	826	579	700
3	1053	806	927
4	1279	1033	1153
5	1506	1260	1380
6	1733	1487	1608
		1493	

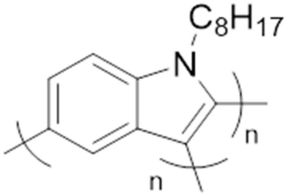

Figure 2.4 MALDI-TOF MS for branched polyindole, with key peaks summarized in the table based on end group identity.

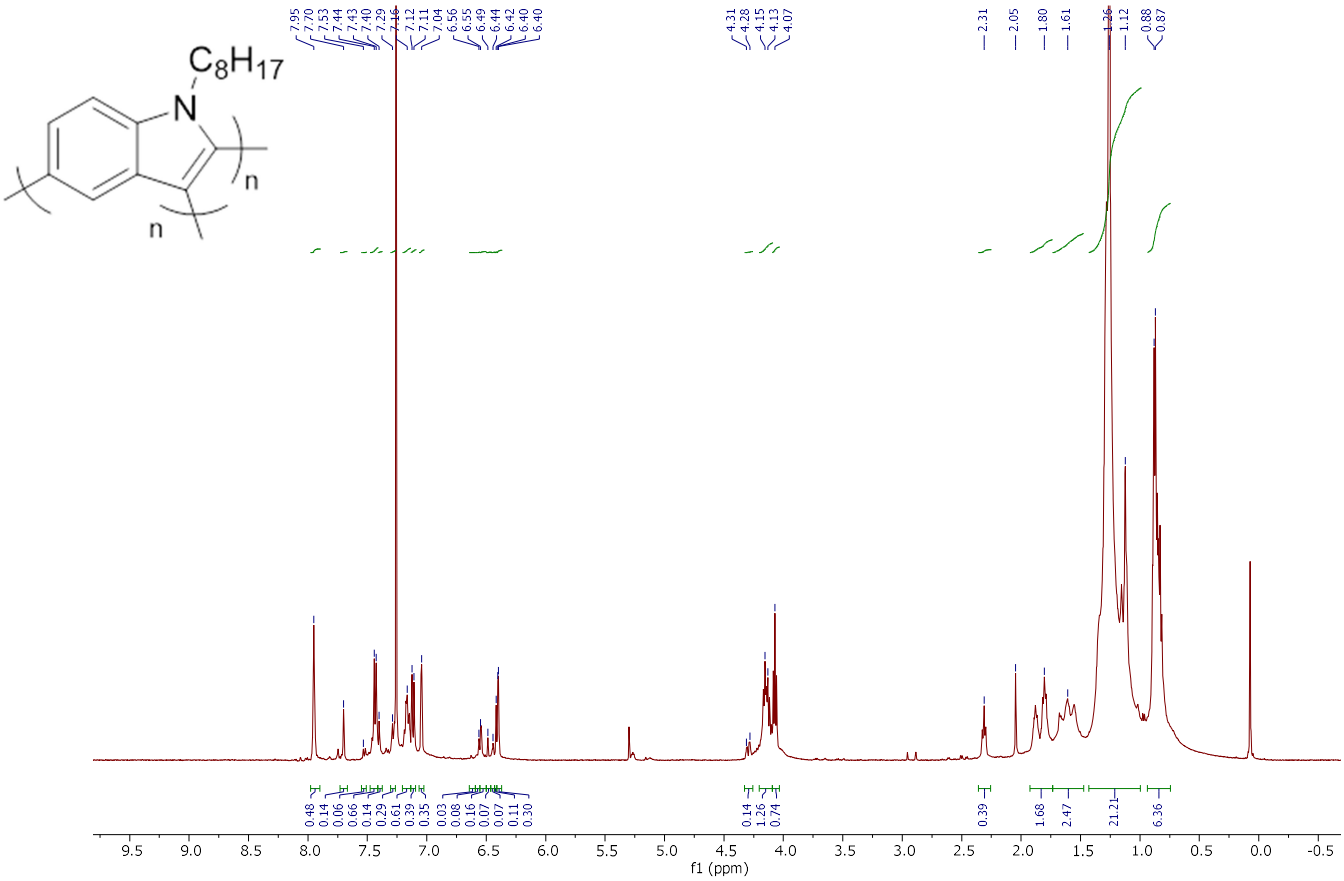

Figure 2.5. ^{1}H NMR of polyindole

2.4.9 *[1]H NMR and [13]C NMR Spectra*

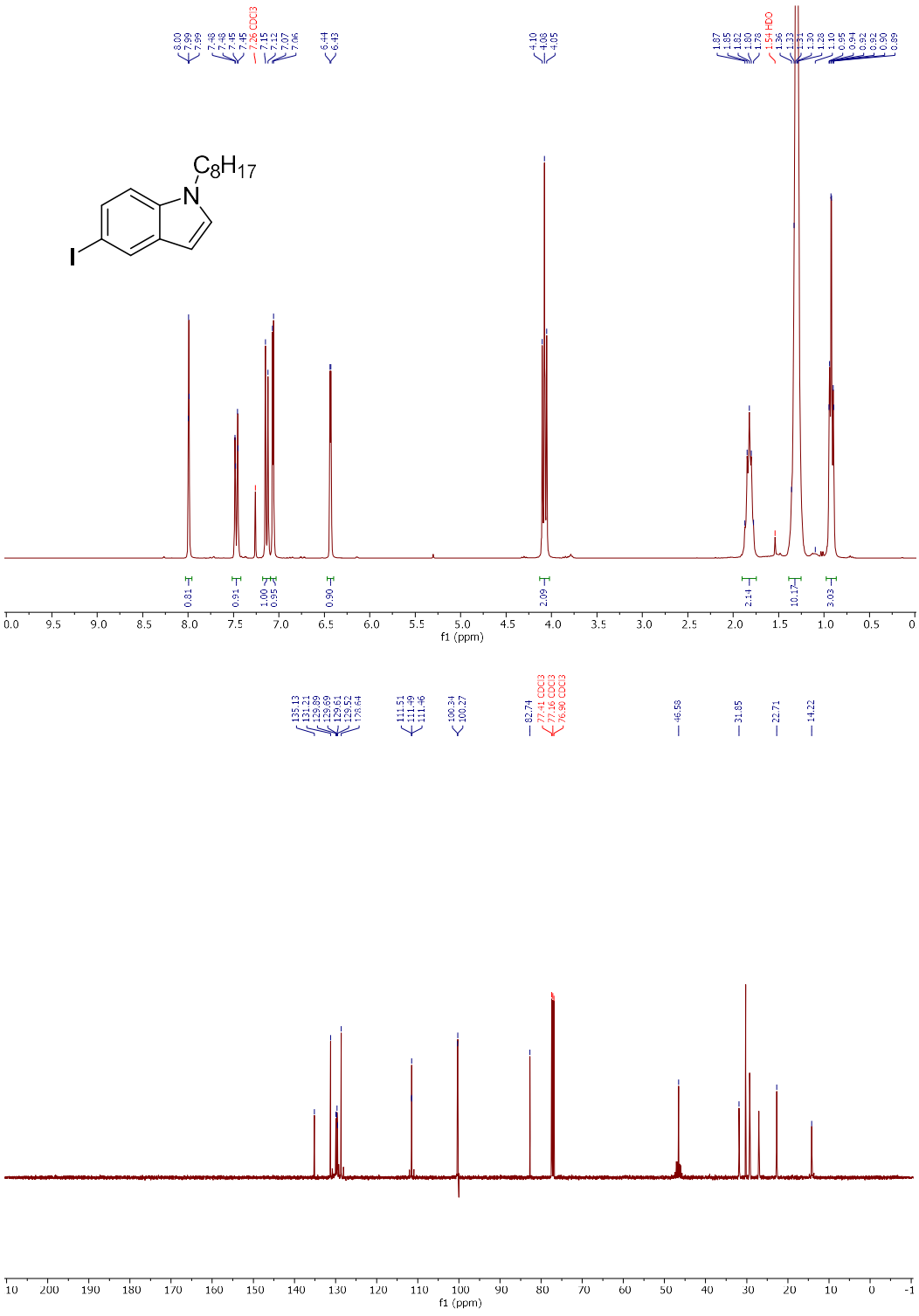

^{1}H NMR (top) and ^{13}C NMR (bottom) of **2.1**.

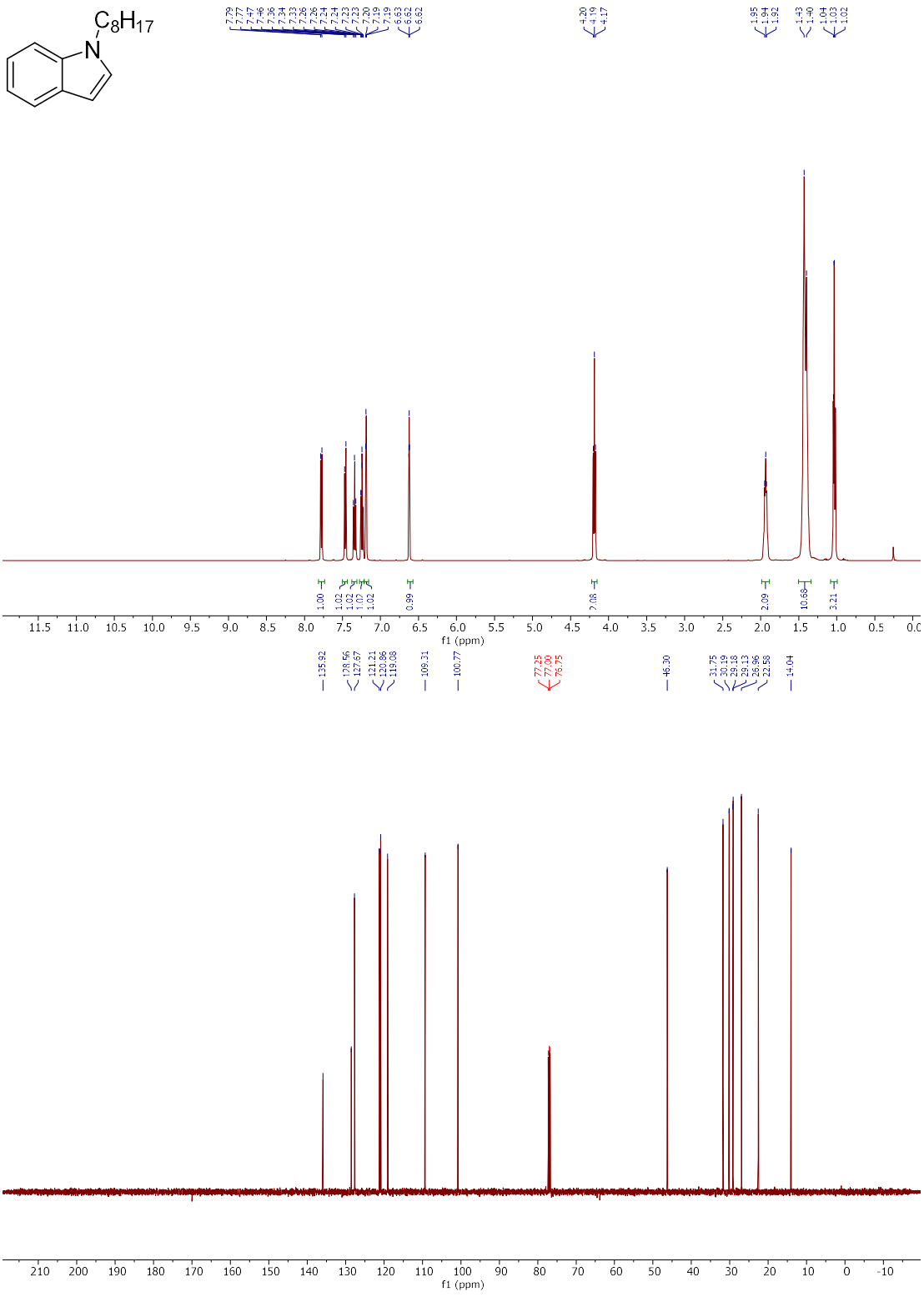

^{1}H NMR (top) and ^{13}C NMR (bottom) of 1-octylindole.

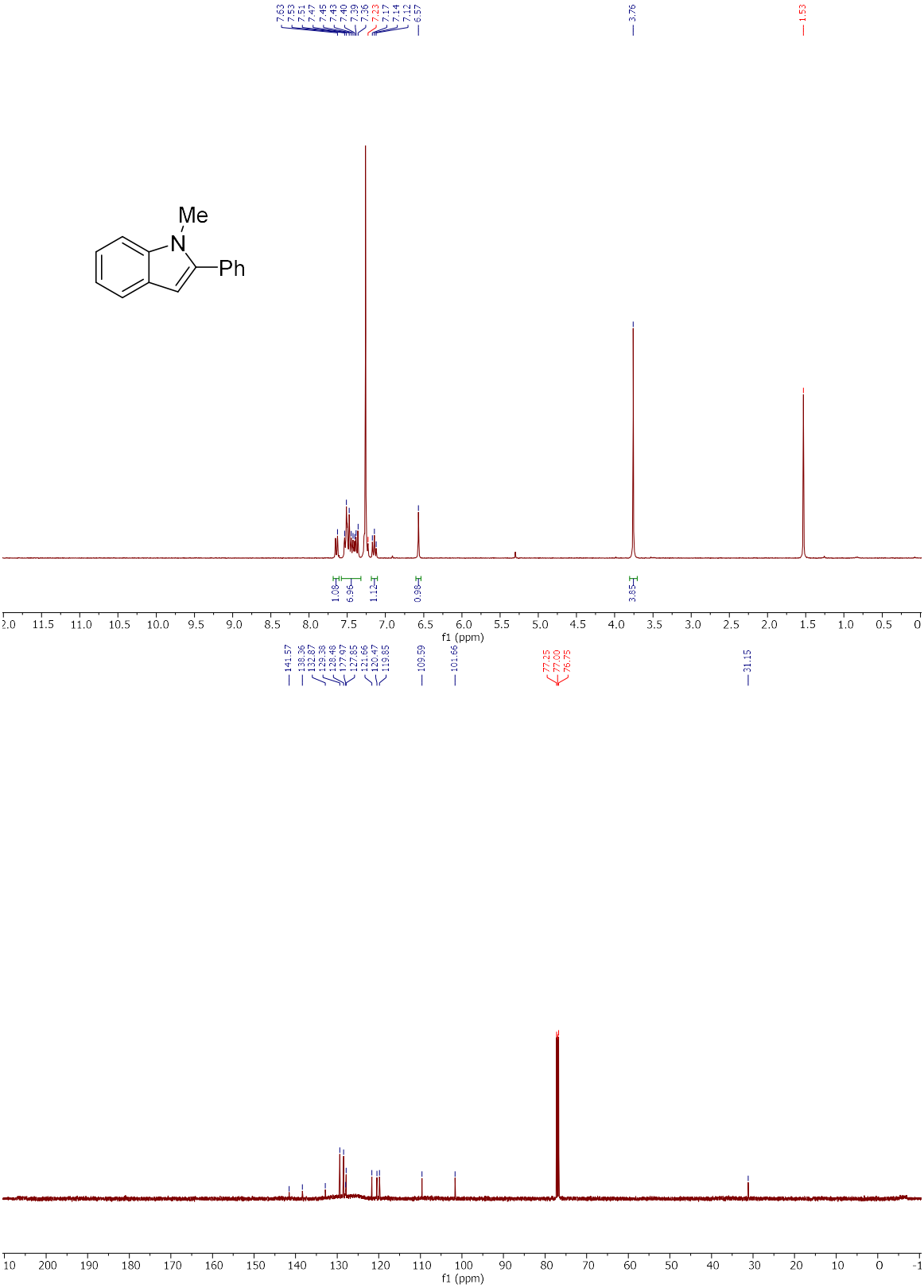

^{1}H NMR (top) and ^{13}C NMR (bottom) of **2.3**.

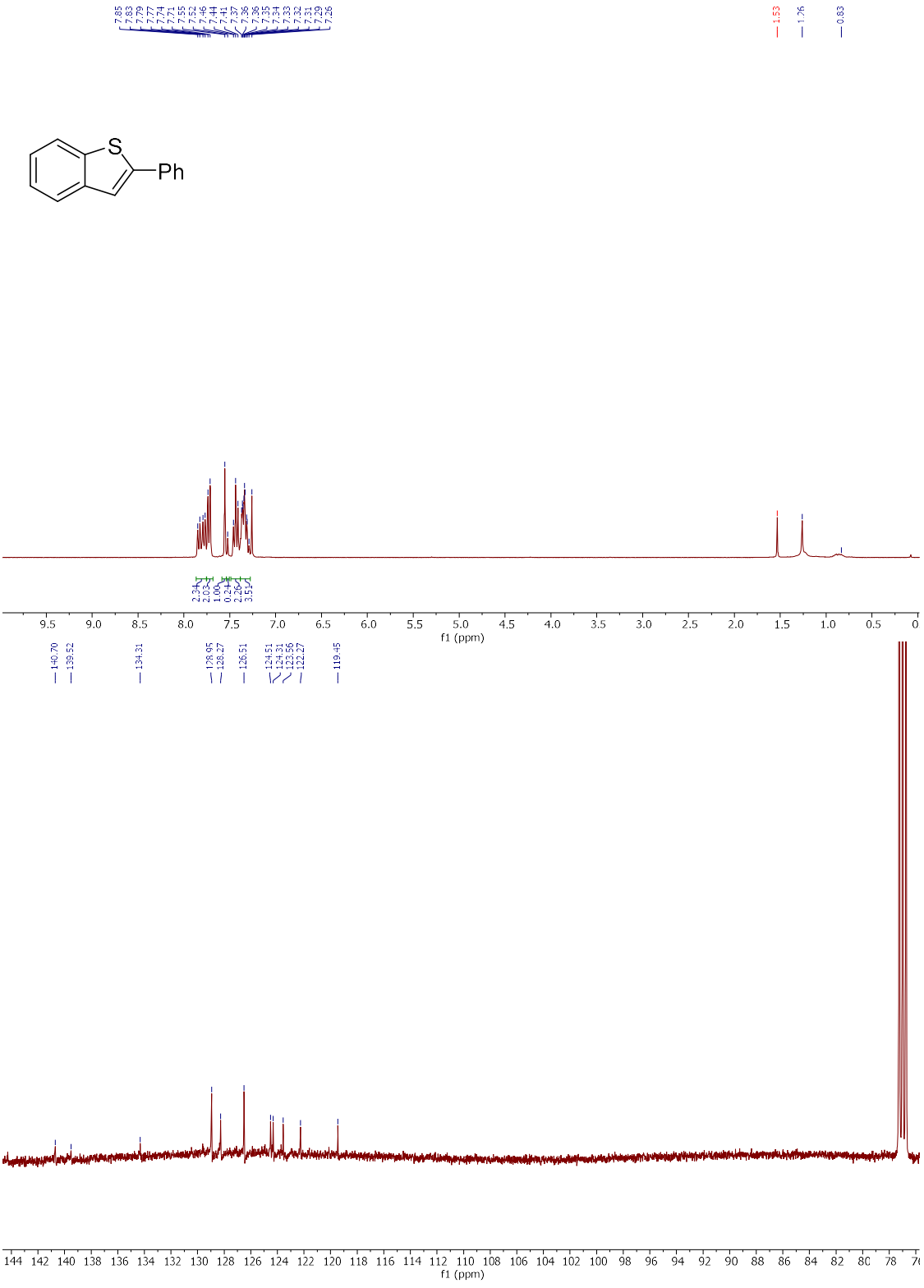

^{1}H NMR (top) and ^{13}C NMR (bottom) of **2.12**.

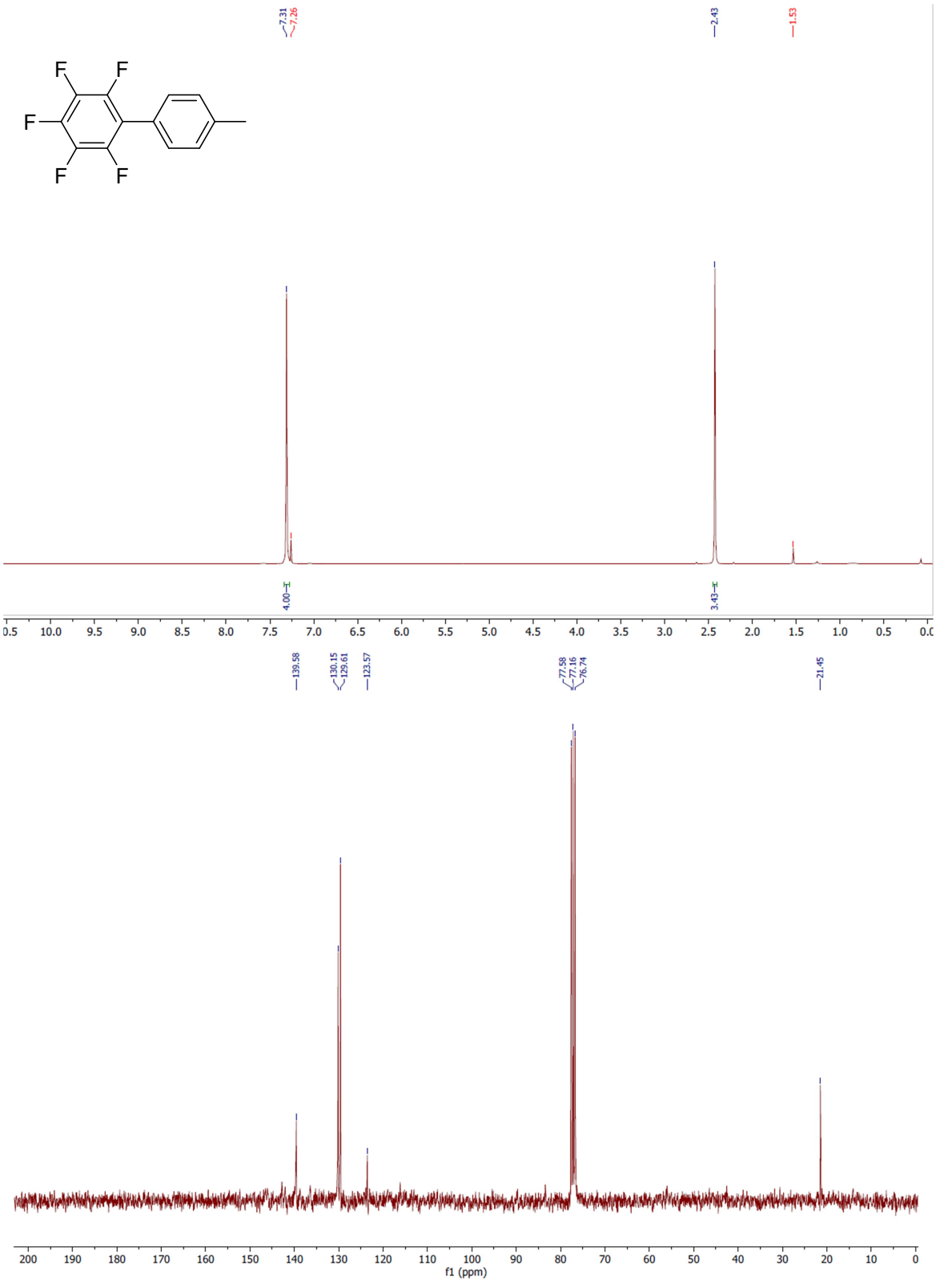

^{1}H NMR (top) and ^{13}C NMR (bottom, excluding C_6F_5) of **2.13**.

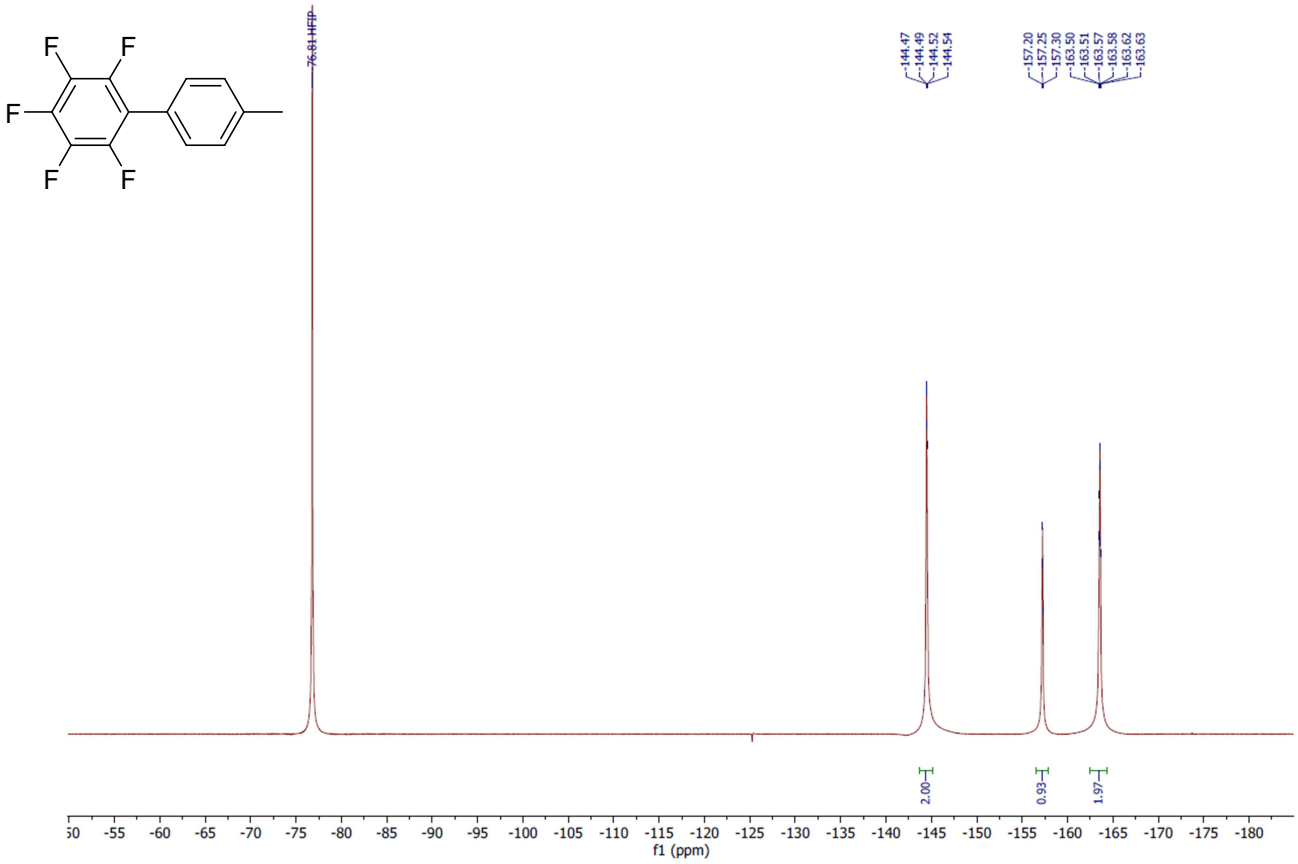

^{19}F NMR of **2.13**.

Chapter 3. Room temperature C-H arylation of benzofurans by aryl iodides

*The work in Chapter 3 is adapted from a previously published article: Reprinted with permission from *Org. Lett.* **2021**, 23, 18, 7079–7082; DOI: 10.1021/acs.orglett.1c02397.

3.1 Introduction

Benzofuran is an interesting pharmaceutical scaffold, with derivatives already utilized in commercial drugs.[94,95] In addition to its pharmaceutical importance, benzofuran derivatives are useful in the materials sector, offering improved electronic properties to the more conventional thiophene-containing polymers.[96,97] In both cases, α-arylation is important to access the desired structures. Although conventional cross-coupling methods are still widely used, there are a growing number of methods for C-H arylation of benzofurans. In spite of the growing methodology, these methods have limited utility because they require elevated temperatures, preventing use on substrates containing heat-sensitive functional groups.[98–103] A small number of mild methods have been reported.[50,104,105] These reports are limited by small substrate scopes, sluggish kinetics under room temperature conditions, and use aryl diazonium salts which have limited commercial availability and can decompose violently.[106]

While the heterobiaryl arylation literature contains methods for robust room temperature C-H arylation of indole,[66] and benzothiophene,[43,68] improvements are still warranted for room temperature arylation of benzofuran. Previous work reported in Chapter 2 hypothesizes a photomediated process enables room temperature arylation of indole (**Scheme 2.5**), and that a

similar process may be influencing a room temperature α-arylation of benzothiophene (**Scheme 2.6**). A report of β-arylation of benzothiophene at room temperature indicates the transformation is governed by a Heck-type process.[43] Looking only at transition metal-catalyzed, room temperature C-H arylation of benzofuran reactions, limited methods exist and amongst those only a preliminary mechanistic work is reported. One such example reports room temperature arylation of benzofuran by aryl diazonium salts, hypothesizing on the basis of DFT studies and in situ NMR experiments the transformation is governed by a Heck-type mechanism.[50] Another room temperature method did not investigate the reaction's mechanism.[105]

With the goal of developing room temperature methods for DArP that can provide target materials with improved selectivity and energy efficiency, the poor regioselectivity outcomes from preparing PIn in Chapter 2 demand further study. In light of the interesting photosensitivity discovered in the PIn study, and to elucidate trends that may exist which enable room temperature reactivity across a broader range of heteroarenes, benzofuran arylation is a worthwhile substrate to investigate. Studies into this heterobiaryl can complement the observed photosensitivity present in indole and benzothiophene in Chapter 2. While substantial work has been done for benzothiophene and indole arylation, limited room temperature methods exist for benzofuran arylation. Thus, optimizing reaction conditions for benzofuran arylation and elucidating the mechanism could indicate if the photosensitivity observed in PIn synthesis is a generalizable process. If not, different mechanisms, such as Heck-type, may provide a more regioselective outcome better suited for polymerization.

3.2 Results and Discussion

We set out to develop a robust method of direct arylation for benzofuran using commercially available aryl iodides. Our preliminary investigations were informed by our previous work on room temperature direct arylation of indole,[107] alongside reports of room temperature conditions for indole and benzothiophene arylation.[43,66,68] The previously known indole conditions did not afford any of the desired product **3.**3a (**Scheme 3.1**, entry 1). Similarly, when the reported benzothiophene room temperature arylation conditions were tried, a small amount of **3.3a** was produced (**Scheme 3.1**, entry 2). Increasing the Pd catalyst led to a modest 16% yield (**Scheme 3.1**, entry 3). Continued trials in hexafluoro-2-propanol (HFIP), regarded as a powerful solvent in C-H functionalization transformations,[108] afforded **3.3a** in high yield and provided our optimized method (**Scheme 3.1**, entry 5).

Scheme 3.1. Reaction conditions optimization

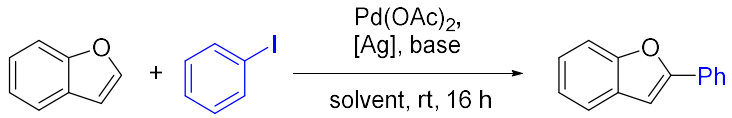

3.1a (1 equiv) **3.2a** (2 equiv) **3.3a**

Entry	Pd (mol %)	Ag (equiv.)	Additive (1.5 equiv.)	Solvent	Yield (%)[a]
(1)	5	Ag_2O (0.75)	2-nitrobenzoic acid	DMF	0
(2)[b]	0.4	Ag_2O (1)	NaOAc	HFIP	5
(3)	2.5	Ag_2O (0.75)	NaOAc	HFIP	16
(4)	0.4	Ag_2O (0.75)	2-nitrobenzoic acid	HFIP	72
(5)	2.5	Ag_2O (0.75)	2-nitrobenzoic acid	HFIP	90
(6)	2.5	-	2-nitrobenzoic acid	HFIP	8
(7)	-	Ag_2O (0.75)	2-nitrobenzoic acid	HFIP	0

[a]Yield determined by ^{1}H NMR using ethylene carbonate as an internal standard. [b]2 equiv. of **3.1a**, 1 equiv. of **3.2a**, 0.5 equiv. base were used.

Having determined the optimized conditions, the scope of aryl iodides were investigated and the results are summarized in **Scheme 3.2**. Aryl iodides bearing electron rich substituents demonstrate high reactivity (**3.3a-3.3h**). The conditions also allow for *ortho*-substituted aryl iodides (**3.3c, 3.3e**). Unprotected alcohols (**3.3g**) are tolerated; since a number of the known pharmaceutically relevant 2-arylbenzofuran derivatives contain alcohol subsitutents,[109] this is an important result. The halogens also show generally good reactivity (**3.3i-3.3l**). This will allow further functionalization of products in additional cross-coupling reactions if needed. Consistently high yields are observed across p*ara*- and *meta*-substituted haloiodoarenes. In addition to the halogens, other weak and moderate electron withdrawing groups show continued good reactivity (**3.3m-3.3n**). Strongly deactivated groups requiring heating to 50 °C to observe any cross coupling (**3.3o**); while high reactivity is lost, modest conversion to product is still accessible under relatively mild conditions. Functional groups that are normally sensitive to high temperatures show desired reactivity - namely, benzyl alcohol **3.3g**, and benzaldehyde **3.3m**. Heteroaryl iodides led to low yields (**Scheme 3.8**). Interestingly, when 2-iodophenol is used, a cascade reaction occurs to produce 4b,9b-dihydrobenzofuro[3,2-*b*]benzofuran (**3.4**) in high yield. Current methods to access these structures are limited to those requiring several steps utilizing high temperatures, highlighting the utility of this work.[110,111]

Scheme 3.2. Room temperature benzofuran arylation: substrate scope[a]

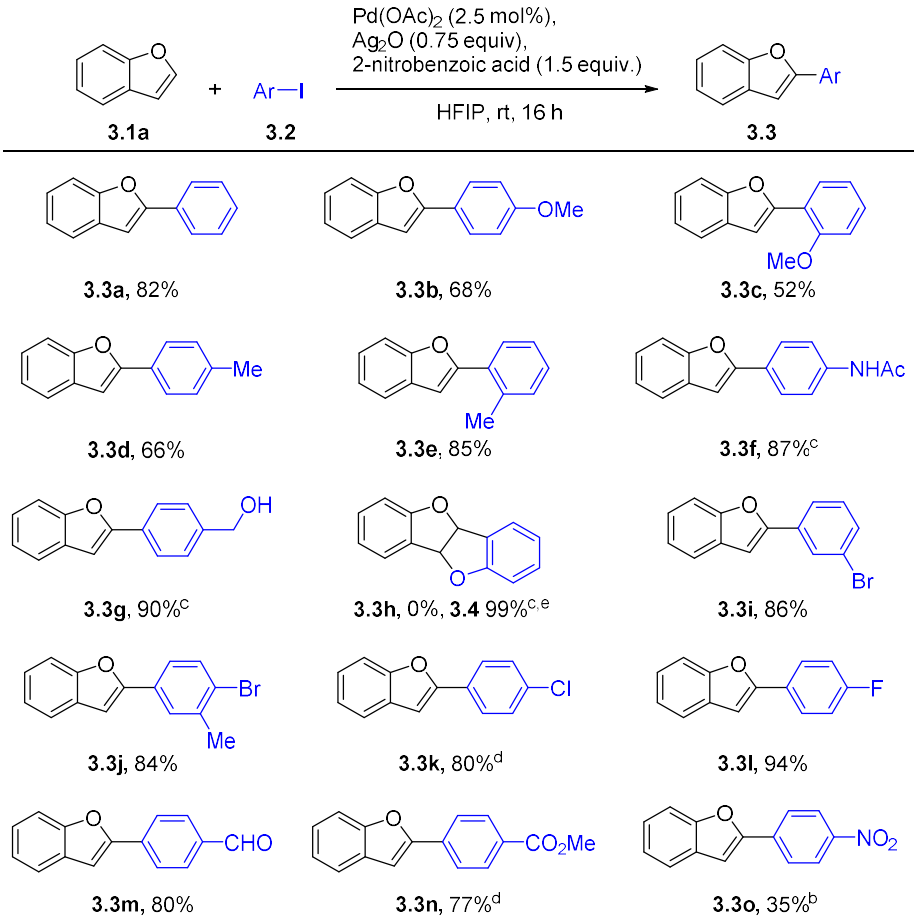

3.3a, 82% **3.3b**, 68% **3.3c**, 52%

3.3d, 66% **3.3e**, 85% **3.3f**, 87%[c]

3.3g, 90%[c] **3.3h**, 0%, **3.4** 99%[c,e] **3.3i**, 86%

3.3j, 84% **3.3k**, 80%[d] **3.3l**, 94%

3.3m, 80% **3.3n**, 77%[d] **3.3o**, 35%[b]

[a]Isolated yields. Standard conditions: **3.1a** 1 mmol, **3.2a** 2 mmol, $Pd(OAc)_2$ 0.05 mmol, Ag_2O 0.75 mmol, 2-nitrobenzoic acid 1.5 mmol, HFIP 1 M, rt, 16 h. [b]50 °C, 20 h. [c]1 equiv. aryl iodide was used. [d]20 h. [e]from 2-iodophenol.

Scheme 3.3 shows the scope of benzofuran derivatives studied. In addition to bromine substitution (**3.3q**), these conditions are suitable for boronic esters (**3.3s**). This allows for multiple reactive functional groups to be present should additional functionalization be required after arylation. The benzofuran coupling partner can tolerate substitution at C-3 (**3.3t**). The notable substrate xanthotoxin (**3.3u**), a compound currently used as a therapeutic agent for various skin conditions, proceeds in high yield albeit requiring elevated temperature (50 °C).

This is in stark comparison to the current method of derivatizing this scaffold which requires a 140°C reaction temperature.[112]

Scheme 3.3. Room temperature benzofuran arylation: benzofuran scope[a]

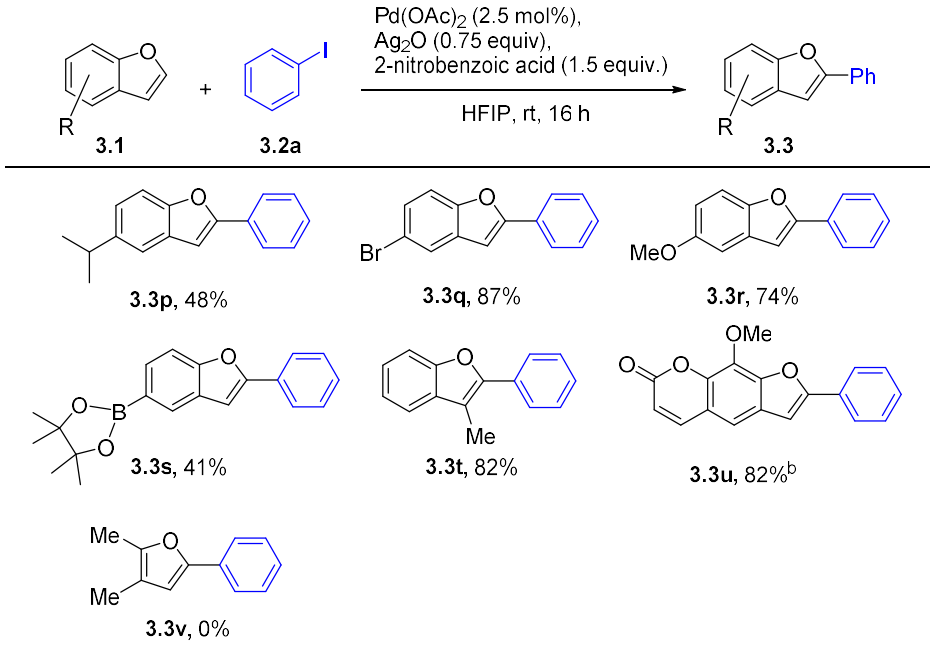

[a]Isolated yields. Standard conditions: **3.1a** 1 mmol, **3.2a** 2 mmol, $Pd(OAc)_2$ 0.05 mmol, Ag_2O 0.75 mmol, 2-nitrobenzoic acid 1.5 mmol, HFIP 1 M, rt, 16 h. [b]50 °C, 20 h.

To begin to elucidate the mechanism operating here, deuterium exchange experiments were undertaken on 2*d*-**3.1a** and 3*d*-**3.1a**, both with and without **3.2a** (**Scheme 3.4a**). Deuterium scrambling was not observed across all conditions evaluated, in contrast to what would be expected by either a Pd or Ag-mediated C-H activation in a concerted metalation-deprotonation (CMD) pathway. In that case, deuterium scrambling should be observed at C-2 if the C-H activation step is non-rate-determining. This makes a non-rate-determining reversible CMD process unlikely.[46,113]

Scheme 3.4. Mechanistic studies

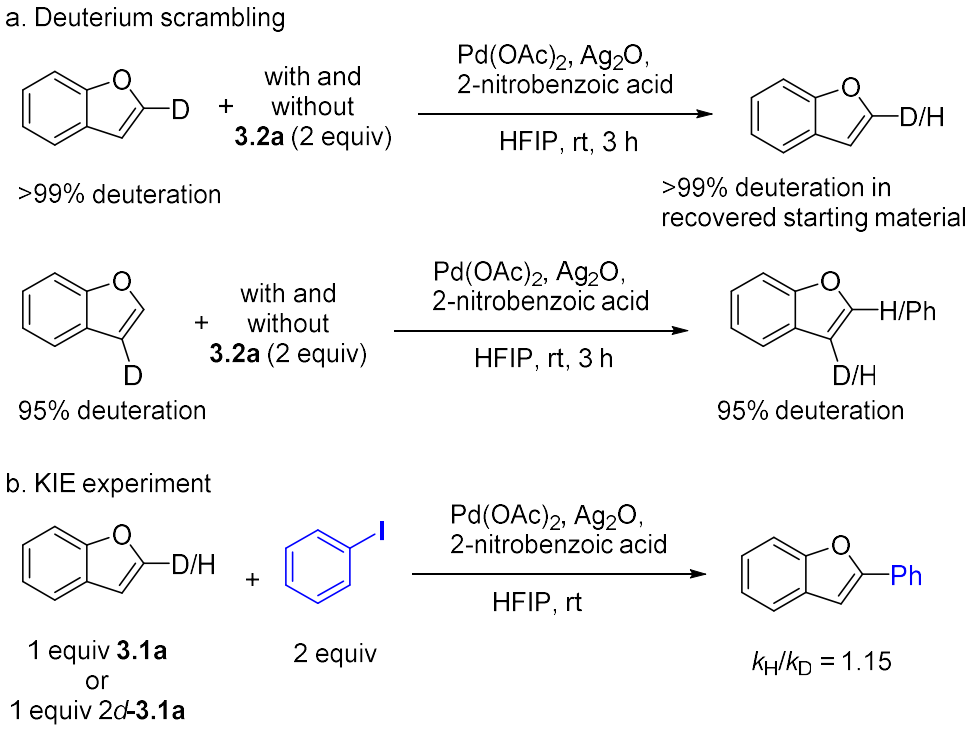

To gain greater insight into what is mechanistically driving this reaction, the kinetic isotope effect (KIE) at benzofuran's C-2 position was studied (**Scheme 3.4b**). A secondary KIE of 1.15 is observed for C-2, suggesting that a CMD mechanism with rate-determining C-H activation is unlikely. Beyond CMD, other commonly discussed mechanisms for Pd-catalyzed C-H arylation events include Heck-type,[43] and electrophilic aromatic substitution (S_EAr).[46] In S_EAr reactions on benzofuran, the electrophilic substitution is expected to occur at C-2, as observed in electrophilic nitrations and acylations.[114] C-2 selectivity is driven by the σ-complex intermediate bearing a stabilized benzylic carbocation, affording the regioselectivity observed in this arylation reaction. The positive secondary KIE at C-2 does not indicate palladation at C-2. That being said, it is common for electrophilic-aromatic substitution reactions to have small to no KIEs, due to the speed of deprotonation compared to forming the arenium ion.[115] For this reason, it does remain possible that an S_EAr mechanism occurs with palladation at C-2.

The cyclization from 2-iodophenol to produce product **3.4** provides good evidence for a C-3-palladium species, showing sp^3 carbon centers. This product is in line with what would be expected for a Heck oxyarylation product, following an established mechanistic pathway, albeit from novel starting materials.[116] In this case, the nearby hydroxyl group displaces the palladium substituent on the benzofuran ring (**Scheme 3.9**). In contrast, under S_EAr with C-2 palladation, C-3 bears a carbocation (**Scheme 3.9**). In acidic medium, the hydroxyl group on the phenol is unlikely to form a bond with a carbocation. The possibility of a secondary C-O bond forming process occurring separate to arylation should be considered. The absence of the arylation product (**3.3h**) even when the reaction was stopped prior to complete conversion, and the stability of other unprotected alcohols to the reaction conditions provide no indication of an S_EAr pathway occurring prior to a C-O cyclization step. Rather, these results are in agreement with Pd catalyzed oxyarylation/C-H functionalization on alkenes,[117] highlighting the similarities between this process and Heck-type chemistry, whilst reducing the likelihood of an S_EAr mechanism at C-2.

With the insights from mechanistic experiments in hand, reflection on the accessible substrates provides additional support for a Heck-type mechanism. Furan **3.3v** is not suited for this reaction. **3.1a** has increased aromaticity compared to furan, where the double bond in the furan ring of **3.1a** is more similar to an alkene and thus will be more susceptible to Heck-type carbopalladation. Moreover, while benzothiophene shows good reactivity under these conditions and has been previously shown to undergo Heck-type arylation,[43] indole does not show desired reactivity (**Scheme 3.7**). Previous work from our group demonstrates that indole proceeds under a photomediated mechanism under similar conditions.[107] We hypothesize that this is due to differences in relative aromaticity of the five membered ring on these heterobiaryl scaffolds,

where benzofuran and benzothiophene show reduced aromatic character compared to indole in the five-membered ring, allowing for pseudo-alkene reactivity.[118–120] Benzofuran in particular is well-documented to behave as (*Z*)-styryl phenyl ether in ring cleavages,[121] accounting for the mechanistic change between indole and benzofuran under similar conditions.

Considering the mechanistic data as a whole, we hypothesize this reaction proceeds in a Heck-type fashion, outlined in **Scheme 3.5**. In this case, after oxidative addition of the aryl iodide to form **II**, the silver species creates a more reactive palladium metal center by halide abstraction, where the newly introduced carboxylate ligand can dissociate from the metal center (**III**). **3.1a** then undergoes carbopalladation to form **IV**, which can undergo base assisted anti-β-elimination to afford product **3.3** and regenerate the Pd(0).[43,45] We hypothesize halide abstraction and subsequent ligand dissociation is a key step in enabling room temperature reactivity. Furthermore, it is possible that HFIP is undergoing acid-base exchange with the silver carboxylate,[43] in addition to its' likely role in stabilizing the active palladium species through H-bonding.[108]

Scheme 3.5. Proposed catalytic cycle

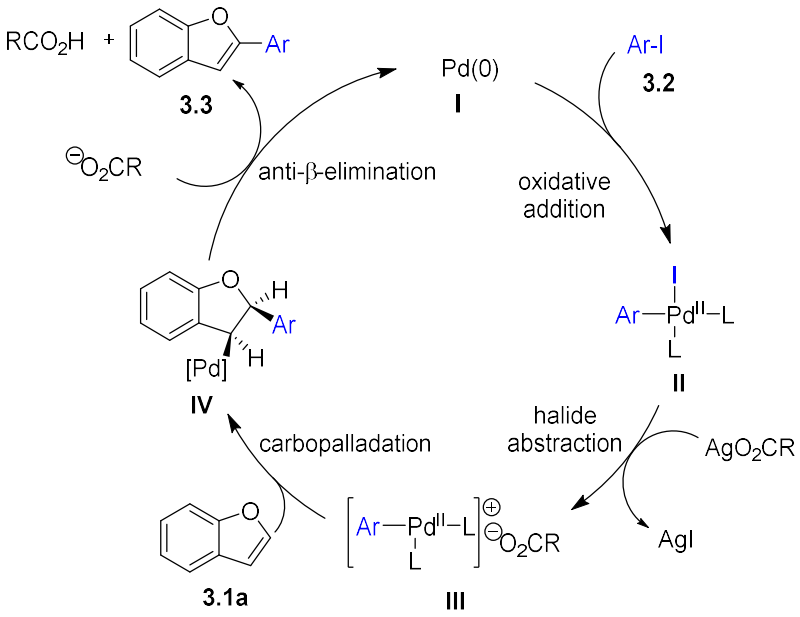

While indole C-2 arylation by aryl iodides under remarkably similar conditions was photosensitive, leading to a proposed Pd-involved radical reaction (**Scheme 2.5**), the benzofuran arylation has different mechanistic features. With evidence for a Heck-type mechanism, and only a small decline in yield when run in the dark compared to exposed to light (**Scheme 3.10**), this reaction is more closely aligned with the similar β-arylation of benzothiophene.[43] This is promising for future studies of room temperature DArP, as the photo-mediated process in synthesizing PIn led to extensive branching. It is reasonable that a Heck-type mechanism for achieving room temperature direct arylation polymerization will have higher fidelity to the regioselectivity observed in the corresponding small molecule reaction than a radical-involved reaction. Moreover, several substrates already investigated demonstrate good reactivity with only one equivalence of the aryl iodide (**3.3g**, **3.3f**). That being said, during the course of reaction optimization, it was clear that while C-2 selectivity is favored, at the end of the reaction, C-3 arylation does occur (**Scheme 3.6**). In the small molecule reaction, this could be easily accounted

for by closely monitoring the reaction time, providing the desired monoarylated product in high yield. In a polymerization, to access high molecular weight, regioregular polymers, high selectivity is needed even at the very end of the reaction. For this reason, if these conditions are to be adapted to polymerization, greater consideration will likely be needed to suppress undesired β-branching at the later stages of the polymerization, when available C-2 C-H sites are scarce.

Scheme 3.6 Disubstitution of benzofuran with extended reaction times

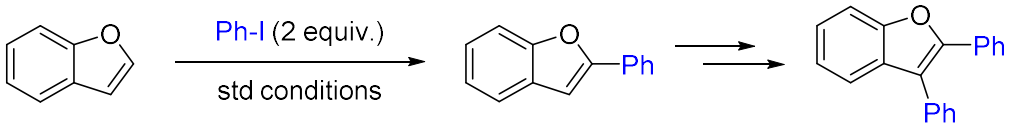

3.3 Conclusion

In this report, we have demonstrated a new and robust method for regioselective C-2 arylation of benzofuran under remarkably mild conditions. The method is tolerant to a wide range of functionalities, including halogens, boronic esters, unprotected alcohols, and carbonyl groups. We propose a Heck-type arylation mechanism alongside the C-H oxyarylation product. When considering other methods reported for room temperature arylation of heterobiaryl substrates, this report is supported by previous work on the β-arylation of benzothiophene and a report investigating indole, benzothiophene, and benzofuran using aryl diazonium salts.[43,50]

In contrast to investigations on indole room temperature, the benzofuran arylation does not show photosensitivity. Unfortunately, the Heck-type mechanism does not show sufficient regioselectivity to be readily amenable to polymerization. At the same time, by having a greater understanding of the mechanism governing this arylation reaction, it may be possible to use strategies proven in conventional Heck reaction settings to improve regioselectivity to inhibit C_{β}-

H activation in Heck-type C-H arylation. As other methods of room temperature direct arylation for heterobiaryls are also suggested to proceed through a Heck-type process, further investigations into strategies for improving regioselectivity could allow for improvements in selectivity for indole, benzothiophene, and benzofuran arylation.

3.4 Supplementary Information

3.4.1 *General Information*

All reactions were carried out under nitrogen atmosphere using standard Schlenk techniques unless otherwise noted. NMR spectra were recorded on Bruker AV-300 and AV-500 spectrometers operating at 300 and 500 MHz, respectively. ^{1}H NMR chemical shifts (δ) are reported in parts per million (ppm) downfield of tetramethylsilane and are referenced relative to the residual solvent signal ($CDCl_3$ (7.26 ppm), DMSO-d_6 (2.50)). ^{13}C NMR chemical shifts (δ) are reported in parts per million (ppm) downfield of tetramethylsilane and are referenced relative to the residual solvent signal ($CDCl_3$ (77.16 ppm), DMSO-d_6 (39.52 ppm)). When indicated, 1,3-dinitrobenzene was used as an internal standard for quantitative NMR. An Agilent 5973 Gas Chromatograph - Mass Spectrometer (EI) was used to perform GC-MS analysis. An AB Sciex 5600 Mass Spectrometer was used for HRMS analysis. HFIP was dried on 4 Å molecular sieves and sparged with nitrogen prior to use. Deuterated solvents were stored over 4 Å molecular sieves. Ethylene carbonate was stored under nitrogen between uses. All other reagents, catalysts, and chemicals were purchased from Sigma-Aldrich or Tokyo Chemical International and used without purification. Column chromatography was performed using VWR Common Silica Gel 60 Å.

3.4.2 *Representative Procedure: Direct Arylation*

To an oven-dried vial and stir bar was added $Pd(OAc)_2$ (2.5 mol %, 0.025 mmol, 5.6 mg), Ag_2O (0.75 equiv., 0.75 mmol, 173.3 mg), 2-nitrobenzoic acid (1.5 equiv., 1.5 mmol, 250.7 mg) (solid iodoarenes are added at this point as well). The vial was evacuated and backfilled with N_2 three times. Hexafluoro-2-propanol was added (1 M, 1 mL), followed by benzofuran (1 equiv., 1 mmol) and iodobenzene (2 equiv., 2 mmol). The reaction was allowed to stir at room temperature (22 °C) for 16 h. After this time, the reaction mixture was filtered through a silica plug using CH_2Cl_2 to transfer and subsequently concentrated under reduced pressure. Purification was performed using column chromatography (hexanes/DCM).

3.4.3 *Product Characterization*

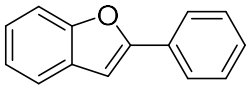

2-phenylbenzo[*b*]furan (3.3a): Product **3.3a** was prepared according to the general procedure (158 mg, 82% yield) and obtained as a white solid. The data is in accordance with the literature.[100] R_f = 0.32 (hexanes). ^{1}H NMR (500 MHz, $CDCl_3$) δ 7.88 (d, *J* = 8.4 Hz, 2H), 7.59 (d, *J* = 8.2 Hz, 1H), 7.53 (d, *J* = 8.1 Hz, 1H), 7.46 (t, *J* = 7.8 Hz, 2H), 7.36 (t, *J* = 7.4 Hz, 1H), 7.31 – 7.27 (m, 1H), 7.23 (d, *J* = 14.8 Hz, 1H), 7.03 (s, 1H). ^{13}C NMR (126 MHz, $CDCl_3$) δ 156.1, 155.0, 130.6, 129.4, 128.9, 125.1, 124.4, 123.1, 121.0, 111.3, 101.4. GC-MS (EI) calculated for [M]+ 194.2, found 194.2.

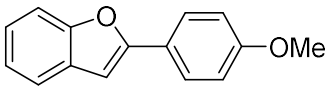

2-(4-methoxyphenyl)benzo[*b*]furan (3.3b): Product **3.3b** was prepared according to the general procedure (158 mg, 68% yield) and obtained as a white solid. The data is in accordance with the

literature.[100] R_f = 0.57 (50% DCM in hexanes). ^{1}H NMR (500 MHz, $CDCl_3$) δ 7.80 (dd, *J* = 9.0, 2.3 Hz, 2H), 7.55 (d, *J* = 7.4 Hz, 1H), 7.50 (d, *J* = 8.0 Hz, 1H), 7.26 – 7.19 (m, 2H), 6.98 (dd, *J* = 9.0, 2.3 Hz, 2H), 6.91 – 6.86 (m, 1H), 3.87 (s, 3H). ^{13}C NMR (126 MHz, $CDCl_3$) δ 160.1, 156.2, 154.9, 129.6, 126.6, 123.9, 123.5, 123.0, 120.7, 114.4, 111.1, 99.8, 55.5. GC-MS (EI) calculated for [M]+ 224.1, found 224.1.

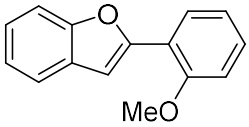

2-(2-methoxyphenyl)benzo[*b*]furan (3.3c): Product **3.3c** was prepared according to the general procedure (119 mg, 52% yield) and obtained as a white solid. The data is in accordance with the literature.[122] R_f = 0.28 (5% DCM in hexanes). ^{1}H NMR (300 MHz, $CDCl_3$) δ 8.08 (d, *J* = 9.2 Hz, 1H), 7.55 (dd, *J* = 25.1, 7.1 Hz, 2H), 7.41 – 7.30 (m, 3H), 7.25 – 7.17 (m, 1H), 7.16 – 6.99 (m, 2H), 4.02 (s, 3H). ^{13}C NMR (126 MHz, $CDCl_3$) δ 156.6, 154.0, 152.3, 129.9, 129.4, 127.2, 124.2, 122.8, 121.2, 120.9, 119.5, 111.2, 110.9, 106.5, 55.5. GC-MS (EI) calculated for [M]+ 224.1, found 224.2.

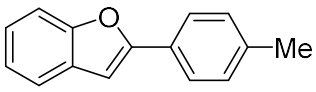

2-(4-methylphenyl)benzo[*b*]furan (3.3d): Product **3.3d** was prepared according to the general procedure (147 mg, 66% yield) and obtained as a white solid. The data is in accordance with the literature.[98] R_f = 0.21 (hexanes). ^{1}H NMR (500 MHz, $CDCl_3$) δ 7.76 (d, *J* = 8.2 Hz, 2H), 7.52 – 7.48 (m, 1H), 7.27 (d, *J* = 6.3 Hz, 3H), 7.22 (td, *J* = 7.5, 1.0 Hz, 1H), 6.97 (s, 1H), 2.40 (s, 3H). ^{13}C NMR (126 MHz, $CDCl_3$) δ 156.4, 154.9, 138.7, 129.6, 129.5, 127.9, 125.1, 124.1, 123.0, 120.9, 111.2, 100.7, 21.5. GC-MS (EI) calculated for [M]+ 208.1, found 208.1.

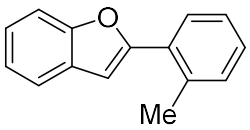

2-(2-methylphenyl)benzo[*b*]furan (3.3e): Product **3.3e** was prepared according to the general procedure (181.4 mg, 85% yield) and obtained as a clear oil. The data is in accordance with the literature.[98] R_f = 0.29 (hexanes). ^{1}H NMR (500 MHz, $CDCl_3$) δ 7.90 (d, *J* = 7.9 Hz, 1H), 7.65 (d, *J* = 8.2 Hz, 1H), 7.58 (d, *J* = 8.1 Hz, 1H), 7.38 – 7.26 (m, 5H), 6.94 (s, 1H), 2.63 (s, 3H). ^{13}C NMR (126 MHz, $CDCl_3$) δ 155.8, 154.5, 135.9, 131.4, 130.1, 129.3, 128.6, 128.3, 126.2, 124.4, 122.9, 121.0, 111.2, 105.2, 22.1. GC-MS (EI) calculated for [M]+ 208.1, found 208.1

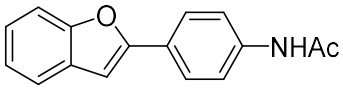

***N*-[4-(2-benzofuranyl)phenyl]acetamide (3.3f):** Product **3.3f** was prepared according to the general procedure with the following modifications: 1 equiv 4-iodoacetamide was used. Product **3.3f** was obtained as a tan solid (221 mg, 87% yield). The data is in accordance with the literature.[123] R_f = 0.64 (EtOAc). ^{1}H NMR (500 MHz, DMSO-d_6) δ 10.14 (s, 1H), 7.85 (d, *J* = 8.6 Hz, 2H), 7.72 (d, *J* = 8.6 Hz, 2H), 7.62 (dd, *J* = 16.1, 7.7 Hz, 2H), 7.35 – 7.21 (m, 3H), 2.08 (s, 3H). ^{13}C NMR (126 MHz, DMSO) δ 168.5, 155.3, 154.1, 139.9, 129.0, 125.3, 124.4, 124.2, 123.1, 120.9, 119.1, 110.9, 100.7, 24.1. GC-MS (EI) calculated for [M]+ 251.1, found 251.1.

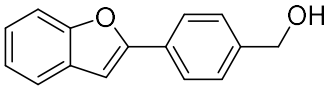

4-(2-Benzofuranyl)benzyl alcohol (3.3g): Product **3.3g** was prepared according to the general procedure with the following modifications: 1 equiv 4-iodobenzyl alcohol was used. Product **3.3g** was obtained as a yellow solid (201 mg, 90% yield). The data is in accordance with the literature.[123] R_f = 0.19 (DCM) ^{1}H NMR (500 MHz, $CDCl_3$) δ 7.90 (s, 1H), 7.80 (d, *J* = 7.8

Hz, 1H), 7.62 – 7.57 (m, 1H), 7.55 – 7.50 (m, 1H), 7.45 (d, *J* = 15.3 Hz, 1H), 7.36 (d, *J* = 7.6 Hz, 1H), 7.29 (td, *J* = 8.2, 7.7, 1.4 Hz, 1H), 7.24 (td, *J* = 7.5, 1.0 Hz, 1H), 7.06 (s, 1H), 4.79 (s, 2H). ^{13}C NMR (126 MHz, $CDCl_3$) δ 155.8, 155.0, 141.4, 130.9, 129.2, 127.2, 124.5, 124.3, 123.5, 123.1, 121.1, 111.3, 101.7, 65.3. GC-MS (EI) calculated for [M]+ 224.1, found 224.2.

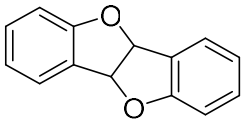

4b,9b-dihydrobenzofuro[3,2-*b*]benzofuran (3.4): Product **3.4** was prepared according to the general with the following modifications: 1 equiv 2-iodophenol was used. Product **3.4** was obtained in as a yellow solid (210 mg, 99% yield). When prepared according to the general procedure, **3.4** was obtained in 67% yield. The data is in accordance with the literature.[110] R_f = 0.33 (10% DCM in hexanes). ^{1}H NMR (500 MHz, $CDCl_3$) δ 7.54 (d, *J* = 7.5 Hz, 2H), 7.28 (td, *J* = 8.1, 7.6, 1.3 Hz, 4H), 6.97 (td, *J* = 7.5, 0.9 Hz, 2H), 6.87 (d, *J* = 8.2 Hz, 2H), 6.29 (s, 2H). ^{13}C NMR (126 MHz, $CDCl_3$) δ 160.2, 131.5, 124.6, 121.3, 111.0, 86.6. GC-MS (EI) calculated for [M]+ 210.1, found 210.1.

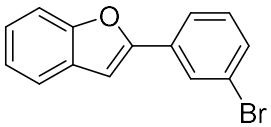

2-(3-bromophenyl)benzo[*b*]furan (3.3i): Product **3.3i** was prepared according to the general procedure and obtained as a white solid (247 mg, 86% yield). The data is in accordance with the literature.[124] R_f = 0.26 (hexanes). ^{1}H NMR (500 MHz, $CDCl_3$) δ 8.02 (t, *J* = 1.8 Hz, 1H), 7.79 (dt, *J* = 7.8, 1.0 Hz, 1H), 7.60 (d, *J* = 8.3 Hz, 1H), 7.55 – 7.50 (m, 1H), 7.47 (ddd, *J* = 7.9, 1.9, 0.9 Hz, 1H), 7.36 – 7.28 (m, 2H), 7.24 (d, *J* = 7.4 Hz, 1H), 7.05 (s, 1H). ^{13}C NMR (126 MHz,

$CDCl_3$) δ 155.0, 154.2, 132.4, 131.3, 130.3, 129.0, 127.8, 124.8, 123.4, 123.2, 123.0, 121.2, 111.3, 102.5. GC-MS (EI) calculated for [M]+ 272.0, found 272.0.

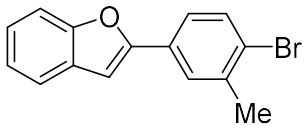

2-(4-bromo-3-methylphenyl)benzo[*b*]furan (3.3j): Product **3.3j** was prepared according to the general procedure and obtained as a white solid (242 mg, 84% yield). R_f = 0.28 (hexanes). ^{1}H NMR (500 MHz, $CDCl_3$) δ 7.74 (s, 1H), 7.56 (d, *J* = 33.3 Hz, 4H), 7.29 (s, 1H), 7.23 (s, 1H), 7.02 (s, 1H), 2.48 (s, 3H). ^{13}C NMR (126 MHz, $CDCl_3$) δ 155.2, 138.5, 132.9, 129.8, 129.3, 127.2, 125.2, 124.6, 123.9, 123.2, 121.1, 111.3, 101.8, 23.2. GC-MS (EI) calculated for [M]+ 286.0, found 286.0

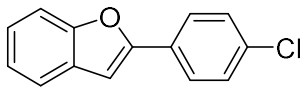

2-(4-chlorophenyl)benzo[*b*]furan (3.3k): Product **3.3k** was prepared according to the general procedure with the following modifications: the reaction was run for 20 h. Product **3.3k** was obtained as a white solid (182 mg, 80% yield). The data is in accordance with the literature.[100] R_f = 0.26 (hexanes). ^{1}H NMR (500 MHz, $CDCl_3$) δ 7.82 – 7.78 (m, 2H), 7.59 (d, *J* = 7.5 Hz, 1H), 7.52 (d, *J* = 8.2 Hz, 1H), 7.45 – 7.40 (m, 2H), 7.30 (td, *J* = 8.3, 7.8, 1.3 Hz, 1H), 7.24 (td, *J* = 7.6, 0.9 Hz, 1H), 7.02 (s, 1H). ^{13}C NMR (126 MHz, $CDCl_3$) δ 155.1, 154.9, 134.5, 129.2, 129.2, 129.1, 126.3, 124.7, 123.3, 121.2, 111.4, 101.9. GC-MS (EI) calculated for [M]+ 228.0, found 228.1.

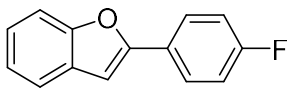

2-(4-fluorophenyl)benzo[*b*]furan (3.3l): Product **3.3l** was prepared according to the general procedure and obtained as a white solid (201 mg, 94% yield). The data is in accordance with the literature.[98] R_f = 0.23 (hexanes). ^{1}H NMR (500 MHz, $CDCl_3$) δ 7.88 – 7.81 (m, 2H), 7.58 (d, *J* = 7.6 Hz, 1H), 7.51 (d, *J* = 8.8 Hz, 1H), 7.29 (td, *J* = 8.2, 7.7, 1.4 Hz, 1H), 7.25 – 7.20 (m, 1H), 7.15 (t, *J* = 8.7 Hz, 2H), 6.96 (s, 1H). ^{13}C NMR (126 MHz, $CDCl_3$) δ 164.0, 162.0, 155.2, 155.0, 129.3, 126.9, 126.9, 124.4, 123.2, 121.0, 116.1, 115.9, 111.3, 101.1. GC-MS (EI) calculated for [M]+ 212.1, found 212.1.

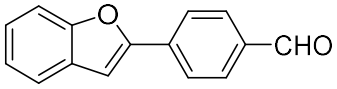

4-(2-benzofuranyl)benzaldehyde (3.3m): Product **3.3m** was prepared according to the general procedure and obtained as a yellow solid (176.1 mg, 80% yield). The data is in accordance with the literature.[99] R_f = 0.52 (50% DCM in hexanes). ^{1}H NMR (500 MHz, $CDCl_3$) δ 10.04 (s, 1H), 8.03 (d, *J* = 8.3 Hz, 2H), 7.96 (d, *J* = 8.4 Hz, 2H), 7.64 (d, *J* = 7.7 Hz, 1H), 7.56 (d, *J* = 8.9 Hz, 1H), 7.35 (t, *J* = 8.4 Hz, 1H), 7.28 (t, *J* = 8.2 Hz, 1H), 7.21 (s, 1H). ^{13}C NMR (126 MHz, $CDCl_3$) δ 191.5, 155.3, 154.3, 135.9, 135.9, 130.3, 128.8, 125.4, 125.2, 123.4, 121.5, 111.4, 104.3. GC-MS (EI) calculated for [M]+ 222.1, found 222.1.

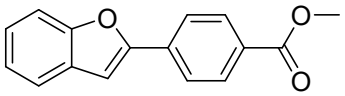

Methyl 4-(benzofuran-2-yl)benzoate (3.3n): Product **3.3n** was prepared according to the general procedure with the following modifications: the reaction was run for 20 h; the mixture obtained after column chromatography was recrystallized in hexanes. Product **3.3n** was obtained as white needles (198 mg, 77% yield). The data is in accordance with the literature.[125] R_f = 0.58 (DCM). ^{1}H NMR (500 MHz, $CDCl_3$) δ 8.12 (d, *J* = 8.7 Hz, 2H), 7.93 (d, *J* = 8.3 Hz, 2H), 7.62

(d, *J* = 8.8 Hz, 1H), 7.54 (d, *J* = 8.8 Hz, 1H), 7.36 – 7.30 (m, 1H), 7.27 (d, *J* = 0.9 Hz, 1H), 7.16 (s, 1H), 3.95 (s, 3H). ^{13}C NMR (126 MHz, $CDCl_3$) δ 166.8, 155.3, 154.8, 134.6, 130.3, 129.9, 129.1, 125.2, 124.8, 123.4, 121.4, 111.5, 103.6, 52.3. GC-MS (EI) calculated for [M]+ 252.1, found 252.1.

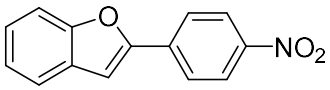

2-(4-nitrophenyl)benzo[*b*]furan (3.3o): Product **3.3o** was prepared according to the general procedure with the following modifications: the reaction was run for 20 h at 50 °C (using an oil bath). Product **3.3o** was obtained as a yellow solid (84 mg, 35% yield). The data is in accordance with the literature.[124] R_f = 0.15 (20% DCM in hexanes). ^{1}H NMR (500 MHz, $CDCl_3$) δ 8.30 (d, *J* = 9.0 Hz, 2H), 7.99 (d, *J* = 9.0 Hz, 2H), 7.65 (s, 1H), 7.55 (s, 1H), 7.39 – 7.35 (m, 1H), 7.30 – 7.26 (m, 1H), 7.24 – 7.21 (m, 1H). ^{13}C NMR (126 MHz, $CDCl_3$) δ 155.6, 153.4, 147.4, 136.4, 128.8, 126.0, 125.3, 124.4, 123.7, 121.8, 111.6, 105.2. GC-MS (EI) calculated for [M]+ 239.1, found 239.1.

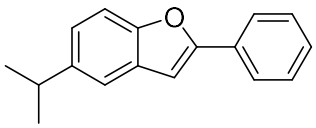

5-isopropyl-2-phenylbenzo[*b*]furan (3.3p): Product **3.3p** was prepared according to the general procedure and obtained as a white solid (112.3 mg, 48% yield). R_f = 0.22 (hexanes). ^{1}H NMR (500 MHz, $CDCl_3$) δ 7.86 (dd, *J* = 8.3, 1.2 Hz, 2H), 7.47 – 7.41 (m, 4H), 7.37 – 7.31 (m, 1H), 7.18 – 7.14 (m, 1H), 7.00 – 6.96 (m, 1H), 3.02 (hept, *J* = 6.9 Hz, 1H), 1.31 (d, *J* = 6.9 Hz, 6H). ^{13}C NMR (126 MHz, $CDCl_3$) δ 156.2, 153.7, 143.9, 130.8, 129.4, 128.9, 128.5, 125.0, 123.4, 118.2, 110.9, 101.5, 34.3, 24.7. HRMS calculated 237.1273, found 237.1280.

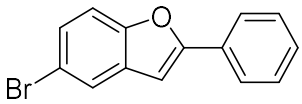

5-bromo-2-phenylbenzo[*b*]furan (3.3q): Product **3.3q** was prepared according to the general procedure and obtained as a white solid (246 mg, 87% yield). The data is accordance with the literature.[126] R_f = 0.26 (hexanes). ^{1}H NMR (300 MHz, $CDCl_3$) δ 7.85 (d, *J* = 7.5 Hz, 2H), 7.73 – 7.68 (m, 1H), 7.46 (t, *J* = 7.5 Hz, 2H), 7.39 (t, *J* = 3.4 Hz, 3H), 6.96 (s, 1H). ^{13}C NMR (126 MHz, $CDCl_3$) δ 157.4, 153.8, 131.4, 130.1, 129.2, 129.0, 127.2, 125.2, 123.6, 116.2, 112.8, 100.8. GC-MS (EI) calculated for [M]+ 272.0, found 272.1.

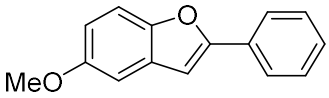

5-methoxy-2-phenylbenzo[*b*]furan (3.3r): Product **3.3r** was prepared according to the general procedure and obtained as a white solid (163.1 mg, 74% yield). The data is in accordance with the literature.[127] R_f = 0.31 (50% DCM in hexanes). ^{1}H NMR (500 MHz, $CDCl_3$) δ 7.88 – 7.82 (m, 2H), 7.48 – 7.38 (m, 3H), 7.35 (t, *J* = 7.4 Hz, 1H), 7.05 (d, *J* = 2.6 Hz, 1H), 6.97 (s, 1H), 6.89 (dd, *J* = 8.9, 2.6 Hz, 1H), 3.86 (s, 3H). ^{13}C NMR (126 MHz, $CDCl_3$) δ 156.9, 156.2, 150.1, 130.7, 129.9, 128.9, 128.6, 125.0, 113.1, 111.7, 103.5, 101.6, 56.1. GC-MS (EI) calculated for [M]+ 224.1, found 224.1.

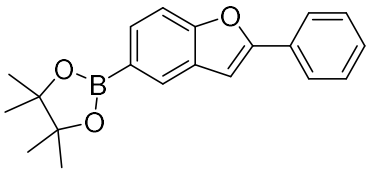

2-phenyl-5-(4,4,5,5-tetramethyl-1,3,2-dioxaborolan-2-yl)benzo[*b*]furan (3.3s): Product **3.3s** was prepared according to the general procedure and obtained as a clear viscous oil (132.5 mg, 41% yield). R_f = 0.64 (DCM). ^{1}H NMR (500 MHz, $CDCl_3$) δ 8.10 (s, 1H), 7.88 (dd, *J* = 8.4, 1.2

Hz, 2H), 7.77 (dd, *J* = 8.2, 1.1 Hz, 1H), 7.55 – 7.52 (m, 1H), 7.46 (t, *J* = 7.7 Hz, 2H), 7.38 – 7.34 (m, 1H), 7.03 (s, 1H), 1.39 (s, 12H). ^{13}C NMR (126 MHz, $CDCl_3$) δ 157.2, 156.1, 131.0, 130.5, 129.1, 128.9, 128.7, 128.4, 125.1, 110.8, 101.5, 83.9, 25.1. HRMS calculated 321.1656, found 321.1659.

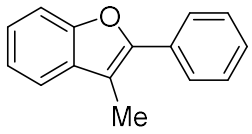

3-methyl-3-phenylbenzo[*b*]furan (3.3t): Product **3.3t** was prepared according to the general procedure and obtained as a clear oil (177 mg, 82% yield). The data is in accordance with the literature.[128] R_f = 0.25 (hexanes) ^{1}H NMR (500 MHz, $CDCl_3$) δ 7.84 (d, *J* = 9.3 Hz, 2H), 7.57 (d, *J* = 7.4 Hz, 1H), 7.50 (t, *J* = 7.7 Hz, 3H), 7.38 (t, *J* = 7.4 Hz, 1H), 7.34 – 7.26 (m, 2H), 2.51 (s, 3H). ^{13}C NMR (126 MHz, $CDCl_3$) δ 153.9, 150.8, 131.6, 131.3, 128.7, 128.0, 126.8, 124.4, 122.5, 119.4, 111.4, 111.0, 9.5. GC-MS (EI) calculated for [M]+ 208.1, found 208.1.

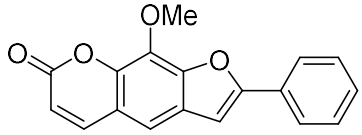

9-methoxy-2-phenyl-7H-furo[3,2-*g*][1]benzopyran-7-one (3.3u): Product **3.3u** was prepared according to the general procedure with the following modifications: the reaction was run for 20 h at 50 °C (using an oil bath). Product **3.3u** was obtained as a yellow solid (219 mg, 82% yield). The data is in accordance with the literature.[112] R_f = 0.79 (EtOAc). ^{1}H NMR (500 MHz, $CDCl_3$) δ 7.90 – 7.84 (m, 2H), 7.76 (d, *J* = 9.6 Hz, 1H), 7.48 (t, *J* = 7.6 Hz, 2H), 7.41 (t, *J* = 7.4 Hz, 1H), 7.32 (s, 1H), 7.04 (s, 1H), 6.38 (d, *J* = 9.6 Hz, 1H), 4.38 (s, 3H). ^{13}C NMR (75 MHz, $CDCl_3$) δ 160.5, 158.1, 147.7, 146.7, 144.3, 132.7, 129.6, 129.4, 129.1, 128.0, 125.2, 116.8, 114.8, 112.6, 101.0, 61.4. GC-MS (EI) calculated for [M]+ 292.1, found 292.1.

3.4.4 *Starting Material Preparation*

All iodoarenes and benzofuran substrates not listed were purchased commercially.

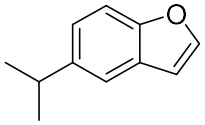

5-isopropylbenzo[*b*]furan (3.1b): Starting material **3.1b** was prepared according to the literature procedure,[129] and collected in 95% yield as a clear liquid. R_f = 0.63 (50% DCM in hexanes). ^{1}H NMR (500 MHz, $CDCl_3$) δ 7.50 (s, 1H), 7.38 – 7.31 (m, 2H), 7.28 – 7.13 (m, 2H), 7.09 (dd, *J* = 8.5, 1.8 Hz, 1H), 6.63 (d, *J* = 2.7 Hz, 1H), 2.94 (s, 1H), 1.21 (s, 6H). ^{13}C NMR (126 MHz, $CDCl_3$) δ 153.7, 145.1, 143.6, 127.6, 123.3, 118.4, 111.1, 106.6, 34.2, 24.7. GC-MS (EI) calculated for [M]+ 160.1, found 160.1.

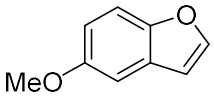

5-methoxybenzo[*b*]furan (3.1c): Starting material **3.1c** was prepared according to the literature procedure,[129] and collected in 40% yield as a yellow liquid. The data is accordance with the literature. R_f = 0.48 (50% DCM in hexanes). ^{1}H NMR (500 MHz, $CDCl_3$) δ 7.59 (d, *J* = 2.1 Hz, 1H), 7.39 (d, *J* = 8.9 Hz, 1H), 7.06 (d, *J* = 2.6 Hz, 1H), 6.90 (dd, *J* = 8.9, 2.6 Hz, 1H), 6.71 (d, *J* = 2.8 Hz, 1H), 3.85 (s, 3H). ^{13}C NMR (126 MHz, $CDCl_3$) δ 156.1, 150.12, 145.9, 128.1, 113.2, 111.9, 106.8, 103.7, 56.0. GC-MS (EI) calculated for [M]+ 148.1, found 148.2.

3-bromobenzo[*b*]furan (3.1d): Starting material **3.1d** was prepared according to the literature report:[130] Br_2 (46.53 mmol, 2.38 mL) dissolved in CH_2Cl_2 (15 mL) was added dropwise to a

solution containing benzo[*b*]furan (42.3 mmol, 4.66 mL) in CH_2Cl_2 (100 mL) at -10 °C. The mixture was stirred for 1 h at -10 °C, then NaOH (1M, 5 mL) was added. The mixture was diluted with H_2O (200 mL) and saturated $Na_2S_2O_3$ (100 mL) was added. The solution was extracted 3 times with CH_2Cl_2. The combined organic layers were dried over $MgSO_4$, filtered, and concentrated under reduced pressure. The crude product was taken up in EtOH (100 mL). Saturated KOH in EtOH (100 mL) was added dropwise at 0 °C. The flask was heated to reflux for 4 h in an oil bath. After the time had elapsed, the reaction was cooled to room temperature and H_2O (50 mL) was added. The EtOH was removed under reduced pressure and the aqueous solution was extracted with EtOAc. The organic layer was washed with H_2O and brine, dried over $MgSO_4$, filtered, and concentrated under reduced pressure. The mixture was purified by column chromatography using hexanes as eluent, affording **3.1d** as white crystals (4.784 g, 58% yield). $R_f = 0.62$ (hexanes). ^{1}H NMR (500 MHz, $CDCl_3$) δ 7.66 (s, 1H), 7.56 (d, $J = 6.8$ Hz, 1H), 7.50 (d, $J = 7.7$ Hz, 1H), 7.39 – 7.31 (m, 2H). ^{13}C NMR (126 MHz, $CDCl_3$) δ 154.5, 142.8, 127.3, 125.6, 123.6, 119.9, 111.9, 98.1. GC-MS (EI) calculated for [M]+ 196.0, found 196.0.

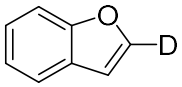

Benzo[*b*]furan-2-*d* (2*d*-3.1a): 3.1a-*d*-2 was prepared based on the literature report:[131] *n*-BuLi (2.5 M in hexanes, 14.7 mmol, 5.90 mL) was added dropwise with vigorous stirring to a solution containing benzo[*b*]furan (8.15 mmol, 0.9 mL) in THF (27.2 mL) at -78 °C. The mixture was stirred for 2 h at -78 °C, then D_2O (4.5 mL) was added dropwise. The mixture was allowed to warm to room temperature. H_2O (5 mL) was added and the aqueous layer was extracted 3 times with Et_2O. The combined organic layers were dried over $MgSO_4$, filtered, and concentrated under reduced pressure. The mixture was purified with a silica plug using hexanes as eluent, affording

2*d*-3.1a as a clear liquid (1.248 g, 72% yield), with >99% deuteration. R_f = 0.28 (hexanes). ^{1}H NMR (500 MHz, $CDCl_3$) δ 7.65 (d, *J* = 7.6 Hz, 1H), 7.57 (d, *J* = 8.2 Hz, 1H), 7.35 (t, *J* = 7.7 Hz, 1H), 7.29 (t, *J* = 7.4 Hz, 1H), 6.81 (s, 1H). ^{2}H NMR (77 MHz, $CDCl_3$) δ 7.79. ^{13}C NMR (126 MHz, $CDCl_3$) δ 155.0, 144.8 (t, *J* = 61.7 Hz, CD) 127.5, 124.3, 122.8, 121.3, 111.5, 106.5. GC-MS (EI) calculated for [M]+ 119.1, found 119.1.

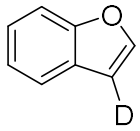

Benzo[*b*]furan-3-*d* (3*d*-3.1a): *n*-BuLi (2.5 M in hexanes, 6 mmol, 2.4 mL) was added dropwise with vigorous stirring to a solution containing 3-bromobenzo[*b*]furan (6 mmol, 1.182 g) in THF (16 mL) at -98 °C. The reaction was quenched with MeOH-d_4 (2 mL) at -98 °C and then allowed to come to room temperature. D_2O (6 mL) was added and the organic were removed under reduced pressure. The aqueous solution was extracted 3 times with Et_2O. The combined organic layers were dried over $MgSO_4$, filtered, and concentrated under reduced pressure. The mixture was purified with a silica plug using hexanes as eluent, affording **3*d*-3.1a** as a clear liquid (476 mg, 65% yield), with 95% deuteration.[132] R_f = 0.32 (hexanes). ^{1}H NMR (500 MHz, $CDCl_3$) δ 7.62 (m, *J* = 13.4 Hz, 2H), 7.52 (d, *J* = 8.8 Hz, 1H), 7.31 (t, *J* = 8.3 Hz, 1H), 7.27 – 7.22 (m, 1H). ^{2}H NMR (77 MHz, $CDCl_3$) δ 6.87 (s, 1H). ^{13}C NMR (126 MHz, $CDCl_3$) δ 155.2, 145.0, 127.5, 124.4, 122.9, 121.3, 111.5, 106.5 (t, *J* = 52.9 Hz, CD). GC-MS (EI) calculated for [M]+ 119.1, found 119.1.

3.4.5 *Heteroatom Comparison*

Scheme 3.7. Comparison of different heterobiaryls[a]

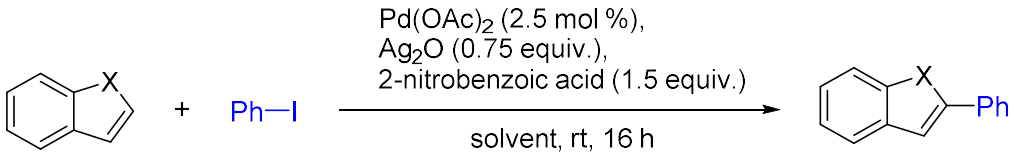

Entry	X	DMF (%)	HFIP (%)	C2:C3
1	N	90	44	>99:1
2	O	0	90	>99:1
3	S	0	71	1:>99

[a]Yield determined by ^{1}H NMR using ethylene carbonate as an internal standard. Run using the general procedure.

Scheme 3.8. Evaluation of heteroaryl iodides[a]

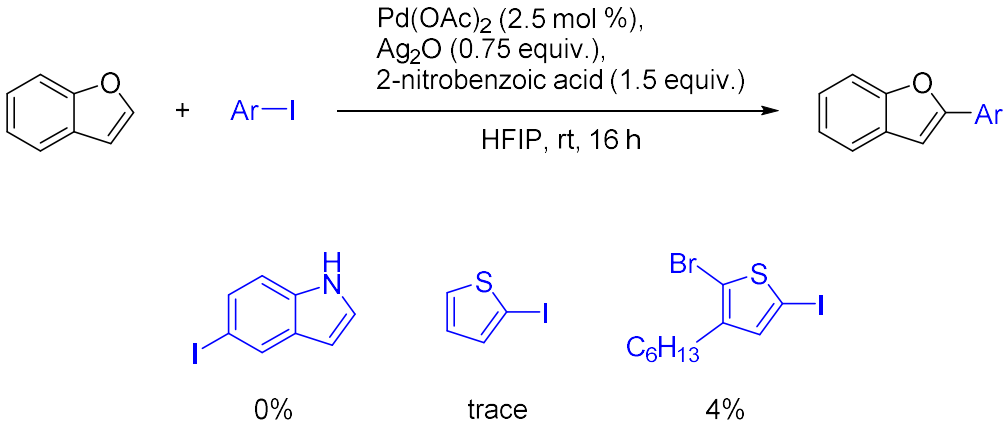

[a]Yield determined by ^{1}H NMR using ethylene carbonate as an internal standard. Run using the general procedure.

As outlined in **Scheme 3.8**, investigations into the utilization of heteroaryl iodides using the optimized methodology did not provide the intended products in meaningful quantities. This is expected in light of the results in **Scheme 3.7**, as the specific heteroaryl iodides investigated have C-H bonds that are reactive under these conditions, leading to competing regioselectivity and a complex mixture of products.

3.4.6 *Mechanistic Experiments*

Deuterium Exchange:

To an oven-dried vial and stir bar was added $Pd(OAc)_2$ (2.5 mol %, 0.005 mmol, 1.12 mg), Ag_2O (0.75 equiv., 0.15 mmol, 34.8 mg), 2-nitrobenzoic acid (1.5 equiv., 0.3 mmol, 50.7 mg). The vial was evacuated and backfilled with N_2 three times. Hexafluoro-2-propanol was added (1 M, 0.2 mL), followed by **2*d*-3.1a** or **3*d*-3.1a** (1 equiv., 0.2 mmol, 24 mg) and, **3.2a** if using (2 equiv., 0.4 mmol, 45 µL). The reaction was allowed to stir at room temperature (22 °C) for 3 h. After this time, the reaction mixture was filtered through a silica plug using CH_2Cl_2 to transfer and subsequently concentrated under reduced pressure. Deuterium scrambling was calculated using ^1H NMR in $CDCl_3$ using 1,3-dinitrobenzene as an internal standard.

KIE:

General Considerations:

Experiments for the deuterated and non-deuterated substrates were done simultaneously utilizing the same catalyst stock solution. The 2-deuterobenzofuran and benzofuran experiments were done in one set of reactions, and the 3-deuterobenzofuran and an additional set of benzofuran experiments were determined in a separate block of experiments. The rate constant for each substrate is determined from the average of four sets of trials for C-2 and three sets of trials for C-3.

Stock solutions:

A stock solution was prepared for the catalyst. In an oven dried vial with stir bar was added $Pd(OAc)_2$ (39.2 mg) and cooled under vacuum. After three N_2/vacuum cycles, 3.5 mL HFIP was added.

A stock solution was prepared for the substrates. In an oven dried vial with stir bar, which was cooled under vacuum, was added the appropriate benzofuran (non-deuterated: 413 mg, deuterated: 416 mg), iodobenzene (1428 mg), and 1.75 mL HFIP.

Reaction set-up:

To an oven-dried vial with stir bar was added Ag_2O (173.3 mg, 0.75 equiv.), 2-nitrobenzoic acid (250.7 mg, 1.5 equiv.), and 1,3-dinitrobenzene (0.5 equiv.) as an internal standard and cooled under vacuum. The vial was cycled through N_2/vacuum three times before 0.5 mL of the catalyst solution and 0.8 mL of the substrate solution were added simultaneously to start the reaction. At the appropriate times, 100 μL aliquots were taken, filtered through SiO_2 using CH_2Cl_2 and subsequently concentrated under reduced pressure. The solution was analyzed using ^1H NMR in $CDCl_3$ using 1,3-dinitrobenzene as an internal standard.

Results:

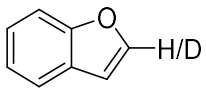

k_h	0.1451
k_d [2*d*-3.1a]	0.1267
KIE (k_h/k_d)	1.14522

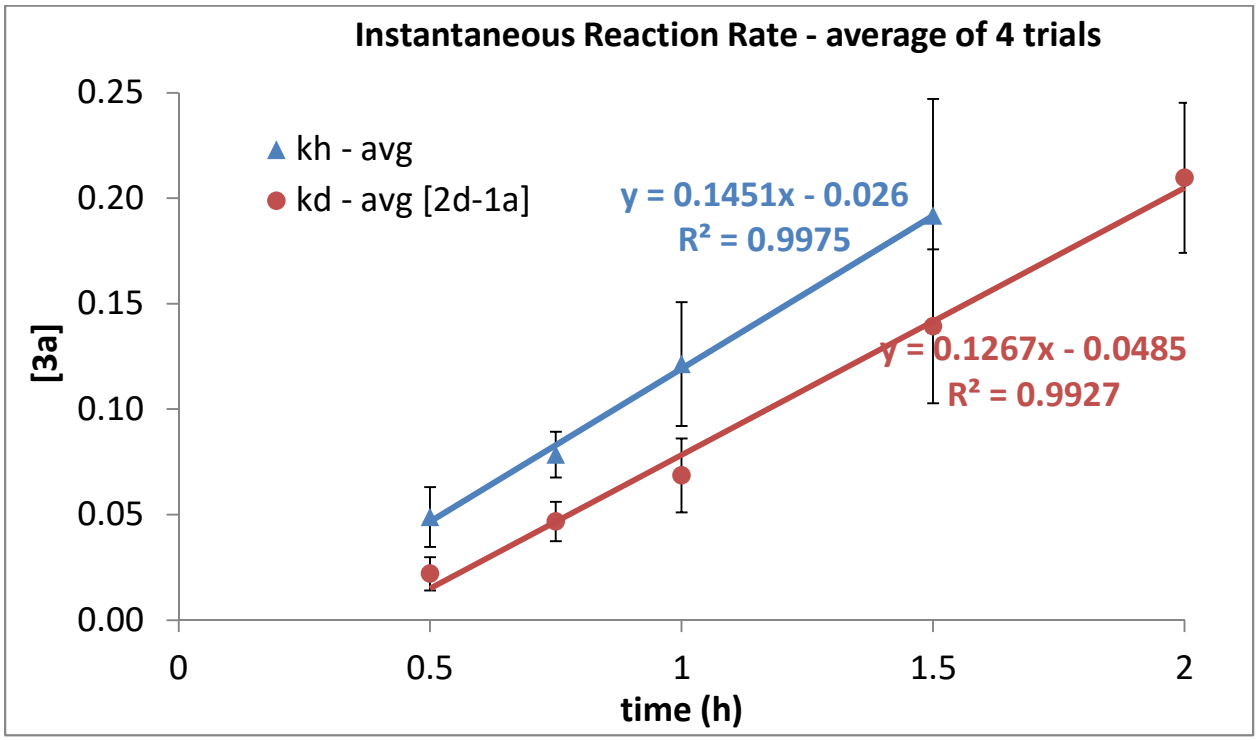

Figure 3.1. Instantaneous reaction rate determination for **3.1a** and **2*d*-3.1a**

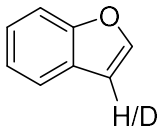

k_h	0.153
k_d [3*d*-3.1a]	0.1658
KIE (k_h/k_d)	0.923

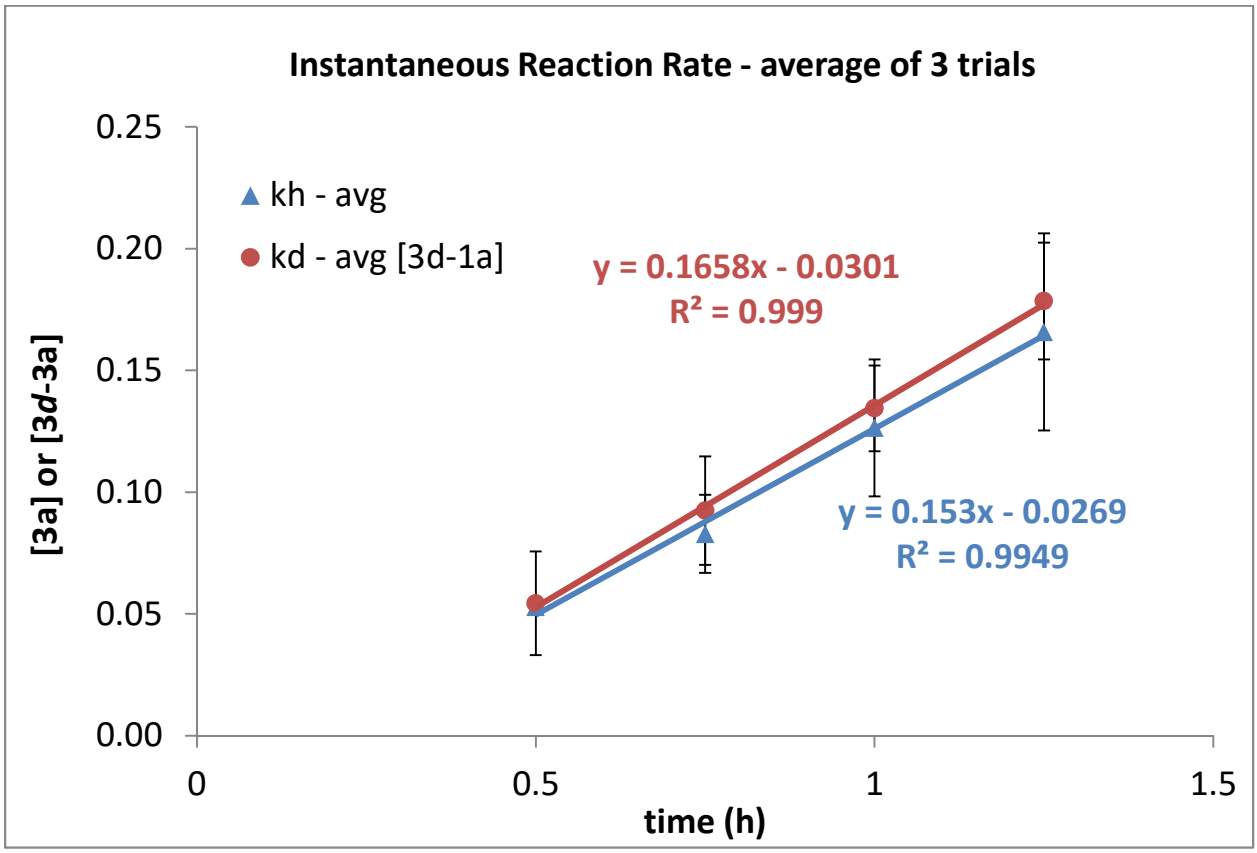

Figure 3.2. Instantaneous reaction rate determination for **3.1a** and **3*d*-3.1a**

Considering the KIE data reported herein, significant error is included in the analysis arising from variations between replicates. While this is exacerbated by the relatively small differences being analyzed, is an inherent challenge with instantaneous reaction rate analysis

exacerbated by the heterogeneity of the reaction mixture. Regardless, the results have still been included as the overall trends for both the KIE values at C-2 and C-3 were replicated many times over and provide reliable insight as a trend although future studies are needed for greater accuracy and precision. While both KIE values are indicative of Heck-type arylation, due to the small differences between k_h and k_d and the relatively large error accompanying the likelihood that an S_EAr pathway may not demonstrate any KIE value, these KIE values aren't able to differentiate between Heck-type and S_EAr pathways with confidence.

3.4.7 *Oxyarylation Mechanism*

Scheme 3.9. Proposed oxyarylation mechanism for the formation of dihydrofuran product 3.4 (top) and contrasting S_EAr mechanism (bottom)

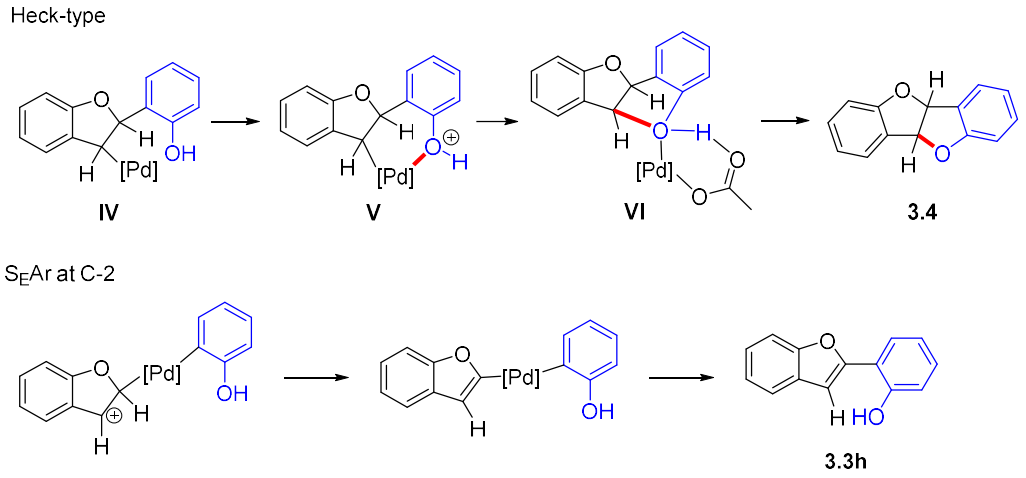

3.4.8 *Dark Experiments*

Scheme 3.10 Benzofuran arylation in the dark

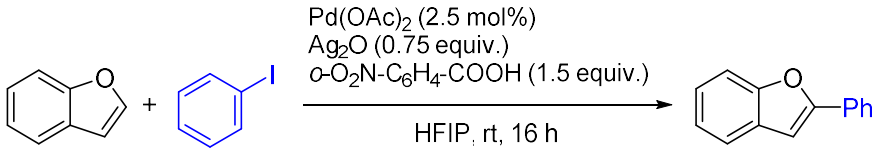

Condition	NMR Yield (%)
light	90
dark	70

3.4.9 *^{1}H NMR and ^{13}C NMR Spectra*

^{1}H NMR (500 MHz, $CDCl_3$)

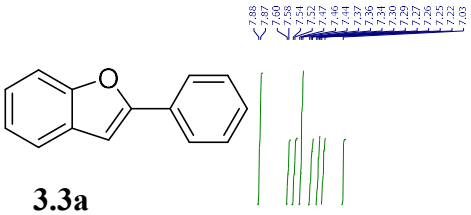

3.3a

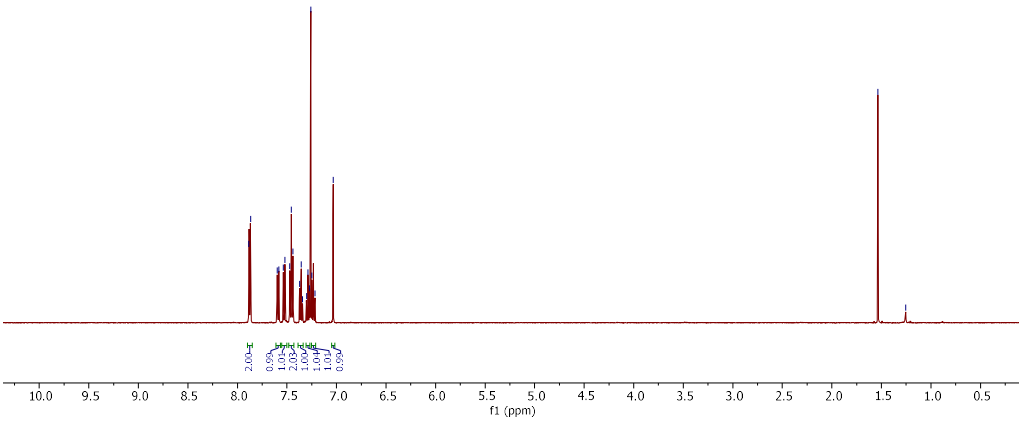

^{13}C NMR (126 MHz, $CDCl_3$)

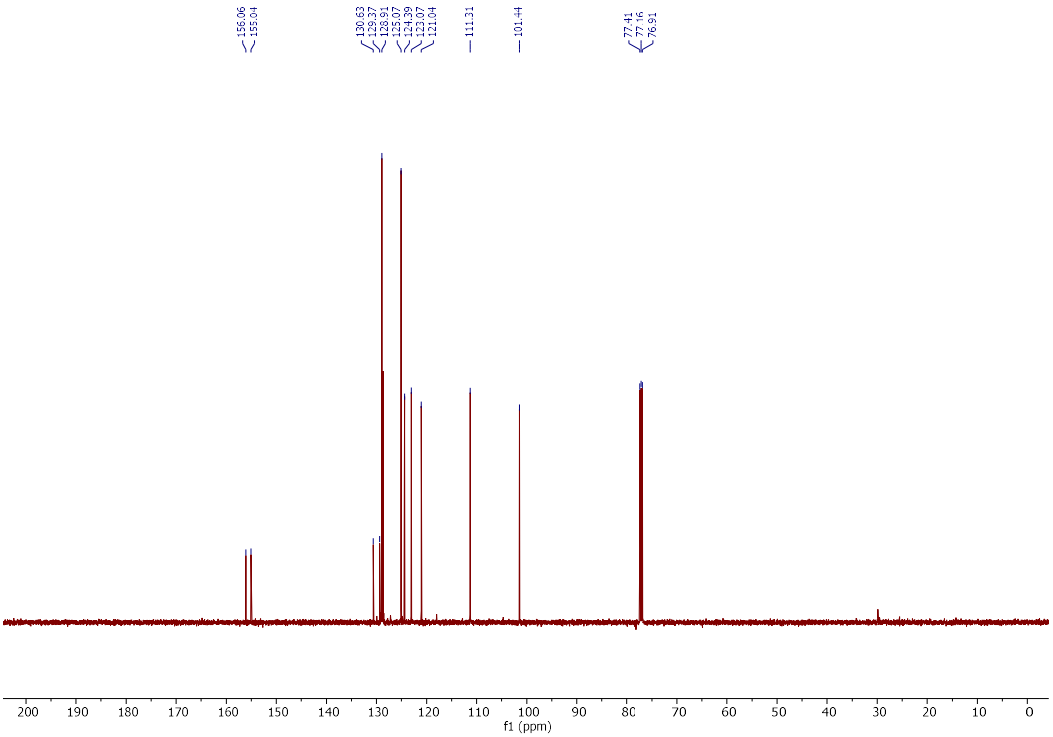

^{1}H NMR (500 MHz, CDCl3)

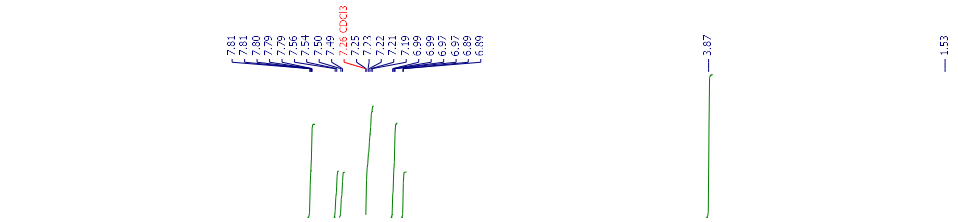

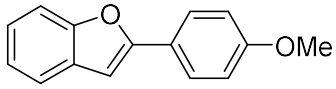

3.3b

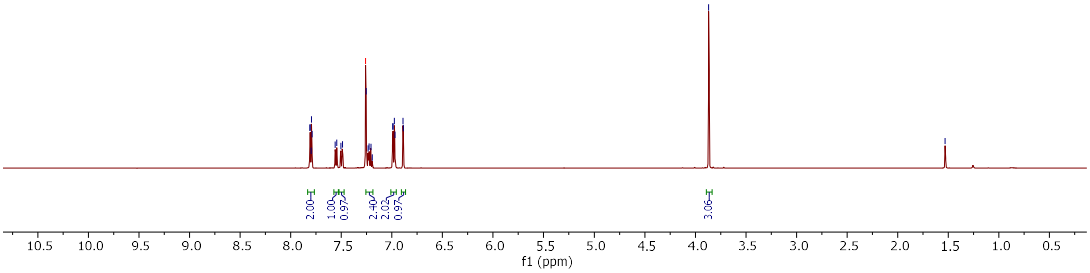

^{13}C NMR (126 MHz, $CDCl_3$)

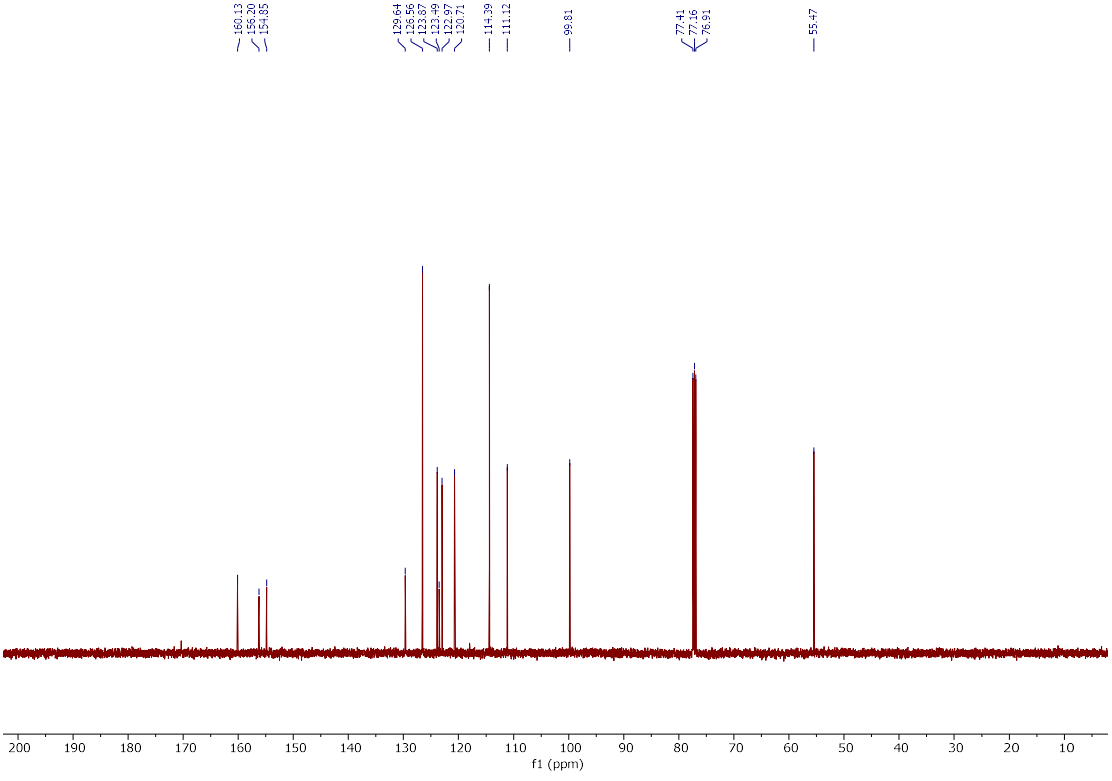

^{1}H NMR (300 MHz, $CDCl_3$)

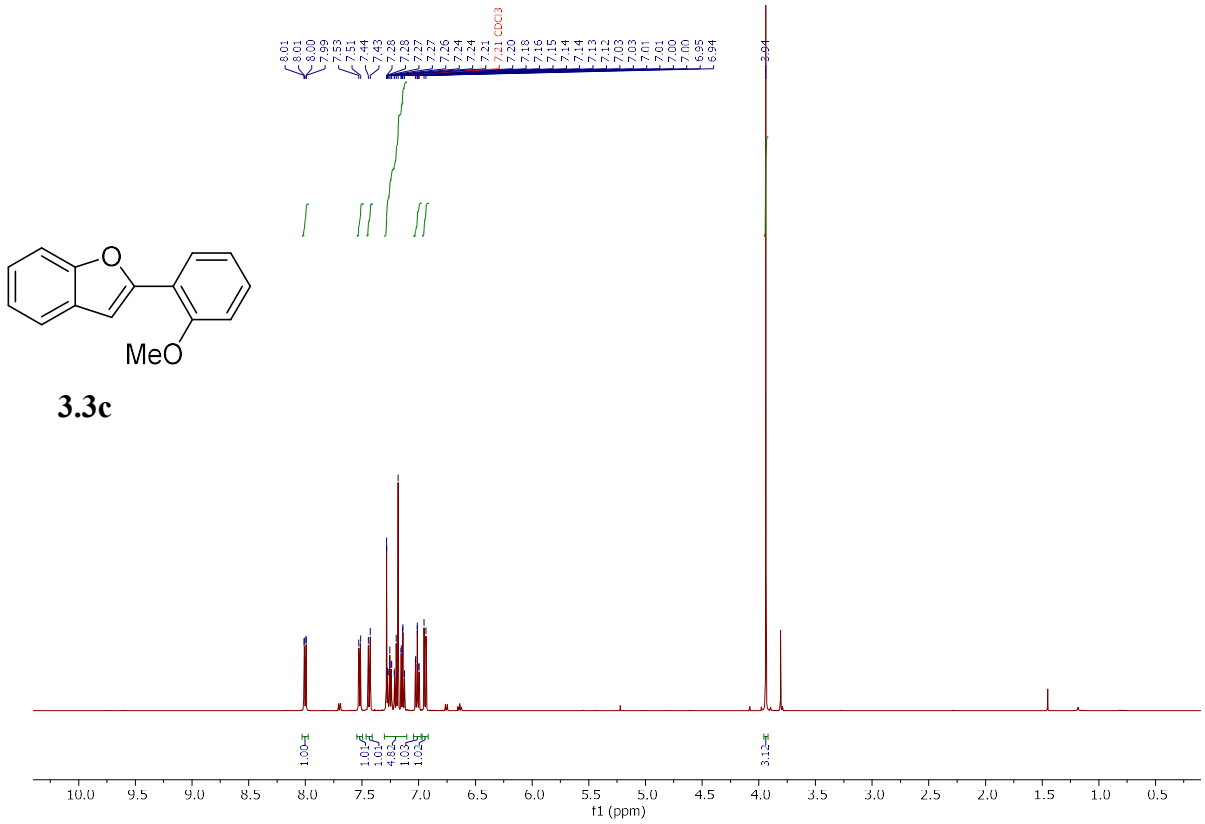

3.3c

^{13}C NMR (126 MHz, $CDCl_3$)

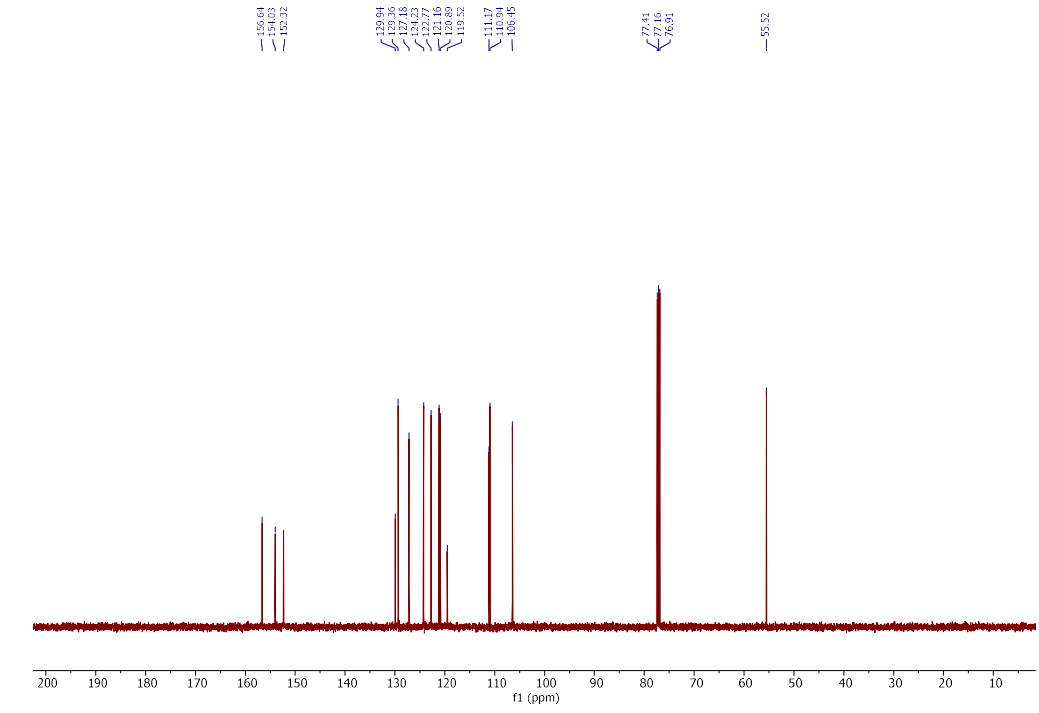

^{1}H NMR (500 MHz, $CDCl_3$)

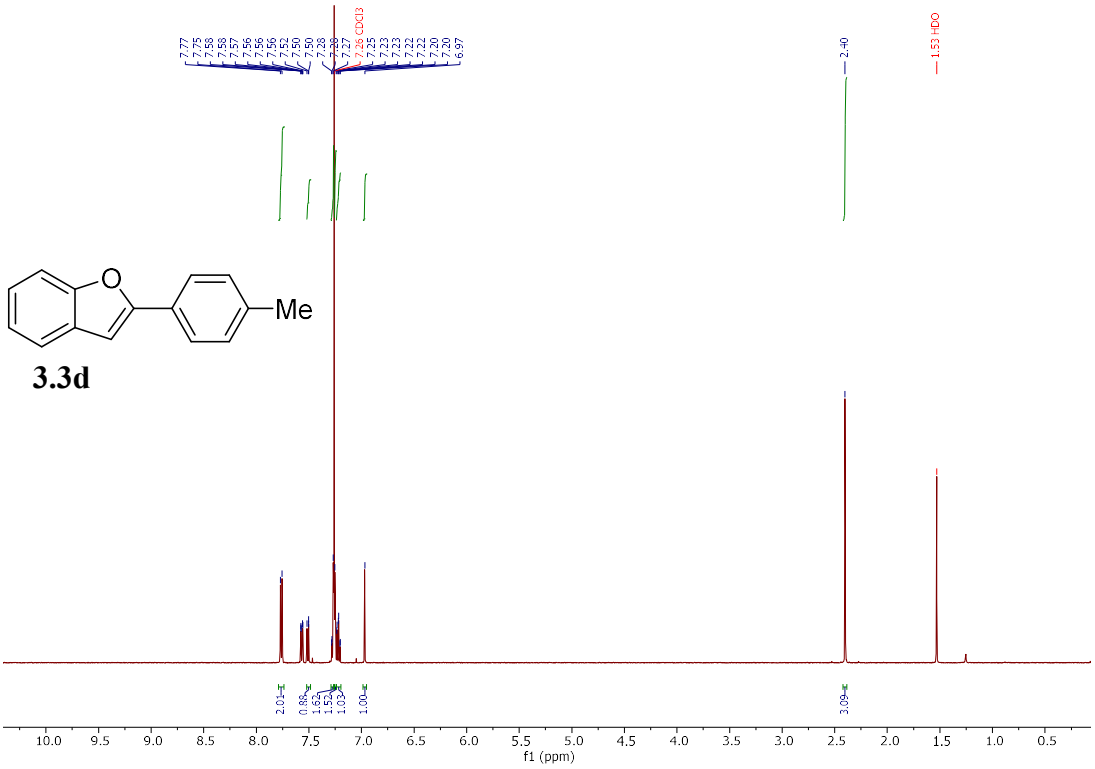

^{13}C NMR (126 MHz, $CDCl_3$)

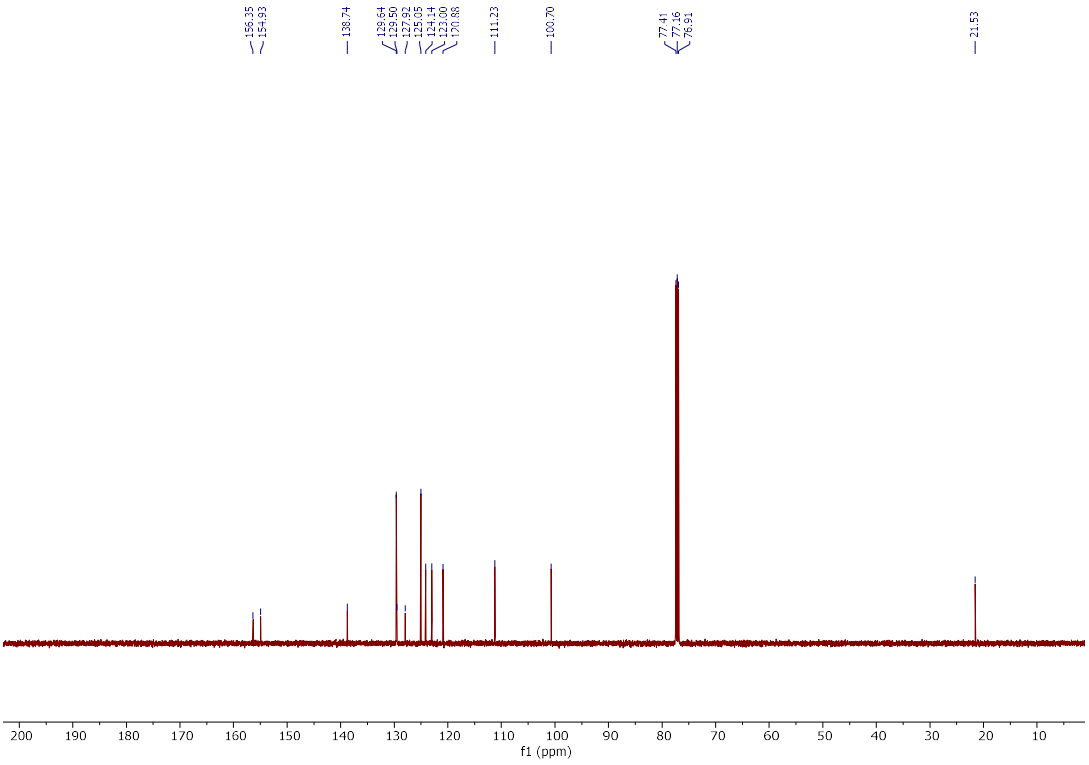

^{1}H NMR (500 MHz, $CDCl_3$)

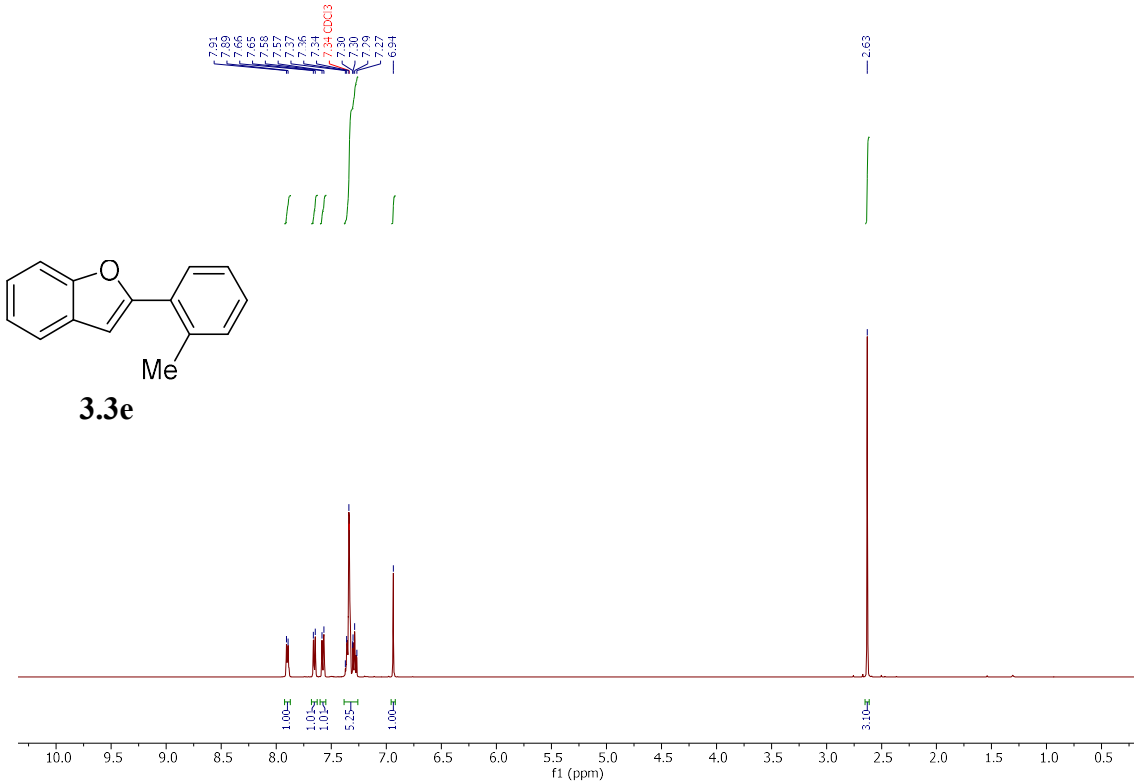

3.3e

^{13}C NMR (126 MHz, $CDCl_3$)

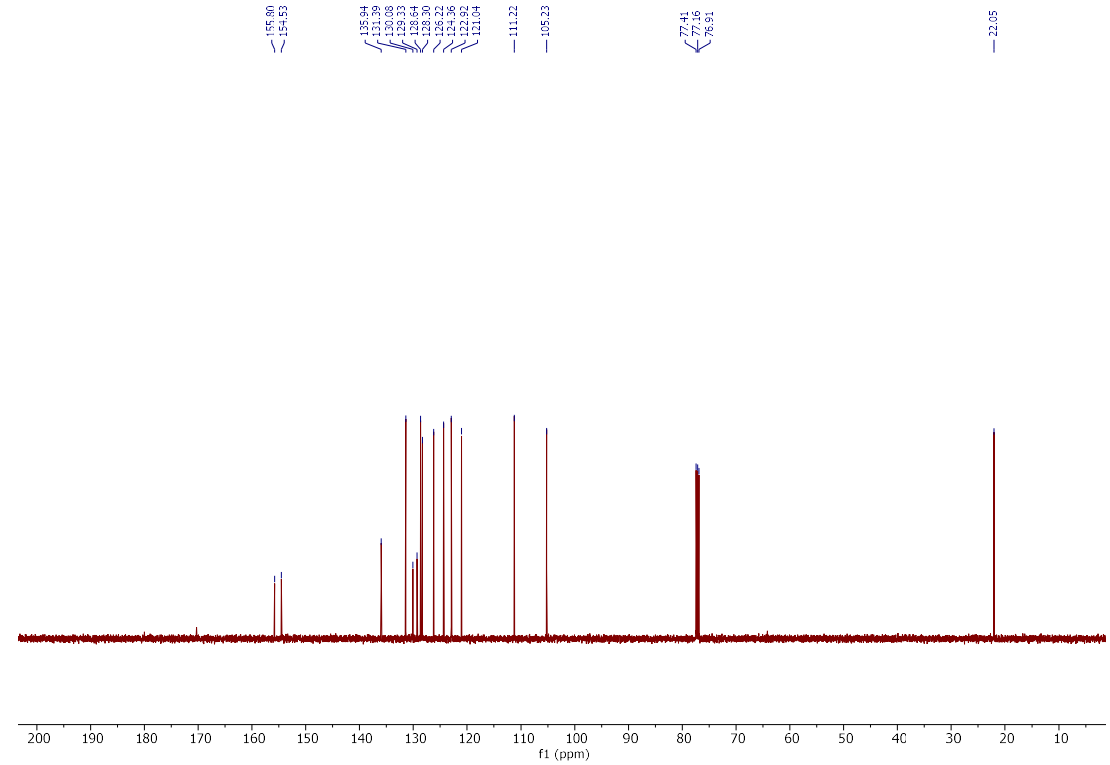

^{1}H NMR (500 MHz, DMSO-d_6)

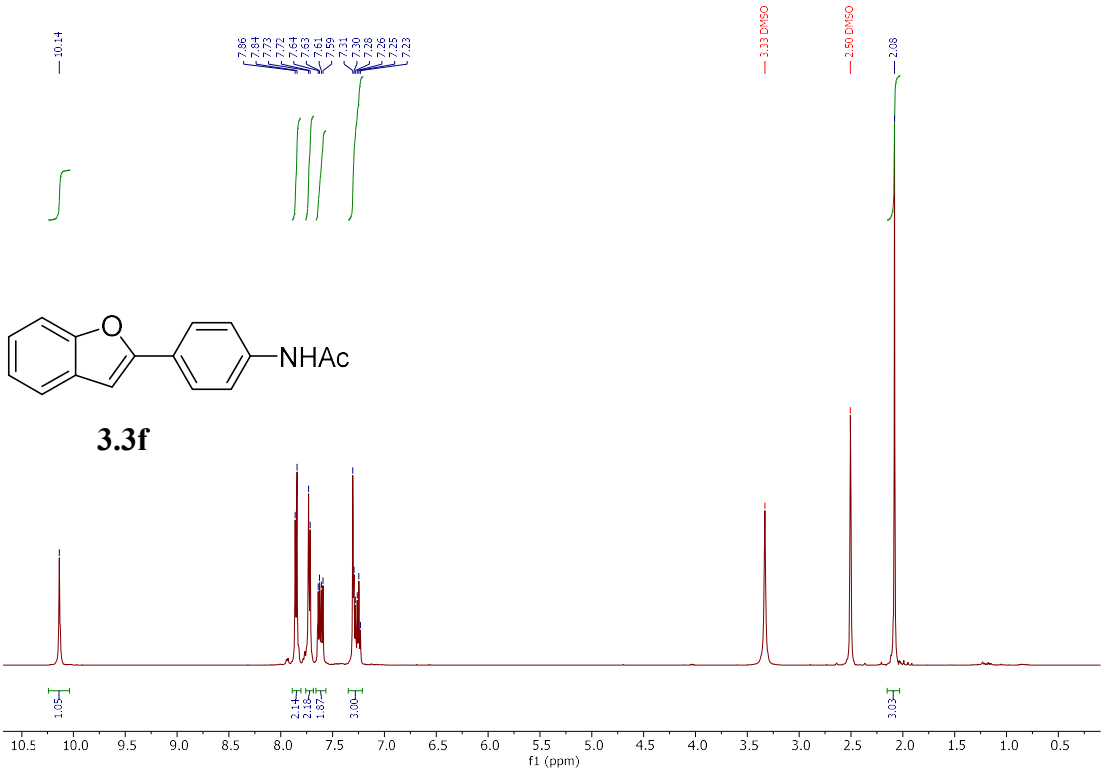

3.3f

^{13}C NMR (126 MHz, DMSO)

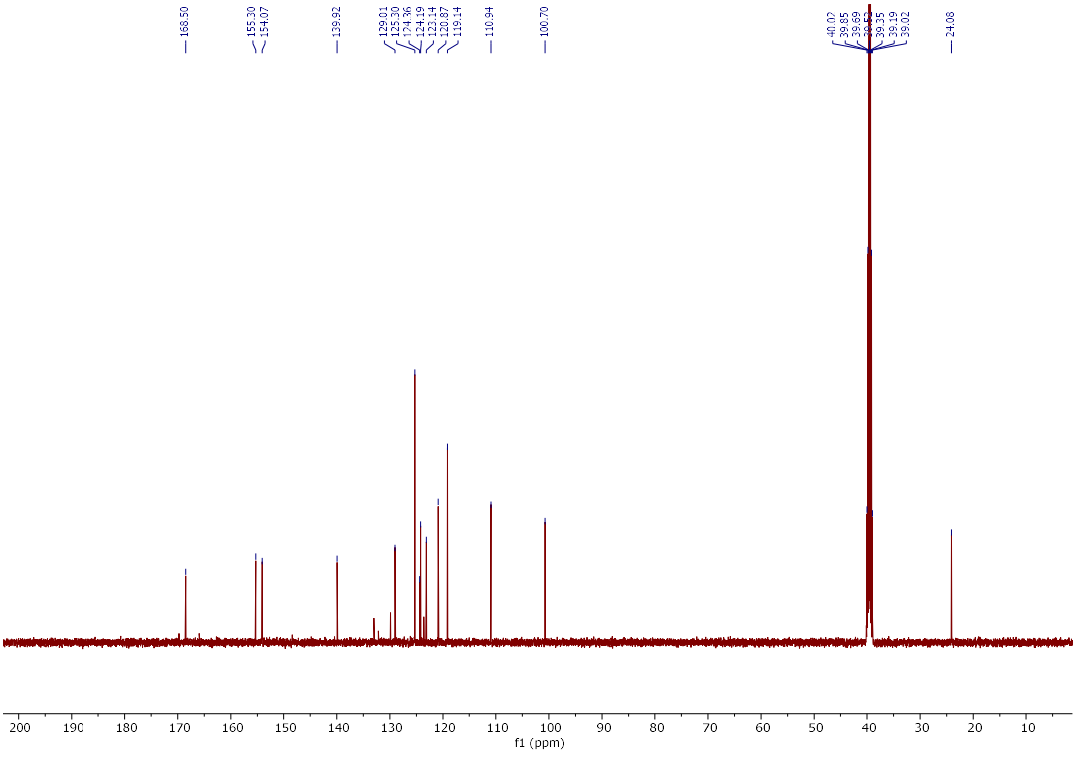

^{1}H NMR (500 MHz, $CDCl_3$)

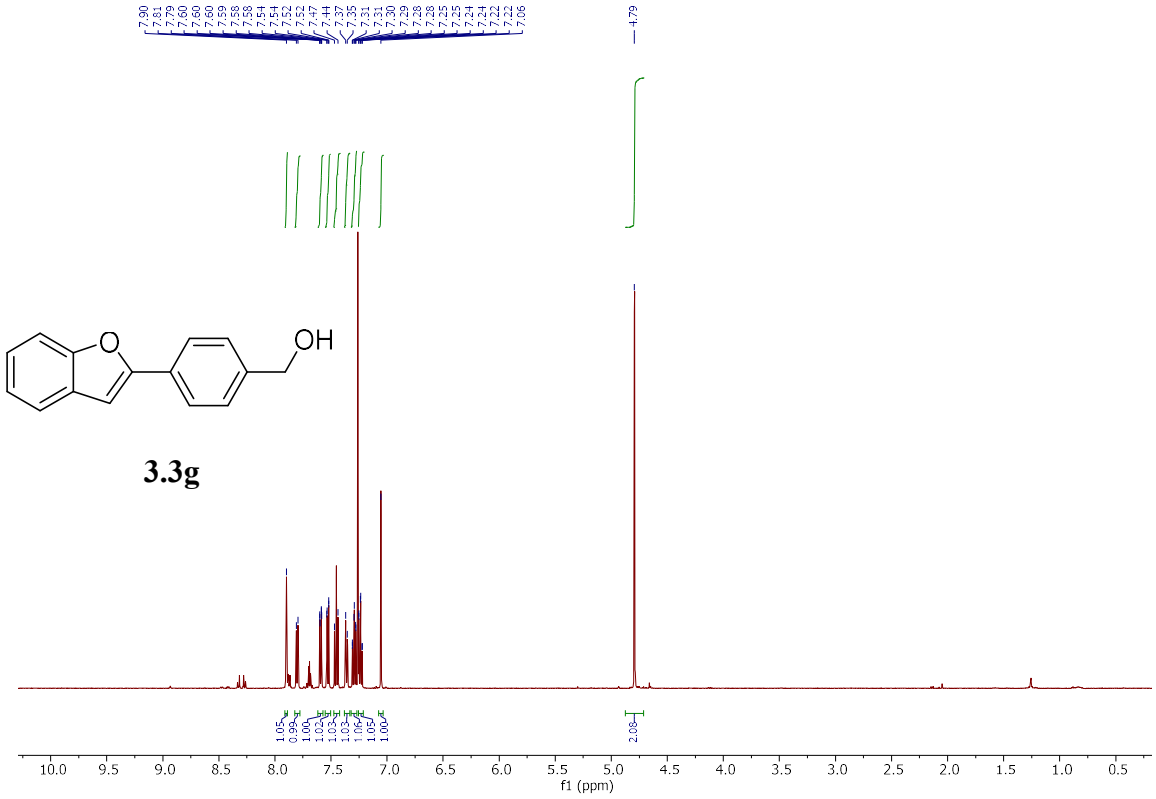

^{13}C NMR (126 MHz, $CDCl_3$)

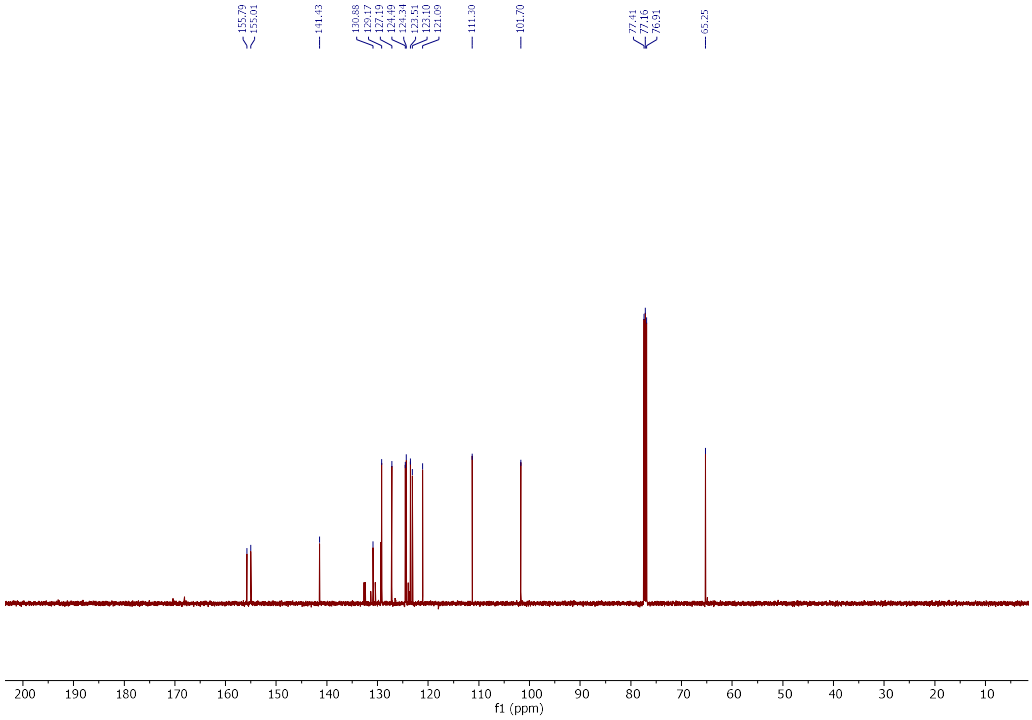

^{1}H NMR (500 MHz, $CDCl_3$)

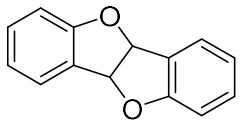

3.4

^{13}C NMR (126 MHz, $CDCl_3$)

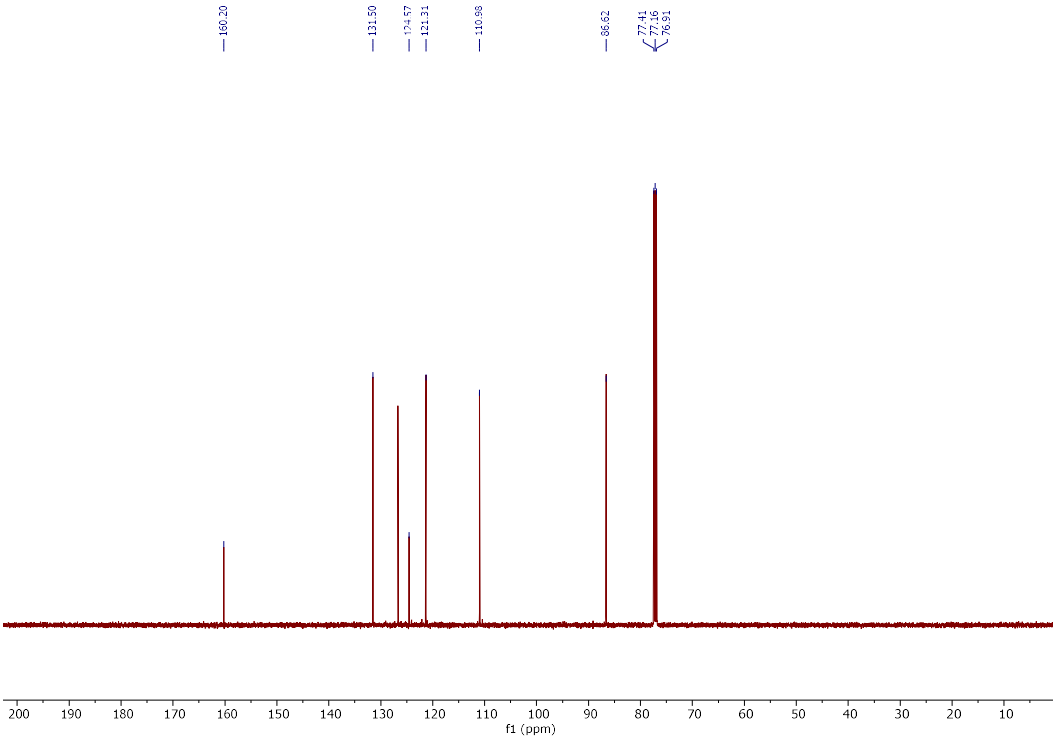

^{1}H NMR (500 MHz, $CDCl_3$)

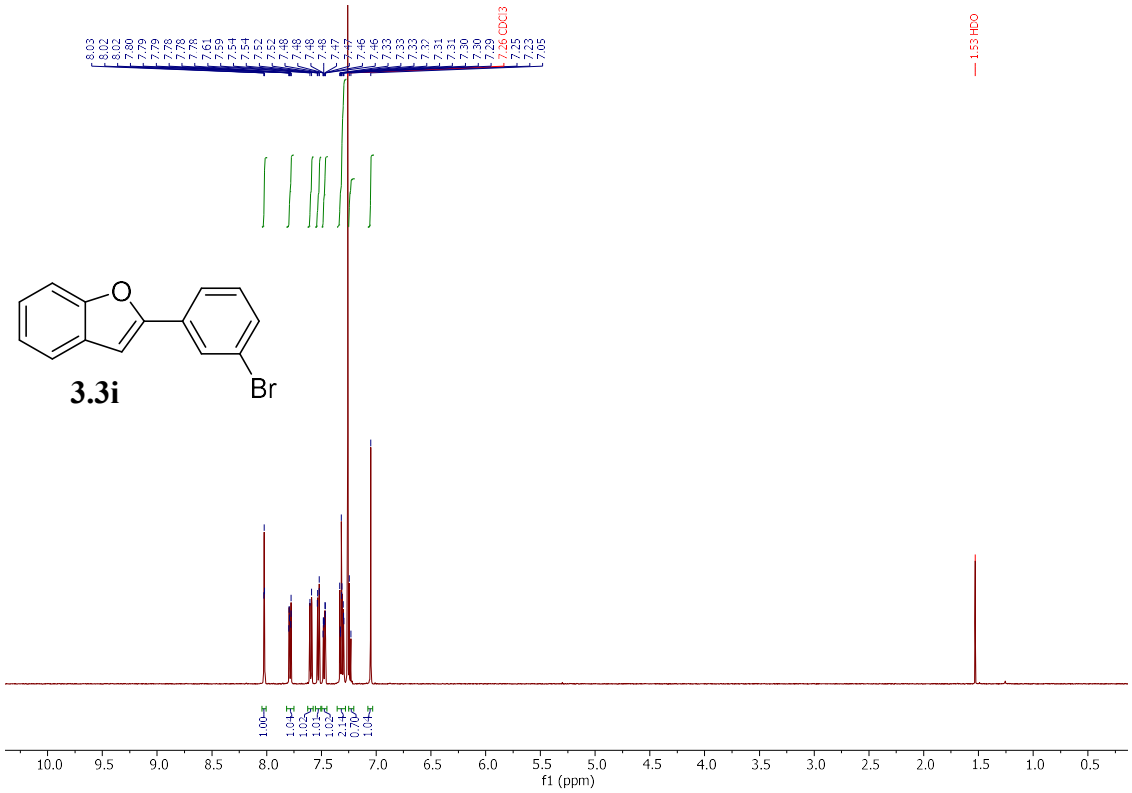

^{13}C NMR (126 MHz, $CDCl_3$)

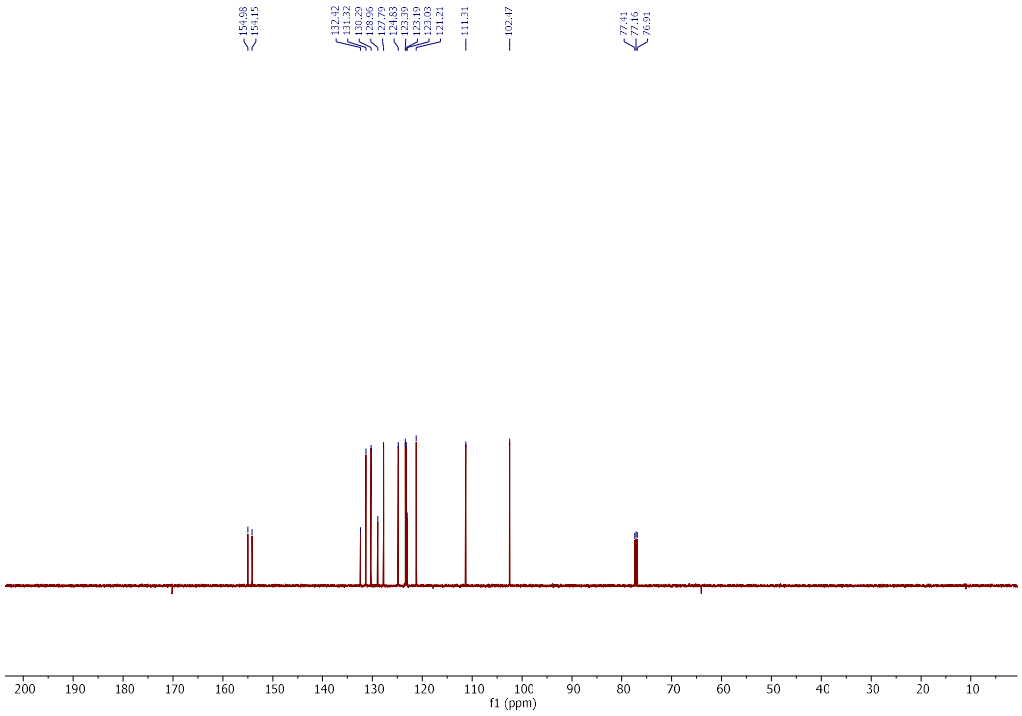

^{1}H NMR (500 MHz, $CDCl_3$)

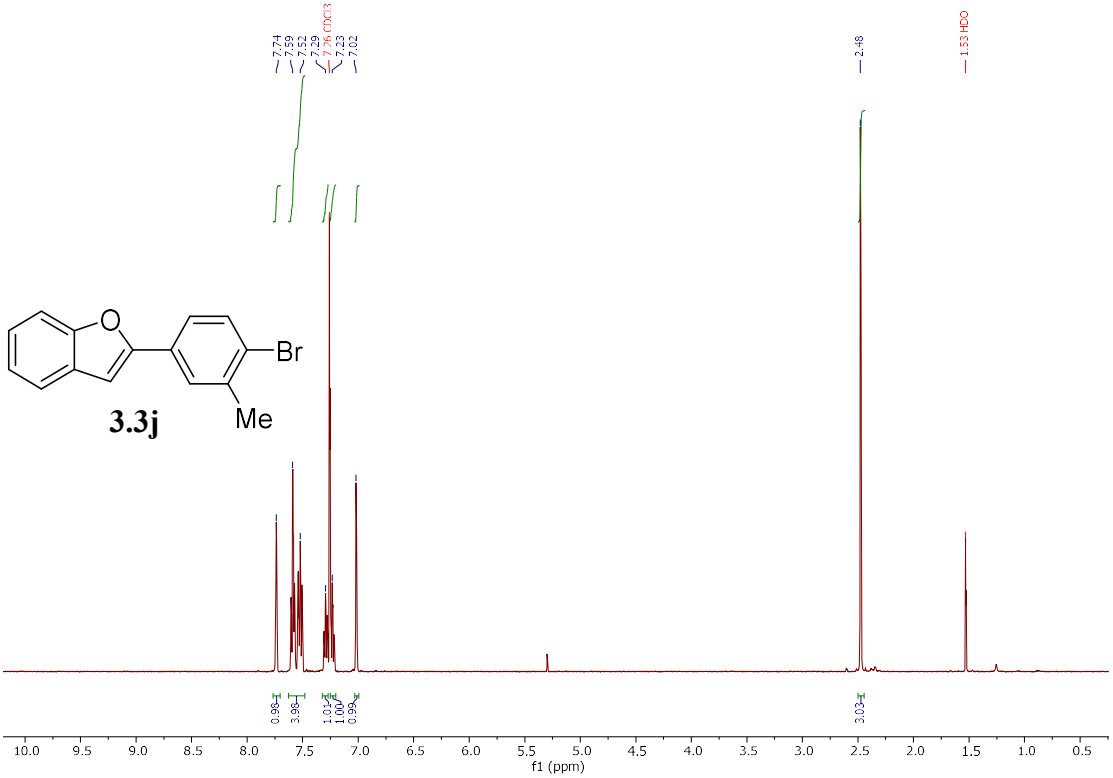

^{13}C NMR (126 MHz, $CDCl_3$)

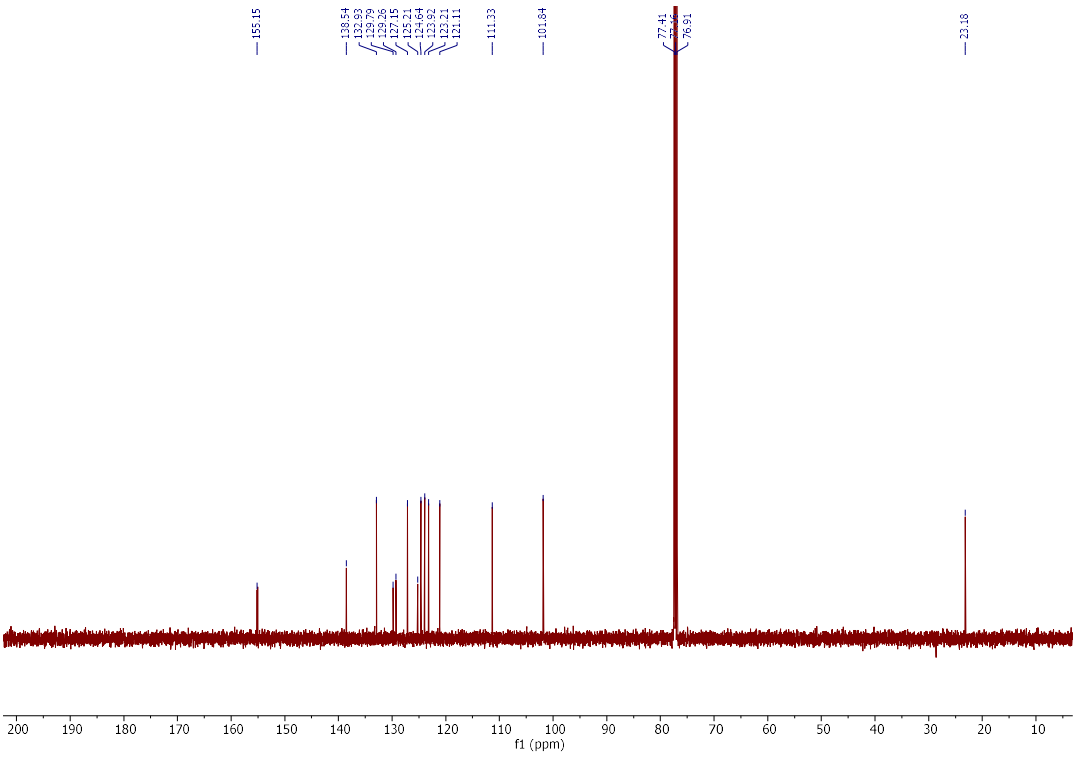

^{1}H NMR (500 MHz, $CDCl_3$)

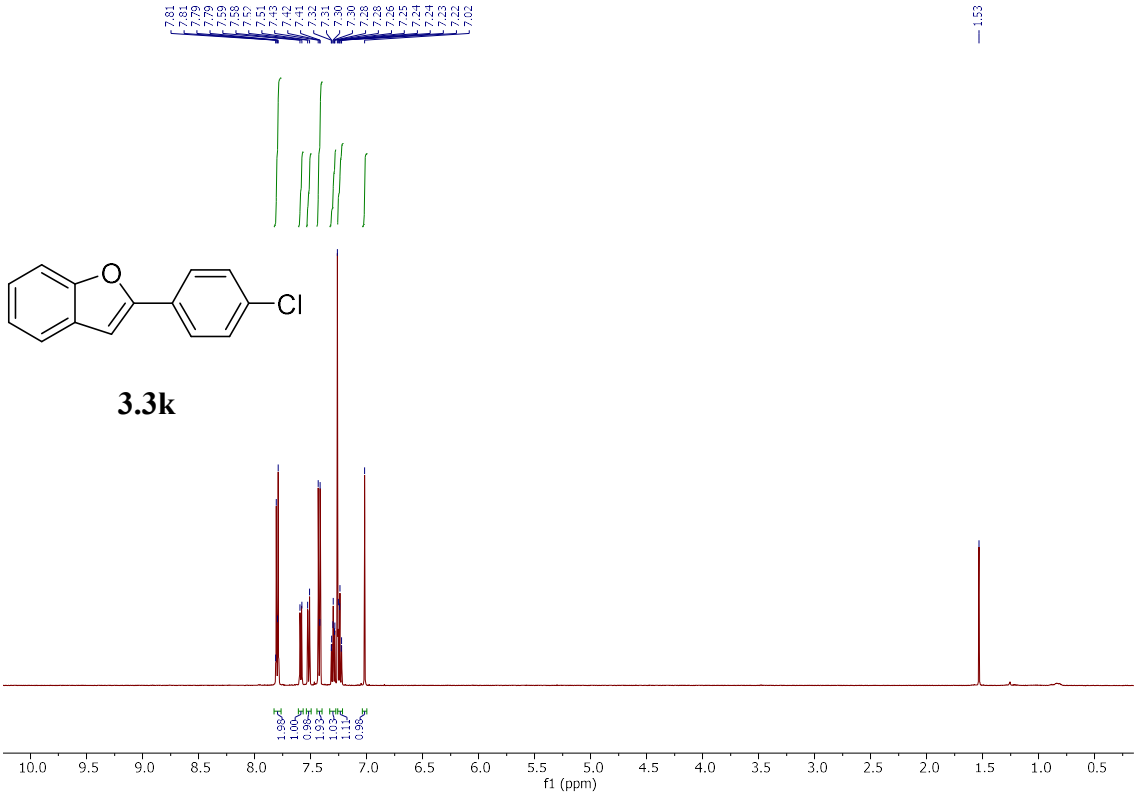

^{13}C NMR (126 MHz, $CDCl_3$)

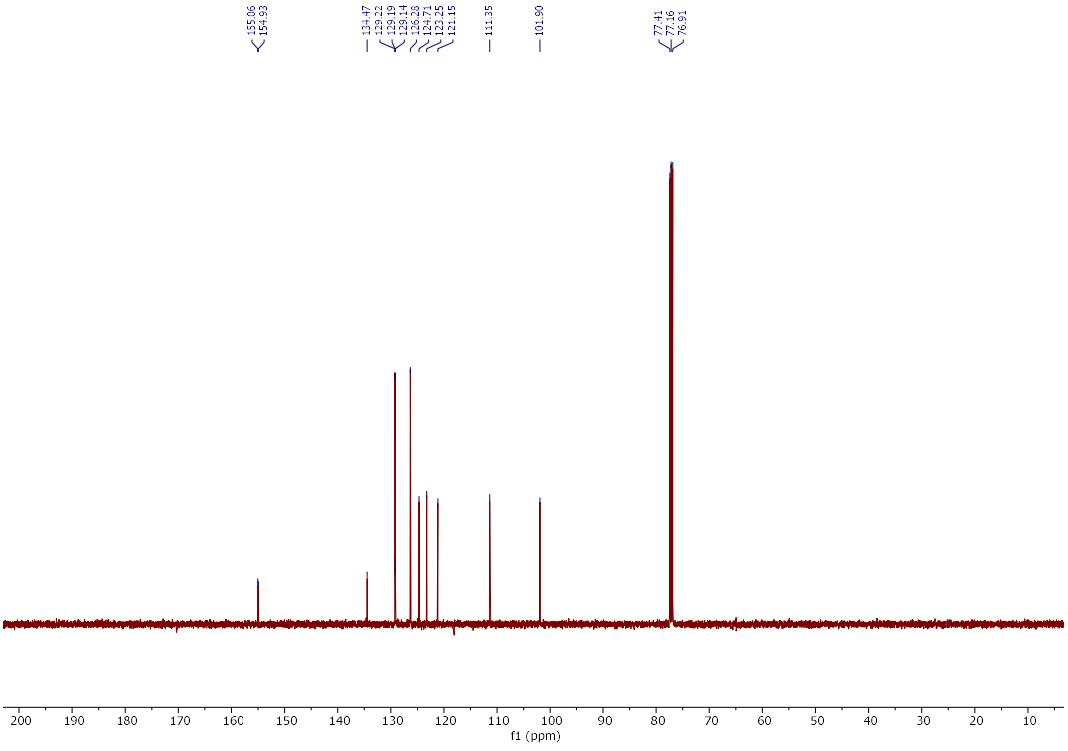

^{1}H NMR (500 MHz, $CDCl_3$)

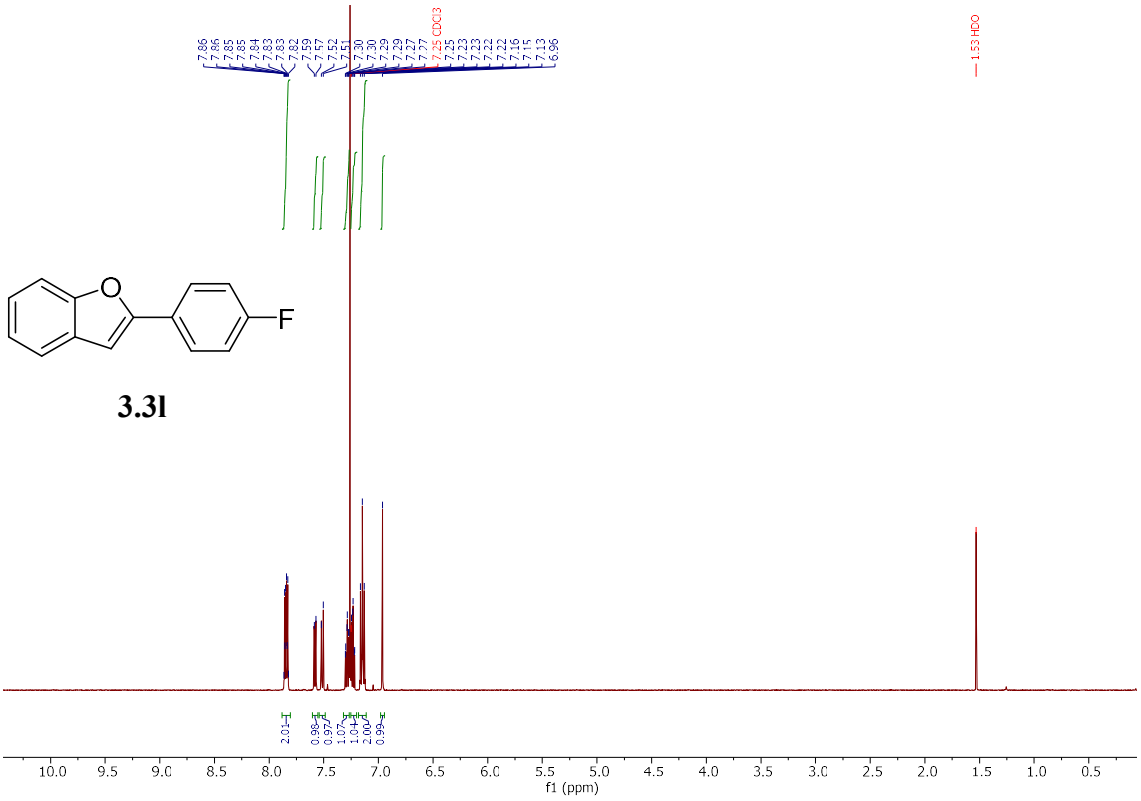

3.31

^{13}C NMR (126 MHz, $CDCl_3$)

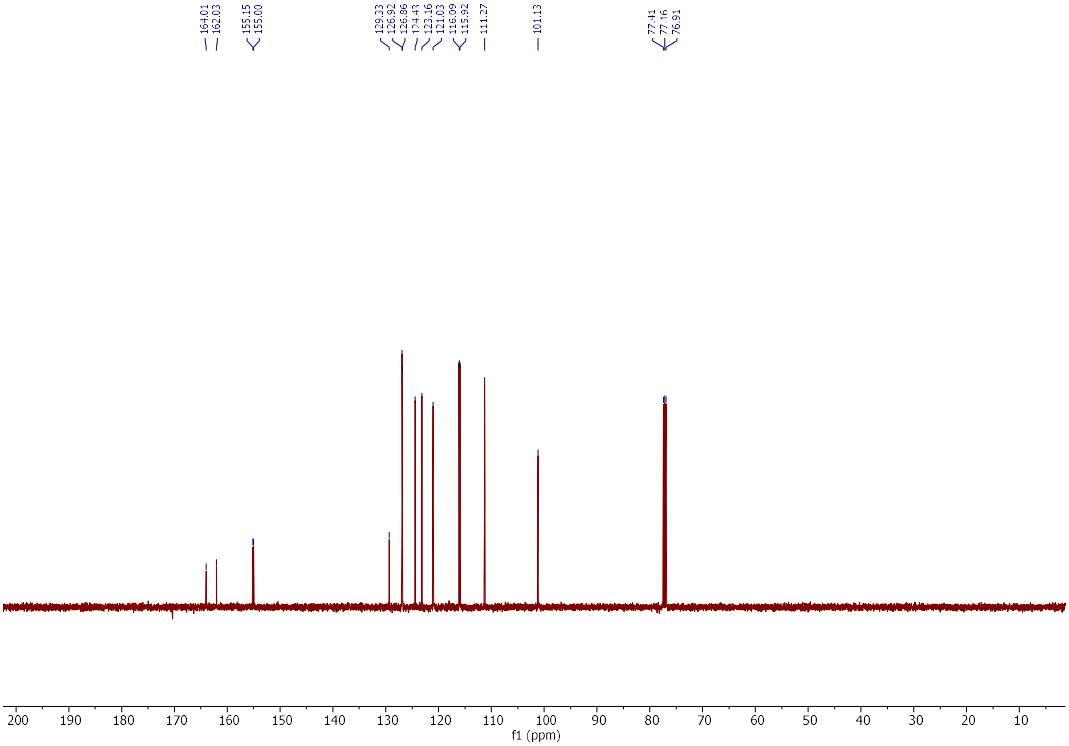

^{1}H NMR (500 MHz, $CDCl_3$)

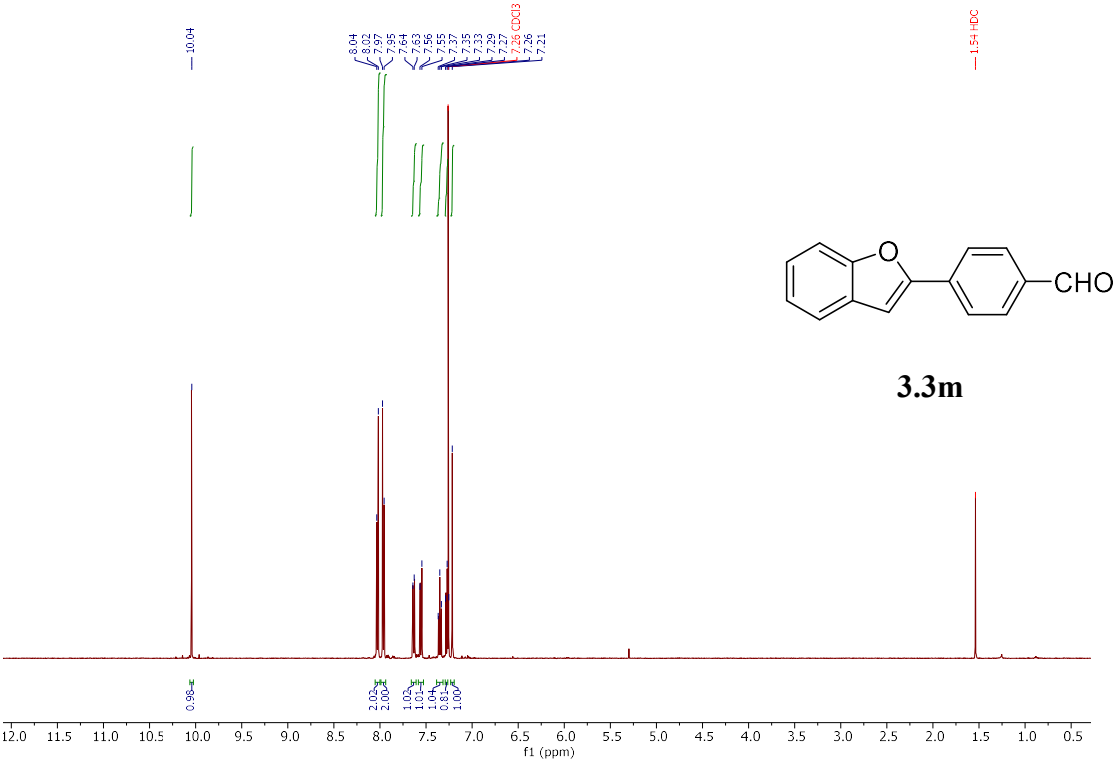

3.3m

^{13}C NMR (126 MHz, $CDCl_3$)

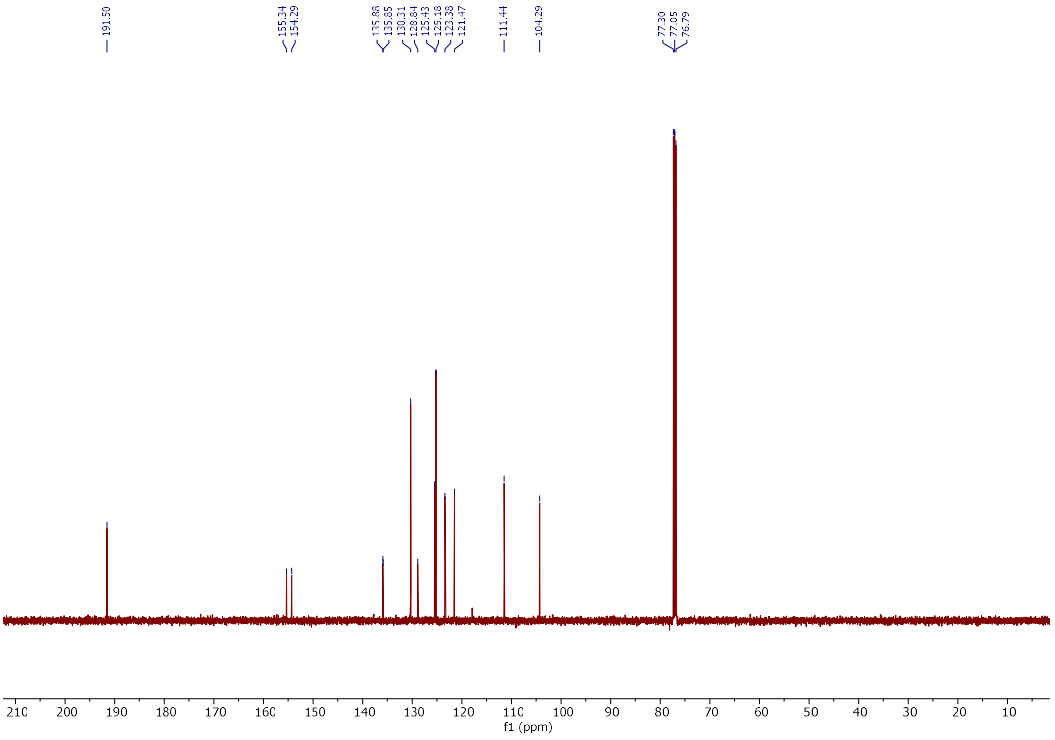

^{1}H NMR (500 MHz, $CDCl_3$)

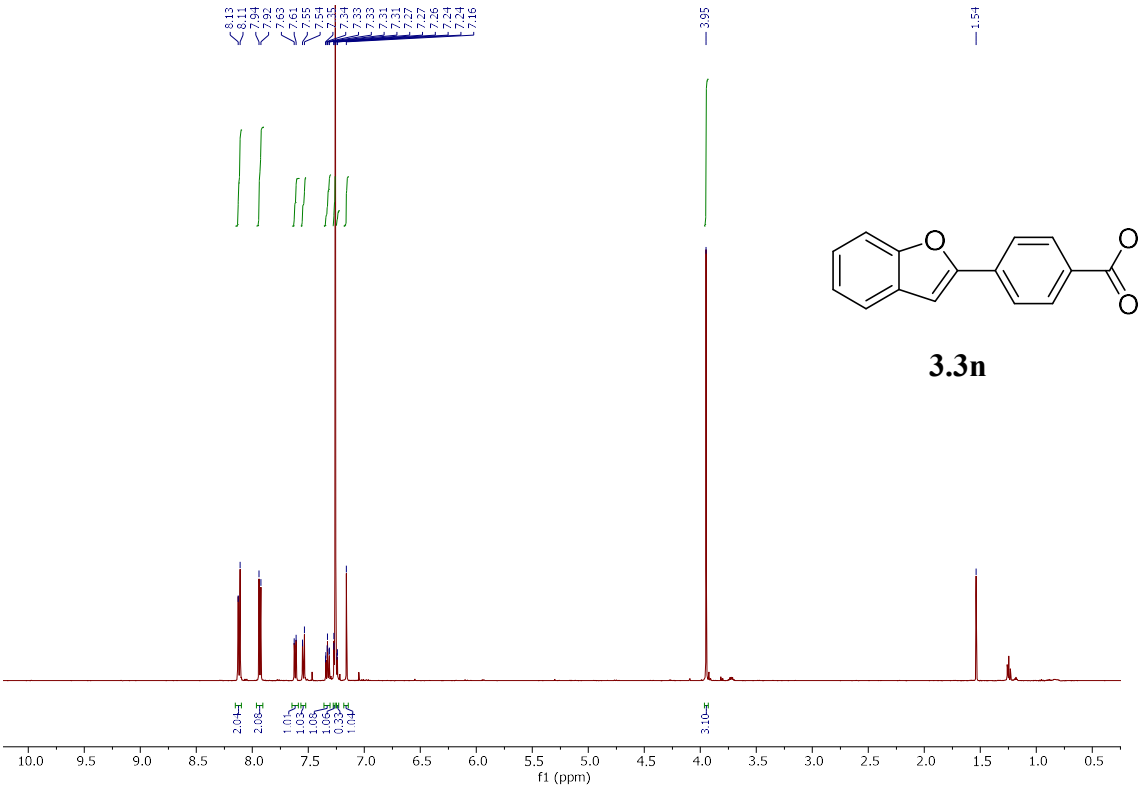

3.3n

^{13}C NMR (126 MHz, $CDCl_3$)

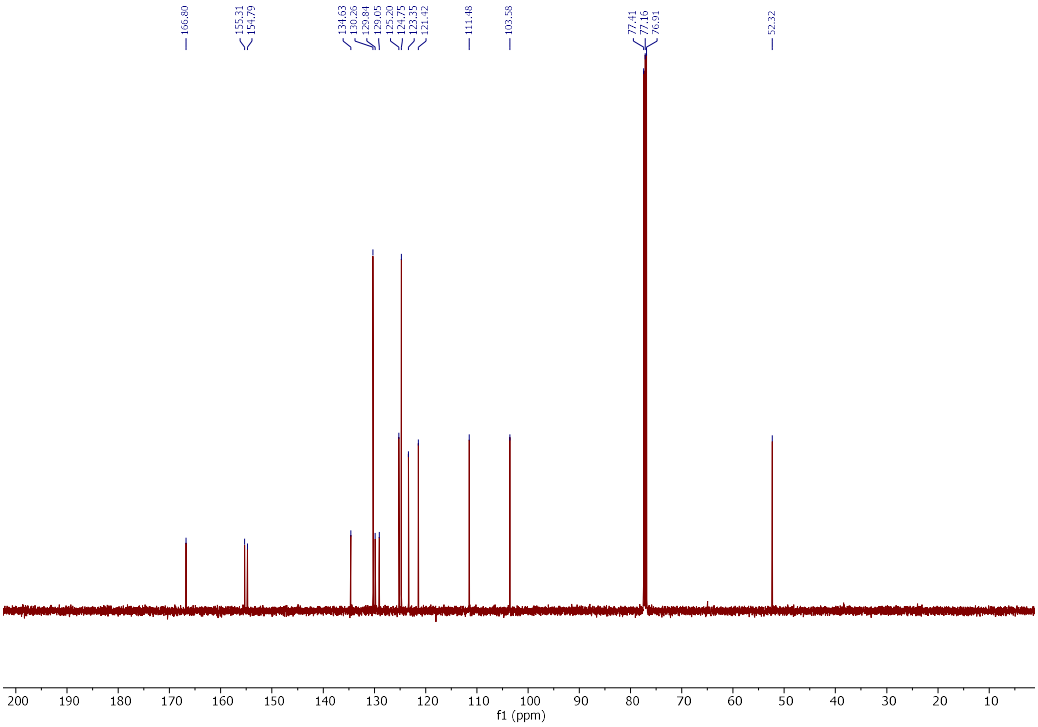

^{1}H NMR (500 MHz, $CDCl_3$)

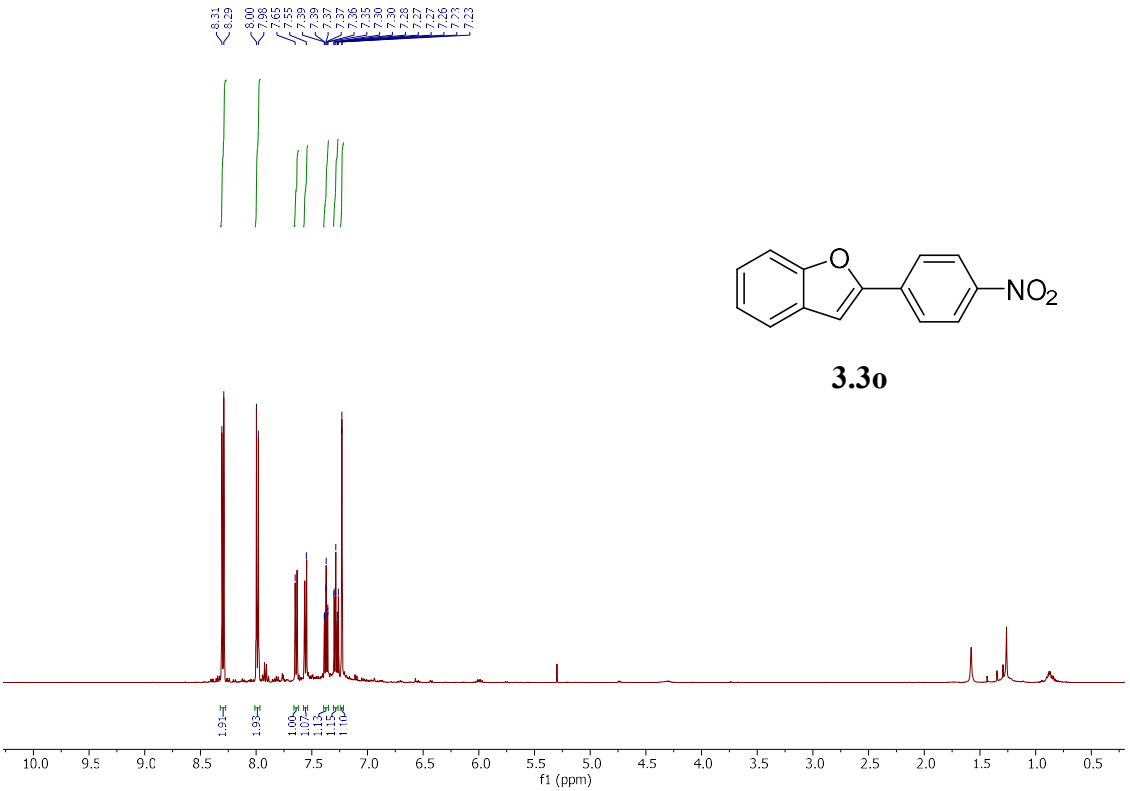

3.3o

^{13}C NMR (126 MHz, $CDCl_3$)

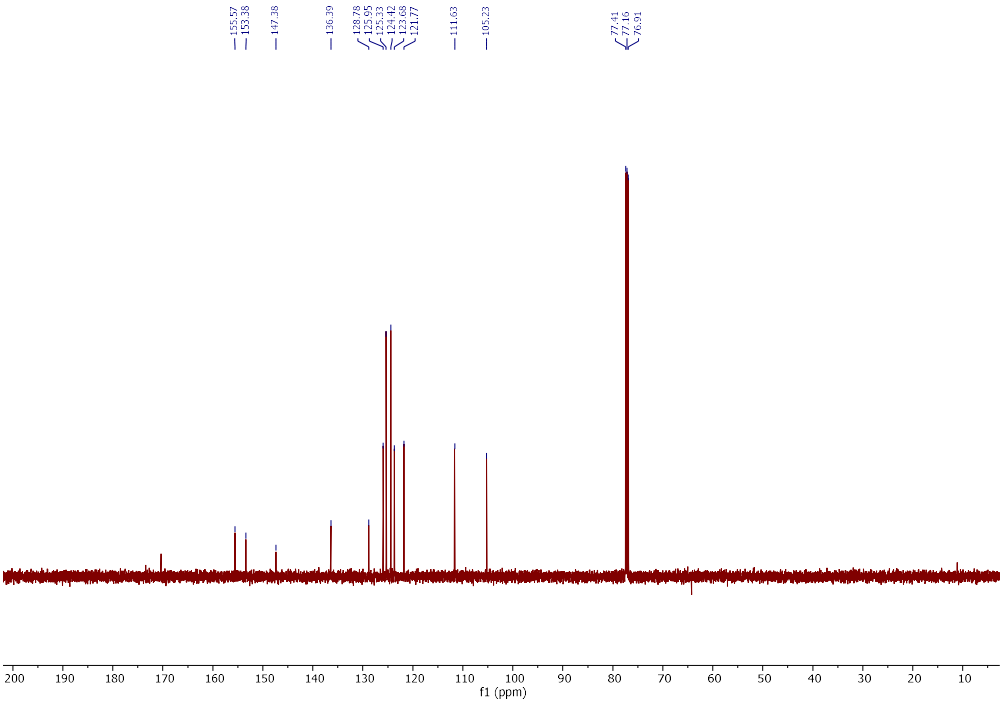

^{1}H NMR (500 MHz, $CDCl_3$)

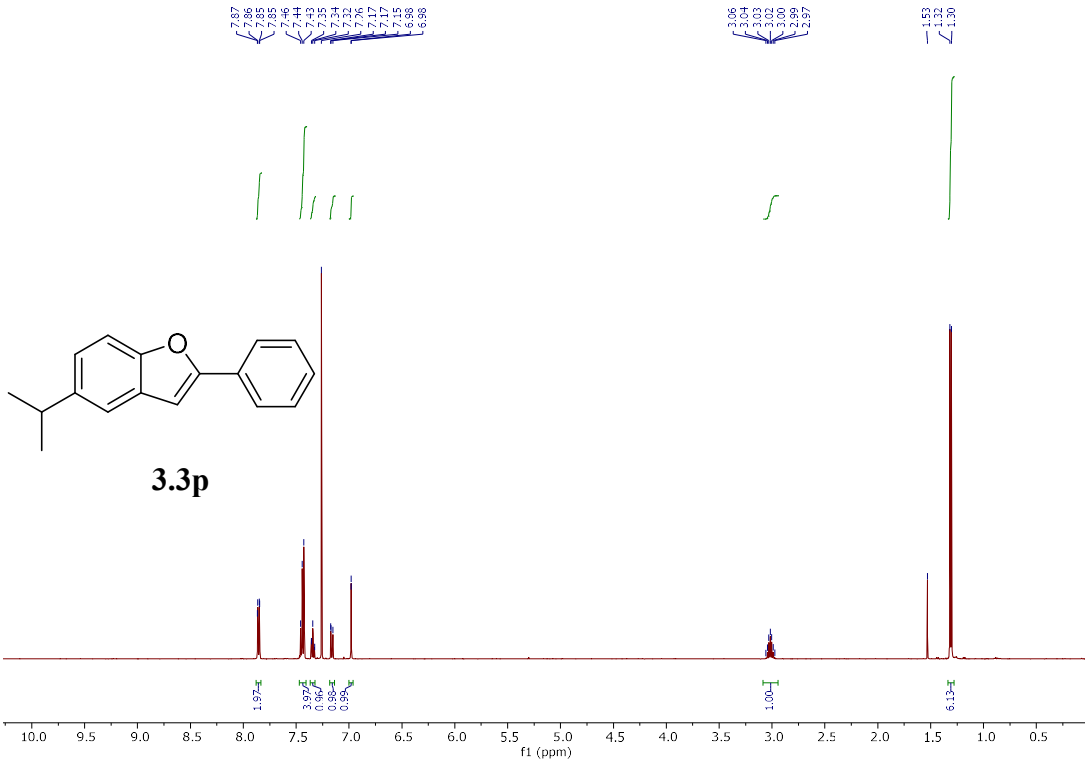

3.3p

^{13}C NMR (126 MHz, $CDCl_3$)

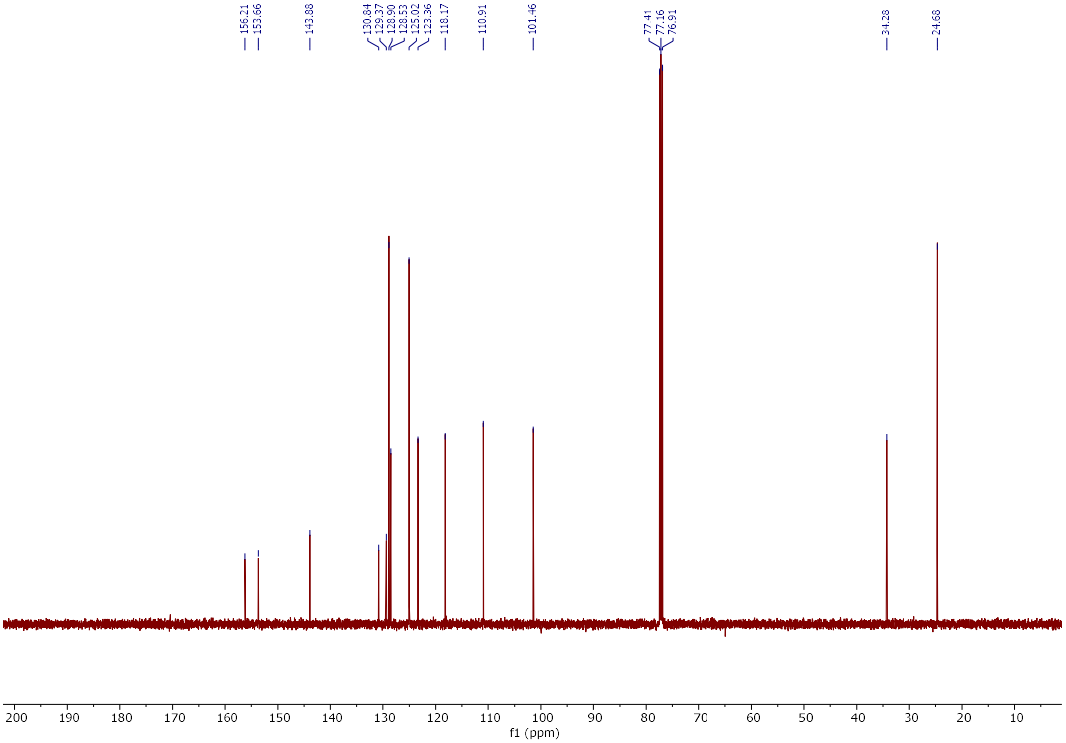

^{1}H NMR (300 MHz, $CDCl_3$)

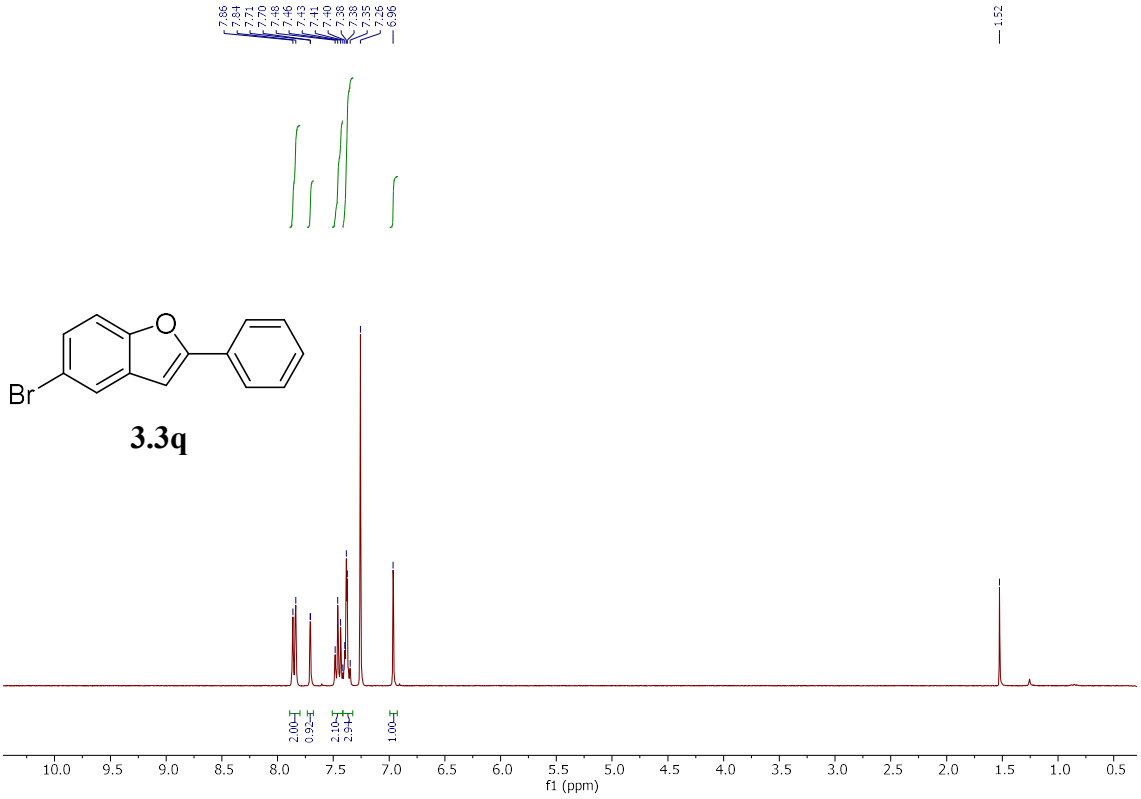

3.3q

^{13}C NMR (126 MHz, $CDCl_3$)

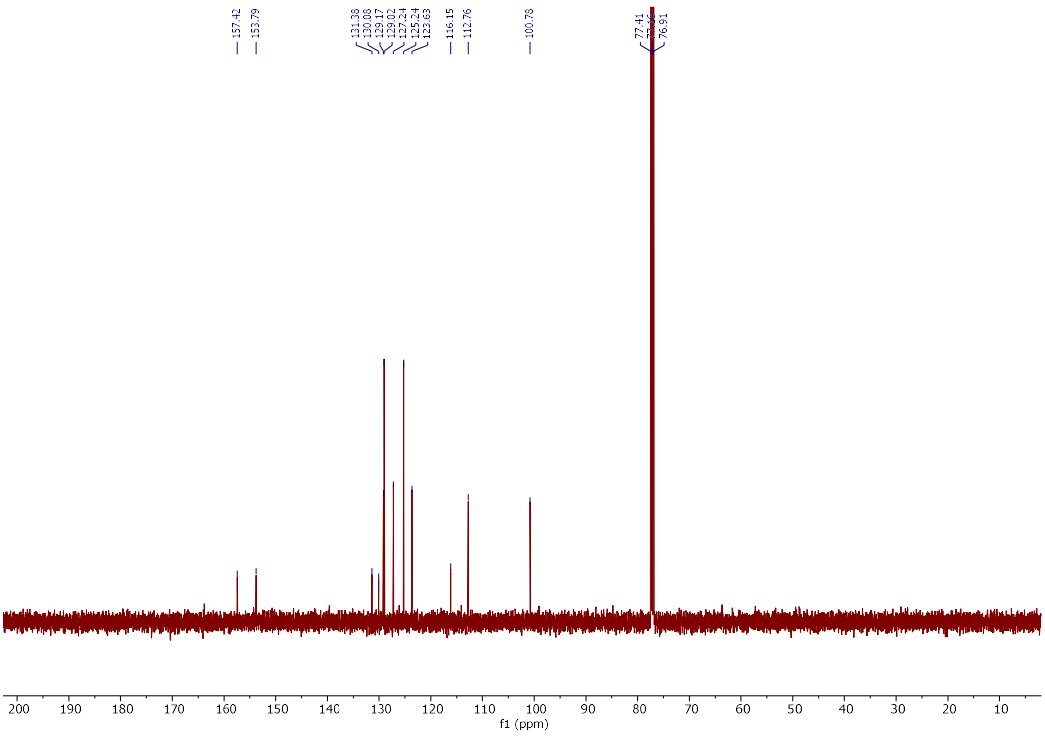

^{1}H NMR (500 MHz, $CDCl_3$)

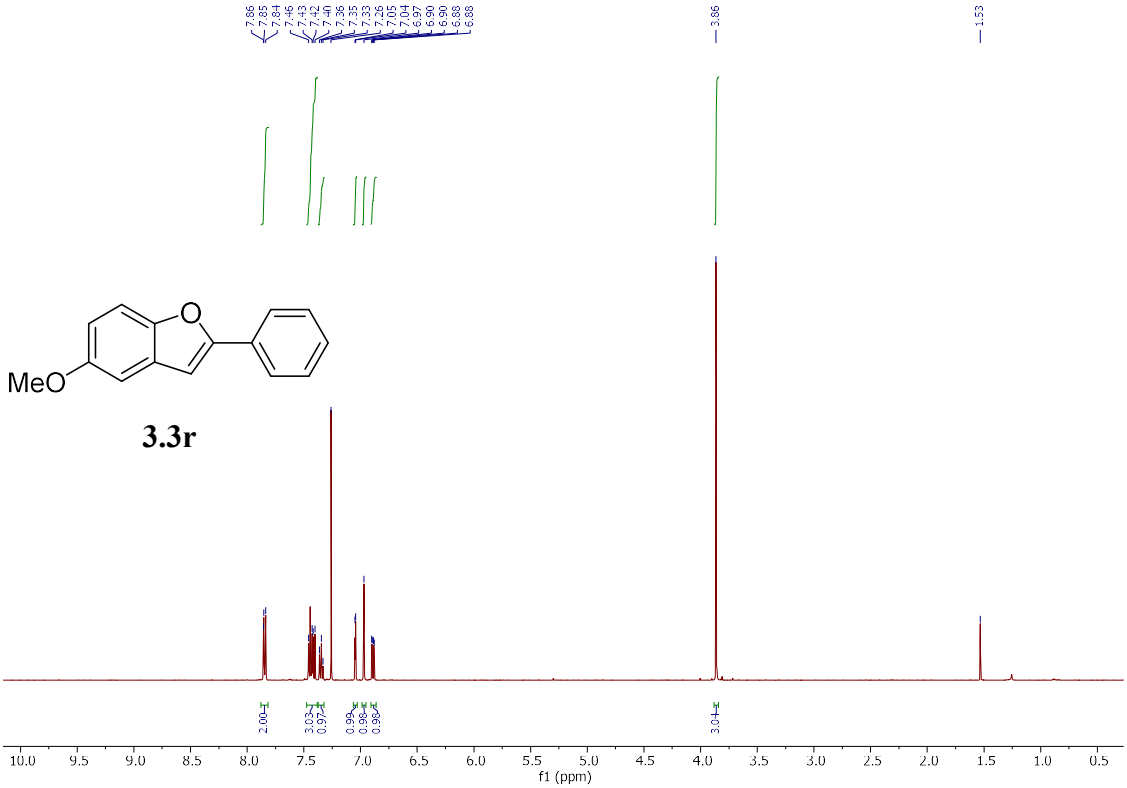

3.3r

^{13}C NMR (126 MHz, $CDCl_3$)

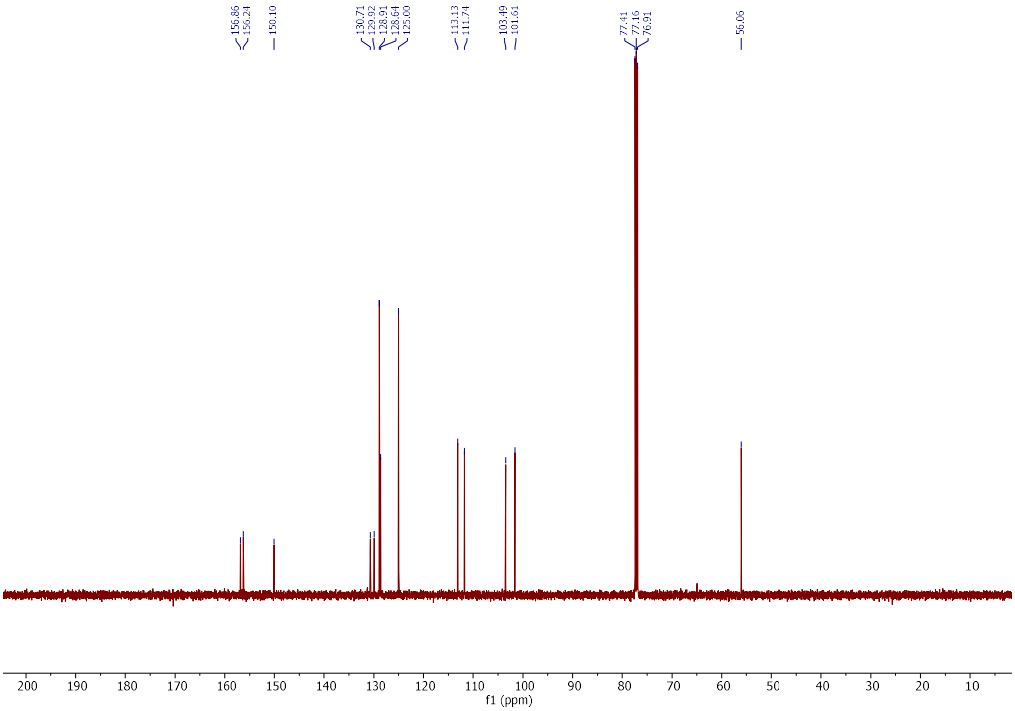

^{1}H NMR (500 MHz, $CDCl_3$)

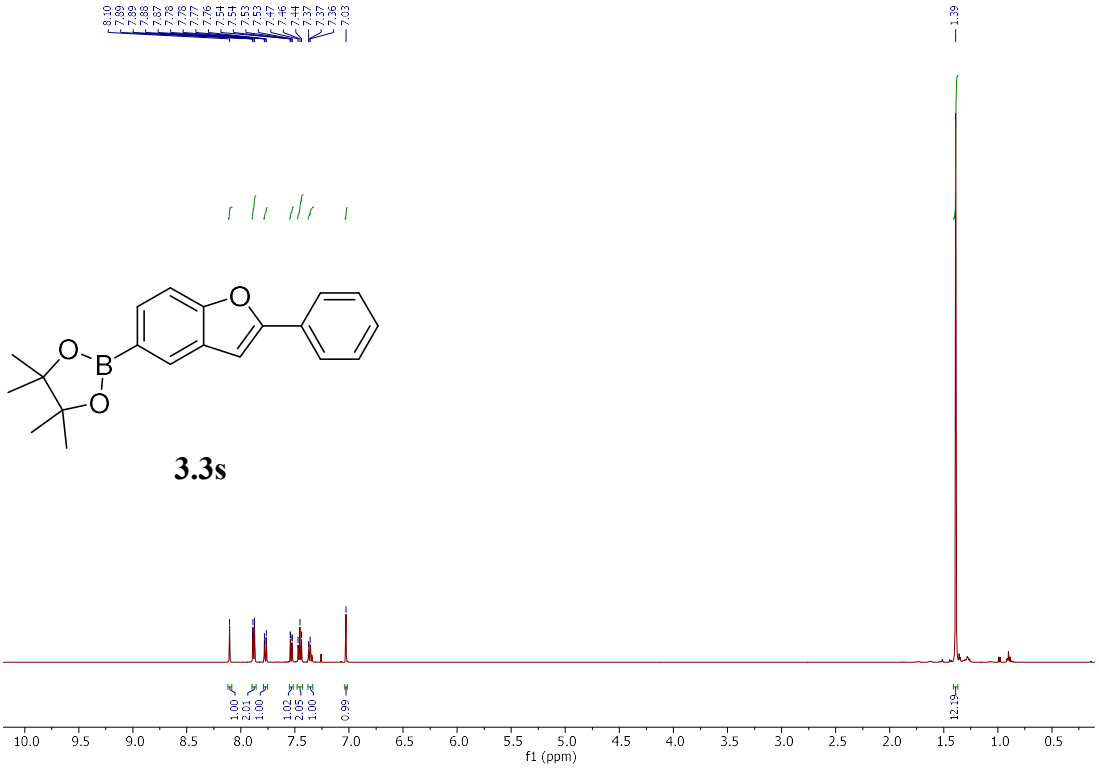

3.3s

^{13}C NMR (126 MHz, $CDCl_3$)

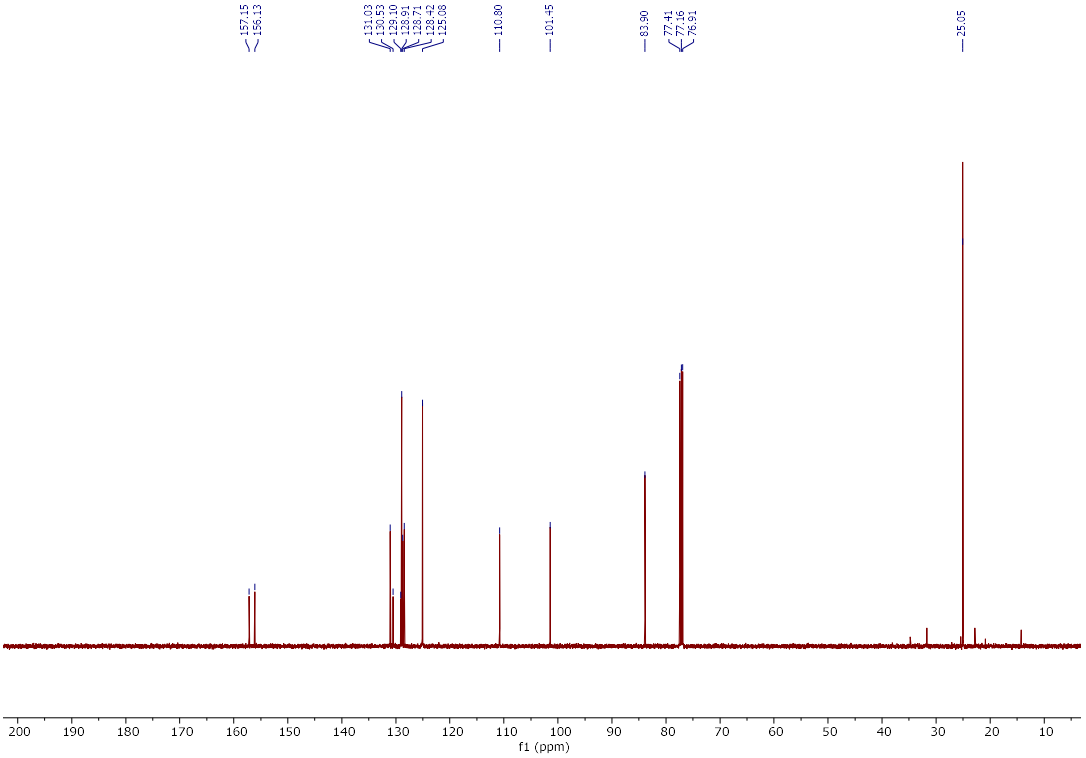

^{1}H NMR (500 MHz, $CDCl_3$)

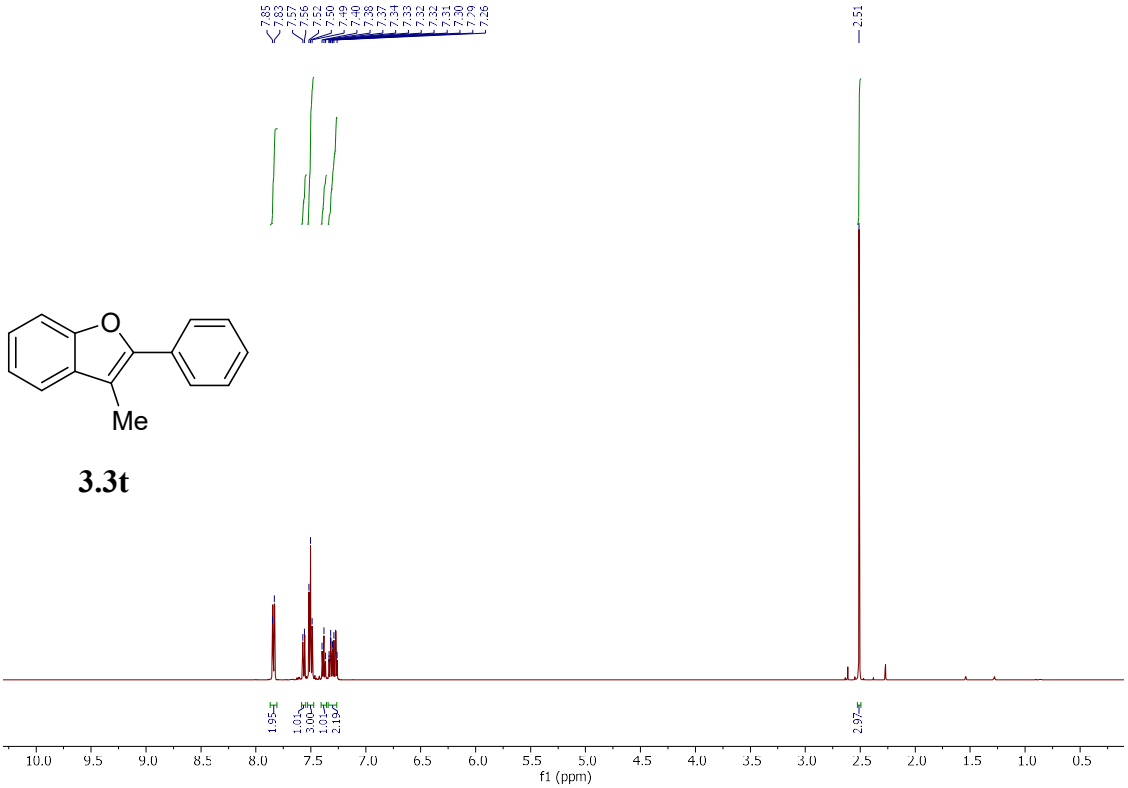

3.3t

^{13}C NMR (126 MHz, $CDCl_3$)

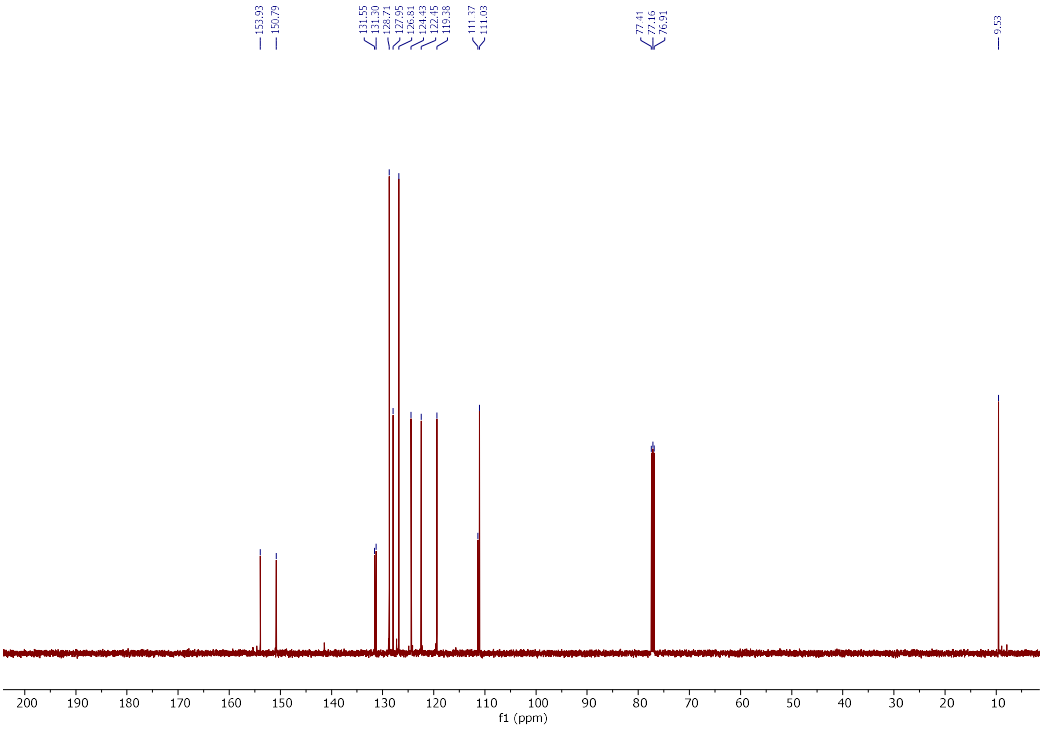

^{1}H NMR (500 MHz, $CDCl_3$)

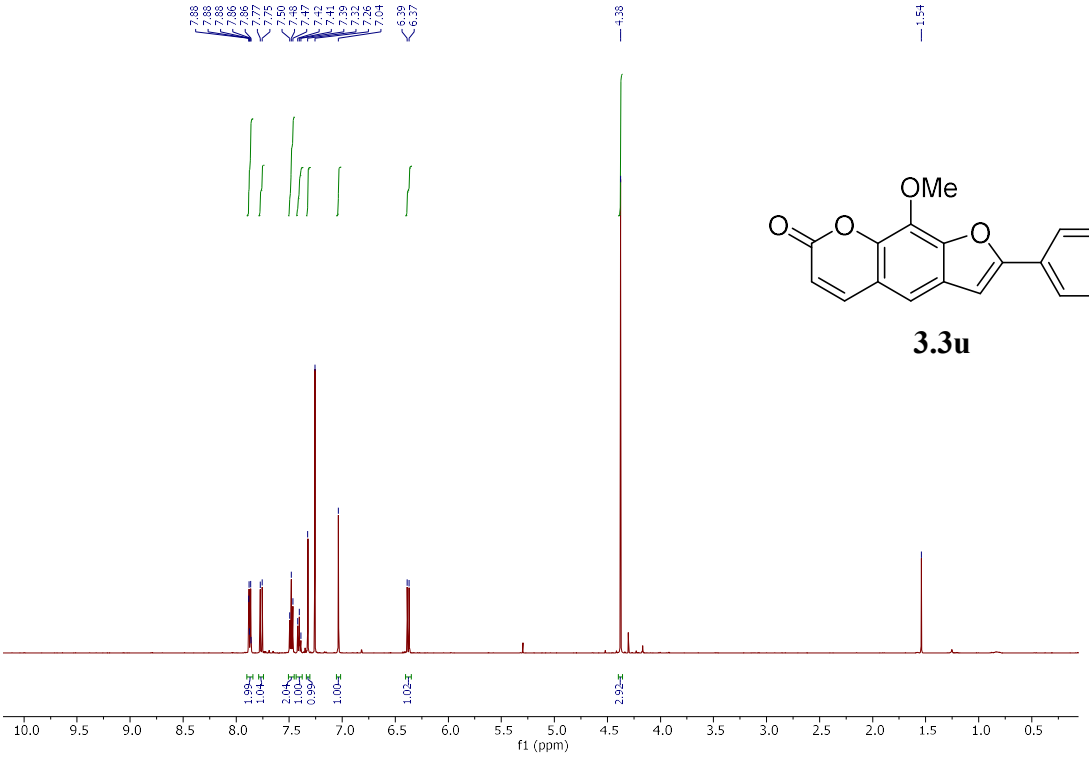

3.3u

^{13}C NMR (75 MHz, $CDCl_3$)

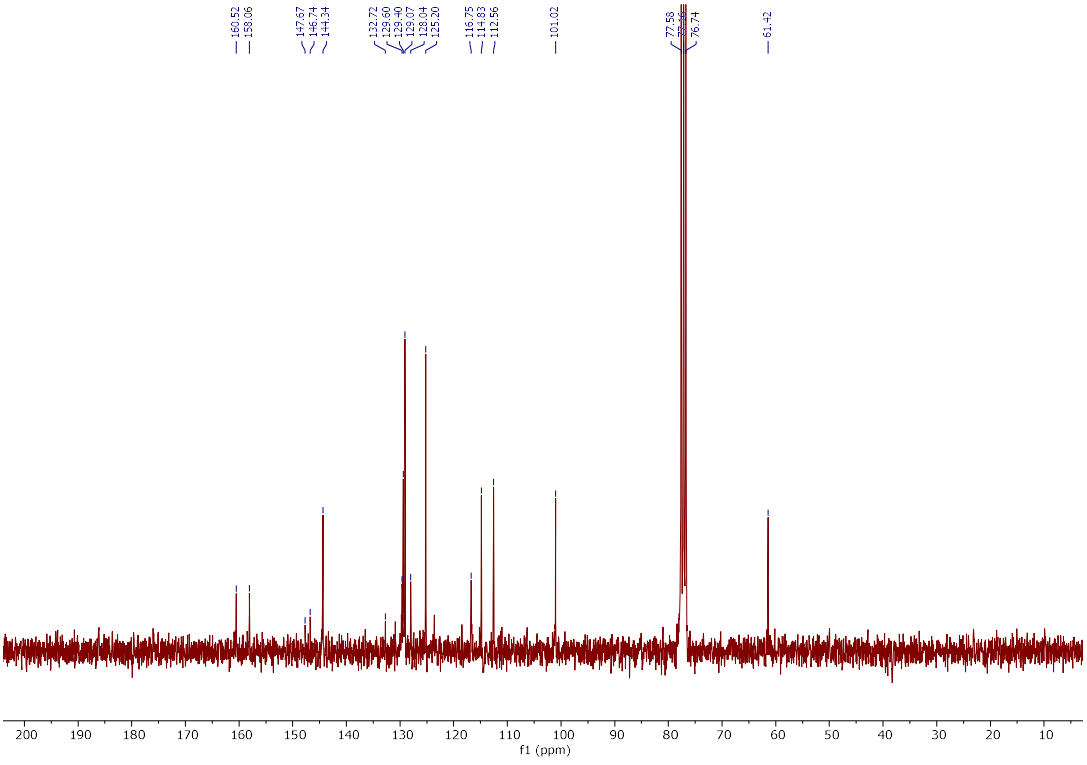

^{1}H NMR (500 MHz, $CDCl_3$)

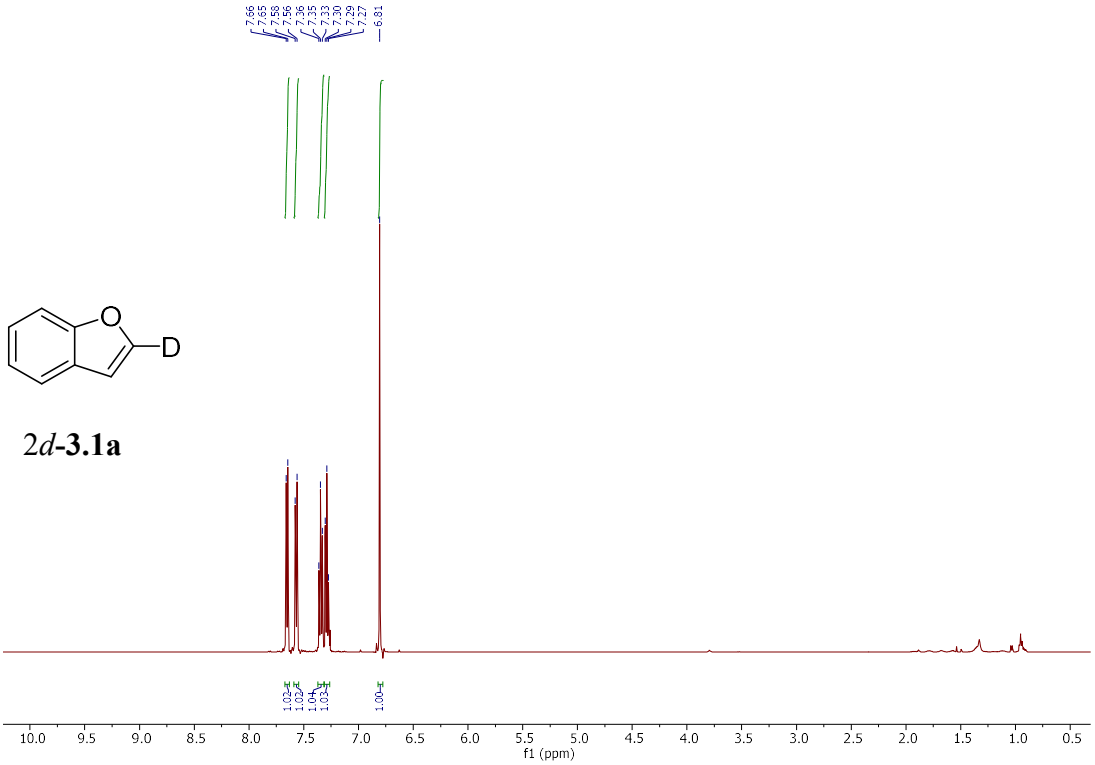

2*d*-3.1a

^{13}C NMR (126 MHz, $CDCl_3$)

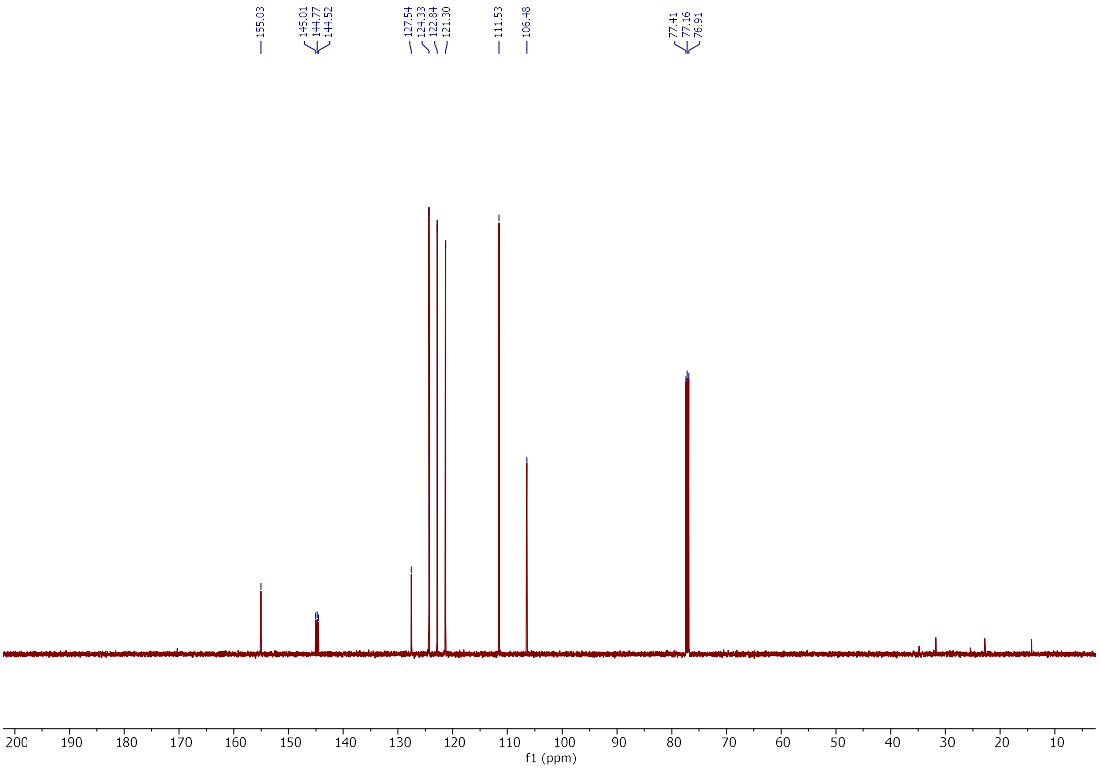

^{1}H NMR (500 MHz, $CDCl_3$)

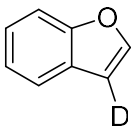

3*d*-**3.1a**

^{13}C NMR (126 MHz, $CDCl_3$)

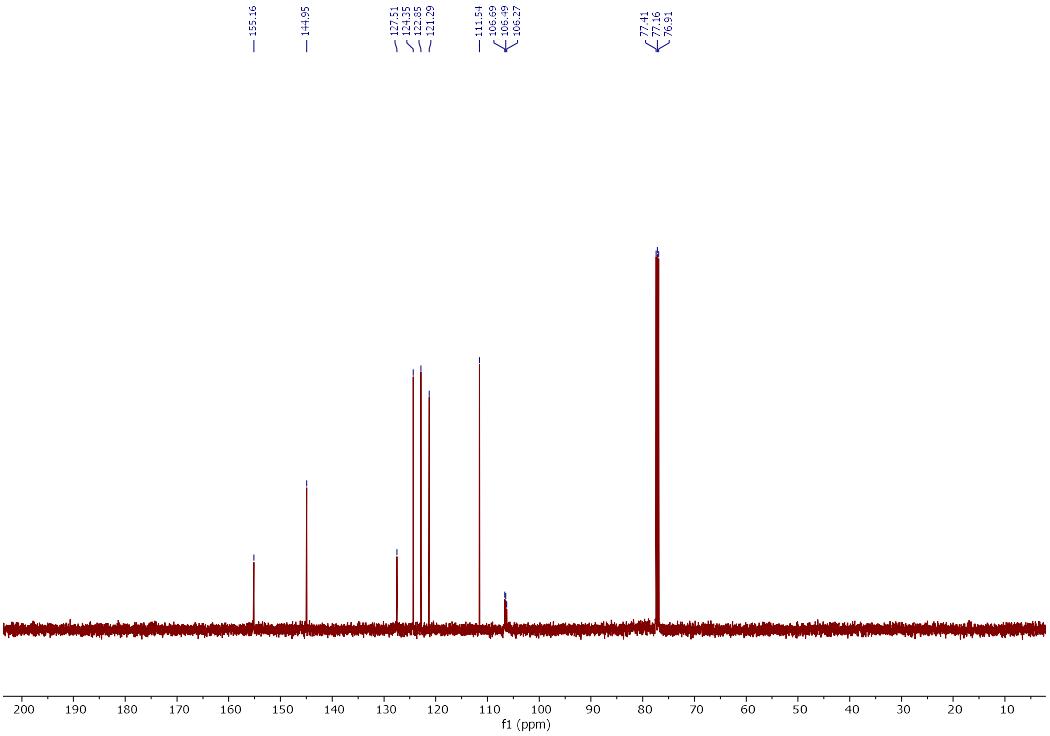

^{1}H NMR (500 MHz, $CDCl_3$)

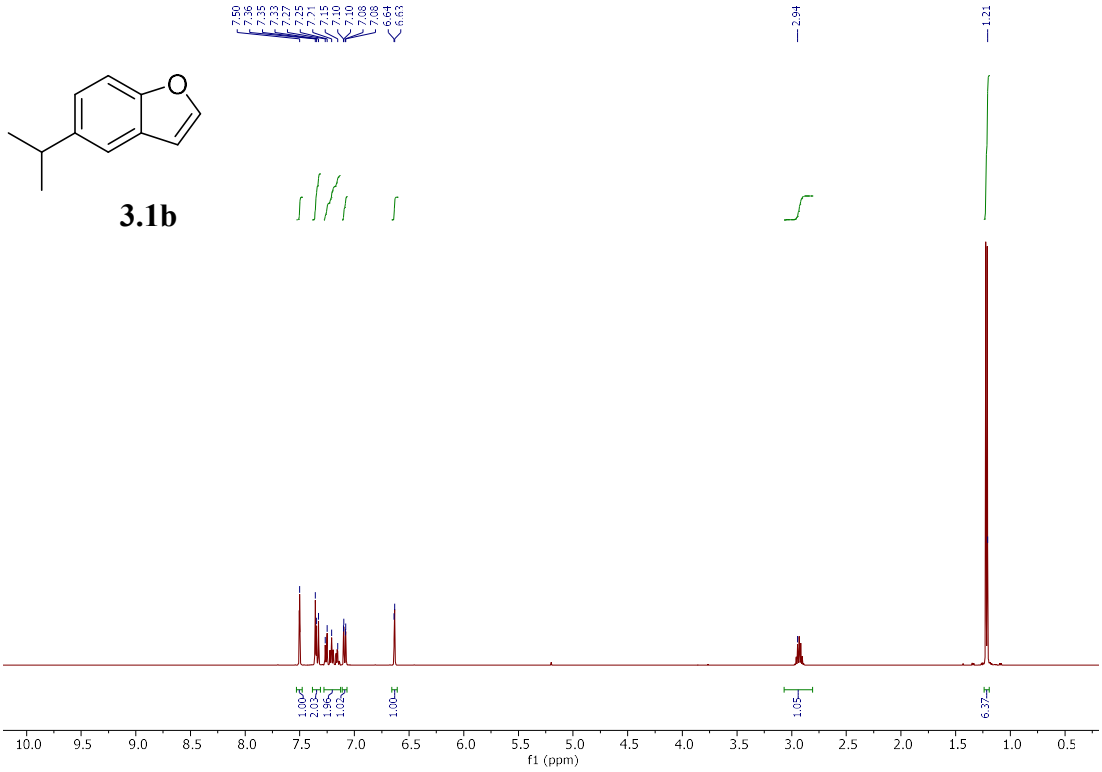

3.1b

^{13}C NMR (126 MHz, $CDCl_3$)

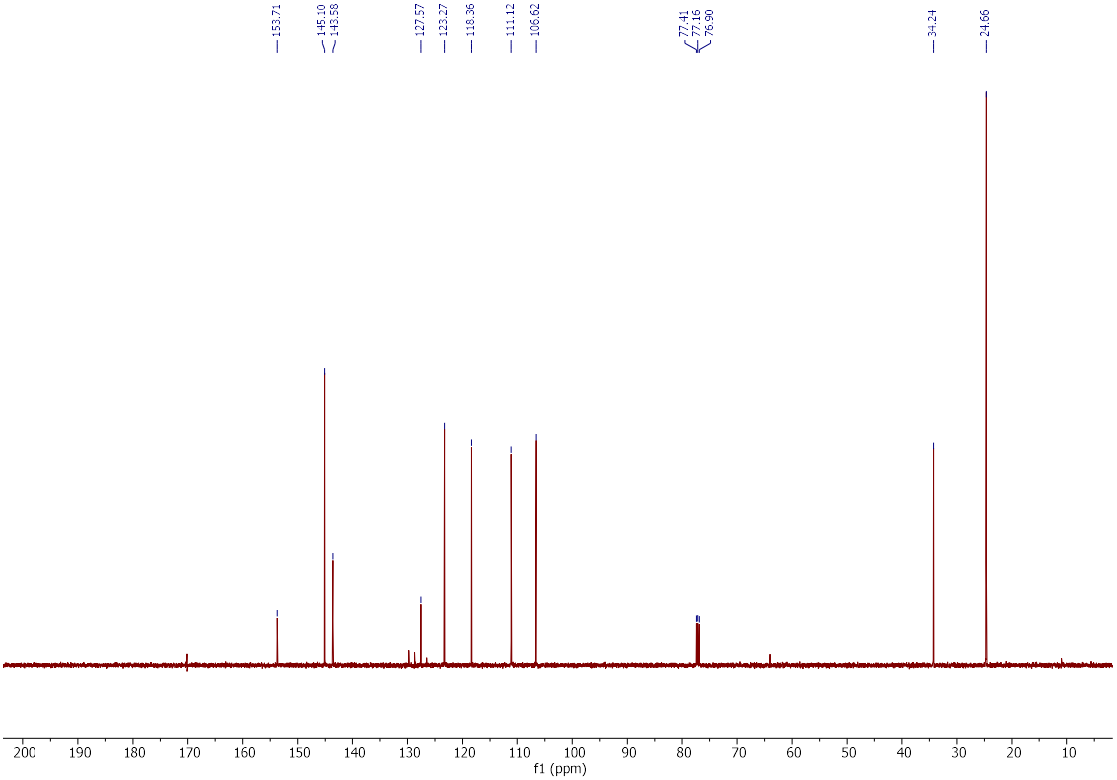

^{1}H NMR (500 MHz, $CDCl_3$)

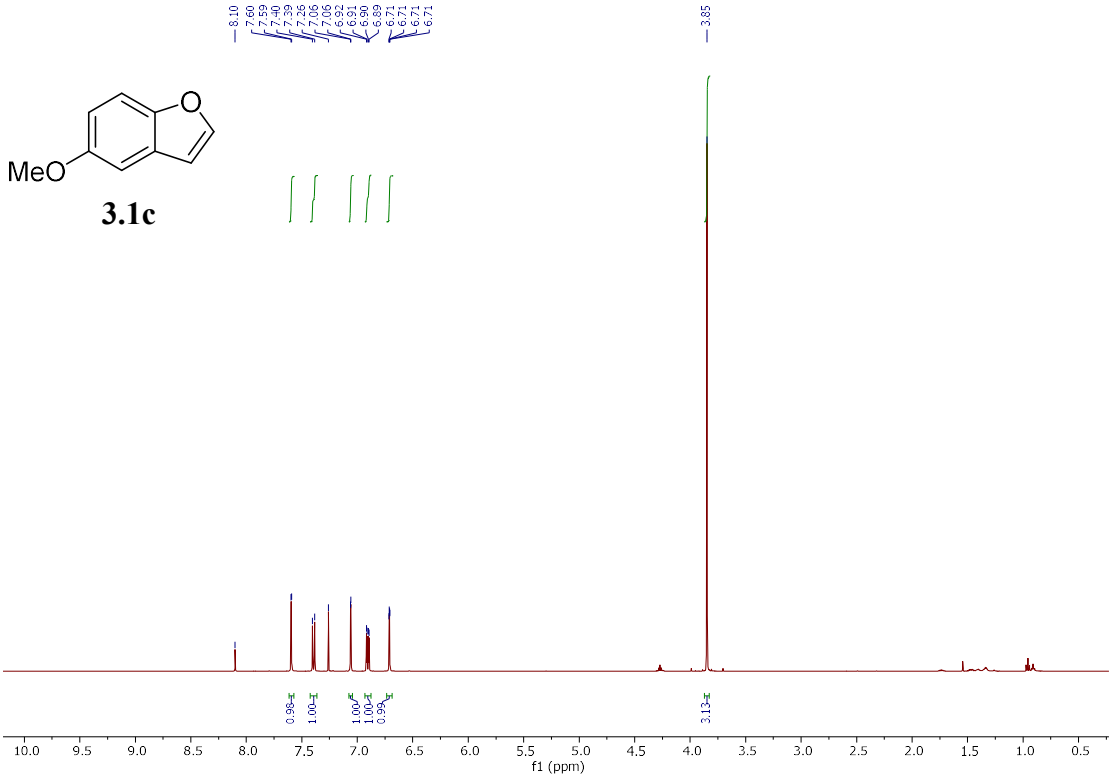

3.1c

^{13}C NMR (126 MHz, $CDCl_3$)

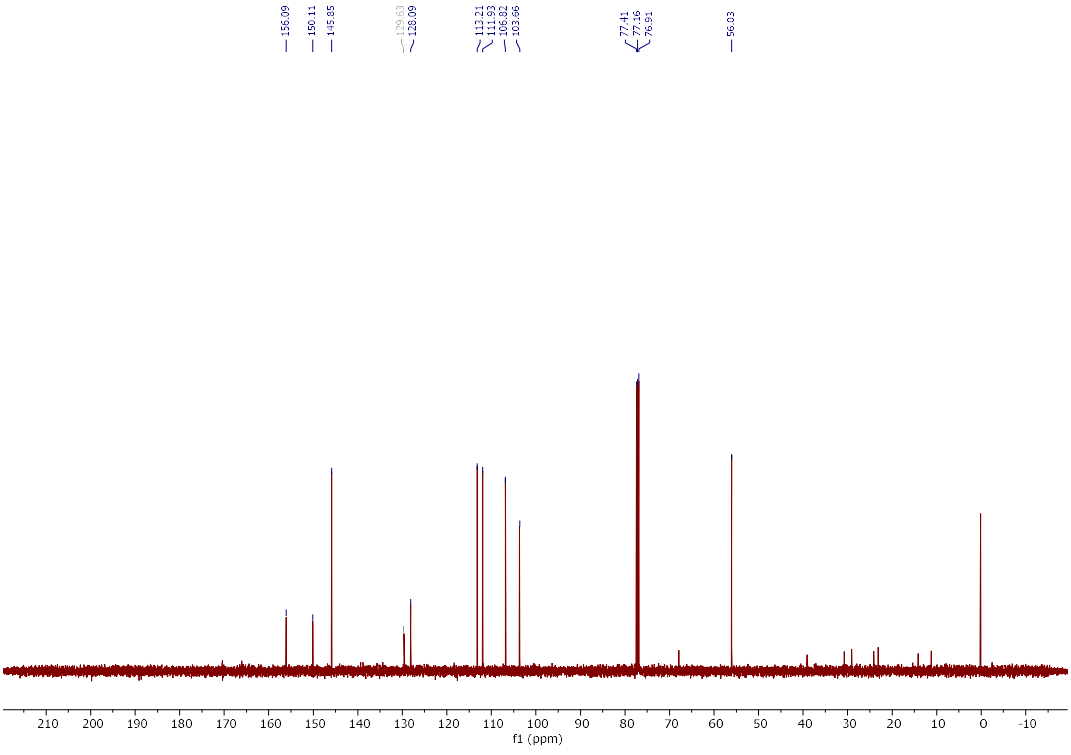

^{1}H NMR (500 MHz, $CDCl_3$)

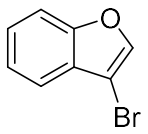

3.1d

^{13}C NMR (126 MHz, $CDCl_3$)

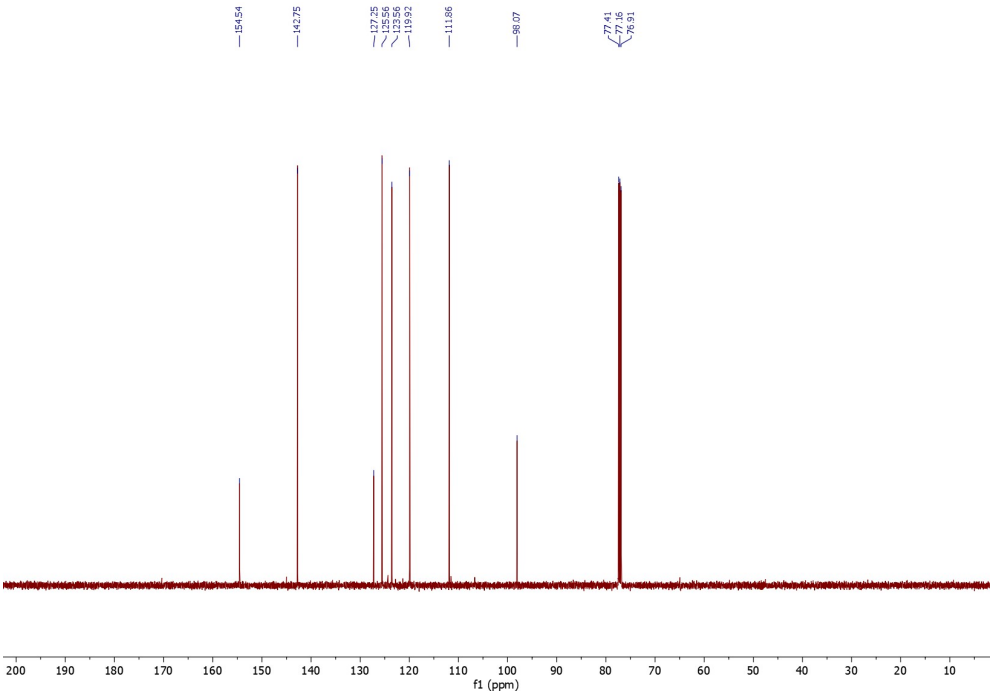

Chapter 4. Circular Discovery in Small Molecule and Conjugated Polymer Synthetic Methodology

*The work in Chapter 4 is adapted from a previously submitted article: Reprinted with permission from *J. Am. Chem. Soc.* **2022**.

4.1 Introduction

The advent and growth of organic electronics can be attributed to the breadth of synthetically accessible conjugated polymers, originating with polyacetylene,[1] and expanding to include recent examples of complex donor-acceptor copolymers.[133] In comparison to inorganic semiconducting materials, desired properties in conjugated polymers can be accessed by fine tuning the molecular structure. Although the development of high-performance conjugated materials has contributed immensely to advancements in the field of organic electronics in the last two decades,[3,134,135] limited access to low-cost synthetic routes still represents a barrier for their large-scale production and commercial applications. Various synthetic methodologies have been developed to obtain high-performance conjugated polymers,[136,137] including conventional cross-coupling polymerizations such as Stille and Suzuki polymerizations (**Scheme 4.1a**).[138,139] These approaches are favored for their ability to generate materials with desired structural and electronic properties. The ability to access high molecular weight, low-defect materials arises from monomer prefunctionalization, which creates site-specific, highly reactive cross-coupling. At the same time, the requisite monomer prefunctionalization gives these conventional synthetic pathways poor atom and step economy. Most notably, the commonly used Stille polymerization generates stoichiometric amounts of toxic organostannane waste.

Developing an efficient, inexpensive, and green synthetic route is important for the large-scale industrial production of conjugated polymers. DArP has emerged as a powerful and competent strategy for the synthesis of organic conjugated materials (**Scheme 4.1b**).[140,141] The most appealing aspects of this approach are reduced organometallic waste and improved step economy as no organometallic prefunctionalization is required. DArP is distinguished as a sustainable and atom-economic approach for constructing C-C bonds over traditional coupling methods by features including generating benign by-products and only requiring functionalization of one component with routine and bench-stable halogens.

Scheme 4.1. Synthetic approaches to conjugated polymers

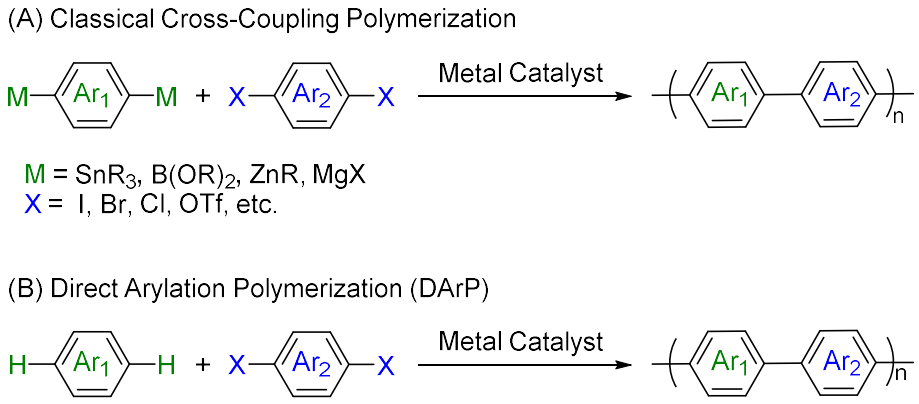

Early DArP studies worked to adapt existing small molecule methodology to polymerizations.[142] Recent work has focused on controlling the C-H bond selectivity to minimize structural defects, and improving the sustainability of the method.[143] Significant progress has been made towards improving DArP methodology, including improving selectivity of C-H bonds, improving reaction yields, broadening substrate scope, and developing first-row transition metal catalysts. Greater improvements in accessing conjugated structures are still needed, both using direct arylation and by novel transformations. Current DArP methodology originates

primarily from adapting seminal small molecule direct arylation reports. As such, continued advancements in synthetic methods for polymer synthesis should look to developments in the small molecule literature. Polymerization studies provide unique perspectives on a transformation, as even small deviations in selectivity and reactivity can have significant impact on a resultant polymer's properties. While it is common for polymerization conditions to be modeled after small molecule reactions (e.g. PIn in Chapter 2), it is uncommon for new small molecule transformations to be born out of the discoveries of polymerization trials. Polymerization studies can offer valuable considerations to improving the efficiencies of both future polymerizations and small molecule transformations.

A wealth of information on DArP can be found in the numerous review articles previously published.[38,39,70,144–146] Topical review articles are also available, addressing topics such as defects in DArP-produced polymers,[59,147] and improving DArP's sustainability.[148–150] To ameliorate the existing literature, this chapter presents a strategy in developing new methodologies for conjugated polymer synthesis. DArP is focused on as a useful example, with guidance on how to adapt existing small molecule methodologies to develop novel polymerizations. Frequently, when this is done, resultant polymers have structural defects not predicted by the small molecule transformations. These defects provide valuable information on the nature of the polymerization and small molecule reaction. This chapter discusses ways polymerizations' strict requirements can improve understanding of small molecule transformations. Examples of this strategy of method development are presented in both DArP and emerging polymerizations, and the work discussed in Chapters 2 and 3 are used as examples for this approach. We propose a synergistic, circular strategy to improved synthetic method development where in addition to the common use of small molecule reports to inspire new

polymerizations, polymerization-based discovery is applied in the development of new small molecule methodologies.

4.2 DArP Method Development

For electronic applications, the π-conjugated backbone of a material is an essential consideration, influencing the material's optical and electronic performance. Sufficiently high molecular weight is a key consideration for many applications of conjugated polymers. Molecular weight affects the polymer's solid-state structure, directly influencing charge transport properties.[151] In addition to molecular weight, there are many parameters affecting the electronic performance of a material, including dispersity and defects. A critical goal of polymer synthesis is having precise structural control with highly reproducible syntheses. Achieving this goal enables accessing the desired structure for a given application, and provides researchers with insight into which structural modifications led to which performance outcomes. There are two main ways well defined, reproducible materials can be realized in DArP. Firstly, homocoupling and branching defects should be limited or absent. Secondly, resultant polymers should have sufficiently high molecular weight to achieve the desired electronic properties.

Cross-coupling polymerizations are governed by a polycondensation mechanism. While different polymerization mechanisms (e.g. chain polymerization) are not readily predictable from small molecule reactions, adapting small molecule methods is an appropriate strategy for developing novel polycondensation reactions. Adapting a small molecule reaction to a polymerization has several considerations, summarized in **Figure 4.1**. It should be noted that these are general guidelines when new small molecule conditions are considered for polymerization studies. Due to the dynamic nature of a growing polymer chain, meeting these

conditions is not guaranteed to provide excellent polymers nor does not meeting these requirements preclude the possibility of successful polymerizations. Nonetheless, they provide helpful guidance.

Polymerization Requirements	***Small Molecule Indication***	***Outcome***
High conversion	High yield	High molecular weight
Stoichiometric monomer loading	Proceeds with stoichiometric substrate loading	High molecular weight
Linear chains	Complete regioselectivity	Fewer branching defects
Alternating copolymers	Complete chemoselectivity	Fewer homocoupling defects
Growing chain stays reactive	Disubstituted substrates react	Polymerization possible

Figure 4.1. Relationship between polycondensation and small molecule reactions

Firstly, molecular weight will be considered. One way to think about polycondensation reactions is that every n-mer displays the same effective reactivity as the monomer, in contrast to chain polymerization where the growing polymer chain reacts preferentially to monomers (**Figure 4.2**).[24] This means that while there is rapid initial conversion of all monomers in a reaction mixture, it is not until the very end of the reaction that high molecular weight is achieved (**Figure 1.2**). Recalling the discussion on the Carothers equation from Chapter 1, this means that exceptionally high conversion is required to achieve a suitably high degree of polymerization (**Equation 1**, **Figure 4.2**).[23] Additionally, this model demands perfect stoichiometry to achieve high molecular weights (r = 1, **Figure 4.2**). When considering a small molecule transformations' suitability to polymerization, this model demonstrates why exceptional reactivity is needed (>98% yield). Moreover, excellent chemoselectivity is need in a small molecule transformation since homocoupling cannot be discouraged via using an excess of one coupling partner.

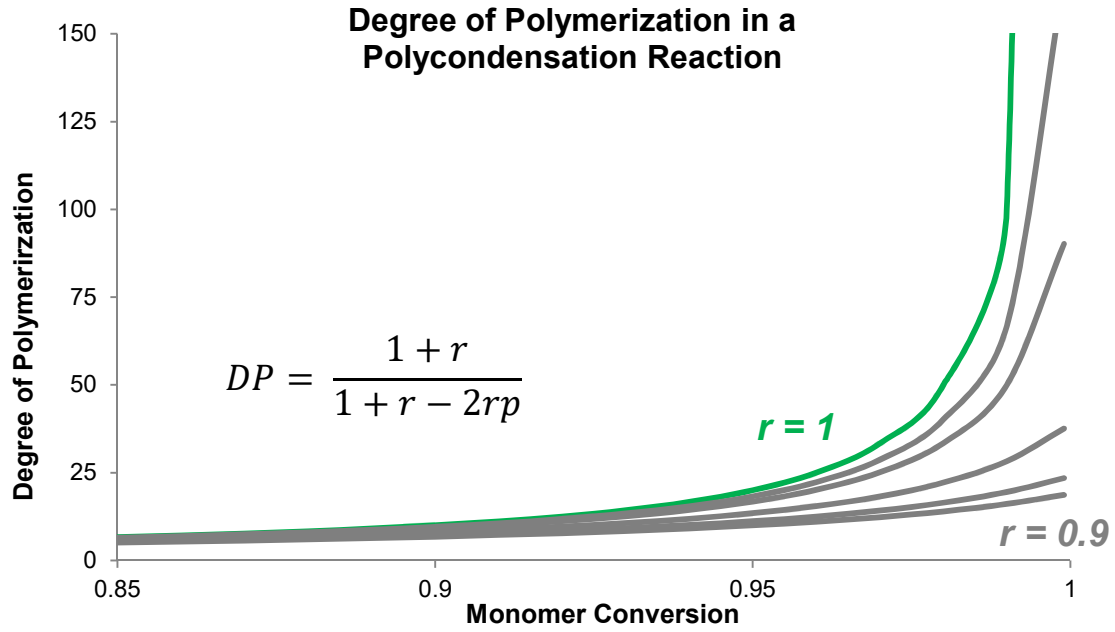

Figure 4.2. Carothers equation model showing the effect of changing monomer molar ratios on degree of polymerization

While the Carothers equation is a valuable model, it does have its limitations and engrained assumptions.[25] Polymerizations are dynamic and as the reactant changes from monomer to dimer to oligomer, the substrate undergoing cross-coupling is changing. As the Carothers equation is founded on the assumption that every n-mer demonstrates the same reactivity whether n = 1 or n = 100 for a monomer or long polymer, it cannot account for variability often introduced in the initial stages of the reaction. For this reason, features observed in the small molecule transformation do not always translate to the subsequent polymerization. This leads to situations where in spite of low yield in a small molecule reaction, excellent polymerization results are achieved.[25] That being said, Carothers does offer a valuable tool for predicting polymerization viability when evaluating small molecule transformations.

4.3 Examples in C-H Arylation

Having reviewed important factors for developing new methods of polymer synthesis, this section presents examples of the types of insights polymerizations can offer. Even when the Small Molecule Indications outlined in **Figure 4.1** are present, there can still be problems with resultant polymers (i.e., low molecular weight, high defect concentration). This discrepancy between what was anticipated from a small molecule reaction and the results of a new polymerization provides insight into mechanistic factors governing regioselectivity, chemoselectivity, and reactivity. Rather than a comprehensive overview, we will primarily focus our discussion on ways that results in polymerization studies can differ from what would be expected from the corresponding small molecule transformations. In addition to presenting some of these challenges and, we highlight ways these deviations can serve as opportunities to inform the broader synthetic community about the nature of a given transformation.

4.3.1 *Defect-Driven DArP Studies*

Selectivity in C-H functionalization reactions can be problematic in substrates with multiple and similar C-H bonds. For example, the C-H bonds on unsubstituted thiophene, a prevalent motif in conjugated polymers, demonstrate reactivity under the same reaction conditions. Unlike in small molecule reactions where undesired regioisomers can be removed using purification techniques, regiodefects in polymers are permanently incorporated into the chain. For optoelectronic applications, these defects are typically detrimental to the electronic performance of a material.[152] Commonly encountered defects in DArP are outlined in **Scheme 4.2** using P3HT as a model system; included are branching defects, as well as head-to-head and tail-to-tail coupling defects.

Scheme 4.2. Defects in DArP P3HT synthesis

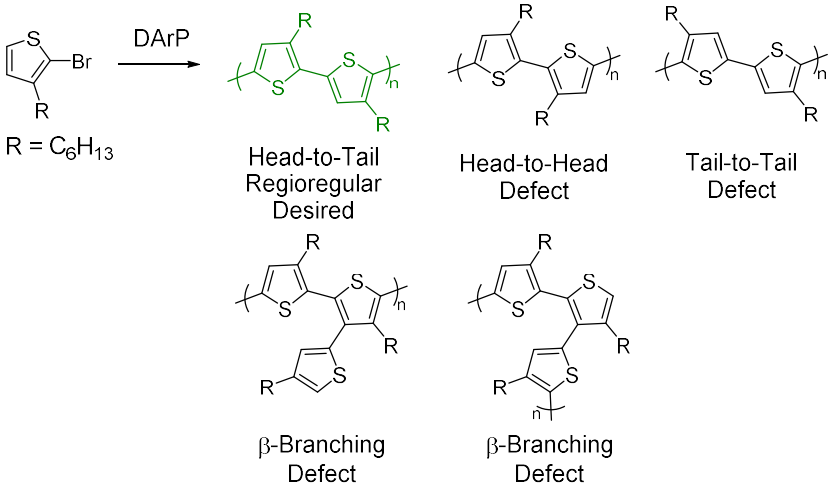

One problem that arises when adapting a small molecule reaction to a polymerization is the changing reactivity of various C-H bonds throughout the growing polymer chain. The activation free energies of both the α-position and the β-position on a substrate change with changing substitution (**Scheme 4.3**).[37,58] In the case of a growing polymer chain the α and β protons' reactivity may differ on the monomer compared to the dimer, and for the terminal repeat units compared to H_β on interior repeat units. These variations will be even more pronounced in donor-acceptor copolymers with changing electronic character of the alternating repeat units. When developing new DArP protocols, it is important to investigate regioselectivity beyond the initial cross-coupling event, as the second and third C-C couplings will have inherently different electronic character that may be detrimental to previously observed regioselectivity.

Polymerization studies lend themselves to exploring factors influencing regioselectivity. As a polymerization proceeds on a thiophene monomer, the free C-H bonds at the desired α-position become scarce, whilst undesired β-position C-H bonds are still abundant for cross-coupling. In light of the need for very high monomer conversion to observe high molecular

weights, polymerizations are often allowed to react longer than analogous small molecule transformations. In small molecule systems, after the initial desired cross-coupling occurs in good-to-excellent yield, the reaction can be stopped prior to undesired cross-coupling events – an approach not possible in the polymerization context. Highlighted below are select studies investigating controlling regioselectivity in DArP.

Scheme 4.3. Activation free energies for CMD of substituted thiophenes[a]

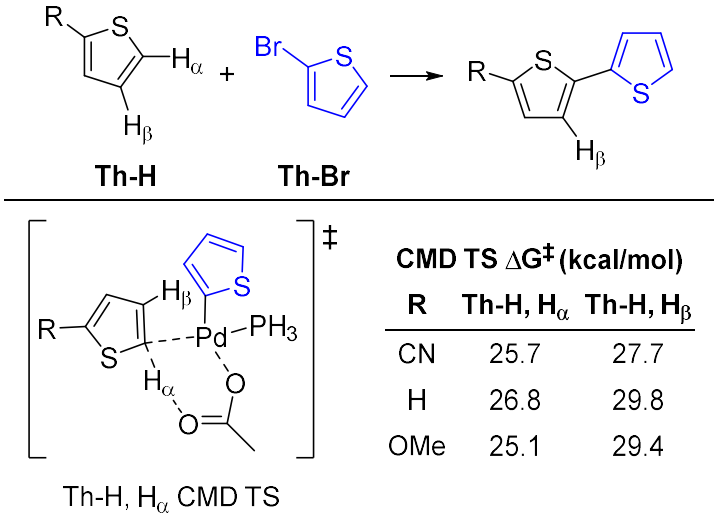

CMD TS ΔG‡ (kcal/mol)

R	Th-H, H_α	Th-H, H_β
CN	25.7	27.7
H	26.8	29.8
OMe	25.1	29.4

[a]Adapted from ref. 58.

For thiophene direct arylation by a CMD process, C-2 selectivity is favored, although β-branching is a known problem in polymerizations (**Scheme 4.2**). Leclerc et al. have reported on the cause of β-defects in polymers involving thiophene C-H arylation.[58] Parameters impacting regioselectivity for substituted thiophenes were evaluated, accounting for both steric and electronic influences on C_α-H and C_β-H bond functionalization by CMD (**Scheme 4.3**). Focusing on thiophene, this work characterizes the increased reactivity of all C-H sites on the halogenated coupling partner, compared to a halogen-free thiophene (**Scheme 4.4,** Th-Br, H_γ, vs. Th-H, H_α). When halogenated, H_γ on Th-Br becomes much more accessible for CMD (26.3 kcal/mol). This

demonstrates that poor selectivity for C_α-H over C_β-H can frequently be attributed to the activating effect bromination has. While addressing a materials-specific problem regarding defect formation in DArP, this report provides analysis on the nature of reactivity at competing C-H bonds useful for small molecule applications as well. To achieve highly selective couplings where a bromothiophene unit is involved, ensuring the C-H coupling partner is electron-rich or electron-poor will make the desired α-position C-H functionalization more competitive to CMD than the C-H adjacent to the C-Br bond on the coupling partner.

Scheme 4.4. Activation free energies for CMD of thiophene[a]

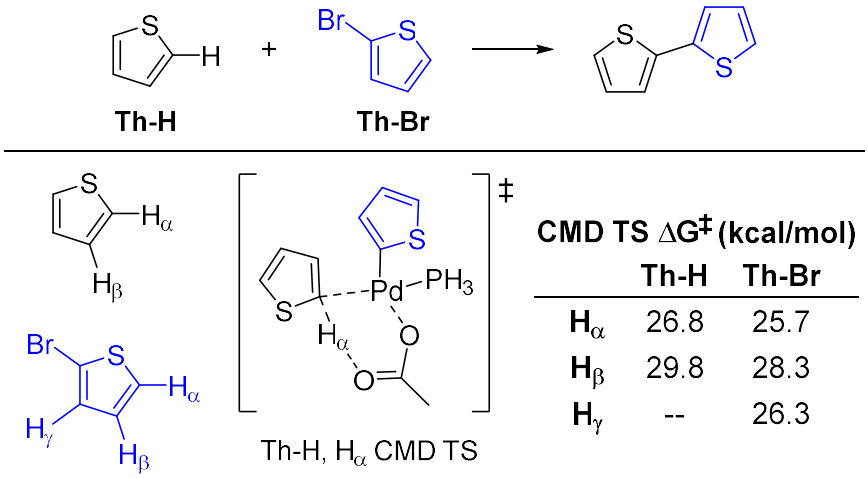

[a]Adapted from ref. 58.

Undesired branching has also been investigated to access novel hyperbranched materials. Our group studied thiophene's β-branching to prepare hyperbranched P3HT, leading to greater understanding of conditions favoring α/β selectivity (**Scheme 4.5**).[74] In this case, β-branching was a feature of the polymerization and was never evidenced in the corresponding small molecule reaction. This highlights the regioselectivity issue of a changing substrate from monomers to oligomers in the early stages of polycondensation reactions (**Scheme 4.3**). The

authors examined how reaction conditions could be used as a tool to tailor degree of branching in thiophene-based polymers, using NMR spectroscopy to quantify the number of α to β couplings in these systems.

Scheme 4.5. Hyperbranched P3HT[a,b,c]

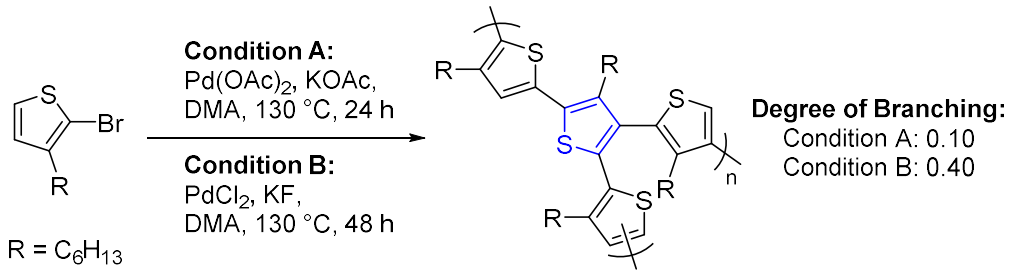

[a]Adapted from ref. 74. [b]Dendritic unit shown in blue [c]Condition A: $Pd(OAc)_2$ (1 mol%), KOAc (2 equiv.), Condition B: $PdCl_2$ (3 mol%), KF (4 equiv.)

Within Condition A, variation in branching could be reduced by adding ligands. Compared with the ligand-free system, phosphine ligands PPh_3, XPhos, and dppe provided high molecular weight polymers but with a decrease in the degree of branching. Polymers prepared with nitrogen-based ligands, bpy and TMEDA, had no dendritic units. More extensive branching was observed with Condition B. Notably, a carboxylate is absent from these reaction conditions, minimizing the likelihood that this process occurs by CMD, which features a carboxylate-assisted deprotonation. This likely difference in mechanism between Conditions A and B contributes to the loss in regioselectivity over the course of the polymerization. Should the mechanism be S_EAr or oxidative polymerization where cations are generated on the polymer backbone, regiodefects are to be expected. This hypothesis is further supported by the fact that when a carboxylate is introduced into Condition B by using $Pd(OAc)_2$ in place of $PdCl_2$, branching is reduced. This is a trend that will be returned to in this article, where for C-H functionalization polymerizations, there is significant opportunity for non-CMD-mediated

polymerizations to offer inherent improvements over transformations governed by CMD, including lower energy requirements, broader substrate tolerance, and greener reaction conditions. At the same time, the mechanistic shift typically results in a loss of regioselectivity creating polymers with intolerable defect concentrations. This is an opportunity in the larger synthetic community to develop greater understanding of the mechanisms for different C-H bond arylations, and of the factors influencing regioselectivity under these different mechanisms.

Regioselectivity is often ameliorated in small molecule reactions by directing groups; this approach is not commonly used in DArP. The installation of directing groups have typically been viewed as negatively influencing the molecular design of the desired material, where commonly used ester or amide directing groups have not frequently been considered valuable structural features. This view is becoming outdated with growing interest in the inclusion of heteroatoms in the sidechains of thiophene-based monomers, arising from the recent attention towards mixed ionic-electronic conductors.[153] Alongside this, some early studies indicate the beneficial impact introducing side chains that can participate in H-bonding has on improving charge mobility through intermolecular H-bonds of nearby side chains.[154] Esters in particular have been evidenced for their ordering morphological effect with demonstrably shorter $\pi - \pi$ stacking distance in polymers with ester-containing side chains.[155,156] The improvements in regioselectivity, and application-specific properties (e.g. ion conductivity, charge mobility) afforded by using pendant directing groups present an opportunity for innovation. Here, creative design of directing groups could be utilized to facilitate improvements in regioselectivity without deleterious effects on polymer properties. With proper design, it may be possible that directing groups could add to the final properties of a material.

The influence directing groups may have on the properties of a polymer is one consideration. A secondary concern arises from the presence of directing groups on repeat units already installed on the polymer chain during synthesis. These mid-chain directing groups can lead to undesired branching and/or cross-linking in polymers when the active catalyst interacts with a mid-chain directing group rather than the desired chain-end site. This problem arises when a secondary suitable C_{aryl}-H bond is present in the monomer structure, as in thiophenes' β and γ positions.[157] Thompson et al. report DArP conditions for a thiophene monomer with an ester directing group at C_β (**Scheme 4.6**).[158] They successfully used the ester directing group to prepare regioregular polymers, showing the promise using the small molecule directing group strategy has for new polymerizations. In order to avoid mid-chain cross-linking/branching couplings, they selected branched alkyl side chains. These sterically bulky side chains prevented undesired reactions along the polymer backbone by improving separation between discrete polymer chains. These rationally designed monomers were utilized to avoid defect formation. Thoughtfully designed monomers containing directing groups should be considered for cases where the end use application of a polymer would benefit from introducing heteroatom-containing functionalities. This may be a path forward to reliably regioregular DArP and Oxi-DArP prepared polymers. Continued work in both the small molecule and polymer communities provides opportunities to make an impact on thoughtfully defined directing groups and directing-group containing polymers.

Scheme 4.6. Ester directed DArP for regioregular P3HT[a]

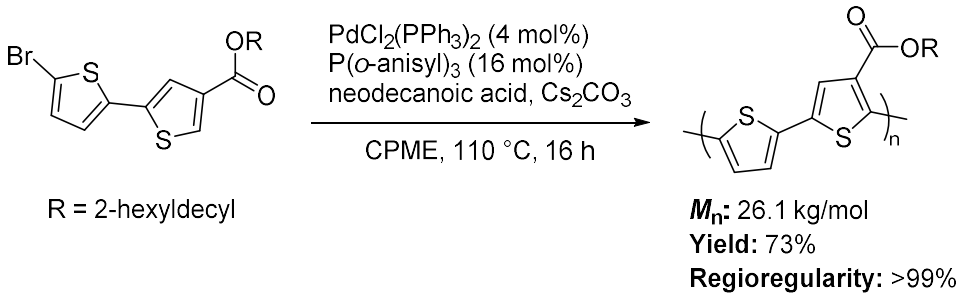

[a]Adapted from ref. 158.

The stringent requirements for successful polycondensation can drive greater understanding of the underlying mechanism. In part, this is due to the very high number of cross-coupling events required for high molecular weight, allowing for deviations in reactivity at the final stages of the reaction to become observable. Moreover, small changes in the steric and electronic properties of the growing polymer chain and the subsequent activation or suppression of desired reactivity can indicate greater details about the nature of catalysis.

One such example investigated preparing polyindole,[107] drawing inspiration from a small molecule method. Here, indole underwent C-H arylation with iodoarene coupling partners (**Scheme 4.7a**).[66] This small molecule report seemed to be a notable precursor for polymerization as it demonstrated complete regioselectivity without the use of a directing group. Secondly, excellent yields were reported even at room temperature. Lastly, this transformation utilized only two equivalents of the aryl iodide, indicating a stoichiometric ratio may be tolerated. The authors proposed the room temperature reactivity could be owed to Ag-mediated halide scavenging, exchanging the iodide ligand after oxidative addition with 2-nitrobenzoate. This carboxylate could dissociate from the metal center, affording a highly electrophilic metal catalyst (**Scheme 4.7b**).

Scheme 4.7. Indole C-H arylation by iodoarenes at room temperature[a]

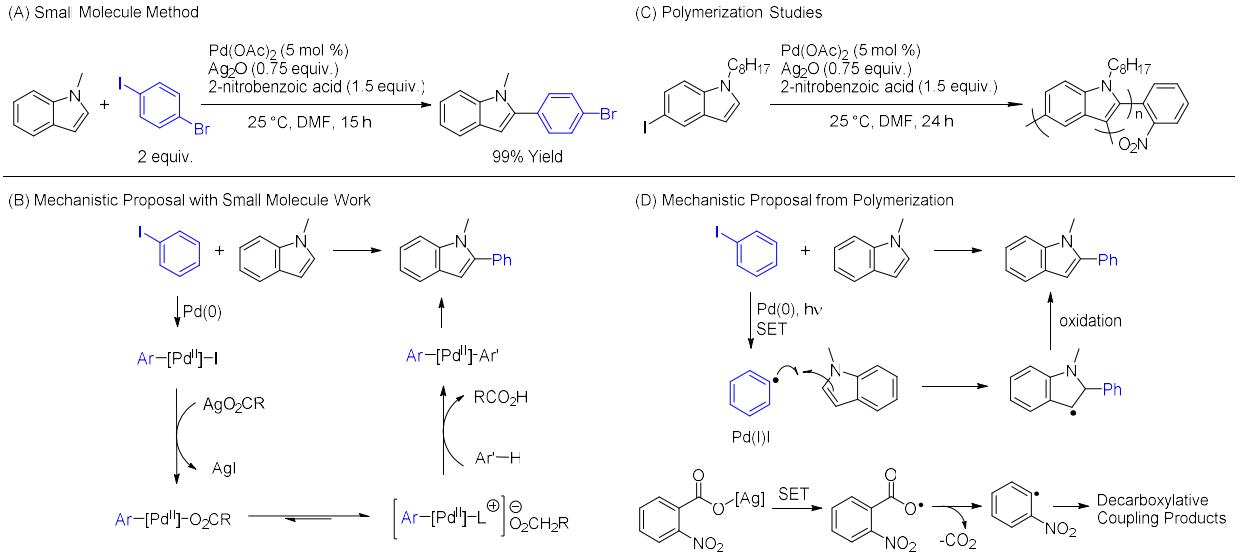

[a]Adapted from ref. 66 (left), 107 (right).

When this was adapted to an iodoindole monomer for polymerization studies, surprising incorporation of the benzoate was observed in the resultant polymer chain, alongside β-branching (**Scheme 4.7c**). Neither structural feature was observed in the small molecule reaction. This observation catalyzed mechanistic studies of the polymerization and corresponding small molecule reaction, revealing a novel photosensitivity atypical of CMD direct arylation without an exogenous photosensitizer. Rather, this light-mediated, room temperature process was likely accessible by a different mechanism (**Scheme 4.7d**). Here, a proposed light-mediated single electron transfer (SET) event occurred between the Pd catalyst and the aryl iodide.[87] The subsequent phenyl radical can be trapped by indole, eventually affording the observed product. The origins of nitrophenyl incorporation were unclear. Commonly, metal benzoates lose CO_2 thermally, providing organometallic arenes for cross-coupling reactions.[159] In the absence of elevated temperatures, metal benzoates can be transformed into aryl radicals through single electron activation.[159,160] While the precise source of an unpaired activating electron has yet to be

elucidated, this is likely the process responsible for nitroarene incorporation in the polymer chain. Since the reaction required palladium, a radical chain reaction initiated by the silver carboxylate decomposition is unlikely as the primary mechanism for the polymerization. The mechanistic studies were replicated in both small molecule and polymer trials, achieving the same results. This indicates the decarboxylative coupling is not indicative of a polymerization-specific mechanism. The photosensitivity is likely responsible for the ability of this reaction to proceed at room temperature, where most CMD-mediated processes require elevated temperatures.

4.3.2 *Defect-Driven Oxi-DArP Studies*

Mechanistic insight arising from polymerization studies can also occurs in oxidative DArP (Oxi-DArP), also referred to as cross dehydrogenative coupling (CDC) polymerization. This is similar to direct arylation, however involves the direct coupling between two aryl C-H/C-H bonds instead of coupling between C-H/C-X bonds as in direct arylation. Some of the original methods of conjugated polymer synthesis, electrochemical and chemical oxidation methods, utilize unfunctionalized monomers.[161,162] These historical methods achieve materials with significant defects, which Oxi-DArP is able to improve upon by using transition metal catalysis. Since Oxi-DArP is still a polycondensation, it shows the same interplay between small molecule couplings and polymerizations as DArP. For donor-acceptor copolymers, it is desired that orthogonal reactivity controls are available to aid in cross-coupling during dual C-H bond activation.

Dialkylbiarylphosphine ligands are widely used in cross-coupling reactions, with extensive examples of their ability to tune reactivity of a given transformation.[163,164] This

category of ligands, often referred to as Buchwald ligands, has undergone screening studies in small molecule direct arylation.[69,165] Minimal efforts to employ this type of catalyst have been seen in the polymerization literature, despite the possibilities to leverage these ligands for improved reactivity and selectivity. One report has systematically screened a selection of Buchwald ligands by using Oxi-DArP on 2,4-propylenedioxythiophene (ProDOT) as a model study (**Scheme 4.8**).[166] By selecting ProDOT monomers, the authors demonstrate a viable strategy for synthesizing regioregular polymers, where potentially problematic C-H bonds are blocked with substituents. Depending on the application of the target material, this can be a simple approach to regioselectivity issues commonly encountered with C-H arylation polymerizations, although is not generalizable.

Scheme 4.8. PolyProDOT prepared via Oxi-DArP using dialkylbiarylphosphine ligands[a]

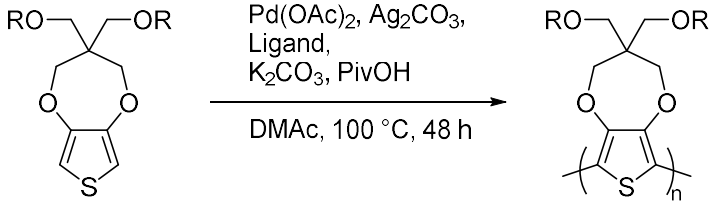

R = 2-ethylhexyl

Ligand	M_n (kg/mol)	Yield (%)
None	8.1	57
CyJohnPhos	5.5	20
JohnPhos	6.6	75
XPhos	7.5	94
t-BuXPhos	12.5	92
t-BuBrettPhos	6.5	88

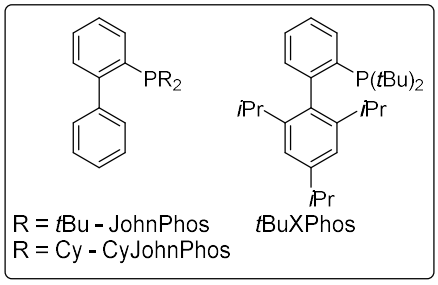

[a]Adapted from ref. 166.

It was clear that ligand selection significantly impacted the polymerization results. Particularly, bulkier ligands utilizing *t*-Bu substituted phosphines, and adding bulky *i*Pr groups to

the lower ring improved both yield and M_n **(Scheme 4.8**). Ligands' impact on catalysis in Pd-mediated cross-couplings has been extensively studied.[164,167,168] These studies demonstrate bulky, electron-donating biarylphosphine ligands effectively stabilize the key catalytic species, monoligated palladium (L_1Pd).[164,167] By affording L_1Pd in place of L_2Pd, these bulky ligands enhance oxidative addition by allowing the substrate and catalyst to interact. Bulky ligands favoring L_1Pd have also been shown to increase the rate of reductive elimination compared to the comparable L_2Pd species.[169,170] These larger ligands accelerate reductive elimination by introducing more strain that can be alleviated upon reductive elimination.[171,172] In Oxi-DArP, the CMD step is analogous to oxidative addition in a traditional cross-coupling reaction, where bulky ligands which favor formation of L_1Pd improve reactivity. Using bulky *t*-Bu phosphine substituents and introducing *ortho*, *ortho'* substitution with a bulky *i*-Pr on the lower ring favors L_1Pd formation by increasing the ligand's size, explaining why *t*-BuXPhos performed the best in the Oxi-DArP report.[164] Thus, oxidative direct arylation shows a similar relationship between ligand selection and catalytic efficiency as C-M/C-X cross-couplings. By studying these ligands for Oxi-DArP, information on ligand's impact on C-H activation and reductive elimination is provided for future small molecule and polymer systems.

Ligand impact on Oxi-DArP performance has also been evaluated in tandem with directing group effect. Thompson et al. evaluated Oxi-DArP for preparing ester-functionalized thiophenes.[173] The authors systematically optimized reaction conditions, comparing the effect of variables including oxidant, additive, and ligand on the resultant polymer's properties (**Scheme 4.9**). By choosing 3-hexylesterthiophene (3-HET) as a model substrate which has three inequivalent but reactive aromatic C-H bonds, this report presents a valuable insight into regioselectivity in oxidative direct arylation. Notably, the authors compared 3-HET to 3-

hexylthiophene (3-HT), showing the dramatic improvement in regioregularity offered by the ester directing group (45% for 3-HT vs. 75% for 3-HET, **Scheme 4.9**, entry 1, 2, 3). From there, improvements in regioregularity were achieved using a phosphine ligand (PCy_3-HBF_4) to achieve polymers around 85% regioregular (**Scheme 4.9**, entry 4). Molecular weight showed similar trends, where the best results used a phosphine ligand. This work highlights the important role directing groups are able to play in achieving regioregular polymers using dual C-H activation. Moreover, the insights gained on regioregularity and molecular weight for monomers provides guidance on achieving regioselective, high yielding small molecule transformations. In particular these trends are valuable for challenging small molecule C-H/C-H coupling reactions with multiple inequivalent C-H bonds, showcasing the value of ester directing groups and phosphine ligands.

Scheme 4.9. Conditions optimization for Oxi-DArP of 3-substituted thiophenes[a]

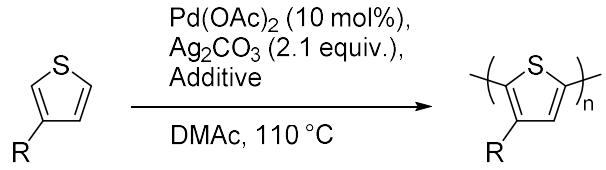

3-HT R = C_6H_{13}
3-HET R = $CO_2C_6H_{13}$

Entry	Monomer	Additive/Ligand	RR (%)	M_n (kg/mol)	Yield (%)
1	3-HT	K_2CO_3 (2.2 equiv.)	45	1.5	16
2	3-HET	K_2CO_3 (2.2 equiv.)	75	10.4	68
3	3-HET	None	78	4.9	24
4	3-HET	PCy_3-HBF_4 (20%)	84	15.1	77

[a]Adapted from ref. 173.

In another example of Oxi-DArP, a promising small molecule reaction was investigated as a polymerization.[174,175] The small molecule report demonstrated orthogonal reactivity between

electron-rich and electron-poor coupling partners (**Scheme 4.10a**). This methodology was demonstrated on heteroaromatic electron-rich species including indole, thiophene, and pyrrole undergoing C-C bond forming events with fluorinated benzenes. These are suitable monomers for a conjugated donor-acceptor copolymer. Moreover, this report was able to achieve cross-coupling selectivity without extreme excess of one of the coupling partners, making it more likely that stoichiometric monomer loadings could be tolerated. Here, the high cross-coupling selectivity came from an infrequently used gold catalyst. In this strategy, it was hypothesized that different oxidation states could be used to change selectivity, rather than in Pd-mediated cross-couplings where only small changes in the ligands must sufficiently turn on and off reactivity for the electron-rich and electron-poor arenes. The authors propose the Au(I) species selectively activates the electron-deficient arene while a Au(III) species in the catalytic cycle selectively activates the electron-rich arene (**Scheme 4.10b**).

Scheme 4.10. Au-Mediated arene oxidative direct arylation[a]

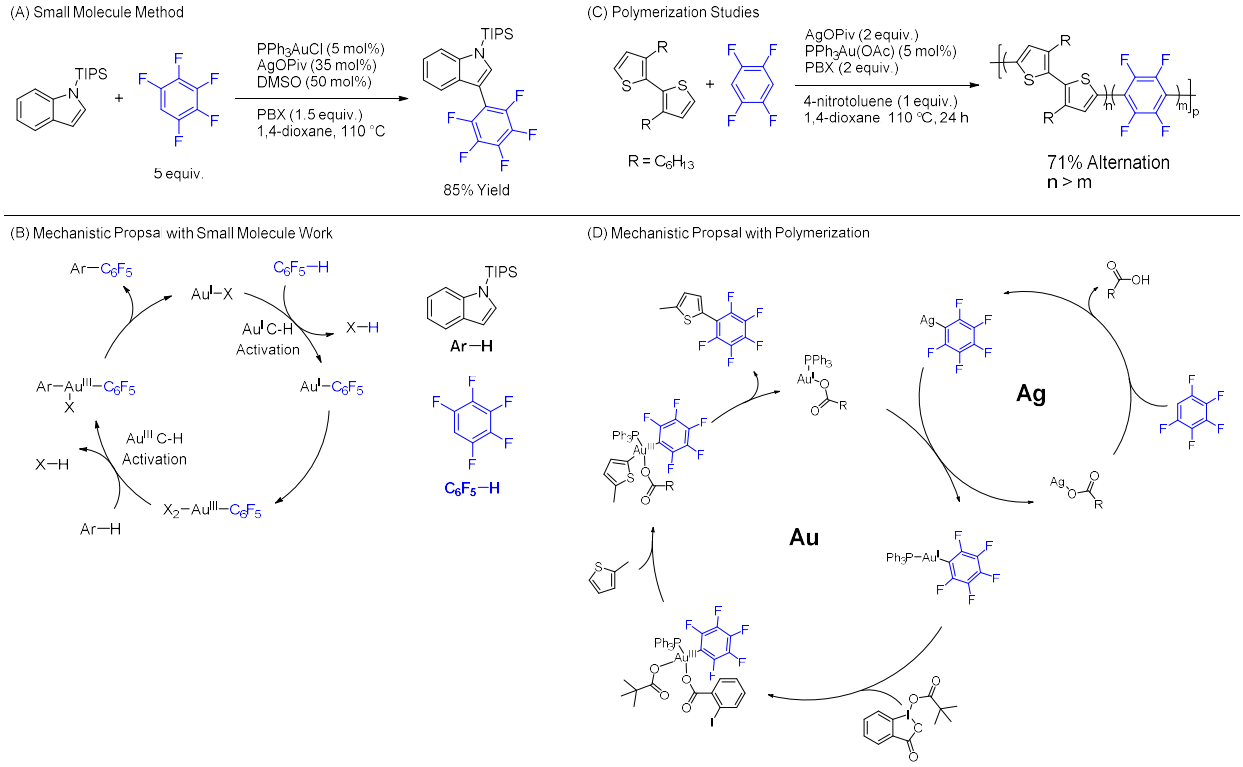

[a]Adapted from ref. 175 (left), 174 (right).

This small molecule oxidative direct arylation report presented an inspiring strategy for donor acceptor copolymers – using a Au(I)/Au(III) catalytic cycle to mediate orthogonal cross-coupling. This could provide an efficient approach to achieving perfectly alternating copolymers. This selective activation approach was subsequently adapted to the polymerization of a thiophene/tetrafluorobenzene copolymer. Unexpectedly, in contrast to the small molecule report, cross-coupling selectivity was lost when polymerization trials were performed (**Scheme 4.10c**). While the fluoroarene did not undergo homocoupling, the thiophene units did. Subsequently, the resultant polymer had a high degree of homocoupling, with 71% alternation between the electron-rich and electron-poor repeat units.

In order to investigate this change from small molecule to polymer conditions, mechanistic studies were performed. Rather than a Au(I)/Au(III) catalytic cycle as proposed in the small molecule work, mechanistic work reported in the polymerization study revealed different mechanistic features. Namely, a dual catalytic cycle enables cross-coupling, where Au and Ag selectively activate electron rich and electron poor substrates, respectively (**Scheme 4.10d**). This cooperative catalysis was later supported by two additional studies.[176,177] In the polymerization, the initial installation of fluorinated benzene on thiophene made the free C-H bond on thiophene meaningfully more reactive to Ag during the second coupling event. This causes Ag to be able to activate C-H bonds on both the electron-poor tetrafluorobenzene monomer, and on the biaryl tetrafluorophenylthiophene. This phenomenon arises from the electron-withdrawing effect of the fluorinated benzene. In the small molecule setting, the biaryl product's reactivity did not need to be considered. However, the biaryl species' reactivity is of fundamental importance for preparing the polymer. The loss of cross-coupling selectivity in the polymerization reveals that the C-H activation selectivity is not driven by the gold catalyst's oxidation state.

This polymerization work discovered in depth information about the catalytic cycle, including the nature of Au/Ag selectivity. Since these reports of Au/Ag dual catalysis, new methods have been reported drawing insight from the Au/Ag transmetalation step initially discovered in this polymerization study. One such example uses stoichiometric Ag in a method of decarboxylative coupling.[178,179] Here, a Ag carboxylate is delivered to the Au metal center using Ag(I) to Au(III) transmetalation. Another report, inspired by a Au/Ag dual catalytic system sought to discover a Pd/Ag system with catalytic amounts of both metals for direct arylation.[180] In this case, silver's demonstrated ability to activate C-H bonds in electron-deficient arenes was

utilized jointly with a Pd-mediated oxidative addition of aryl bromides. Both of these reports apply findings originating from mechanistic studies on a polymerization, showing cooperative discovery between small molecule and polymerization transformations.

In addition to work highlighting mechanistic shifts and factors influencing regioselectivity, reactivity has also been assessed.[25] Kanbara et al. reported a Pd/Ag Oxi-DArP system with high molecular weights and low homocoupling that used the same substrates as the Au/Ag system outlined in **Scheme 4.10c**.[181] While high homocoupling was observed in the Au/Ag system, the Pd/Ag report showed excellent cross-coupling selectivity (**Scheme 4.11a**). Luscombe et al. investigated this deviation, observing the Pd/Ag polymerization result was in contrast to small molecule model studies, where the equivalent small molecule cross-coupling showed poor yield and poor selectivity (**Scheme 4.11b**). Considering the Carothers equation (**Figure 4.2**), **Scheme 4.11b** does not forecast the successful polymerization achieved by Kanbara. Luscombe et al. investigated the origins of the discrepancy, and found that the second cross-coupling event occurs much more readily than the first (**Scheme 4.11b** vs. **Scheme 4.11c**), approximately 10 times faster. Through kinetic and computational experiments, they demonstrated the activating effect the thienyl substituent has on the fluoroaryl coupling partner. This activating effect fundamentally changes the reactivity of the monomer with growing polymer chains, subverting the Carothers equation's assumptions. The change in reactivity from the first cross-coupling step to the second demonstrates the limitations of studying small molecules as precursors to polymerizations, indicating that studying the second cross-coupling step may be more accurate. Moreover, this work also may inform oxidative direct arylation on small molecule substrates, particularly in late-stage functionalization settings. In cases where

addition of thiophene to electron-deficient scaffolds is desired or tolerable, it may provide more efficient access to target cross-coupled products.

Scheme 4.11. First and second cross-coupling steps, compared to Oxi-DArP study[a]

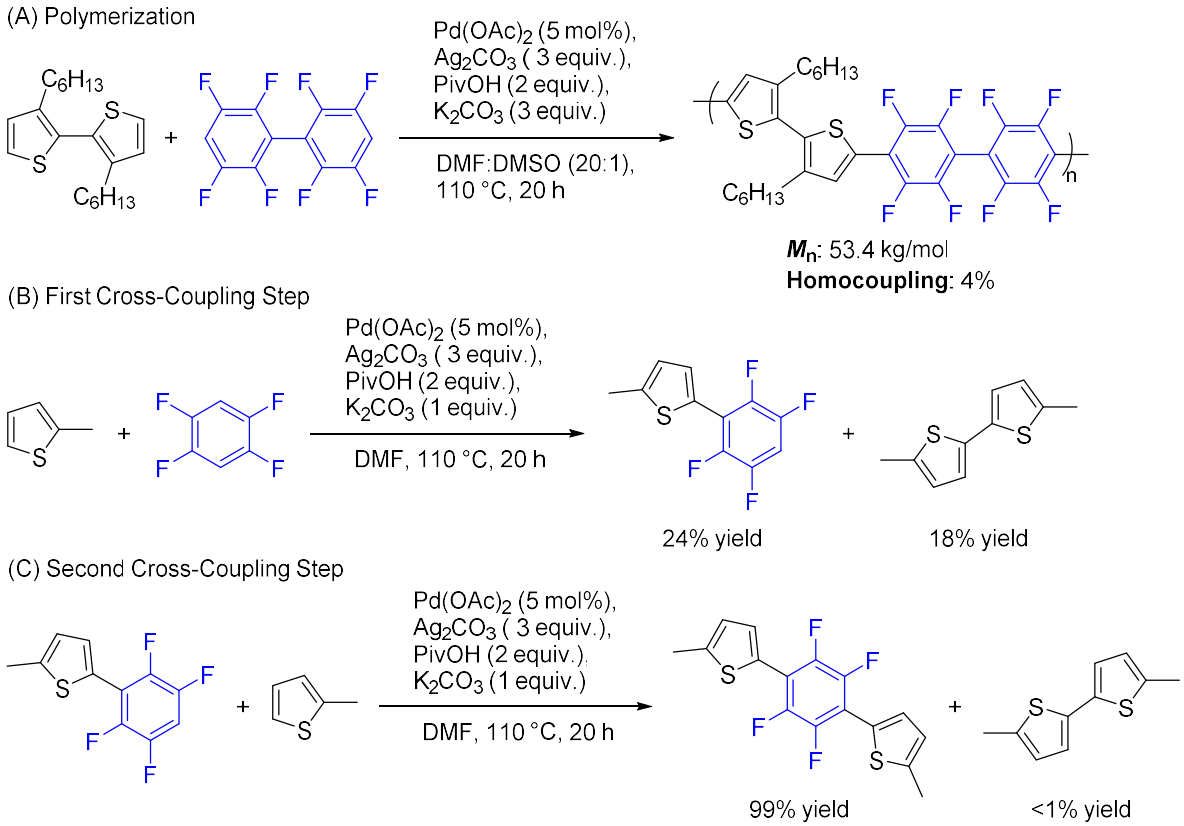

[a]Adapted from ref. 181 (Scheme A). Adapted from ref. 25 (Scheme B and C).

4.3.3 *Improvements to Small Molecule Methodologies Inspired by Polymerizations*

Examples have been presented of new methods of polymer synthesis inspired from efficient small molecule reactions. This is a common and useful approach, especially as new and significantly improved transformations are developed in the small molecule literature. Of particular value are those transformations that offer a significant improvement in atom economy, environmental and economic impact of the conditions (e.g. solvents, catalysts), as well as those that offer access to novel polymeric architectures. A few of these polymerization-based

discoveries have subsequently led to new innovations for small molecule transformations and targets. This strategy could be more broadly utilized for developing novel and improved transformations in the small molecule literature.

An example of this small molecule → polymer → small molecule innovation pipeline is from the study on room temperature arylation of indole (**Scheme 4.7**). As discussed in Chapter 4.3.1, the original small molecule work for indole direct arylation with iodoarenes was adapted to polymerization.[66,107] In the course of these polymerization studies, new mechanistic insights on the room temperature transformation were discovered. Namely, photosensitivity was observed and proposed to be the driving force enabling this transformation to proceed at room temperature. Curious about the generality of this process, exploratory work was performed, eventually leading to improved conditions for benzofuran C-H arylation (**Scheme 4.12**).[44] This small molecule report was inspired directly from our studies on adjacent polymerizations. While it is common for new polymerization methods to be informed by small molecule work, it is worth considering in what ways new polymerizations can inform new small molecule synthetic methods as well. The indole/polyindole/benzofuran progression is one example of this circular pathway to developing greater insight into a type of transformation.

Scheme 4.12. Benzofuran direct arylation by aryl iodides[a]

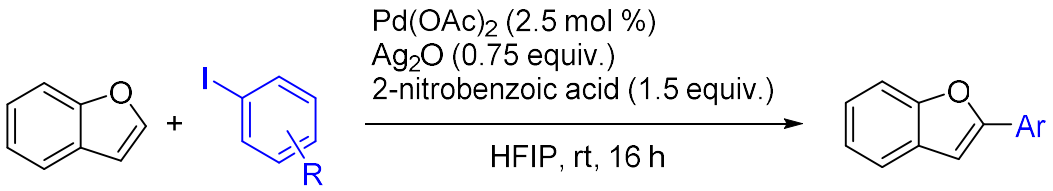

[a]Adapted from ref. 44.

The benzofuran small molecule C-H arylation method offers significant improvement over existing methodologies, with improved functional group tolerance, mild conditions, and commercially available aryl iodides. This method shows a number of similarities in conditions to those for indole room temperature arylation (**Scheme 4.7a**), with the only meaningful difference arising from a change in solvent from DMF to HFIP. Interestingly, despite these similarities a significantly different mechanism was evidenced using dark conditions screenings, deuterium exchange and kinetic isotope effect experiments. Rather than a photosensitive transformation as with indole, the benzofuran report appears to be governed by a Heck-type process, similar to a method for β-arylation of benzothiophene.[43] Notably, neither the indole nor the benzofuran room temperature direct arylation systems can be described by a more conventional CMD mechanism. It is likely these mechanistic changes are what enable such mild reaction conditions compared to elevated temperatures typically found in direct arylation conditions. While still accessible from small molecule studies, polymerizations served as a valuable driving force to gain increased fundamental insight into the processes underlying these room temperature transformations. This serves as an example of how considering polymerization studies in small molecule methodology is a useful strategy for gaining new insights and inspiration for small molecule methods.

4.4 Emerging Polymerization Methodologies Beyond DArP

Examples presented thus far have focused on ways in which DArP has grown out of existing small molecule methodologies. Mechanistic insights driving the properties of a given method, including regioselectivity have also been discussed. Some examples have also been presented on ways in which DArP studies can inform future small molecule work on a given transformation. Beyond DArP methodology, there are emerging methods of polymerization, both

for fully conjugated and nonconjugated optoelectronic materials that have been informed by the small molecule literature.

A preliminary example of a novel approach to new polymer structures is based off of a small molecule report detailing the utility of a dinuclear nickel catalyst in preparing aryl azides.[182] A wide range of aromatic groups are tolerated, including heteroarenes. This work included a preliminary polymerization example, highlighting the efficiency of the reaction. Later, a full report was published on the preparation of azopolymers using several different heteroaromatic monomers (**Scheme 4.13a**).[183] Azopolymers have not been thoroughly explored in conjugated polymers; this methodology opens up an efficient synthetic route to their greater study.

A secondary example of adopting established small molecule methods to polymerization utilizes C-O cross-coupling. While C-H bond arylation has been discussed earlier in this article, polycondensation using C-O and C-N bond forming events is a developing strategy to access different polymeric structures. A number of synthetic strategies exist for preparing diaryl ethers from C-O cross-couplings.[184,185] Recently, the small molecule understanding of Pd-catalyzed C-O cross-coupling was applied to synthesize a unique class of poly(arylene ethers) not previously accessible by the more conventional S_NAr approach (**Scheme 4.13b**).[186] Here, cross-coupling occurs between aryl halides and hydroquinone's hydroxyl groups. This specific report focuses on space-promoting repeat units for porous organic polymers, but the approach should be generalizable to prepare other poly(arylene ethers). Similar to the previously discussed Oxi-DArP study exploring Buchwald ligands (**Scheme 4.8**), this report provides useful information into the efficiencies of different pairings of ligands with aryl halides. This information is certainly useful

for further advancements in the polymerization context but could also inform conditions screening for similar small molecule reactions.

Scheme 4.13. Representative polymers prepared from aryl azides and by C-O cross-coupling[a]

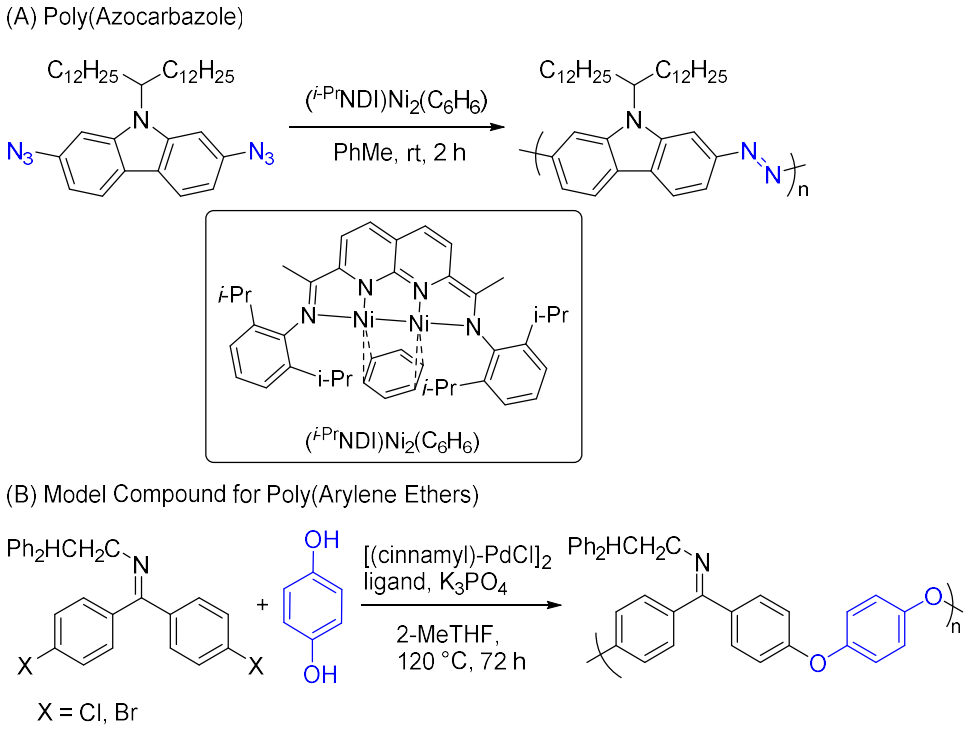

[a]Adapted from ref. 183 (Scheme A). Adapted from ref. 186 (Scheme B).

The C-O cross-coupling polymerization demonstrates some interplay between insights from new polymerization strategies and applications in small molecule methodologies, primarily for guiding conditions screenings. There are other examples of this in recent polymerization approaches. Focusing on a different transformation utilizing C-H bond functionalization, C-H amidation has been extensively studied in the small molecule literature.[187–190] One such study reported by Chang et al. detailed an iridium-catalyzed C-H amidation of substrates with weakly coordinating directing groups (esters and ketones) (**Scheme 4.14a**).[187] This methods' ability to form C-N bonds under mild conditions and with excellent yields later inspired a novel method of

polymerization, direct C-H amidation polymerization (DCAP) (**Scheme 4.14b**). A suite of unique, fluorogenic polysulfonamides were produced, all with high yields and good molecular weights.[191] During characterization of these materials, it was observed that these polysulfonamides were blue-light emitters with high quantum yields, arising from hydrogen bonds between the sulfonamide and adjacent carbonyl. Notably, these polymerization conditions were later applied to a new set of small molecule substrates, focusing on C-H amidation of aryl amides by tosyl azide.[192] Using the insights from the polymer synthesis, the materials prepared contained various substitution patterns to provide a collection of multicolor fluorophores. These three methods, starting from a small molecule method, then a novel polymerization, and lastly a new small molecule approach, demonstrate the synergistic discovery accessible between small molecule methodology and new methods of polycondensation.

Scheme 4.14. Iridium-catalyzed C-H amidation[a]

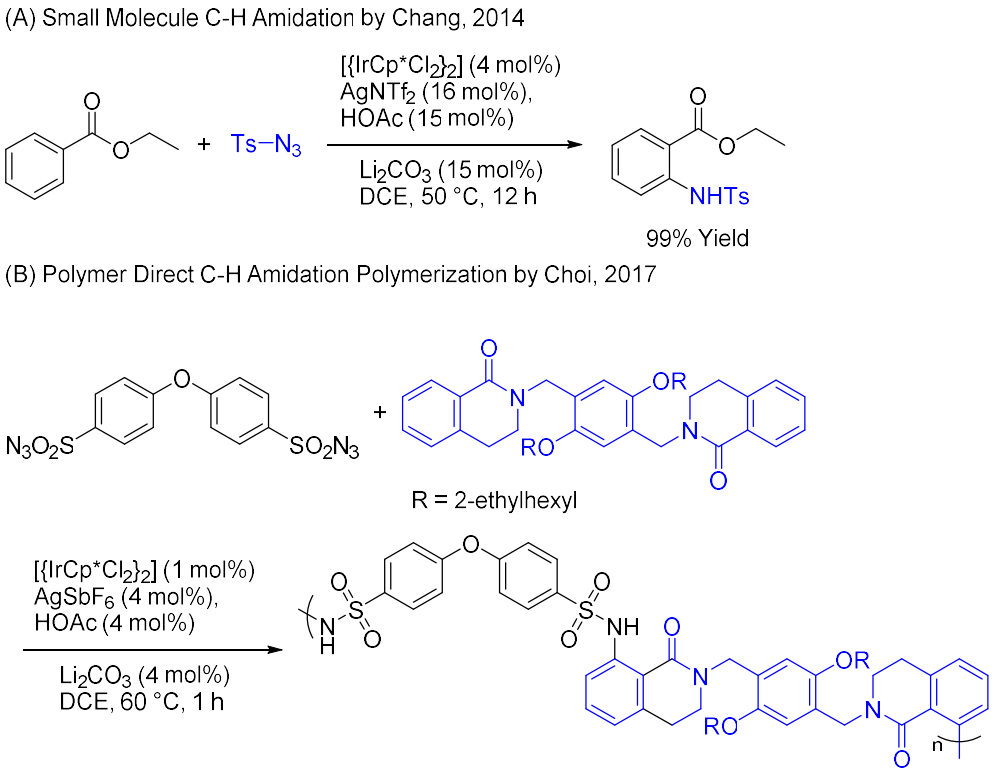

[a]Adapted from ref. 187 (Scheme A). Adapted from ref. 191 (Scheme B).

A similar pathway to new conditions has emerged with a type of $S_{RN}1$ reactions, where aryl Grignard coupling partners are used as anionic nucleophiles with an aryl halide. This strategy was first reported by Hayashi et al., providing a transition metal-free approach to biaryls from aryl Grignards and haloarenes (**Scheme 4.15a**).[193] This method is able to achieve transition metal-free cross-coupling by a thermally initiated SET event between the aryl Grignard and the aryl halide, successfully activating the aryl halide. Later, Studer et al. developed an analogous TEMPO-initiated cross-coupling polymerization between aryl Grignards and aryl halides (**Scheme 4.15b**).[194] This report hypothesizes this is a chain polymerization. Building off of both of these contributions, Kalow et al. later reported a method of photocontrolled synthesis of a range of conjugated polymers (**Scheme 4.15c**).[64]

Scheme 4.15. $S_{RN}1$-Mediated cross-coupling between aryl Grignards and aryl halides[a]

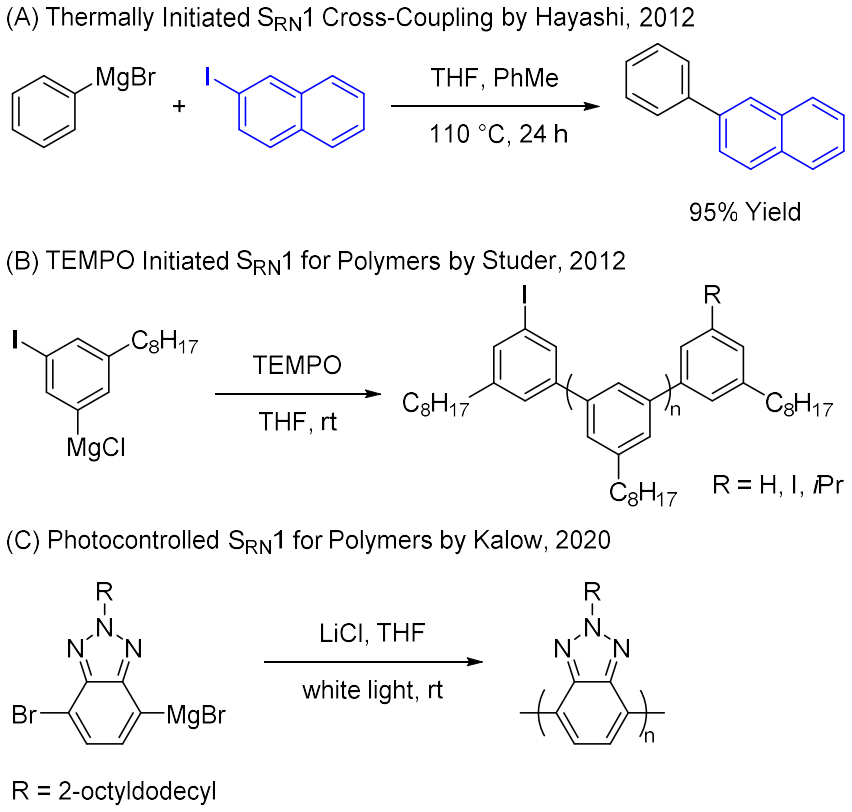

[a]Adapted from ref. 193 (Scheme A). Adapted from ref. 194 (Scheme B). Adapted from ref. 64 (Scheme C).

The photocontrolled polymerization was demonstrated to have the properties of chain polymerization. Later, extensive mechanistic work was reported on this transformation investigating the role of light.[195] The initial stages of the polymerization proceed readily without photoexcitation, but as the chain grows, the Grignard has problematic preferential interactions with internal repeat units; interaction at the chain ends is required for continued propagation. Light excites the growing chain, causing a shift in electron density away from internal repeat units and towards the chain ends. This causes the Grignard monomer to move from internal repeat units to the chain end, leading to chain propagation. The dynamic changes in electron density make polymer chains accessible, whereas without the use of light only oligomeric

materials with around four repeat units are observed. This work indicates that there could be a small molecule method accessible for heteroaryl Grignard cross-couplings with aryl halides without photoexcitation, and without the high temperatures used in the previous report, which required a heating to 110 °C for sufficient cross-coupling.

4.5 Outlook

In this perspective, we summarize important advances in conjugated polymer synthesis, highlighting the circular discoveries in small molecule and polymer C-H arylation methodologies. Direct arylation has become an important synthetic approach to conjugated molecules due to its' improved simplicity and efficiency over conventional methods of cross-coupling. As with many polymerization strategies, DArP was inspired by small molecule reports. As improvements are continually made in the small molecule C-H arylation literature, superior polymerization protocols will be developed. The stringent reactivity and selectivity requirements of preparing high quality polymers require efficient synthetic methods, and can provide insight into small deviations in selectivity not readily observable in all small molecule studies. This is valuable for not just future polymerizations, but also addresses needs in industrial scale-up of small molecules in pharmaceutical settings. In these cases, improved yield and regioselectivity are important for scalable synthetic routes, arising from the practicalities of purifying the target product. As improved methods in the small molecule and polymerization fields are discovered, new approaches for C-H arylation transformations are being utilized. These present challenges to achieving the high yields and selectivity needed for both polymerization and practical scale-up of pharmaceutical compounds. At the same time, they also hold significant promise for developing

the next generation of C-H arylation conditions that can allow for novel disconnections, controlled polymerization, and sustainable syntheses.

A number of examples have been discussed within this article for areas most promising for continued innovation. Amongst these, ligand design, greater inclusion and exploration of directing groups, improved understanding of new mechanisms for direct arylation for greater regioselectivity are important themes. Within DArP specifically, creating methods with improved control over molecular weight is a key advancement needed that could arise from polymerization-specific studies as has been developed in the controlled Grignard metathesis method of polymer synthesis.

In the future, we anticipate new, emerging reactions will continue to improve upon the simplicity and efficiency of conjugated polymer synthesis, while allowing study of more diverse polymer structures. As has occurred with DArP, these methods can be inspired by continued innovation in small molecule transformations. Greater advancements will be achieved if the results of these polymerization trials are also accounted for in developing new small molecule reactions. A circular path of methodology development and understanding where new small molecule and polymerization discoveries inform the other is a useful strategy to new synthetic method discovery. This approach showcases the utility of collaborative research efforts between synthetic research groups working on small molecules and those working on materials as an improved strategy for synthetic method development.

Chapter 5. Conclusions and Future Recommendations

5.1 Mechanism and Selectivity when Developing New DArP Protocols

Room temperature methods investigated in this work demonstrate the challenges in achieving high selectivity at low temperatures. In the case of CMD-mediated transformations, selectivity has been previously shown to improve with reduced temperature, as there is less energy available to activate the undesired and less reactive β-position on five-membered heteroarenes. On the contrary, high-yielding room temperature transformations may be allowed to proceed so efficiently at room temperature due to fundamental changes in mechanism which reduce the transformations' energetic needs. When this is the case, the activation free energy for competing C-H sites on a substrate may be entirely different than in CMD. For this reason, understanding the mechanism allowing for a highly reactive room temperature transformation is important to understand and predict regioselectivity outcomes.

While extensive work has been conducted in the CMD literature to understand and optimize regioselectivity in direct arylation, site-selectivity in direct arylation governed by different mechanisms is poorly understood. As successful polycondensation reactions are dependent on maximizing reactivity to achieve high molecular weight materials, developing a similar level of insight into factors determining regioselectivity in non-CMD transformations can offer access to improved DArP protocols featuring energy efficient conditions. At the same time, understanding the mechanistic origins controlling regioselectivity in direct arylation systems that diverge from conventional CMD will be of value to both the small molecule and polymer communities. As demonstrated by the PIn study in Chapter 2 and further contextualized in Chapter 4, polymerization trials are a great tool to the synthetic community for understanding

trends in regioselectivity. When small molecule studies indicate excellent regioselectivity, subsequent polymerization studies are a competent strategy to discover regiodivergent outcomes not readily observable in the small molecule transformation due to the exceptional monomer conversion required for polymerization.

5.2 Advances in Room Temperature DArP Methodology

Photomediated transformations are an attractive strategy for achieving room temperature reactivity. As demonstrated with the PIn work in Chapter 2, photomediated transformations are a viable tactic for mild polymerizations, albeit this process still requires improvements for achieving regioselective polymerization. While visible light photocatalysis has seen a renaissance in recent years, including for aryl-heteroaryl C-C bond forming reactions, it is largely unexplored in the literature for conjugated polymers. Achieving controlled chain polymerizations is an important goal yet to be broadly achieved in the synthesis of high performing conjugated polymers, photocatalyzed/photoinitiated polymerizations are a promising strategy. Considering that conjugated polymers are themselves photoactive materials, an optimized light-mediated system could selectively active growing polymer chains in place of monomers, dimers, or shorter oligomers due to their changing photoredox properties. As has been shown by the Kalow group, irradiation can move electron density from midchain to the chain ends of a growing conjugated polymer, potentially reducing branching defects.[195]

It is still unclear what drives the photosensitivity observed in DArP-prepared PIn, but understanding this will be an enabling discovery to develop new photomediated transformations, and creating regioselective DArP protocols. While a Pd-involved radical reaction is proposed herein based off of work from the Gevorgyan group, it may be that silver is playing an important

role as a photosensitizer. Silver nanoparticles are effective photosensitizers, previously used in such a role with other types of palladium catalyzed cross-coupling reactions.[196] DMF is known to be capable of reducing silver to Ag^0 for nanoparticle formation, which could be facilitation this process. Alternatively, in HFIP, Ag_2O is known to undergo a SET process with heteroarenes.[197] It is possible that light is enabling Ag-mediated C-H activation through such a process. Either way, subsequent studies investigating how silver behaves in a photomediated system are recommended to advance this work.

5.3 Improved Regioselectivity in Heck-Type Direct Arylation

While CMD is a widely observed mechanism for direct arylation reactions, there are growing reports for Heck-type couplings for five-membered heteroarenes and heterobiaryls as presented in Chapter 3. Up until this point, this type of mechanism is not known to have been used in a polymerization. One hindrance to pursuing Heck-type DArP arises from insufficient regioselectivity. For pyrrole/indole and furan/benzofuran, these small molecule transformations afford the desired C-2 selectivity as the major regioisomers produced.[50] Significant work has been completed to understand regioselectivity trends in the Heck olefination reaction, as well as to facilitate room temperature reactivity with Jeffery conditions.[198] These insights provide an excellent starting point from which to explore perfecting regioselectivity and maximizing reactivity at low temperatures for Heck-type DArP. Since the current small molecule reports for Heck-type C-H arylation are often at room temperature, studies seeking to improve regioselectivity for this type of mechanism are an important approach to achieving efficient DArP protocols.

For thiophene/benzothiophene, Heck-type transformations afford β-selective arylation under both ambient and elevated temperatures.[29,30,43,45] β-selectivity is a nice feature for small molecule transformations, offering access to the inaccessible regioisomers by CMD direct arylation, but is not desired in conjugated polymers. Heck-type arylation has been shown to occur simultaneously with CMD arylation when the reaction is run at high temperatures, requiring specific conditions to shut down one pathway to afford a single regioisomer.[45] This likely also causes the poor regioselectivity present in one method of primarily α-selective C-H arylation of benzothiophene.[68] Improved understanding of features enabling Heck-type arylation to compete with other mechanisms of direct arylation would enable designing conditions that shut off this undesired, β-selective reactivity.

In the case of pyrrole/indole and furan/benzofuran, promoting and improving selectivity for Heck-type arylation is a means of achieving room temperature Heck-type DArP. On the contrary, for thiophene/benzothiophene, shutting down the Heck-type C-H arylation pathway can lead to improved regioselectivity outcomes and could enable adaptation of a current α-selective room temperature benzothiophene arylation to polymerization. In both cases, more work is needed to understand fundamental origins allowing the Heck-type mechanism to occur preferentially to CMD and other direct arylation mechanisms. Looking to the existing literature from Heck olefination reactions will be a valuable starting place to guide experimental design and conditions-based approaches to improving desired reactivity and selectivity in both small molecule transformations and polymerizations.

References

(1) Shirakawa, H.; Louis, E. J.; MacDiarmid, A. G.; Chiang, C. K.; Heeger, A. J. Synthesis of Electrically Conducting Organic Polymers: Halogen Derivatives of Polyacetylene, (CH)X. *J. Chem. Soc. Chem. Commun.* **1977**, No. 16, 578–580.

(2) MacDiarmid, A. G.; Heeger, A. J. Organic Metals and Semiconductors: The Chemistry of Polyacetylene, (CH)x, and Its Derivatives. *Synth. Met.* **1980**, *1* (2), 101–118.

(3) Bronstein, H.; Nielsen, C. B.; Schroeder, B. C.; McCulloch, I. The Role of Chemical Design in the Performance of Organic Semiconductors. *Nat. Rev. Chem.* **2020**, *4* (2), 66–77.

(4) Liu, C.; Wang, K.; Gong, X.; Heeger, A. J. Low Bandgap Semiconducting Polymers for Polymeric Photovoltaics. *Chem. Soc. Rev.* **2016**, *45* (17), 4825–4846.

(5) Cui, C.; Li, Y. High-Performance Conjugated Polymer Donor Materials for Polymer Solar Cells with Narrow-Bandgap Nonfullerene Acceptors. *Energy Environ. Sci.* **2019**, *12* (11), 3225–3246.

(6) Beaujuge, P. M.; Amb, C. M.; Reynolds, J. R. Spectral Engineering in π-Conjugated Polymers with Intramolecular Donor-Acceptor Interactions. *Acc. Chem. Res.* **2010**, *43* (11), 1396–1407.

(7) Gibson, G. L.; McCormick, T. M.; Seferos, D. S. Atomistic Band Gap Engineering in Donor-Acceptor Polymers. *J. Am. Chem. Soc.* **2012**, *134* (1), 539–547.

(8) Mei, J.; Bao, Z. Side Chain Engineering in Solution-Processable Conjugated Polymers. *Chem. Mater.* **2014**, *26* (1), 604–615.

(9) Cui, C.; Wong, W. Y. Effects of Alkylthio and Alkoxy Side Chains in Polymer Donor Materials for Organic Solar Cells. *Macromol. Rapid Commun.* **2016**, *37* (4), 287–302.

(10) Wudl, F.; Kobayashi, M.; Heeger, A. J. Poly(Isothianaphthene). *J. Org. Chem.* **1984**, *49* (18), 3382–3384.

(11) Liang, Y.; Feng, D.; Wu, Y.; Tsai, S. T.; Li, G.; Ray, C.; Yu, L. Highly Efficient Solar Cell Polymers Developed via Fine-Tuning of Structural and Electronic Properties. *J. Am. Chem. Soc.* **2009**, *131* (22), 7792–7799.

(12) Gendron, D.; Leclerc, M. New Conjugated Polymers for Plastic Solar Cells. *Energy Environ. Sci.* **2011**, *4* (4), 1225–1237.

(13) Jadoun, S.; Riaz, U. Conjugated Polymer Light-Emitting Diodes. In *Polymers for Light-Emitting Devices and Displays*; John Wiley & Sons, Ltd, 2020; pp 77–98.

(14) Wang, S.; Oh, J. Y.; Xu, J.; Tran, H.; Bao, Z. Skin-Inspired Electronics: An Emerging Paradigm. *Acc. Chem. Res.* **2018**, *51* (5), 1033–1045.

(15) Paulsen, B. D.; Fabiano, S.; Rivnay, J. Mixed Ionic-Electronic Transport in Polymers. *Annu. Rev. Mater. Res.* **2021**, *51*, 73–99.

(16) Søndergaard, R.; Hösel, M.; Angmo, D.; Larsen-Olsen, T. T.; Krebs, F. C. Roll-to-Roll Fabrication of Polymer Solar Cells. *Mater. Today* **2012**, *15* (1–2), 36–49.

(17) Picca, R. A.; Manoli, K.; Macchia, E.; Sarcina, L.; Di Franco, C.; Cioffi, N.; Blasi, D.; Österbacka, R.; Torricelli, F.; Scamarcio, G.; et al. Ultimately Sensitive Organic Bioelectronic Transistor Sensors by Materials and Device Structure Design. *Adv. Funct. Mater.* **2020**, *30* (20), 1904513.

(18) Osedach, T. P.; Andrew, T. L.; Bulović, V. Effect of Synthetic Accessibility on the

Commercial Viability of Organic Photovoltaics. *Energy Environ. Sci.* **2013**, *6* (3), 711–718.

(19) Lizin, S.; Van Passel, S.; De Schepper, E.; Maes, W.; Lutsen, L.; Manca, J.; Vanderzande, D. Life Cycle Analyses of Organic Photovoltaics: A Review. *Energy Environ. Sci.* **2013**, *6* (11), 3136–3149.

(20) Tian, S.; Yue, Q.; Liu, C.; Li, M.; Yin, M.; Gao, Y.; Meng, F.; Tang, B. Z.; Luo, L. Complete Degradation of a Conjugated Polymer into Green Upcycling Products by Sunlight in Air. *J. Am. Chem. Soc.* **2021**, *143* (27), 10054–10058.

(21) Bronstein, H. A.; Luscombe, C. K. Externally Initiated Regioregular P3HT with Controlled Molecular Weight and Narrow Polydispersity. *J. Am. Chem. Soc.* **2009**, *131* (36), 12894–12895.

(22) Yokozawa, T.; Yokoyama, A. Chain-Growth Condensation Polymerization for the Synthesis of Well-Defined Condensation Polymers and π-Conjugated Polymers. *Chem. Rev.* **2009**, *109* (11), 5595–5619.

(23) Cowie, J.; Arrighi, V. Polymers: Chemistry and Physics of Modern Materials; CRC Press: Boca Raton, FL, 2007; pp 31–32.

(24) Yokozawa, T.; Ohta, Y. Scope of Controlled Synthesis via Chain-Growth Condensation Polymerization: From Aromatic Polyamides to π-Conjugated Polymers. *Chem. Commun.* **2013**, *49* (75), 8281–8310.

(25) Xing, L.; Liu, J.-R.; Hong, X.; Houk, K. N.; Luscombe, C. K. An Exception to the Carothers Equation Caused by the Accelerated Chain Extension in a Pd/Ag Cocatalyzed Cross Dehydrogenative Coupling Polymerization. *J. Am. Chem. Soc.* **2022**, *144* (5), 2311–2322.

(26) Tiwari, V. K.; Kapur, M. Catalyst-Controlled Positional-Selectivity in C-H Functionalizations. *Org. Biomol. Chem.* **2019**, *17* (5), 1007–1026.

(27) Liu, W.; Ren, Z.; Bosse, A. T.; Liao, K.; Goldstein, E. L.; Bacsa, J.; Musaev, D. G.; Stoltz, B. M.; Davies, H. M. L. Catalyst-Controlled Selective Functionalization of Unactivated C-H Bonds in the Presence of Electronically Activated C-H Bonds. *J. Am. Chem. Soc.* **2018**, *140* (38), 12247–12255.

(28) Roizen, J. L.; Zalatan, D. N.; Du Bois, J. Selective Intermolecular Amination of C-H Bonds at Tertiary Carbon Centers. *Angew. Chemie - Int. Ed.* **2013**, *52* (43), 11343–11346.

(29) Ueda, K.; Yanagisawa, S.; Yamaguchi, J.; Itami, K. A General Catalyst for the β-Selective C-H Bond Arylation of Thiophenes with Iodoarenes. *Angew. Chemie Int. Ed.* **2010**, *49* (47), 8946–8949.

(30) Yanagisawa, S.; Ueda, K.; Sekizawa, H.; Itami, K. Programmed Synthesis of Tetraarylthiophenes through Sequential C-H Arylation. *J. Am. Chem. Soc.* **2009**, *131* (41), 14622–14623.

(31) Wang, H.; Li, G.; Engle, K. M.; Yu, J. Q.; Davies, H. M. L. Sequential C-H Functionalization Reactions for the Enantioselective Synthesis of Highly Functionalized 2,3-Dihydrobenzofurans. *J. Am. Chem. Soc.* **2013**, *135* (18), 6774–6777.

(32) Bedell, T. A.; Hone, G. A. B.; Valette, D.; Yu, J.-Q.; Davies, H. M. L.; Sorensen, E. J. Rapid Construction of a Benzo-Fused Indoxamycin Core Enabled by Site-Selective C−H Functionalizations. *Angew. Chemie* **2016**, *128* (29), 8410–8414.

(33) Brückl, T.; Baxter, R. D.; Ishihara, Y.; Baran, P. S. Innate and Guided C-H Functionalization Logic. *Acc. Chem. Res.* **2012**, *45* (6), 826–839.

(34) Engle, K. M.; Mei, T. S.; Wasa, M.; Yu, J. Q. Weak Coordination as a Powerful Means for Developing Broadly Useful C-H Functionalization Reactions. *Acc. Chem. Res.* **2012**, *45* (6), 788–802.
(35) Jacob, C.; Maes, B. U. W.; Evano, G. Transient Directing Groups in Metal−Organic Cooperative Catalysis. *Chem. - A Eur. J.* **2021**, *27* (56), 13899–13952.
(36) Gorelsky, S. I.; Lapointe, D.; Fagnou, K. Analysis of the Concerted Metalation-Deprotonation Mechanism in Palladium-Catalyzed Direct Arylation across a Broad Range of Aromatic Substrates. *J. Am. Chem. Soc.* **2008**, *130* (33), 10848–10849.
(37) Gorelsky, S. I. Origins of Regioselectivity of the Palladium-Catalyzed (Aromatic)CH Bond Metalation-Deprotonation. *Coord. Chem. Rev.* **2013**, *257* (1), 153–164.
(38) Blaskovits, J. T.; Leclerc, M. C-H Activation as a Shortcut to Conjugated Polymer Synthesis. *Macromol. Rapid Commun.* **2019**, *40* (1), 1800512.
(39) Gobalasingham, N. S.; Thompson, B. C. Direct Arylation Polymerization: A Guide to Optimal Conditions for Effective Conjugated Polymers. *Prog. Polym. Sci.* **2018**, *83*, 135–201.
(40) Okamoto, K.; Zhang, J.; Housekeeper, J. B.; Marder, S. R.; Luscombe, C. K. C-H Arylation Reaction: Atom Efficient and Greener Syntheses of π-Conjugated Small Molecules and Macromolecules for Organic Electronic Materials. *Macromolecules* **2013**, *46* (20), 8059–8078.
(41) Sambiagio, C.; Schönbauer, D.; Blieck, R.; Dao-Huy, T.; Pototschnig, G.; Schaaf, P.; Wiesinger, T.; Zia, M. F.; Wencel-Delord, J.; Besset, T.; et al. A Comprehensive Overview of Directing Groups Applied in Metal-Catalysed C-H Functionalisation Chemistry. *Chem. Soc. Rev.* **2018**, *47* (17), 6603–6743.
(42) Choi, H.; Min, M.; Peng, Q.; Kang, D.; Paton, R. S.; Hong, S. Unraveling Innate Substrate Control in Site-Selective Palladium-Catalyzed C-H Heterocycle Functionalization. *Chem. Sci.* **2016**, *7* (6), 3900–3909.
(43) Colletto, C.; Islam, S.; Juliá-Hernández, F.; Larrosa, I. Room-Temperature Direct β-Arylation of Thiophenes and Benzo[b]Thiophenes and Kinetic Evidence for a Heck-Type Pathway. *J. Am. Chem. Soc.* **2016**, *138* (5), 1677–1683.
(44) Mayhugh, A. L.; Luscombe, C. K. Room Temperature C–H Arylation of Benzofurans by Aryl Iodides. *Org. Lett.* **2021**, *23* (18), 7079–7082.
(45) Tang, S. Y.; Guo, Q. X.; Fu, Y. Mechanistic Origin of Ligand-Controlled Regioselectivity in Pd-Catalyzed C-H Activation/Arylation of Thiophenes. *Chem. - A Eur. J.* **2011**, *17* (49), 13866–13876.
(46) Gorelsky, S. I.; Lapointe, D.; Fagnou, K. Analysis of the Palladium-Catalyzed (Aromatic)C-H Bond Metalation- Deprotonation Mechanism Spanning the Entire Spectrum of Arenes. *J. Org. Chem.* **2012**, *77* (1), 658–668.
(47) Wang, L.; Carrow, B. P. Oligothiophene Synthesis by a General C-H Activation Mechanism: Electrophilic Concerted Metalation-Deprotonation (ECMD). *ACS Catal.* **2019**, *9* (8), 6821–6836.
(48) Carrow, B. P.; Sampson, J.; Wang, L. Base-Assisted C−H Bond Cleavage in Cross-Coupling: Recent Insights into Mechanism, Speciation, and Cooperativity. *Isr. J. Chem.* **2020**, *60* (3–4), 230–258.
(49) Gorsline, B. J.; Wang, L.; Ren, P.; Carrow, B. P. C-H Alkenylation of Heteroarenes: Mechanism, Rate, and Selectivity Changes Enabled by Thioether Ligands. *J. Am. Chem.*

Soc. **2017**, *139* (28), 9605–9614.
(50) Gemoets, H. P. L. L.; Kalvet, I.; Nyuchev, A. V; Erdmann, N.; Hessel, V.; Schoenebeck, F.; Noël, T.; Nö, T. Mild and Selective Base-Free C-H Arylation of Heteroarenes: Experiment and Computation. *Chem. Sci.* **2017**, *8* (2), 1046–1055.
(51) Beletskaya, I. P.; Cheprakov, A. V. Heck Reaction as a Sharpening Stone of Palladium Catalysis. *Chem. Rev.* **2000**, *100* (8), 3009–3066.
(52) Sévignon, M.; Papillon, J.; Schulz, E.; Lemaire, M. New Synthetic Method for the Polymerization of Alkylthiophenes. *Tetrahedron Lett.* **1999**, *40* (32), 5873–5876.
(53) Hassan, J.; Schulz, E.; Gozzi, C.; Lemaire, M. Palladium-Catalyzed Synthesis of Oligo(Alkylthiophenes). *J. Mol. Catal. A Chem.* **2003**, *195* (1–2), 125–131.
(54) Kumar, A.; Kumar, A. Single Step Reductive Polymerization of Functional 3,4-Propylenedioxythiophenes via Direct C-H Arylation Catalyzed by Palladium Acetate. *Polym. Chem.* **2010**, *1* (3), 286–288.
(55) Lafrance, M.; Rowley, C. N.; Woo, T. K.; Fagnou, K. Catalytic Intermolecular Direct Arylation of Perfluorobenzenes. *J. Am. Chem. Soc.* **2006**, *128* (27), 8754–8756.
(56) Wang, Q.; Takita, R.; Kikuzaki, Y.; Ozawa, F. Palladium-Catalyzed Dehydrohalogenative Polycondensation of 2-Bromo-3-Hexylthiophene: An Efficient Approach to Head-to-Tail Poly(3-Hexylthiophene). *J. Am. Chem. Soc.* **2010**, *132* (33), 11420–11421.
(57) Aldrich, T. J.; Dudnik, A. S.; Eastham, N. D.; Manley, E. F.; Chen, L. X.; Chang, R. P. H.; Melkonyan, F. S.; Facchetti, A.; Marks, T. J. Suppressing Defect Formation Pathways in the Direct C-H Arylation Polymerization of Photovoltaic Copolymers. *Macromolecules* **2018**, *51* (22), 9140–9155.
(58) Blaskovits, J. T.; Johnson, P. A.; Leclerc, M. Mechanistic Origin of β-Defect Formation in Thiophene-Based Polymers Prepared by Direct (Hetero)Arylation. *Macromolecules* **2018**, *51* (20), 8100–8113.
(59) Rudenko, A. E.; Thompson, B. C. Optimization of Direct Arylation Polymerization (DArP) through the Identification and Control of Defects in Polymer Structure. *J. Polym. Sci. Part A Polym. Chem.* **2015**, *53* (2), 135–147.
(60) Rudenko, A. E.; Thompson, B. C. Influence of the Carboxylic Acid Additive Structure on the Properties of Poly(3-Hexylthiophene) Prepared via Direct Arylation Polymerization (DArP). *Macromolecules* **2015**, *48* (3), 569–575.
(61) Khlyabich, P. P.; Burkhart, B.; Rudenko, A. E.; Thompson, B. C. Optimization and Simplification of Polymerefullerene Solar Cells through Polymer and Active Layer Design. *Polymer (Guildf).* **2013**, *54*, 5267–5298.
(62) Rudenko, A. E.; Wiley, C. A.; Tannaci, J. F.; Thompson, B. C. Optimization of Direct Arylation Polymerization Conditions for the Synthesis of Poly(3-Hexylthiophene). *J. Polym. Sci. Part A Polym. Chem.* **2013**, *51* (12), 2660–2668.
(63) Li, Z.; Shi, Q.; Ma, X.; Li, Y.; Wen, K.; Qin, L.; Chen, H.; Huang, W.; Zhang, F.; Lin, Y.; et al. Efficient Room Temperature Catalytic Synthesis of Alternating Conjugated Copolymers via C-S Bond Activation. *Nat. Commun.* **2022**, *13* (1).
(64) Woods, E. F.; Berl, A. J.; Kalow, J. A. Photocontrolled Synthesis of N-Type Conjugated Polymers. *Angew. Chemie - Int. Ed.* **2020**, *59* (15), 6062–6067.
(65) Koyuncu, S.; Hu, P.; Li, Z.; Liu, R.; Bilgili, H.; Yagci, Y. Fluorene-Carbazole-Based Porous Polymers by Photoinduced Electron Transfer Reactions. *Macromolecules* **2020**, *53* (5), 1645–1651.

(66) Lebrasseur, N.; Larrosa, I. Room Temperature and Phosphine Free Palladium Catalyzed Direct C-2 Arylation of Indoles. *J. Am. Chem. Soc.* **2008**, *130* (10), 2926–2927.
(67) Islam, S.; Larrosa, I. On Water Phosphine-Free Palladium-Catalyzed Room Temperature C-H Arylation of Indoles. *Chem. - A Eur. J.* **2013**, *19* (45), 15093–15096.
(68) Colletto, C.; Panigrahi, A.; Fernández-Casado, J.; Larrosa, I. Ag(I)-C-H Activation Enables Near-Room-Temperature Direct α-Arylation of Benzo[b]Thiophenes. *J. Am. Chem. Soc.* **2018**, *140* (30), 9638–9643.
(69) René, O.; Fagnou, K. Room-Temperature Direct Arylation of Polyfluorinated Arenes under Biphasic Conditions. *Org. Lett.* **2010**, *12* (9), 2116–2119.
(70) Pouliot, J. R.; Grenier, F.; Blaskovits, J. T.; Beaupré, S.; Leclerc, M. Direct (Hetero)Arylation Polymerization: Simplicity for Conjugated Polymer Synthesis. *Chem. Rev.* **2016**, *116* (22), 14225–14274.
(71) Wencel-Delord, J.; Dröge, T.; Liu, F.; Glorius, F. Towards Mild Metal-Catalyzed C–H Bond Activation. *Chem. Soc. Rev.* **2011**, *40* (9), 4740–4761.
(72) Gensch, T.; Hopkinson, M. N.; Glorius, F.; Wencel-Delord, J. Mild Metal-Catalyzed C–H Activation: Examples and Concepts. *Chem. Soc. Rev.* **2016**, *45* (10), 2900–2936.
(73) Zhou, C.; Liang, Y.; Liu, F.; Sun, C.; Huang, X.; Xie, Z.; Huang, F.; Roncali, J.; Russell, T. P.; Cao, Y. Chain Length Dependence of the Photovoltaic Properties of Monodisperse Donor-Acceptor Oligomers as Model Compounds of Polydisperse Low Band Gap Polymers. *Adv. Funct. Mater.* **2014**, *24* (47), 7538–7547.
(74) Okamoto, K.; Housekeeper, J. B.; Michael, F. E.; Luscombe, C. K. Thiophene Based Hyperbranched Polymers with Tunable Branching Using Direct Arylation Methods. *Polym. Chem.* **2013**, *4* (12), 3499–3506.
(75) Gooßen, L. J.; Deng, G.; Levy, L. M. Synthesis of Biaryls via Catalytic Decarboxylative Coupling. *Science* **2006**, *313* (5787), 662–664.
(76) Cornella, J.; Lahlali, H.; Larrosa, I. Decarboxylative Homocoupling of (Hetero)Aromatic Carboxylic Acids. *Chem. Commun.* **2010**, *46* (43), 8276–8278.
(77) Cornelia, J.; Lu, P.; Larrosa, I. Intermodular Decarboxylative Direct C-3 Arylation of Indoles with Benzoic Acids. *Org. Lett.* **2009**, *11* (23), 5506–5509.
(78) Stateman, L. M.; Nakafuku, K. M.; Nagib, D. A. Remote C-H Functionalization via Selective Hydrogen Atom Transfer. *Synth.* **2018**, *50* (8), 1569–1586.
(79) *Radicals in Organic Synthesis*; Renaud, P., Sibi, M. P., Eds.; Wiley-VCH Verlag, 2000; Vol. 48.
(80) Lapointe, D.; Fagnou, K. Overview of the Mechanistic Work on the Concerted Metallation-Deprotonation Pathway. *Chem. Lett.* **2010**, *39* (11), 1118–1126.
(81) Lebrasseur, N.; Larrosa, I. Recent Advances in the C2 and C3 Regioselective Direct Arylation in Indoles. *Adv. Heterocycl. Chem.* **2012**, *105*, 309–351.
(82) Seregin, I. V; Gevorgyan, V. Direct Transition Metal-Catalyzed Functionalization of Heteroaromatic Compounds. *Chem. Soc. Rev.* **2007**, *36* (7), 1173–1193.
(83) Lane, B. S.; Brown, M. A.; Sames, D. Direct Palladium-Catalyzed C-2 and C-3 Arylation of Indoles: A Mechanistic Rationale for Regioselectivity. *J. Am. Chem. Soc.* **2005**, *127* (22), 8050–8057.
(84) Deprez, N. R.; Kalyani, D.; Krause, A.; Sanford, M. S. Room Temperature Palladium-Catalyzed 2-Arylation of Indoles. *J. Am. Chem. Soc.* **2006**, *128* (15), 4972–4973.
(85) Kurokhtina, A. A.; Larina, E. V; Yarosh, E. V; Lagoda, N. A.; Schmidt, A. F. Mechanistic

Study of Direct Arylation of Indole Using Differential Selectivity Measurements: Shedding Light on the Active Species and Revealing the Key Role of Electrophilic Substitution in the Catalytic Cycle. *Organometallics* **2018**, *37* (13), 2054–2063.

(86) Zhou, W. J.; Cao, G. M.; Shen, G.; Zhu, X. Y.; Gui, Y. Y.; Ye, J. H.; Sun, L.; Liao, L. L.; Li, J.; Yu, D. G. Visible-Light-Driven Palladium-Catalyzed Radical Alkylation of C−H Bonds with Unactivated Alkyl Bromides. *Angew. Chemie - Int. Ed.* **2017**, *56* (49), 15683–15687.

(87) Kurandina, D.; Parasram, M.; Gevorgyan, V. Visible Light-Induced Room-Temperature Heck Reaction of Functionalized Alkyl Halides with Vinyl Arenes/Heteroarenes. *Angew. Chemie - Int. Ed.* **2017**, *56* (45), 14212–14216.

(88) Parasram, M.; Chuentragool, P.; Sarkar, D.; Gevorgyan, V. Photoinduced Formation of Hybrid Aryl Pd-Radical Species Capable of 1,5-HAT: Selective Catalytic Oxidation of Silyl Ethers into Silyl Enol Ethers. *J. Am. Chem. Soc.* **2016**, *138* (20), 6340–6343.

(89) Liu, Q.; Dong, X.; Li, J.; Xiao, J.; Dong, Y.; Liu, H. Recent Advances on Palladium Radical Involved Reactions. *ACS Catal.* **2015**, *5* (10), 6111–6137.

(90) Punji, B.; Song, W.; Shevchenko, G. A.; Ackermann, L. Cobalt-Catalyzed C-H Bond Functionalizations with Aryl and Alkyl Chlorides. *Chem. - A Eur. J.* **2013**, *19* (32), 10605–10610.

(91) Guo, X. K.; Zhang, L. B.; Wei, D.; Niu, J. L. Mechanistic Insights into Cobalt(Ii/Iii)-Catalyzed C-H Oxidation: A Combined Theoretical and Experimental Study. *Chem. Sci.* **2015**, *6* (12), 7059–7071.

(92) Sun, Q. K.; Liu, W.; Ying, S. A.; Wang, L. L.; Xue, S. F.; Yang, W. J. 9,10-Bis(N-Alkylindole-3-Yl-Vinyl-2)Anthracenes as a New Series of Alkyl Length-Dependent Piezofluorochromic Aggregation-Induced Emission Homologues. *RSC Adv.* **2015**, *5* (89), 73046–73050.

(93) Korenaga, T.; Kosaki, T.; Fukumura, R.; Ema, T.; Sakai, T. Suzuki-Miyaura Coupling Reaction Using Pentafluorophenylboronic Acid. *Org. Lett.* **2005**, *7* (22), 4915–4917.

(94) Naik, R.; Harmalkar, D. S.; Xu, X.; Jang, K.; Lee, K. Bioactive Benzofuran Derivatives: Moracins A-Z in Medicinal Chemistry. *Eur. J. Med. Chem.* **2015**, *90*, 379–393.

(95) Hu, X.; Wu, J. W.; Wang, M.; Yu, M. H.; Zhao, Q. S.; Wang, H. Y.; Hou, A. J. 2-Arylbenzofuran, Flavonoid, and Tyrosinase Inhibitory Constituents of Morus Yunnanensis. *J. Nat. Prod.* **2012**, *75* (1), 82–87.

(96) Huang, P.; Du, J.; Biewer, M. C.; Stefan, M. C. Developments of Furan and Benzodifuran Semiconductors for Organic Photovoltaics. *J. Mater. Chem. A* **2015**, *3* (12), 6244–6257.

(97) Dou, K.; Wang, X.; Du, Z.; Jiang, H.; Li, F.; Sun, M.; Yang, R. Synergistic Effect of Side-Chain and Backbone Engineering in Thieno[2,3-f] Benzofuran-Based Conjugated Polymers for High Performance Non-Fullerene Organic Solar Cells. *J. Mater. Chem. A* **2019**, *7* (3), 958–964.

(98) Yin, S. C.; Zhou, Q.; Zhao, X. Y.; Shao, L. X. N-Heterocyclic Carbene-Palladium(II)-1-Methylimidazole Complex Catalyzed Direct C-H Bond Arylation of Benzo[b]Furans with Aryl Chlorides. *J. Org. Chem.* **2015**, *80* (17), 8916–8921.

(99) Dao-Huy, T.; Haider, M.; Glatz, F.; Schnürch, M.; Mihovilovic, M. D. Direct Arylation of Benzo[b]Furan and Other Benzo-Fused Heterocycles. *European J. Org. Chem.* **2014**, *2014* (36), 8119–8125.

(100) Cao, J.; Chen, Z. L.; Li, S. M.; Zhu, G. F.; Yang, Y. Y.; Wang, C.; Chen, W. Z.; Wang, J.

T.; Zhang, J. Q.; Tang, L. Palladium-Catalyzed Regioselective C-2 Arylation of Benzofurans with N′-Acyl Arylhydrazines. *European J. Org. Chem.* **2018**, *2018* (22), 2774–2779.

(101) Mao, S.; Shi, X.; Soulé, J. F.; Doucet, H. Direct Arylations of Heteroarenes with Benzenesulfonyl Chlorides Using Pd/C Catalyst. *European J. Org. Chem.* **2020**, *2020* (1), 91–97.

(102) Dwight, T. A.; Rue, N. R.; Charyk, D.; Josselyn, R.; DeBoef, B. C-C Bond Formation via Double C-H Functionalization: Aerobic Oxidative Coupling as a Method for Synthesizing Heterocoupled Biaryls. *Org. Lett.* **2007**, *9* (16), 3137–3139.

(103) Hegde, R. V.; Ong, T. G.; Ambre, R.; Jadhav, A. H.; Patil, S. A.; Dateer, R. B. Regioselective Direct C2 Arylation of Indole, Benzothiophene and Benzofuran: Utilization of Reusable Pd NPs and NHC-Pd@MNPs Catalyst for C–H Activation Reaction. *Catal. Letters* **2021**, *151* (5), 1397–1405.

(104) Biajoli, A. F. P.; Da Penha, E. T.; Correia, C. R. D. Palladium Catalysed Regioselective Arylation of Indoles, Benzofuran and Benzothiophene with Aryldiazonium Salts. *RSC Adv.* **2012**, *2* (31), 11930–11935.

(105) Xu, Z.; Xu, Y.; Lu, H.; Yang, T.; Lin, X.; Shao, L.; Ren, F. Efficient and C2-Selective Arylation of Indoles, Benzofurans, and Benzothiophenes with Iodobenzenes in Water at Room Temperature. *Tetrahedron* **2015**, *71* (18), 2616–2621.

(106) Firth, J. D.; Fairlamb, I. J. S. A Need for Caution in the Preparation and Application of Synthetically Versatile Aryl Diazonium Tetrafluoroborate Salts. *Org. Lett.* **2020**, *22* (18), 7057–7059.

(107) Mayhugh, A. L.; Luscombe, C. K. Room-Temperature Pd/Ag Direct Arylation Enabled by a Radical Pathway. *Beilstein J. Org. Chem.* **2020**, *16* (1), 384–390.

(108) Bhattacharya, T.; Ghosh, A.; Maiti, D. Hexafluoroisopropanol: The Magical Solvent for Pd-Catalyzed C-H Activation. *Chem. Sci.* **2021**, *12* (11), 3857–3870.

(109) Miao, Y. H.; Hu, Y. H.; Yang, J.; Liu, T.; Sun, J.; Wang, X. J. Natural Source, Bioactivity and Synthesis of Benzofuran Derivatives. *RSC Adv.* **2019**, *9* (47), 27510–27540.

(110) Imrich, H. G.; Conrad, J.; Beifuss, U. Copper-Catalyzed Double Intramolecular Ullmann Coupling for the Synthesis of Diastereomerically and Enantiomerically Pure 4b,9b-Dihydrobenzofuro[3,2-b]Benzofurans. *European J. Org. Chem.* **2015**, *2015* (35), 7718–7734.

(111) Zhang, Z.-J.; Zhou, X.; Li, D.; Chen, Y.; Xiao, W.-W.; Li, R.-T.; Shao, L.-D. Aerobic Copper-Catalyzed Intramolecular Cascade Oxidative Isomerization/[4+4] Cyclization of 2,2′-Disubstituted Stilbenes. *J. Org. Chem.* **2021**, *86* (11), 7609–7624.

(112) Li, H.; Roisnel, T.; Soulé, J. F.; Doucet, H. Regiocontrolled Palladium-Catalyzed Direct C2-Arylations of Methoxalen Using Benzenesulfonyl Chlorides and C2,C3-Diarylations Using Aryl Bromides as the Aryl Sources. *Tetrahedron Lett.* **2020**, *61* (1).

(113) Lotz, M. D.; Camasso, N. M.; Canty, A. J.; Sanford, M. S. Role of Silver Salts in Palladium-Catalyzed Arene and Heteroarene C-H Functionalization Reactions. *Organometallics* **2017**, *36* (1), 165–171.

(114) Kantam, M. L.; Ranganath, K. V. S.; Sateesh, M.; Kumar, K. B. S.; Choudary, B. M. Friedel-Crafts Acylation of Aromatics and Heteroaromatics by Beta Zeolite. *J. Mol. Catal. A Chem.* **2005**, *225* (1), 15–20.

(115) Liljenberg, M. Quantum Chemical Studies of Aromatic Substitution Reactions, KTH

Royal Institute of Technology, 2017.
(116) Rao, V. K.; Shelke, G. M.; Tiwari, R.; Parang, K.; Kumar, A. A Simple and Efficient Synthesis of 2,3-Diarylnaphthofurans Using Sequential Hydroarylation/Heck Oxyarylation. *Org. Lett.* **2013**, *15* (9), 2190–2193.
(117) Zhu, R.; Buchwald, S. L. Combined Oxypalladation/C-H Functionalization: Palladium(II)-Catalyzed Intramolecular Oxidative Oxyarylation of Hydroxyalkenes. *Angew. Chemie - Int. Ed.* **2012**, *51* (8), 1926–1929.
(118) von Ragué Schleyer, P.; Jiao, H.; Goldfuss, B.; Freeman, P. K. Aromaticity and Antiaromaticity in Five-Membered C4H4X Ring Systems: "Classical" and "Magnetic" Concepts May Not Be "Orthogonal." *Angew. Chemie Int. Ed. English* **1995**, *34* (3), 337–340.
(119) Delaere, D.; Minh, T. N.; Vanquickenborne, L. G. Influence of Building Block Aromaticity in the Determination of Electronic Properties of Five-Membered Heterocyclic Oligomers. *Phys. Chem. Chem. Phys.* **2002**, *4* (9), 1522–1530.
(120) Cyrañski, M. K.; Krygowski, T. M.; Katritzky, A. R.; Schleyer, P. V. R. To What Extent Can Aromaticity Be Defined Uniquely? *J. Org. Chem.* **2002**, *67* (4), 1333–1338.
(121) Saito, H.; Yorimitsu, H. Ring-Expanding and Ring-Opening Transformations of Benzofurans and Indoles with Introducing Heteroatoms. *Chem. Lett.* **2019**, *48* (9), 1019–1028.
(122) Qin, D. D.; Chen, W.; Tang, X.; Yu, W.; Wu, A. A.; Liao, Y.; Chen, H. Bin. Accessing 2-Arylbenzofurans by CuI2(Pip)2-Catalyzed Tandem Coupling/Cyclization Reaction: Mechanistic Studies and Application to the Synthesis of Stemofuran A and Moracin M. *Asian J. Org. Chem.* **2016**, *5* (11), 1345–1352.
(123) Baxendale, I. R.; Griffiths-Jones, C. M.; Ley, S. V.; Tranmer, G. K. Microwave-Assisted Suzuki Coupling Reactions with an Encapsulated Palladium Catalyst for Batch and Continuous-Flow Transformations. *Chem. - A Eur. J.* **2006**, *12* (16), 4407–4416.
(124) Chakrabarty, I.; Akram, M. O.; Biswas, S.; Patil, N. T. Visible Light Mediated Desilylative C(Sp2)-C(Sp2) Cross-Coupling Reactions of Arylsilanes with Aryldiazonium Salts under Au(i)/Au(Iii) Catalysis. *Chem. Commun.* **2018**, *54* (52), 7223–7226.
(125) Wang, Z.; Li, Y.; Yan, B.; Huang, M.; Wu, Y. Palladium-Catalyzed Phosphine-Free Direct C-H Arylation of Benzothiophenes and Benzofurans Involving MIDA Boronates. *Synlett* **2015**, *26* (4), 531–536.
(126) Ranjbari, M. A.; Tavakol, H. Catalyst-Free Synthesis of Benzofuran Derivatives from Cascade Reactions between Nitroepoxides and Salicylaldehydes. *J. Org. Chem.* **2021**, *86* (6), 4756–4762.
(127) Henry, M. C.; Sutherland, A. Synthesis of Benzo[b]Furans by Intramolecular C-O Bond Formation Using Iron and Copper Catalysis. *Org. Lett.* **2020**, *22* (7), 2766–2770.
(128) Shin, T.; Kim, M.; Jung, Y.; Cho, S. J.; Kim, H.; Song, H. Characterization of Heterogeneous Aryl-Pd(Ii)-Oxo Clusters as Active Species for C-H Arylation. *Chem. Commun.* **2020**, *56* (92), 14404–14407.
(129) Ma, W.; Huang, J.; Huang, X.; Meng, S.; Yang, Z.; Li, C.; Wang, Y.; Qi, T.; Li, B. Direct Construction of 2,3-Unsubstituted Benzofurans and Benzothiophenes: Via a Metal-Free Catalyzed Intramolecular Friedel-Crafts Reaction. *Org. Chem. Front.* **2019**, *6* (4), 493–497.
(130) Reddy, A. C. S.; Ramachandran, K.; Reddy, P. M.; Anbarasan, P. Rhodium-Catalyzed

Sommelet-Hauser Type Rearrangement of α-Diazoimines: Synthesis of Functionalized Enamides. *Chem. Commun.* **2020**, *56* (42), 5649–5652.
(131) Pu, X.; Zhang, M.; Lan, J.; Chen, S.; Liu, Z.; Liang, W.; Yang, Y.; Zhang, M.; You, J. Tandem Rh(III)-Catalyzed C-H Heteroarylation of Indolyl Ketones and Cu(II)-Promoted Intramolecular Cyclization: One-Pot Access to Blue-Emitting Phenanthrone-Type Polyheterocycles. *Org. Lett.* **2019**, *21* (4), 1139–1143.
(132) Baciocchi, E.; Sebastiani, G. V; Ruzziconi, R. Kinetic Study of the Base-Induced Anti and Syn Eliminations from 2, 3-Dihalogeno-2, 3-Dihydrobenzofurans in Different Base-Solvent Systems. *J. Org. Chem.* **1979**, *44* (1), 28–31.
(133) Zhang, M.; Zhu, L.; Zhou, G.; Hao, T.; Qiu, C.; Zhao, Z.; Hu, Q.; Larson, B. W.; Zhu, H.; Ma, Z.; et al. Single-Layered Organic Photovoltaics with Double Cascading Charge Transport Pathways: 18% Efficiencies. *Nat. Commun.* **2021**, *12* (1).
(134) Holliday, S.; Li, Y.; Luscombe, C. K. Recent Advances in High Performance Donor-Acceptor Polymers for Organic Photovoltaics. *Prog. Polym. Sci.* **2017**, *70*, 34–51.
(135) Rasmussen, S. C. Conjugated and Conducting Organic Polymers: The First 150 Years. *Chempluschem* **2020**, *85* (7), 1412–1429.
(136) Okamoto, K.; Luscombe, C. K. Controlled Polymerizations for the Synthesis of Semiconducting Conjugated Polymers. *Polym. Chem.* **2011**, *2* (11), 2424–2434.
(137) Reynolds, J. R. Pi-Conjugated Polymers: The Importance of Polymer Synthesis. In *Conjugated Polymers: A Practical Guide to Synthesis*; Müllen, K., Reynolds, J. R., Masuda, T., Eds.; 2013; pp 1–11.
(138) Carsten, B.; He, F.; Son, H. J.; Xu, T.; Yu, L. Stille Polycondensation for Synthesis of Functional Materials. *Chem. Rev.* **2011**, *111* (3), 1493–1528.
(139) Sakamoto, J.; Rehahn, M.; Wegner, G.; Schlüter, A. D. Suzuki Polycondensation: Polyarylenes à La Carte. *Macromol. Rapid Commun.* **2009**, *30* (9–10), 653–687.
(140) Stepek, I. A.; Itami, K. Recent Advances in C-H Activation for the Synthesis of π-Extended Materials. *ACS Mater. Lett.* **2020**, *2* (8), 951–974.
(141) Dalton, T.; Faber, T.; Glorius, F. C-H Activation: Toward Sustainability and Applications. *ACS Cent. Sci.* **2021**, *7* (2), 245–261.
(142) Lu, W.; Kuwabara, J.; Kanbara, T. Polycondensation of Dibromofluorene Analogues with Tetrafluorobenzene via Direct Arylation. *Macromolecules* **2011**, *44* (6), 1252–1255.
(143) Bura, T.; Beaupré, S.; Légaré, M. A.; Quinn, J.; Rochette, E.; Blaskovits, J. T.; Fontaine, F. G.; Pron, A.; Li, Y.; Leclerc, M. Direct Heteroarylation Polymerization: Guidelines for Defect-Free Conjugated Polymers. *Chem. Sci.* **2017**, *8* (5), 3913–3925.
(144) Bura, T.; Blaskovits, J. T.; Leclerc, M. Direct (Hetero)Arylation Polymerization: Trends and Perspectives. *J. Am. Chem. Soc.* **2016**, *138* (32), 10056–10071.
(145) Suraru, S.-L.; Lee, J. A.; Luscombe, C. K. C–H Arylation in the Synthesis of π-Conjugated Polymers. *ACS Macro Lett.* **2016**, *5* (6), 724–729.
(146) Bohra, H.; Wang, M. Direct C-H Arylation: A "Greener" Approach towards Facile Synthesis of Organic Semiconducting Molecules and Polymers. *J. Mater. Chem. A* **2017**, *5* (23), 11550–11571.
(147) Leclerc, M.; Brassard, S.; Beaupré, S. Direct (Hetero)Arylation Polymerization: Toward Defect-Free Conjugated Polymers. *Polym. J.* **2020**, *52* (1), 13–20.
(148) Ye, L.; Thompson, B. C. Improving the Efficiency and Sustainability of Catalysts for Direct Arylation Polymerization (DArP). *J. Polym. Sci.* **2021**, 1–36.

(149) Wakioka, M.; Ozawa, F. Highly Efficient Catalysts for Direct Arylation Polymerization (DArP). *Asian J. Org. Chem.* **2018**, *7* (7), 1206–1216.
(150) Pankow, R. M.; Thompson, B. C. Approaches for Improving the Sustainability of Conjugated Polymer Synthesis Using Direct Arylation Polymerization (DArP). *Polym. Chem.* **2020**, *11* (3), 630–640.
(151) Dixon, A. G.; Visvanathan, R.; Clark, N. A.; Stingelin, N.; Kopidakis, N.; Shaheen, S. E. Molecular Weight Dependence of Carrier Mobility and Recombination Rate in Neat P3HT Films. *J. Polym. Sci. Part B Polym. Phys.* **2018**, *56* (1), 31–35.
(152) Kim, J. S.; Kim, J. H.; Lee, W.; Yu, H.; Kim, H. J.; Song, I.; Shin, M.; Oh, J. H.; Jeong, U.; Kim, T. S.; et al. Tuning Mechanical and Optoelectrical Properties of Poly(3-Hexylthiophene) through Systematic Regioregularity Control. *Macromolecules* **2015**, *48* (13), 4339–4346.
(153) Onorato, J.; Wang, Z.; Sun, Y.; Nowak, C.; Flagg, L.; Li, R.; Dong, B. X.; Richter, L.; Escobedo, F.; Nealey, P. F.; et al. Side Chain Engineering Control of Mixed Conduction in Oligoethylene Glycol-Substituted Polythiophenes. *J. Mater. Chem. A* **2021**, *9*, 21410–21423.
(154) Yu, X.; Li, C.; Gao, C.; Zhang, X.; Zhang, G.; Zhang, D. Incorporation of Hydrogen-bonding Units into Polymeric Semiconductors toward Boosting Charge Mobility, Intrinsic Stretchability, and Self-healing Ability. *SmartMat* **2021**, *2* (3), 347–366.
(155) Kim, H. J.; Pei, M.; Ko, J. S.; Ma, M. H.; Park, G. E.; Baek, J.; Yang, H.; Cho, M. J.; Choi, D. H. Influence of Branched Alkyl Ester-Labeled Side Chains on Specific Chain Arrangement and Charge-Transport Properties of Diketopyrrolopyrrole-Based Conjugated Polymers. *ACS Appl. Mater. Interfaces* **2018**, *10* (47), 40681–40691.
(156) Maria, I. P.; Paulsen, B. D.; Savva, A.; Ohayon, D.; Wu, R.; Hallani, R.; Basu, A.; Du, W.; Anthopoulos, T. D.; Inal, S.; et al. The Effect of Alkyl Spacers on the Mixed Ionic-Electronic Conduction Properties of N-Type Polymers. *Adv. Funct. Mater.* **2021**, *31* (14), 2008718.
(157) Pankow, R. M.; Ye, L.; Thompson, B. C. Influence of an Ester Directing-Group on Defect Formation in the Synthesis of Conjugated Polymers: Via Direct Arylation Polymerization (DArP) Using Sustainable Solvents. *Polym. Chem.* **2019**, *10* (33), 4561–4572.
(158) Pankow, R. M.; Ye, L.; Thompson, B. C. Influence of the Ester Directing Group on the Inhibition of Defect Formation in Polythiophenes with Direct Arylation Polymerization (DArP). *Macromolecules* **2020**, *53* (9), 3315–3324.
(159) Hu, X. Q.; Liu, Z. K.; Hou, Y. X.; Gao, Y. Single Electron Activation of Aryl Carboxylic Acids. *iScience* **2020**, *23* (7), 101266.
(160) Twilton, J.; Le, C. C.; Zhang, P.; Shaw, M. H.; Evans, R. W.; MacMillan, D. W. C. The Merger of Transition Metal and Photocatalysis. *Nat. Rev. Chem.* **2017**, *1*.
(161) Sapurina, I.; Stejskal, J. The Mechanism of the Oxidative Polymerization of Aniline and the Formation of Supramolecular Polyaniline Structures. *Polym. Int.* **2008**, *57* (12), 1295–1325.
(162) Heinze, J.; Frontana-Uribe, B. A.; Ludwigs, S. Electrochemistry of Conducting Polymers-Persistent Models and New Concepts. *Chem. Rev.* **2010**, *110* (8), 4724–4771.
(163) Ruiz-Castillo, P.; Buchwald, S. L. Applications of Palladium-Catalyzed C-N Cross-Coupling Reactions. *Chem. Rev.* **2016**, *116* (19), 12564–12649.
(164) Martin, R.; Buchwald, S. L. Palladium-Catalyzed Suzuki-Miyaura Cross-Coupling

Reactions Employing Dialkylbiaryl Phosphine Ligands. *Acc. Chem. Res.* **2008**, *41* (11), 1461–1473.

(165) Campeau, L. C.; Parisien, M.; Leblanc, M.; Fagnou, K. Biaryl Synthesis via Direct Arylation: Establishment of an Efficient Catalyst for Intramolecular Processes. *J. Am. Chem. Soc.* **2004**, *126* (30), 9186–9187.

(166) Collier, G. S.; Reynolds, J. R. Exploring the Utility of Buchwald Ligands for C-H Oxidative Direct Arylation Polymerizations. *ACS Macro Lett.* **2019**, *8* (8), 931–936.

(167) Christmann, U.; Vilar, R. Monoligated Palladium Species as Catalysts in Cross-Coupling Reactions. *Angew. Chemie - Int. Ed.* **2005**, *44* (3), 366–374.

(168) Hartwig, J. F.; Paul, F. Oxidative Addition of Aryl Bromide after Dissociation of Phosphine from a Two-Coordinate Palladium(0) Complex, Bis(Tri-o-Tolylphosphine)Palladium(0). *J. Am. Chem. Soc.* **1995**, *117* (19), 5373–5374.

(169) Hartwig, J. F. Electronic Effects on Reductive Elimination to Form Carbon-Carbon and Carbon-Heteroatom Bonds from Palladium(Ll) Complexes. *Inorg. Chem.* **2007**, *46* (6), 1936–1947.

(170) Barder, T. E.; Buchwald, S. L. Insights into Amine Binding to Biaryl Phosphine Palladium Oxidative Addition Complexes and Reductive Elimination from Biaryl Phosphine Arylpalladium Amido Complexes via Density Functional Theory. *J. Am. Chem. Soc.* **2007**, *129* (39), 12003–12010.

(171) Mann, G.; Shelby, Q.; Roy, A. H.; Hartwig, J. F. Electronic and Steric Effects on the Reductive Elimination of Diaryl Ethers from Palladium(II). *Organometallics* **2003**, *22* (13), 2775–2789.

(172) Molander, G. A.; Canturk, B. Organotrifluoroborates and Monocoordinated Palladium Complexes as Catalysts - A Perfect Combination for Suzuki-Miyaura Coupling. *Angew. Chemie - Int. Ed.* **2009**, *48* (49), 9240–9261.

(173) Gobalasingham, N. S.; Noh, S.; Thompson, B. C. Palladium-Catalyzed Oxidative Direct Arylation Polymerization (Oxi-DArP) of an Ester-Functionalized Thiophene. *Polym. Chem.* **2016**, *7* (8), 1623–1631.

(174) Kang, L. J.; Xing, L.; Luscombe, C. K. Exploration and Development of Gold- and Silver-Catalyzed Cross Dehydrogenative Coupling toward Donor–Acceptor π-Conjugated Polymer Synthesis. *Polym. Chem.* **2019**, *10* (4), 486–493.

(175) Cambeiro, X. C.; Ahlsten, N.; Larrosa, I. Au-Catalyzed Cross-Coupling of Arenes via Double C-H Activation. *J. Am. Chem. Soc.* **2015**, *137* (50), 15636–15639.

(176) Li, W.; Yuan, D.; Wang, G.; Zhao, Y.; Xie, J.; Li, S.; Zhu, C. Cooperative Au/Ag Dual-Catalyzed Cross-Dehydrogenative Biaryl Coupling: Reaction Development and Mechanistic Insight. *J. Am. Chem. Soc.* **2019**, *141* (7), 3187–3197.

(177) Liu, J. R.; Duan, Y. Q.; Zhang, S. Q.; Zhu, L. J.; Jiang, Y. Y.; Bi, S.; Hong, X. C-H Acidity and Arene Nucleophilicity as Orthogonal Control of Chemoselectivity in Dual C-H Bond Activation. *Org. Lett.* **2019**, *21* (7), 2360–2364.

(178) Daley, R. A.; Morrenzin, A. S.; Neufeldt, S. R.; Topczewski, J. J. Gold Catalyzed Decarboxylative Cross-Coupling of Iodoarenes. *J. Am. Chem. Soc.* **2020**, *142* (30), 13210–13218.

(179) Daley, R. A.; Morrenzin, A. S.; Neufeldt, S. R.; Topczewski, J. J. Mechanistic Investigation into the Gold-Catalyzed Decarboxylative Cross-Coupling of Iodoarenes. *ACS Catal.* **2021**, *11* (15), 9578–9587.

(180) Panigrahi, A.; Whitaker, D.; Vitorica-Yrezabal, I. J.; Larrosa, I. Ag/Pd Cocatalyzed Direct Arylation of Fluoroarene Derivatives with Aryl Bromides. *ACS Catal.* **2020**, *10* (3), 2100–2107.
(181) Aoki, H.; Saito, H.; Shimoyama, Y.; Kuwabara, J.; Yasuda, T.; Kanbara, T. Synthesis of Conjugated Polymers Containing Octafluorobiphenylene Unit via Pd-Catalyzed Cross-Dehydrogenative-Coupling Reaction. *ACS Macro Lett.* **2018**, *7* (1), 90–94.
(182) Powers, I. G.; Andjaba, J. M.; Luo, X.; Mei, J.; Uyeda, C. Catalytic Azoarene Synthesis from Aryl Azides Enabled by a Dinuclear Ni Complex. *J. Am. Chem. Soc.* **2018**, *140* (11), 4110–4118.
(183) Andjaba, J. M.; Rybak, C. J.; Wang, Z.; Ling, J.; Mei, J.; Uyeda, C. Catalytic Synthesis of Conjugated Azopolymers from Aromatic Diazides. *J. Am. Chem. Soc.* **2021**, *143* (10), 3975–3982.
(184) Salvi, L.; Davis, N. R.; Ali, S. Z.; Buchwald, S. L. A New Biarylphosphine Ligand for the Pd-Catalyzed Synthesis of Diaryl Ethers under Mild Conditions. *Org. Lett.* **2012**, *14* (1), 170–173.
(185) Burgos, C. H.; Barder, T. E.; Huang, X.; Buchwald, S. L. Significantly Improved Method for the Pd-Catalyzed Coupling of Phenols with Aryl Halides: Understanding Ligand Effects. *Angew. Chemie - Int. Ed.* **2006**, *45* (26), 4321–4326.
(186) Guo, S.; Swager, T. M. Versatile Porous Poly(Arylene Ether)s via Pd-Catalyzed C-O Polycondensation. *J. Am. Chem. Soc.* **2021**, *143* (30), 11828–11835.
(187) Kim, J.; Chang, S. Iridium-Catalyzed Direct C-H Amidation with Weakly Coordinating Carbonyl Directing Groups under Mild Conditions. *Angew. Chemie - Int. Ed.* **2014**, *53* (8), 2203–2207.
(188) Shang, M.; Sun, S. Z.; Dai, H. X.; Yu, J. Q. Cu(II)-Mediated C-H Amidation and Amination of Arenes: Exceptional Compatibility with Heterocycles. *J. Am. Chem. Soc.* **2014**, *136* (9), 3354–3357.
(189) Xiao, B.; Gong, T. J.; Xu, J.; Liu, Z. J.; Liu, L. Palladium-Catalyzed Intermolecular Directed C-H Amidation of Aromatic Ketones. *J. Am. Chem. Soc.* **2011**, *133* (5), 1466–1474.
(190) Ryu, J.; Kwak, J.; Shin, K.; Lee, D.; Chang, S. Ir(III)-Catalyzed Mild C-H Amidation of Arenes and Alkenes: An Efficient Usage of Acyl Azides as the Nitrogen Source. *J. Am. Chem. Soc.* **2013**, *135* (34), 12861–12868.
(191) Jang, Y.-J.; Hwang, S.-H.; Choi, T.-L. Iridium-Catalyzed Direct C−H Amidation Polymerization: Step-Growth Polymerization by C−N Bond Formation via C−H Activation to Give Fluorescent Polysulfonamides. *Angew. Chemie* **2017**, *129* (46), 14666–14670.
(192) Hwang, S. H.; Choi, T. L. Iridium-Catalyzed Direct C-H Amidation Producing Multicolor Fluorescent Molecules Emitting Blue-to-Red Light and White Light. *Org. Lett.* **2020**, *22* (8), 2935–2940.
(193) Shirakawa, E.; Hayashi, Y.; Itoh, K. I.; Watabe, R.; Uchiyama, N.; Konagaya, W.; Masui, S.; Hayashi, T. Cross-Coupling of Aryl Grignard Reagents with Aryl Iodides and Bromides through S RN1 Pathway. *Angew. Chemie - Int. Ed.* **2012**, *51* (1), 218–221.
(194) Murarka, S.; Studer, A. Radical/Anionic SRN1-Type Polymerization for Preparation of Oligoarenes. *Angew. Chemie - Int. Ed.* **2012**, *51* (49), 12362–12366.
(195) Woods, E. F.; Berl, A. J.; Kantt, L. P.; Eckdahl, C. T.; Wasielewski, M. R.; Haines, B. E.;

Kalow, J. A. Light Directs Monomer Coordination in Catalyst-Free Grignard Photopolymerization. *J. Am. Chem. Soc.* **2021**, *143*, 18755–18765.

(196) Xiao, Q.; Sarina, S.; Bo, A.; Jia, J.; Liu, H.; Arnold, D. P.; Huang, Y.; Wu, H.; Zhu, H. Visible Light-Driven Cross-Coupling Reactions at Lower Temperatures Using a Photocatalyst of Palladium and Gold Alloy Nanoparticles. *ACS Catal.* **2014**, *4* (6), 1725–1734.

(197) Yang, S.; Cheng, R.; Zhang, M.; Bin, Z.; You, J. Rh/Ag-Mediated Peri-Selective Heteroarylation/Single Electron Transfer Annulation Cascade of 1-(Methylthio)Naphthalenes and Analogues: Road Less Traveled to Benzo[de]Thioacenes. *ACS Catal.* **2019**, *9* (7), 6188–6193.

(198) Jeffery, T. On the Efficiency of Tetraalkylammonium Salts in Heck Type Reactions. *Tetrahedron* **1996**, *52* (30), 10113–10130.

Vita

Amy Mayhugh is from Portland, Oregon. She began her research career as an undergraduate student at Pacific University, where she worked with Prof. David Cordes on developing facile methods for the hydrodehalogenation of aryl halides. Graduating with a B.S. in Chemistry in 2015, Amy was inspired by the idea of generating fundamentally new solutions to existing problems, particularly regarding sustainability. Subsequently, she joined Prof. Christine Luscombe's research group at the University of Washington as a member of the Chemistry Department. While at UW, Amy completed an internship with Procter & Gamble, developing analytical techniques for compositional analysis of recycled materials. She was awarded the CEI Graduate Fellowship and the Simeon Endowed Research Fellowship. She was involved with the Students in Clean Energy student organization for 3 years, and mentored several junior researchers. Her research focused on developing more environmentally friendly and economically viable methods of conjugated polymer synthesis, focusing on mild C-H functionalization reactions.